CHARACTERIZING ASCL1-DEPENDENT NEUROENDOCRINE NON-SMALL CELL LUNG CANCERS

APPROVED BY SUPERVISORY COMMITTEE

John D. Minna, M.D. (Mentor)

James F. Amatruda, M.D., Ph.D. (Chairman)

Jane E. Johnson, Ph.D.

Michael A. White, Ph.D.

Dedicated to

My parents Edward and Elizabeth Augustyn
And my sisters Caroline, Veronica, and Renata

CHARACTERIZING ASCL1-DEPENDENT NEUROENDOCRINE NON-SMALL CELL LUNG CANCERS

by

ALEXANDER AUGUSTYN

DISSERTATION

Presented to the Faculty of the Graduate School of Biomedical Sciences

The University of Texas Southwestern Medical Center at Dallas

In Partial Fulfillment of the Requirements

For the Degree of

DOCTOR OF PHILOSOPHY

The University of Texas Southwestern Medical Center at Dallas

Dallas, Texas

June, 2013

ACKNOWLEDGMENTS

I would like to express my sincere and unconditional gratitude to the many people who have made my research training possible, first among them my mentor, Dr. John D. Minna, whose patience, generosity, and enthusiasm I hope to emulate in my future career. I am deeply thankful for the opportunity to have trained in such an independent environment and greatly appreciate the time and resources Dr. Minna invested in my training, and for the many hours I spent in his office discussing, writing, and re-writing our work. I would also like to thank Dr. Adi Gazdar for his input and encouragement.

I thank my committee members Dr. James Amatruda, Dr. Jane Johnson, and Dr. Michael White for challenging me and for the animated and helpful discussions we had during my committee meetings. I am especially thankful for all of the help provided by Dr. Johnson in editing my scientific writing and helping me understand how to properly prepare figures for publication.

The research I performed during my training could not have been accomplished without an immensely helpful network of collaborators. I would like to thank Dr. Yang Xie and her graduate student Tao Wang for their help in performing bioinformatics analysis; Dr. Ignacio Wistuba and his team at MD Anderson Cancer Center for providing microarray data and stained tissue samples; Dr. Luc Girard for developing bioinformatics software for the Minna lab. I also had the opportunity to train two wonderfully gifted undergraduate students, Christopher Tan and Victoria Lee, whose help performing experiments was greatly appreciated.

I would like to extend a special thank you to Mark Borromeo, a graduate student in Dr. Jane Johnson's lab for his help in performing the ChIP-Seq experiments and always replying to my many emails in rapid fashion.

I am grateful to my colleagues in the lab, past and present, for providing lively discussion during lab meetings, answering my technical questions, giving intellectual input, as well as providing support, friendship, and "essential" happy hours. In particular I would like to thank Dr. Chunli Shao for answering my never-ending series of questions and Dr. Jill Larsen for always helping me maintain perspective in my project.

My training would not have been possible without the generous support of the Ruth L. Kirschstein Individual Predoctoral Fellowship for Dual Degree Candidates, afforded to me by the National Cancer Institute division of the National Institutes of Health.

Finally, I would like to thank my family for their constant support and encouragement, particularly from my parents, Edward and Elizabeth, whose love and sacrifice are unparalleled.

CHARACTERIZING ASCL1-DEPENDENT NEUROENDOCRINE NON-SMALL CELL LUNG CANCERS

Publication No._____

Alexander Augustyn, Ph.D.

The University of Texas Southwestern Medical Center at Dallas, 2013

Supervising Professor: John D. Minna, M.D.

In order to achieve personalized medicine for the treatment of lung cancer, it is important to accurately classify tumors using a combination of factors, including patho-physiological features, tumor gene expression profiles, response to therapy, and oncogene/tumor suppressor mutation status. Gene expression analyses, including immunohistochemistry, single mRNA transcript analyses, and genome-wide mRNA expression profiling, performed over the course of the last three decades suggest that distinct, poorly performing neuroendocrine tumors occur in about 10% of otherwise pathologically indistinguishable non-small cell lung cancers. A complete molecular characterization of these tumors is lacking because no pre-clinical model exists.

Utilizing genome-wide mRNA expression profiling from lung cancer cell lines established from a variety of patients, it was discovered that a rare subgroup of non-small cell lung cancer (NSCLC) lines demonstrated similar gene expression compared to a known neuroendocrine tumor, small cell lung cancer (SCLC). Validation of transcript analysis verified this data, and demonstrated that a particular transcription factor, ASCL1, required during development for the formation of pulmonary neuroendocrine cells, is dramatically upregulated in the subgroup of non-small cell lung cancer with neuroendocrine features (NE-NSCLC). Other cancer models have demonstrated addiction of tumors to developmental transcription factors and termed these genes "lineage oncogenes." By showing that NE-NSCLC cell lines are addicted to ASCL1 expression and function, it was established that ASCL1 is also a lineage oncogene.

Transcription factors of the basic helix-loop-helix category are historically difficult to target with small molecules, so a downstream target analysis was performed in order to understand the ASCL1 transcriptome. ChIP-Seq analysis demonstrated that ASCL1 regulates many genes, including several that are inherently druggable. Further studies proved that ASCL1 directly regulates the transcription of the anti-apoptotic regulator BCL2. Inhibition of BCL2 *in vitro* and *in vivo* led to induction of apoptosis and tumor xenograft regression suggesting that BCL2 is a potential therapeutic target in ASCL1-dependent NE-NSCLCs.

Analysis of the upstream regulation of ASCL1 showed that it depends on a paradoxical activation of the RAS/RAF/MEK/ERK pathway. Small molecule agonists of this pathway were utilized to demonstrate reduction of ASCL1 levels and induction of apoptosis. The combination of ERK activation with BCL2 inhibition was then shown to be a viable therapeutic strategy for ASCL1-dependent tumors *in vitro*.

TABLE OF CONTENTS

PRIOR PUBLICATIONS

Augustyn, A., Borromeo, M, Wang, T., Shao, C., Lee, V., Tan, C., Larsen, J.E., Girard, L., Behrens, C., Wistuba, I., Xie, Y., Gazdar, A.F., Johnson, J.E., and Minna, J.D. (2013) ASCL1 is a Lineage Oncogene in a Novel Neuroendocrine Subtype of Non-Small Cell Lung Cancer. Nat Med, *submitted.*

Shao, C., Sullivan, J.P., Girard, L., **Augustyn, A.,** Rodriguez, J., Behrens, C., Wistuba, I., and Minna, J.D. (2013) Aldehyde Dehydrogenase 1A3 is a Functional Marker of Non-Small Cell Lung Cancer Stem Cells. Stem Cell, *submitted.*

LIST OF FIGURES AND TABLES

LIST OF ABBREVIATIONS

A-SC – achaete-scute complex

AC – adenocarcinoma or atypical carcinoid

ALDH – aldehyde dehydrogenase

APL – acute promyelocytic leukemia

ASCL1 – achaete-scute homolog 1

ATRA – all-trans retinoic acid

BCL2 – B-cell lymphoma 2

bHLH – basic helix loop helix

BRAF – v-Raf murine sarcoma viral oncogene homolog B1

cGRP – calcitonin gene related peptide

ChIP-Seq – chromatin immunoprecipitation – sequencing

CML – chronic myelogenous leukemia

CZ – cabozantinib

DLL1 – delta-like protein 1

DLL3 – delta-like protein 3

DMSO – dimethyl sulfoxide

EGFR – epidermal growth factor receptor

ERK – extracellular signal regulated kinase

FACS – fluorescence activated cell sorting

GFP – green fluorescent protein

GREAT – genomic regions enrichment of annotations tools

GRP – gastrin-releasing peptide

HBEC – human bronchial epithelial cell

HOMER – hypergeometric optimization of motif enrichment

HRAS – v-Ha-Ras Harvey rat sarcoma viral oncogene homolog

IHC – immunohistochemistry

KRAS – v-Ki-Ras2 Kirsten rat sarcoma viral oncogene homolog

LCNEC – large cell neuroendocrine carcinoma

MACS – model-based analysis of ChIP-Seq

MAPK – mitogen activated protein kinase

MEK1/2 – mitogen activated protein kinase kinase 1/2

MITF – microphtalmia-associated transcription factor

miR – microRNA

MTS – 3-(4,5-dimethylthiazol-2-yl)-5-(3-carboxymethoxyphenyl)-2-(4-sulfophenyl)-2H-tetrazolium

NE – neuroendocrine

NE-NSCLC – non-small cell lung cancer with neuroendocrine features

NOD/SCID – non-obsese diabetic severe combined immunodeficiency mouse

NSCLC – non-small cell lung cancer

P53 – tumor protein 53

PI – propidium iodide

PMA – phorbol 12-myristate 13-acetate

PML – promyelocytic leukemia

PNEC – pulmonary neuroendocrine cell

qRT-PCR – quantitative real-time polymerase chain reaction

RARA – retinoic acid receptor alpha

RB – retinoblastoma

RET – ret proto-oncogene

RPMI – Roswell Park Memorial Institute medium

SCC – squamous cell carcinoma

SCLC – small cell lung cancer

SHH – sonic hedgehog

shRNA – short-hairpin ribonucleic acid

siRNA – short-interfering ribonucleic acid

SOR - sorafenib

SNP – single nucleotide polymorphism

TC – typical carcinoid

TMA – tissue microarray

XN - xanthohumol

CHAPTER ONE

LINEAGE DEPENDENCE IN HUMAN CANCER

1.1 Introduction to Lineage-Based Carcinogenesis Models

Cancer is invariably a genetic disease that arises from mutations in the DNA of specific cell types, leading to uncontrolled growth and division. The last decade of cancer research has brought to the forefront array technologies with the ability to carefully detail many genetic characteristics of tumors. Such array technologies can be used to profile tumors for whole-genome mRNA expression, complete DNA sequencing, single nucleotide polymorphisms (SNP), and genome-wide methylation patterns, among others. The explosion of high-throughput genetic arrays raises the possibility of reclassifying human cancers based on their genetic traits rather than solely through histopathological analysis. The main challenge will be to discern essential cellular dependencies that are the result of genetic lesions, and to use this information to uncover novel therapeutic advances in the clinic (Garraway and Sellers 2006).

Human development and cancer are intrinsically linked (Berman 2004). Embedded in the aberrant genetic programs of a given human cancer is a molecular assumption that these tumor cells must cannibalize various cellular mechanisms that function in their normal ancestral cell type (Garraway and Sellers 2006). Indeed, histopathologists have long noted a close phenotypic association between a particular cancer and the cells of the organ from which the tumor was excised (Berman 2004; Berman 2005). Cellular dependencies that are imprinted during normal

cell development may shape the course of genetic alterations in a given cancer and perhaps reveal a class of lineage-associated cancer genes (Garraway, Weir et al. 2005). This suggests that normal developmental lineages must play a critical role in shaping the course of human cancer, and that progress towards improving our understanding of cancer and developing novel therapies will depend on understanding how genetic lesions can utilize normal developmental pathways to lead to unchecked growth.

Four hypotheses have been recently developed in order to explain the range of human tumorigenesis (Table 1.1). The implication of each hypothesis (explained below, briefly) is the idea that cancer biology is linked to and influenced by the lineage and differentiation states of normal cells, including precursor (stem) cells.

1.1.1 Differentiation Hypothesis

The differentiation hypothesis defines cancer as an abnormality arising from cell maturation or differentiation. Hematological malignancies typically exemplify the differentiation hypothesis, and one specific cancer is acute promyelocytic leukemia (APL). In APL, neoplastic cells gain genetic mutations that block their ability to differentiate past the promyelocytic stage of myeloid differentiation (Fenaux and Degos 1997). Treatment efficacy with all-trans retinoic acid (ATRA) depends on the ability of ATRA to displace the tumor-driving fusion protein and restoring normal myeloid differentiation (Tallman, Andersen et al. 1997).

Prior to the discovery that forcing differentiation in APL is an attractive therapeutic option, the only treatment was a full stem cell transplant (Fenaux and Degos 1997). Normal

Hypothesis	Definition	Example	Targeted Therapy
Differentiation	Abnormal differentiation is tumorigenic	Acute leukemias	ATRA (APL)
Tissue-Lineage	Tumorigenesis of specific cells from distinct tissues	Breast adenocarcinoma vs. lung adenocarcinoma	Herceptin (Breast) Erlotinib (Lung)
Embryological	Tumorigensis of embryonal cells	Sarcoma vs. carcinoma	None (Surgery, Chemotherapy, Radiation)
Cell-Lineage	Transformation of histologically distinct cells	Squamous cell carcinoma vs. adenocarcinoma	Vismodegib (SCC of the skin) Crizotinib (Lung Adenocarcinoma)

Table 1.1: Hypotheses for tumorigenesis. Four hypotheses can be used to explain the range of human cancer and are reviewed briefly in this table. Adapted from Garraway and Sellers, 2006.

myeloid lineage differentiation relies on the proteins promyelocytic leukemia (PML) and retinoic acid receptor alpha (RARA) dimerizing (PML homodimerizing, RARA homodimerizing or heterodimerizing with retinoic X receptor). The t(15;17) chromosomal translocation seen in APL creates a fusion protein between PML and RARA, removing the cell's ability to properly differentiate past the promyelocytic stage. Treatment with ATRA causes APL blasts to differentiate into polymorphonuclear leukocytes, relieving the tumor burden. The major therapeutic effect appears to be degradation of the PML-RARA fusion protein (Tallman, Andersen et al. 1997). In the case of APL, improper lineage development is the direct cause of the tumor, while the resulting treatment relies on relieving the cell of this aberrant differentiation block.

1.1.2 Tissue Lineage, Embryological, and Cell Lineage Hypotheses

The tissue lineage hypothesis can be explained as a malignant transformation of characteristic cells from distinct tissue types. This lineage model is the implied clinical approach to most solid tumors largely due to the organ-specific developmental history that is associated with these cancers. For example, adenocarcinoma of the breast is a different disease than adenocarcinoma of the lung or colon, with different mutations and different treatment paradigms (Garraway and Sellers 2006). Tumors with endocrine-based treatments such as breast cancer and prostate cancer have lineage-specific dependencies that vary dramatically from each other, yet each relies on a similar principle: hormonal blockade in order to stop tumor growth and

progression (Heinlein and Chang 2004; Lumachi, Luisetto et al. 2011; Bourke, Kirkbride et al. 2013).

The embryological hypothesis is defined as the malignant transformation of embryologically distinct cell types (Garraway and Sellers 2006). This is best explained as the difference between carcinomas, which develop from endodermal or ectodermal cells, and sarcomas, which develop from mesenchymal cells.

The cell lineage hypothesis is defined as the malignant transformation of histologically distinct cell types, and explains the difference between tumors such as squamous cell lung carcinoma, which arises from lung basal cells, and lung adenocarcinoma, which arises from epithelial alveolar cells (Garraway and Sellers 2006). Although little is known about the stem cell hierarchy in the human lung, precluding the ability of researchers to study stem cell associations with cancer, recent evidence has demonstrated the existence of a differentiation hierarchy in the adult mammary gland (Perou, Sorlie et al. 2000; Sorlie, Perou et al. 2001).

Mammary stem cells, presumed to be important for organ development and tissue maintenance, give rise to both the luminal and myoepithelial lineages via a series of lineage-restricted intermediate progenitors. The luminal lineage can be subdivided into ductal and alveolar cells, which line the ducts and make up the alveolar units, respectively, while the myoepithelial cells are specialized contractile cells that exist at the basal surface of the epithelium adjacent to the basement membrane (Visvader 2009). Major expansion of breast tissue occurs during puberty and pregnancy, suggesting the existence of a stem-like cell with impressive regenerative potential. The existence of adult stem cells in the breast makes them

attractive targets for oncogenic transformation. Committed progenitors are also susceptible to tumorigenesis. Currently, the human breast epithelial hierarchy can be used to describe the six types of breast cancer. First, the claudin low "normal-like" subtype of breast cancer expresses a gene signature similar to that of mammary stem cells. Next, basal-like tumors share many genes in common with a luminal progenitor, while luminal A and luminal B subtypes express genes indicative of a continuum between the luminal progenitor and a fully-differentiated ductal cell. Finally, HER2+ tumors arise from an oncogenic event activating HER2 at some point during a cell's progression between luminal progenitor and ductal cell (Visvader 2009). Establishing similarities between tumor subtypes and normal cellular subsets can have dramatic implications for the development of therapeutically useful interventions and prognostic markers.

Taken together, these hypotheses can adequately explain the range of human cancers by distinguishing between cancer type, tissue type, cell type, and differentiation stage. Advances in understanding the molecular mechanisms guiding lineage programs that govern differentiation of cells, tissues, and ultimately organisms and understanding how cancers subvert these pathways will improve our ability to develop useful therapies in the clinic.

1.1.3 Lineage Specification in Development and Cancer

Vertebrate development is modeled primarily through genome-wide chromatin rearrangement and spatiotemporal regulation of transcription factors that direct expression of lineage-specific genes (Muller and Leutz 2001; Kluger, Lian et al. 2004). Epigenetic remodeling mechanisms function in an ordered, sequential manner to activate gene expression patterns that

govern axis formation, body segmentation, and lineage differentiation (Warburton, Schwarz et al. 2000; Ringrose and Paro 2004; Fraga, Ballestar et al. 2005). Following epigenetic modeling, tissue and cell-specific transcription factors begin to activate, and in conjunction with microenvironmental cues and cell-autonomous migration, allow for the eventual maturation of a specific cell type (Nagamura-Inoue, Tamura et al. 2001; Kluger, Lian et al. 2004).

Many cancers are known to have deregulated epigenetic programs and these occur as mutations in chromatin remodeling genes such as SNF5 or BMI1, which occur either causally or in strong association with tumor progression and metastasis (Davis and Brackmann 2003; Dukers, van Galen et al. 2004; Sawa, Yamamoto et al. 2005; Garraway and Sellers 2006). Deregulated expression of essential transcription factors that govern pattern formation and lineage development also occurs in conjunction with tumorigenesis (Abate-Shen 2002; Grier, Thompson et al. 2005; Garraway and Sellers 2006). Interestingly, a comparison between the genome-wide mRNA expression of certain cancer types and their associated normal tissue indicates that certain tumor subsets may be characterized by their molecular similarity to a particular developmental stage (Kho, Zhao et al. 2004). This suggests that a given cancer only has a finite molecular repertoire to genetically exploit, and that this depends on the lineage-restricted pattern of development. If true, it is reasonable to expect a primarily lineage-restricted pattern of cancer mechanisms across human cancer and that lineage-survival factors that operate during normal development are prime candidates for oncogenic dependency (Garraway, Weir et al. 2005; Garraway and Sellers 2006; Garraway and Sellers 2006).

1.1.4 Somatic Mutations in Cancer are Lineage-Restricted

The spectrum of somatic mutations in cancer is affected by lineage. Genome-era high-throughput technology allows for the characterization of cancer mutations on a global scale and the combination of genetic and lineage cancer development hypotheses. Though the idea that cancer is fundamentally a genetic disease has gained prevalence in recent years, it is also known that lineage restriction is associated with the distribution of genetic alterations in human cancers. A combination of genetic and lineage hypotheses will likely lead to a more thorough understanding of cancer, its genesis, and underlying essential dependencies that can be exploited therapeutically.

Surveying well-known oncogenes such as BRAF, KRAS, and EGFR demonstrates that mutations in these genes are attributed to high frequency occurrences in a small number of cancers, such that their overall prevalence can be restricted to a small number of cell lineages. For example, BRAF mutations are very frequent in melanoma yet infrequent in other tumors (Davies, Bignell et al. 2002). KRAS mutations occur in the lung, colon, and prostate, but few other tumors, and EGFR is mutated in lung cancers and glioblastoma, but not others (Smit, Boot et al. 1988; Burmer, Rabinovitch et al. 1991; Batra, Castelino-Prabhu et al. 1995; Vachtenheim, Horakova et al. 1995). In addition, mutation patterns can also be attributed to lineage. Though the common tumor suppressor gene TP53 is frequently mutated in all cancer types, a mutation in TP53 paired with a mutation in RB1 is seen in approximately 90% of small cell lung cancer tumors (Gazdar 1992). Similarly, macro-genomic alterations such as chromosomal translocations, deletions, and amplifications are also lineage-restricted. In leukemia, balanced

translocations group distinct molecular subtypes of hematological malignancies according to cell lineage (Cork 1983; Wang 2012). Amplifications of genes in solid tumors, including CCND1, HER2, and EGFR also show lineage-restricted patterns (Wong, Bigner et al. 1987; Tal, Wetzler et al. 1988; Fantl, Smith et al. 1993). Finally, clustering analysis of high-density SNP arrays profiling a large number of human cancers for gain or loss of genomic material demonstrates a clear grouping of cancers by tissue-of-origin, which suggests lineage-driven genetic perturbations drive human cancer (Garraway, Widlund et al. 2005). These observations support the premise that tumor mutations and associated reliance on their continued aberrant function is intrinsically linked with the lineage specification that occurs in the relevant progenitor cells (Garraway and Sellers 2006). Therefore, a careful analysis of model systems including cell lines, animal models, and human tumor samples is necessary in order to discover how lineage-associated genes are affected by genetic lesions and whether it is possible to use such an approach to develop therapeutic interventions for human cancers.

1.1.5 Lineage Addiction in Human Cancer

Lineage addiction is a combination of the lineage dependence and genome-centric hypotheses of cancer. Lineage-survival pathways may operate aberrantly during tumor progression as the result of genetic alterations, leading to the dependency or addiction of a particular tumor to its parental lineage-signaling program (Bass, Watanabe et al. 2009). In contrast to oncogene addiction, in which tumors rely on pathways not normally activated in adjacent normal tissue (Weinstein 2002), lineage addiction suggests that tumors rely on the

persistence and deregulation of survival mechanisms that operate during normal development (Hemesath, Steingrimsson et al. 1994; Garraway, Widlund et al. 2005; Gontan, de Munck et al. 2008). Although both models are similar in the reliance of tumors on a key genetic alteration, the origin and basis of the oncogene addiction and lineage addiction models are quite different.

Well-known examples of oncogene addiction often involve growth-promoting genes such as tyrosine kinases that have developed a point mutation or fusion that allows for their constitutive activation. The best example of oncogene addiction is the BCR-ABL fusion protein that is a hallmark of chronic myelogenous leukemia (CML) (Rowley 1973). Identification of the BCR-ABL fusion protein led to the development of imatinib, a highly effective tyrosine kinase inhibitor for the treatment of CML (Schindler, Bornmann et al. 2000). Other examples of oncogene addiction include activating KIT mutations in gastrointestinal tumors, and EGFR mutations in non-small cell lung cancer (Batra, Castelino-Prabhu et al. 1995; Hirota, Isozaki et al. 1998). Often times, these mutated genes are able to confer a transformed phenotype in a well-known model system such as induction of anchorage-independent growth in NIH-3T3 cells and tumor formation in xenograft models (Batra, Castelino-Prabhu et al. 1995).

Lineage addiction, by contrast, involves deregulation of master regulator genes such as transcription factors that activate pro-growth and pro-survival (lineage survival) signaling pathways during normal development (Garraway, Widlund et al. 2005; Kwei, Kim et al. 2008; Bass, Watanabe et al. 2009). Cancers hijack these pathways in order to maintain a positive growth and survival phenotype. Lineage survival genes have critical roles during tissue development. The normal cellular changes experienced by a cell during development condition

the genetic lesions necessary to form a tumor. Context-specific mutations that occur during a particular spatiotemporal phase of cell development may have cancer-causing effects in one cell, but not in another cell, which is in a separate phase of development (Garraway and Sellers 2006). Genetic and epigenetic alterations during development can subvert lineage survival genes for carcinogenesis, tumor survival, and subsequent metastasis.

1.1.6 MITF as a Prototypical Lineage Oncogene

The master transcriptional regulator microphthalmia associated transcription factor (MITF) has a critical role during melanocyte development (Hemesath, Steingrimsson et al. 1994). Knockout studies in mice demonstrates that loss of MITF is associated with loss of the melanocyte lineage (Goding 2000; Dupin and Le Douarin 2003; Widlund and Fisher 2003), while further studies demonstrate that MITF directly activates the transcription of BCL2, an anti-apoptotic gene necessary for cell lineage survival (McGill, Horstmann et al. 2002). The success of the melanocyte lineage therefore depends on survival and proliferation signals that converge on and emanate from MITF.

Studies have shown that MITF is amplified in 15-20% of metastatic melanomas and functional assays demonstrated cooperation with activated BRAF mutations and cell cycle deregulation to transform human melanocytes (Sharpless and Chin 2003). Loss-of-function studies in melanoma cancer models show that these tumors are addicted to continued MITF expression and function (Garraway, Widlund et al. 2005). It is critical to note that the transformative capacity of MITF occurred in conjunction with activated MAPK signaling and

cell cycle deregulation via p16-RB1 pathway inactivation (Wellbrock, Rana et al. 2008). Therefore, by directing melanocyte lineage survival and promoting carcinogenesis in conjunction with specific genetic alterations, MITF seems to act as a lineage oncogene (Garraway and Sellers 2006). A deeper look into MITF function in melanoma reveals how a lineage differentiation program can be subverted through conditioned genetic alterations in order to develop a tumor. MITF, during normal development, has two critical roles. One is to initiate the developmental transcription program for melanocytes, which is associated with growth and cell cycle arrest through the involvement of CDK2 (Du, Widlund et al. 2004), while the other is to promote lineage survival through the aforementioned MITF-BCL2 axis (McGill, Horstmann et al. 2002). It seems that MITF-dependent melanomas must overcome the cell cycle block by removing growth-inhibitory signals through genetic and/or epigenetic mutations in order to proliferate unchecked. Studies show that MITF-dependent melanomas escape growth arrest by losing p16 expression and/or RB function via deletion of CDKN2A (Chin 2003). Additionally, MITF-dependent melanomas incur frequent BRAF or NRAS mutations, which are functionally important as the MEK/ERK pathway directly phosphorylates MITF and allows for its constitutive activity in the cancer cell (Davies, Bignell et al. 2002; Omholt, Platz et al. 2003; Reifenberger, Knobbe et al. 2004). Therefore, it seems that melanocytes that develop mutations in both the p16/RB and MAPK pathways are distinctly positioned for carcinogenesis, suggesting that conditioned genetic alterations in melanocytes can lead to cancer directly through the master transcriptional regulator MITF. The lineage addiction model also explains why these mutations occur much more frequently in melanomas than in tumors of other cell lineages.

Lineage oncogenes are also described in other tumor types and include androgen receptor (AR) in prostate cancer, estrogen receptor (ESR1) in breast cancer, thyroid transcription factor 1 (TTF1) in lung adenocarcinoma, SRY-box 2 (SOX2) in squamous cell lung carcinoma, as well as achaete-scute homolog 1 (ASCL1) in small cell lung cancer, among others (Heinlein and Chang 2004; Osada, Tatematsu et al. 2005; Bass, Watanabe et al. 2009). Additionally, lineage-specific inactivation of tumor suppressor genes is also reported. Prominent examples include loss of adenomatosis polyposis coli (APC) in colon cancer, RB in retinoblastoma and small cell lung cancer, and neurofibromatosis 1 (NF1) in neurofibromatosis (Nishi and Saya 1991; Classon and Harlow 2002; de la Chapelle 2004; Garraway and Sellers 2006). In the case of lineage-specific tumor suppressor inactivation, different cell lineages may preferentially acquire genetic mutations in these loci and/or the tumor suppressor gene may have a critical dominant negative role within a master regulator pathway as outlined earlier.

Expanding evidence demonstrates that normal lineage development may profoundly influence carcinogenesis and metastasis (Gupta, Kuperwasser et al. 2005; Winslow, Dayton et al. 2011; Xiang, Liao et al. 2011). The lineage dependency model places emphasis on the continuum between normal processes and tumor development, and describes a functional aspect for commonly found lineage-restricted somatic mutations (Garraway and Sellers 2006). Additionally, therapies developed from lineage dependency studies have already proven fruitful: vemurafenib, which targets mutant BRAF V600E has been approved for the treatment of late stage melanoma (Chapman, Hauschild et al. 2011), while the aforementioned ATRA treatment

for APL is now commonplace (Tallman, Andersen et al. 1997). Future studies will invariably lead to other dramatic therapeutic interventions for lineage-dependent human cancers.

1.2 Achaete-Scute Homolog 1 Pathway in Lung Development and Lung Cancer

Achaete-scute homolog 1 (ASCL1, MASH1) is a basic helix-loop-helix (bHLH) transcription factor responsible for the differentiation of several neural and neuroendocrine (NE) tissues in mammals, including specific cells within the central nervous system, autonomic nervous system, adrenal medulla, thyroid, lung, prostate, and others (Guillemot, Lo et al. 1993; Hirsch, Tiveron et al. 1998; Casarosa, Fode et al. 1999; Torii, Matsuzaki et al. 1999; Ito, Udaka et al. 2000; Huber, Bruhl et al. 2002; Kameda, Nishimaki et al. 2007). bHLH transcription factors are an evolutionarily ancient family of proteins that contain a dimerization domain and a DNA binding domain, and are utilized throughout eukaryotes (Skinner, Rawls et al. 2010). Class II bHLH proteins direct transcription in a tissue-restricted fashion by binding E-box sites with the canonical CANNTG sequence (Kewley, Whitelaw et al. 2004) and heterodimerize with the widely expressed E proteins E12, E47, E2-2, and HEB. Following dimerization and DNA binding, bHLH proteins recruit the histone acetylators p300 and pCAF, resulting in transcriptional activation (Puri, Sartorelli et al. 1997). Transcriptional inhibition of bHLH proteins is achieved by Id proteins, which compete for and sequester the E proteins (Perk, Iavarone et al. 2005). A number of signaling pathways are implicated in bHLH regulation; a major regulator of bHLH expression is the Notch pathway (Ball 2004). Targets of Notch signaling are HES1 and HES5, which are potent transcriptional repressors at N-box DNA

sequences (Iso, Sartorelli et al. 2001). Known targets of HES1 include Ascl1 in the nervous system and in the lung (Sriuranpong, Borges et al. 2002). ASCL1 in vertebrates are homologs of achaete-scute (A-SC) genes first discovered to regulate neurogenesis and bristle development in *Dropsophila* (Garcia-Bellido and de Celis 2009).

The large bristles of files, known as machrochaetes, are sensory organs that form at precise locations on the thorax and head. The first mutant *Dropsophila* that lacked bristles, termed *scute*, was discovered in 1916 – subsequent genetic analyses revealed that different A-SC alleles removed different subset of bristles (Campuzano, Carramolino et al. 1985). These genes became known as *achaete, scute, lethal of scute,* and *asense*, each residing within a 100kb chromosomal segment. Deletion of *achaete* demonstrated a loss of sense organs along with the loss of central neurons, demonstrating the gene's requirement during neural development (Jimenez and Campos-Ortega 1979; Campos-Ortega and Knust 1990). Spatial distribution of A-SC transcripts in the embryo accumulate in regions where neuroblasts will later segregate from the epidermis, confirming that A-SC is involved in the initial decision to form neural cells (Simpson 1990).

Mammalian ASCL1 was reported in 1990 from analysis performed in a sympathoadrenal progenitor cell line (MAH) by using degenerate oligonucleotide primers and the polymerase chain reaction (Johnson, Birren et al. 1990). Primers were based solely on the amino acid sequence of the proteins encoded by genes of the A-SC *Drosophila* complex, yielding two clones with closely related but distinct sequences. The two clones were termed MASH-1 and MASH-2 (mammalian achaete-scute homologues). Importantly, the sequence identity of MASH-1/2 was

closer to that of the A-SC genes than to other mammalian members of the bHLH family. This parallel conservation of lineage-specificity and sequence may indicate invariant amino-acid residues required for the determination of particular cell types. Mammalian and *Drosophila* A-SC genes share a pattern of conserved residues in the basic region along with a three-residue gap not found in other members of the bHLH gene family. Expression of MASH-1 is significantly higher than MASH-2 in most tissues tested, and was first detected in PC12 cells (derived from the same sympathoadrenal lineage as MAH cells) and in a medullary thyroid carcinoma cell line, but not in schwannoma or melanoma cell lines, demonstrating that non-neuronal/neuroendocrine neural crest derivatives do not express MASH-1 (Johnson, Birren et al. 1990). Small amounts of MASH-1 transcript were detected in the developing rat lung, corresponding to pulmonary neuroendocrine cells, and also in the developing adrenal gland, which contains a subpopulation of sympathoadrenal progenitor cells. Human MASH1 (termed ASCL1) resides on chromosome 12q23.2, and encodes a protein spanning 236 amino acids.

Besides the aforementioned regulation by HES1, regulation of ASCL1 expression has also been associated with the RAS/RAF/MEK/ERK pathway as well as the sonic hedgehog (SHH) pathway. Treatment of a neuroblastoma-derived cell line expressing high amounts of ASCL1 with phorbol 12-myristate 13-acetate (PMA) induced rapid degradation of ASCL1 mRNA and protein (Benko, Winkelmann et al. 2011). PMA is a diacylglycerol mimic and is known for its ability to activate the RAS/RAF/MEK/ERK pathway by binding to and activating protein kinase C (PKC) (Tahara, Kadara et al. 2009). Reporter gene constructs were utilized to demonstrate that the decreased expression of ASCL1 occurred at the transcript level initially, and

at the promoter level subsequently, leading to a rapid and long-lasting inhibition of expression (Benko, Winkelmann et al. 2011). The paradoxical activation of a pro-tumorigenic growth pathway inhibiting ASCL1 expression is surprising but not novel in the subset of neuroendocrine lung cells. A mouse model utilizing inducible h-Ras under the control of a pulmonary neuroendocrine cell-specific cGRP promoter resulted in primarily non-NE bronchial adenocarcinomas (Sunday, Haley et al. 1999). This unexpected result demonstrates that activation of the RAS/RAF/MEK/ERK pathway is likely leading to inhibition of neuroendocrine differentiation in the lung and that this effect is potentially mediated by reduction of ASCL1 expression.

The SHH pathway is important for stem cell maintenance in different tissue types. During neurogenesis *in vivo*, the SHH effector GLI transcription factors are activated and critical for proper development (Brewster, Lee et al. 1998). Overexpression of GLI2 in an embryonal carcinoma cell line resulted in neuronal differentiation and the upregulation of several neural-specific bHLH proteins such as NeuroD, Neurog1, and ASCL1 (Voronova, Fischer et al. 2011). Chromatin immunoprecipitation (ChIP) assays revealed that GLI2 bound directly to multiple regulatory regions in the ASCL1 promoter and enhancer sites. A dominant-negative GLI2 resulted in a reduction of neurogenesis and a significant downregulation of ASCL1 expression. Much research is still required to determine other direct activators or repressors of ASCL1 expression. It is likely that different tissues will utilize varied tissue-specific effectors to control ASCL1.

1.2.1 ASCL1 in Lung Development

ASCL1 first becomes detectable in the developing mouse lung around E13.5 in neuroepithelial bodies (NEBs), which are clusters of NE cells found near branch points of large and medium-sized airways (Borges, Linnoila et al. 1997). NE cells are the first defined epithelial cell type found in the lung during development (Linnoila 2006). ASCL1 expression coincides with NE markers cGRP and synaptophysin, and ASCL1 expression peaks shortly after birth and declines in adulthood, mirroring the presence of NE cells in the lung (Borges, Linnoila et al. 1997; Ito, Udaka et al. 2000). Mice with no functional ASCL1 die shortly after birth due to hypoventilation, though this effect is potentially attributed to brain stem or autonomic nervous system abnormalities rather than lung-specific deficiencies, as the lung is morphologically normal in ASCL1-null mice, with the exception of a lack of NE cells (Guillemot, Lo et al. 1993; Dauger, Guimiot et al. 2001). Overall lung morphology is retained along with the appearance of Clara cells and type II pneumocytes. Knockout mice clearly lack pulmonary neuroendocrine cells (PNECs), important for oxygen sensing and ventilation-perfusion matching, suggesting that ASCL1 is a required lineage transcription factor for their development (Borges, Linnoila et al. 1997).

The importance of ASCL1 in lung development is highlighted by findings that HES1 knockout mice contain dramatically elevated ASCL1 expression, and PNECs are approximately 10 times more abundant (Ito, Udaka et al. 2000). HES1 deficient mice show disordered endocrine and non-endocrine epithelial lineages, emphasized by a dramatic reduction of Clara cells and a 20% reduction in overall lung size. HES1 is a major effector of the Notch pathway,

and activation of the Notch pathway is sufficient to reduce ASCL1 expression (Sriuranpong, Borges et al. 2002). ASCL1 also participates in this signaling loop by directly activating the expression of the Notch ligands Delta1 (DLL1) and Delta3 (DLL3), which signal through adjacent cells to activate the Notch pathway and inhibit neuroendocrine differentiation in those cells (Castro, Skowronska-Krawczyk et al. 2006; Henke, Meredith et al. 2009; Castro, Martynoga et al. 2011) (Figure 1.1). Interestingly, DLL1 is believed to sequester Notch proteins inside the Golgi apparatus of neuronal precursors (Jacobsen, Brennan et al. 1998; Sakamoto, Ohara et al. 2002). Transgenic loss of ASCL1 (Post, Ternet et al. 2000) coincides with a total loss of DLL1 in the lung, while other Notch ligands such as Jagged1 or 2 lack this characteristic pattern (Post, Ternet et al. 2000). Activation of Notch signaling in adjacent cells is an example of lateral inhibition and is highly reminiscent of *Drosophila* neurogenesis, where such mechanisms are required for generating sequential waves of neuronal precursors (Chen, Thiagalingam et al. 1997).

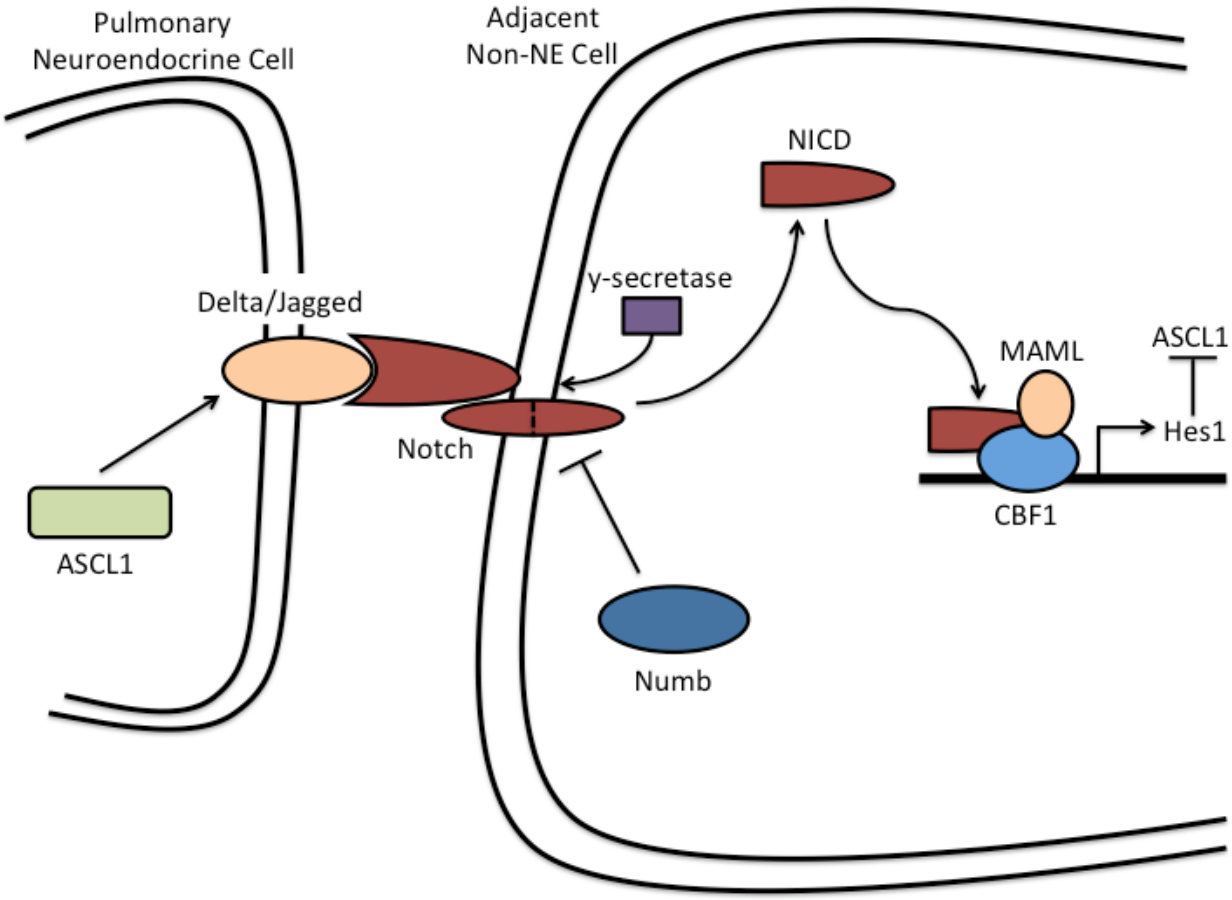

Figure 1.1: The Notch pathway regulates neuroendocrine differentiation in the lung. ASCL1 expression is regulated by the Notch pathway via lateral inhibition mechanisms. Notch receptor activation via DLL1 or DLL3 signals to a cell to repress ASCL1 expression and inhibit neuroendocrine differentiation.

1.2.2 Introduction to Neuroendocrine Lung Cancers

The leading cause of cancer mortality for both men and women in the United States is lung cancer with an estimated 160,000 Americans dying each year from the disease and approximately 200,000 new cases diagnosed each year (Jemal, Siegel et al. 2007). Small cell lung cancer (SCLC) is a neuroendocrine tumor tightly associated with cigarette smoking and accounts for 10-20% of all lung cancer cases (Rodriguez and Lilenbaum 2010). The proportion of lung cancers diagnosed as SCLC has decreased steadily, from 17% in 1986 to 13% in 2002, possibly reflecting a decrease in the number of smokers and improvements in cigarette filters (Rodriguez and Lilenbaum 2010). Interestingly, the number of women diagnosed with SCLC has increased from 28% to 50% of all SCLC cases between 1972 and 2002 likely mirroring the rise of female smokers (Rodriguez and Lilenbaum 2010).

Distinctive features of SCLC include expression of neuroendocrine genes such as chromogranin A and B, the amine synthetic enzyme L-dopa decarboxylase, and synaptophysin (D'Angelo and Pietanza 2010). Additionally, SCLC is marked by a lack of dysplastic or metaplastic precursor lesions, early and widespread metastasis, initial responsiveness to chemo and radiotherapy followed by rapid chemoresistance (Rodriguez and Lilenbaum 2010). Another characteristic feature of SCLC is the ectopic expression of hormones such as ACTH, calcitonin, cGRP, GRP, and vasopressin, which lead to associated paraneoplastic syndromes (Bondy 1981). SCLC is a more aggressive cancer than non-small cell lung cancer (NSCLC), with late-stage patients having a median survival of several months and only 5% of patients surviving past their second year of diagnosis (Garcia-Yuste, Matilla et al. 2008). Current treatment modalities for

SCLC have changed little in the past three decades and the gold-standard therapy remains a combination of carboplatin and etoposide given concurrently with radiotherapy, including prophylactic cranial irradiation for patients presenting with limited or extensive disease (Rodriguez and Lilenbaum 2010). Patients initially show tremendous response to this combined treatment, however remission is brief and relapse occurs in nearly every single patient, resulting in a very aggressive and chemo-resistant cancer (D'Angelo and Pietanza 2010). The lack of second-line therapy for SCLC makes this an overwhelmingly lethal disease. The only FDA-approved second-line therapy is Topotecan and the response in patients with refractory disease is less than 10%. Survival is 3-4 months (Garst 2007). Trials of targeted therapies including angiokinase inhibitors and tyrosine kinase inhibitors have been a major focus of SCLC patient trials over the last decade. However, unlike NSCLC, these therapies have not resulted in any clinical benefit for SCLC. Clinical trials in late-stage, therapy-resistant SCLC have been a dismal failure necessitating the need to study this aggressive tumor in the laboratory in order to achieve sustained clinical response.

Other than SCLC, neuroendocrine differentiation in NSCLC may appear in up to 20% of NSCLC tumors, predominantly as typical or atypical carcinoids, as well as adenocarcinomas and large cell cancers (Righi, Volante et al. 2007). Carcinoids represent 1-2% of all lung cancer cases. Typical carcinoids (TC), contrary to other neuroendocrine lung cancers, are not related to smoking (Garcia-Yuste, Matilla et al. 2008). TCs are well-differentiated, slow-growing tumors with a near 100% 5-year survival and represent the least aggressive pulmonary neuroendocrine cancer. Atypical carcinoids (AC) are rarer than TC, more often associated with smoking, and

have predominance for diagnosis in males. Diagnosis between TC and AC is made on the basis of detectable necrosis and higher mitotic count in ACs. The 5-year survival for AC is about 70% and represents an intermediate-grade neuroendocrine tumor (Skov, Krasnik et al. 2008). For both TC and AC patients, surgery is the established treatment at an early stage (Garcia-Yuste, Matilla et al. 2008; Skov, Krasnik et al. 2008).

Large cell neuroendocrine carcinoma (LCNEC) was recognized as a separate cancer entity in 1991 based on the observation that a group of highly aggressive NE lung carcinomas exists apart from SCLC (Gollard, Jhatakia et al. 2010). LCNEC comprises up to 3% of lung cancers, with male predominance, and virtually all patients are cigarette smokers (Gollard, Jhatakia et al. 2010). Survival for LCNEC is very similar to that of SCLC – a study of 318 patients from 10 Japanese institutions demonstrated a 5-year survival rate of 40.3% for LCNEC compared to 35.7% for SCLC when all tumor stages were considered (Asamura, Kameya et al. 2006). Stage-for-stage, no difference was noted between LCNEC and SCLC and their survival curves overlapped. A separate study performed in Spain demonstrated a 5-year survival rate of 21% for LCNEC and 14% for SCLC (Garcia-Yuste, Matilla et al. 2000). LCNEC has been understudied and to this day, no standard has been determined for treatments. Efforts to determine if LCNEC patients would benefit from a SCLC regimen including cotreatment with etoposide and cisplatin with prophylactic radiotherapy have demonstrated some efficacy, but studies are generally too small to ascertain any profound clinical impact (Sun, Ahn et al. 2012).

Besides formally recognized carcinoid and LCNEC tumors, NSCLCs with neuroendocrine features are also known to appear in lung adenocarcinomas, where they are most

frequent, but also in squamous cell carcinomas, and large cell (non-neuroendocrine) cancers (Berendsen, de Leij et al. 1989; Chejfec, Cosnow et al. 1990; Schleusener, Tazelaar et al. 1996; Abbona, Papotti et al. 1998). Together, these tumors appear in about 10-15% of NSCLC patients. IHC analysis for NE markers such as chromogranin A (CHGA) may be positive in up to 25% of the cancer cells in these cases (Abbona, Papotti et al. 1998). A recent study suggests that NE differentiation in NSCLC as measured by IHC is of no prognostic or clinical benefit, although this is in contention with prior studies, which found that NE differentiation confers a worse prognosis in stage I NSCLC (Schleusener, Tazelaar et al. 1996; Ionescu, Treaba et al. 2007). Little is known about the significance of NE differentiation in NSCLC and controversial data exist in the literature about the different behavior and response to therapy for NE-NSCLC and conventional NSCLC (Pelosi, Pasini et al. 2003; Howe, Chapman et al. 2005). To complicate matters, NSCLCs that do not stain positive for any NE markers may express the full array of NE genes as measured by a variety of methods, including qRT-PCR, northern blot, and whole-genome cDNA microarray (Jensen, Gazdar et al. 1990; Abbona, Papotti et al. 1998; Bhattacharjee, Richards et al. 2001; Jones, Virtanen et al. 2004; Howe, Chapman et al. 2005).

Prior studies have shown that neuroendocrine gene expression in NSCLC confers a poor prognosis in about 10% of patients with otherwise pathologically unremarkable adenocarcinoma, occurring even in tumors that do not express neuroendocrine markers by immunohistochemistry (IHC) (Bhattacharjee, Richards et al. 2001). Currently, no pre-clinical models including cell lines and/or xenografts for NSCLC with neuroendocrine features (NE-NSCLC) exist. Clinically there is little evidence available regarding adequate treatment options for patients that present with

NE-NSCLC dictating the need for additional study of this tumor subtype. Recent research suggests that NE-NSCLC patients may benefit from a SCLC-like treatment, including co-administration of carboplatin and etoposide, however these studies lack the statistical power to clearly demonstrate a therapeutic advantage (Sun, Ahn et al. 2012). A summary of neuroendocrine lung cancers is presented in Table 1.2.

Type	Cell Size	Cytoplasm	Five Year Survival	Prevalence	Treatment
Small Cell	Small	Scant	< 10%	~15%	Carboplatin/etoposide, radiotherapy
Large Cell Neuroendocrine	Large	Abundant	25%	~3%	Chemotherapy
Atypical Carcinoid	Large	Abundant	70%	< 1%	Surgery
Typical Carcinoid	Large	Abundant	100%	< 1%	Surgery
Non-small cell with neuroendocrine features	Large	Abundant	Undetermined	~10%	Undetermined

Table 1.2: Overview of pulmonary neuroendocrine tumors. An overview of the known neuroendocrine cancers in the lung is presented, including survival rates, prevalence among all lung cancers, and treatment options.

1.2.3 Molecular Studies of Neuroendocrine Lung Cancers

SCLC has a unique natural history with a shorter doubling time, higher growth fraction, early development of widespread metastases, and uniform initial response to chemo and radiotherapy followed by nearly unilateral chemoresistance (Gazdar 1992). The molecular and cellular abnormalities of SCLC as well as NE-NSCLC are unique and provide a basis of knowledge from which to determine novel therapeutic targets.

The majority of SCLCs contain multiple chromosomal aberrations including amplifications and deletions. Recurrent genetic loss occurs at 3p, 5p, 13q, and 17q, with the latter containing the TP53 tumor suppressor gene (D'Angelo and Pietanza 2010). Comparative genomic hybridization analyses (CGH) revealed that SCLCs contain amplifications in regions including 1p, 2p, 3q, 5p, 8q, and 19p (Balsara and Testa 2002). Allelic loss of chromosome 3p occurs in greater than 90% of SCLCs, with distinct areas including 3p12, 3p14, 3p21.3. and 3p24 (Sato, Shames et al. 2007). Known tumor suppressor genes are contained in these genomic locations including RASSF1A, FUS1, SEMA3B, and SEMA3F at 3p21 (Burbee, Forgacs et al. 2001; Tomizawa, Sekido et al. 2001; Ji and Roth 2008). RASSF1A is involved in cell cycle regulation, apoptosis, and microtubule stability and is deleted in nearly 90% of SCLC, while FUS1 is lost in 100% of SCLC and is involved in inducing G1 arrest and apoptosis (Burbee, Forgacs et al. 2001; Ji and Roth 2008). 3p12, 3p14, and 3p24 also contain tumor suppressor genes commonly lost during SCLC pathogenesis (Sattler and Salgia 2003).

The protein product of the TP53 tumor suppressor gene located on chromosome 17q is a negative regulator of proliferation in the cell by inducing cell cycle arrest and apoptosis. p53 acts

on downstream genes such as p21 (cell cycle), GADD45 (DNA repair), and BAX (apoptosis) (Wistuba, Gazdar et al. 2001). TP53 plays an important role in SCLC pathogenesis due to the fact that it is inactivated in approximately 90% of tumors (Sato, Shames et al. 2007). Importantly, most TP53 mutations are GC-TA transversions, which have been demonstrated to be caused by the carcinogen benzo(A) pyrene in cigarette smoke (Sattler and Salgia 2003). TP53 mutations occur in tandem with mutations in the Retinoblastoma1 (RB1) gene in up to 90% of SCLC cases (Harbour, Lai et al. 1988; Shimizu, Coxon et al. 1994; Modi, Kubo et al. 2000). Together with retinoblastoma, SCLC is the only tumor to harbor RB1 mutations in nearly every case (Sherr and McCormick 2002). RB1 is required for a proper transition from the G1 to the S phase of the cell cycle by controlling the E2F family of transcription factors (Sekido, Fong et al. 2003) and is also involved in regulating apoptosis pathways (Rodina, Vilenchik et al. 2007).

To study the role of p53 and RB1 in lung tumorigenesis, Berns and colleagues developed a conditional knockout mouse harboring loss of both alleles of TP53 and RB1 specifically in the lung epithelium. Somatic inactivation of both tumor suppressors resulted in the development of tumors with histology and immunophenotype closely resembling human SCLC, including the formation of early and widespread distal metastases (Meuwissen, Linn et al. 2003). Retention of one RB1 allele, even in the context of $TP53^{-/-}$, results in repression of neuroendocrine tumor formation, underscoring the need for cell cycle deregulation within the lung epithelium in order to form robust tumors. This is in agreement with prior research in neural and neuroendocrine tumors demonstrating frequent mutation events in the RB1 gene, including tumors such as medulloblastomas, pituitary tumors, and retinoblastomas (Marino, Vooijs et al. 2000; Wechsler-

Reya and Scott 2001; Classon and Harlow 2002). In addition to expressing neuroendocrine markers such as cGRP and SYP, lung tumors resulting from $TP53^{-/-}$ and $RB1^{-/-}$ mice also express high levels of ASCL1, mimicking the clinical features of human SCLC. Normal NEBs in $TP53^{-/-}$ and $RB1^{-/-}$ mice stained intensely for cGRP and SYP, while demonstrating a diminished expression of ASCL1 compared to tumor and hyperplasias, which stained more intensely for ASCL1 (Meuwissen, Linn et al. 2003). The expression pattern of ASCL1 in early NE hyperplasia and in primary human NE lung tumor samples suggests that mouse $TP53^{-/-}$ and $RB1^{-/-}$ NE tumors formed from progenitors of pulmonary NE cells. Although not all RB1-dependent neural/neuroendocrine tumors express ASCL1, there is evidence showing that RB1 may be involved in modulating the expression of HES1, a direct transcriptional repressor of ASCL1 (Lasorella, Noseda et al. 2000; Toma, El-Bizri et al. 2000; Jogi, Persson et al. 2002). The argument for a lineage-specific necessity for TP53 and RB1 loss in pulmonary NE cells is demonstrated by the fact that in cGRP-driven HRAS mice, expression of HRAS in PNECs leads only to bronchial adenocarcinomas. This suggests a repression of neuronal differentiation in the original PNEC lineage by an active RAS pathway (Sunday, Haley et al. 1999).

Recent research utilizing the $TP53^{-/-}RB1^{-/-}$ mouse model demonstrates the essentiality of sonic hedgehog (SHH) signaling in the tumorigenesis of SCLC. Constitutive activation of the Hedgehog signaling molecule Smoothened was sufficient to promote clonogenicity of human SCLC *in vitro* and the progression of mouse SCLC *in vivo (Park, Martelotto et al. 2011)*. The reciprocal experiment, deleting SMO in RB1/TP53 mutant lung epithelial cells, resulted in a strong suppression of SCLC initiation and progression in mice. Blockade of Hedgehog signaling

with pharmacological agents inhibited the growth of mouse and human SCLC, particularly following chemotherapy. This research demonstrates the activity of a stem cell-associated pathway, SHH, and its role in progressing and maintaining a largely undifferentiated tumor. Additionally, this work suggests a potential therapeutic benefit to targeting SCLC with SHH inhibitors, particularly following chemotherapy, which currently represents a population of patients with no treatment options beyond palliative care or early-stage clinical trials.

1.2.4 The Role of ASCL1 in Pulmonary Neuroendocrine Tumors

The expression and function of ASCL1 in human tumors is of critical importance. Initially, ASCL1 transcript expression was detected in pulmonary carcinoids and SCLCs, among other neuroendocrine tumors such as pheochromocytomas, MTC, olfactory neuroblastomas, and thymic carcinoids (Ball, Azzoli et al. 1993). ASCL1 expression in cancer is frequently associated with the expression of neuroendocrine markers such as chromogranins, synaptophysin, and dopa decarboxylase indicating the association between ASCL1 expression and the neuroendocrine phenotype (Song, Yao et al. 2012). Despite the high expression of ASCL1 in SCLC, there exist no reported genomic amplifications of the 12q23.2 region where the ASCL1 gene resides. Data gathered by the Minna lab along with collaborators corroborates this finding. This is in contrast to other lineage-based carcinogenesis models, such as MITF in melanoma and TITF1 in lung adenocarcinoma, where regions of local amplification are responsible for the overexpression of those genes (Garraway, Widlund et al. 2005; Kwei, Kim et al. 2008). Additionally, no spontaneous somatic mutations have been reported for the ASCL1 gene.

The importance of ASCL1 in neuroendocrine tumors was highlighted by experimental findings demonstrating that antisense oligonucleotides targeting ASCL1 were sufficient to reduce viability of SCLC compared to controls. Viral vector-based, RNAi-driven ASCL1 knockdown was first reported by Takahashi, et al. to inhibit colony forming ability of a SCLC cell line (Osada, Tatematsu et al. 2005). Subsequent experiments determined that ASCL1 knockdown was associated with apoptosis induction and that SCLCs depleted of ASCL1 injected into the subcutaneous flank of mice demonstrated delayed tumorigenesis *in vivo*. Experiments such as these were the first to show that ASCL1 mediates survival of SCLCs. The nature of SCLC behavior *in vitro*, namely the propensity to grow as tumor spheres rather than adherent colonies, prohibits the use of lipid-based siRNA transfections in order to study short-term knockdown of essential genes.

ASCL1 is a developmental transcription factor, essential for the differentiation of several neural and neuroendocrine tissues, including pulmonary neuroendocrine cells, underscoring its relationship to stem cell processes. Research by Ball, et al, suggests that ASCL1 mediates part of its tumorigenic effect in SCLC by regulating the cancer stem cell-associated markers CD133 and ALDH1A1 (Jiang, Collins et al. 2009). Cancer stem cells are a subpopulation of cells theorized to exist within the bulk tumor mass that are able to self-renew and divide to replenish the tumor mass (Sullivan and Minna 2010). Both CD133 (PROM1) and ALDH1A1 are markers that select a subpopulation of cancer cells associated with "stemness" in various blood and solid tumors (Jiang, Collins et al. 2009; Sullivan, Spinola et al. 2010). By way of viral-based ASCL1 knockdown, Ball and colleagues showed that ASCL1 regulates the transcription of CD133 and

ALDH1A1 in a SCLC cell line by binding directly to the promoter region of each gene. Further work demonstrated that a subpopulation of highly tumorigenic $ASCL1^{+}/ALDH^{+}/CD133^{+}$ cells exists in a patient-derived xenograft. Knockdown of ASCL1 significantly decreases the percentage of $ALDH^{+}$ and $CD133^{+}$ cells, resulting in significant tumor reduction *in vivo*. These data suggest that ASCL1 may mediate its tumorigenic effect at least partially through the regulation of cancer stem cell-associated mechanisms in SCLC (Jiang, Collins et al. 2009).

The transcriptional network of ASCL1 also includes regulation of microRNAs. microRNAs are short, 22-base pair nucleotides that bind the 3' UTR of mRNA and inhibit gene expression through mRNA degradation or translational repression (He and Hannon 2004). microRNAs are critically involved in the development of nearly every organ and proliferate their effect by fine-tuning the expression of many genes (Dong, Jiang et al. 2010; Ucar, Vafaizadeh et al. 2010). In cancer, microRNAs are generally downregulated, suggesting a major role of microRNAs as tumor suppressors (Iorio and Croce 2012). Indeed, the potential of microRNA replacement therapy has spurred the development of novel delivery methods in order to maximize their therapeutic potential (Wiggins, Ruffino et al. 2010). ASCL1, as a developmental transcription factor, likely regulates microRNAs that fine tune the expression of genes required during differentiation. During tumorigenesis, these microRNAs may be silenced if they act as tumor suppressors or utilized as oncogenes in order to progress cancer. ASCL1 has been shown to regulate miR-375 directly by binding to a proximal promoter in front of the miR-375 genomic locus (Nishikawa, Osada et al. 2011). Takahashi and colleagues demonstrated that ASCL1 directly transactivates miR-375, and that induction of neuroendocrine features by ASCL1 at least

partially requires the presence of miR-375. Finally, it was shown that miR-375 targets the YAP1 transcription factor, and YAP1 overexpression in ASCL1+ lung cancer lines was growth inhibitory. These experiments demonstrate that the ASCL1 signaling network mediates part of its effect by regulating the expression of microRNAs, which in turn regulate the expression of key downstream genes. Potential therapeutic applications may be based on targeting the ASCL1-associated microRNAs in neuroendocrine lung cancers.

Besides the high expression in SCLC, ASCL1 expression in NSCLC clinical samples has been noted for some time, although a pre-clinical model for these tumors has yet to be discovered. In 1989, Berendson and colleagues set out to analyze NSCLC tumor samples for neuroendocrine differentiation by immunohistochemical staining (IHC). They discovered that some NSCLCs (up to 30%), particularly adenocarcinomas, displayed prominent neuroendocrine features (Berendsen, de Leij et al. 1989). A cDNA genome-wide microarray analysis performed by the Meyerson lab on 139 pathologically unremarkable lung adenocarcinomas demonstrated a subclass of NSCLC that expressed neuroendocrine genes, including ASCL1 (Bhattacharjee, Richards et al. 2001). This subtype accounted for 9% of adenocarcinomas in the study and was associated with a significantly reduced overall survival. An IHC and RNA-RNA *in situ* hybridization analysis of lung cancer cell lines, including SCLC and NSCLC demonstrated ASCL1 expression in 6/6 SCLCs, 5/5 carcinoids, 6/7 NSCLCs with NE features, and 3/14 other NSCLCs. In primary tissue samples, ASCL1 was detected in 2/2 SCLCs, 5/5 pulmonary carcinoids, and 10/41 NSCLCs only four of which demonstrated overt neuroendocrine features (Miki, Ball et al. 2012). Analyses such as these demonstrate the existence of a prominent subtype

of NSCLC with neuroendocrine features (NE-NSCLC) demonstrating the need for a defined pre-clinical model to study these tumors.

Attempts to introduce ASCL1 into NSCLC cell lines without native ASCL1 expression have resulted in the formation of lines with partial neuroendocrine transformation. Takahashi, et al, infected NSCLC A549 and NCI-H460 cells with a vector carrying ASCL1 and noted the significant induction of neuroendocrine markers such as chromogranin and synaptophysin. Similarly, transfection of miR-375 into A549 and NCI-H460 resulted in a partial neuroendocrine transformation (Osada, Tatematsu et al. 2005; Osada, Tomida et al. 2008; Nishikawa, Osada et al. 2011). A key experiment demonstrating the lineage-specificity of ASCL1 was performed involving normal immortalized bronchial epithelial cells (BEAS-2B) infected with ASCL1. Lung epithelial cells carrying the ASCL1 vector demonstrated little transformative capacity and no induction of neuroendocrine markers such as chromogranin A, gastrin-releasing peptide, or calcitonin (Jensen-Taubman, Wang et al. 2010). This suggests that in normal non-NE cells, ASCL1 is not sufficient to transform cells to a neuroendocrine phenotype. However, as this effect is quite readily apparent in cancer cells, it is likely that genetic abnormalities present in tumors allow for ASCL1 to carry out its transcriptional profile. Similarly, ASCL1 likely requires a specific genetic and epigenetic background to function properly as a neuroendocrine-specific transcription factor. Since lung epithelial cells are non-NE, they do not carry the necessary background to maintain ASCL1 function.

Several studies have overexpressed ASCL1 in the lung in order to study its effect on tumor formation. In particular, Linnoila and colleagues performed the overexpression in non-

endocrine cells in order to determine ASCL1's ability to transform lung tissue into cancer. Constitutive ASCL1 expression under the CC10 promoter ensures that ASCL1 was only expressed in Clara cells, which may act as a stem cell-like pool to replenish lung epithelial cells following injury (Linnoila, Sahu et al. 2000). Beginning three weeks after birth, CC10-ASCL1 mice began to demonstrate airway hyperplasia located at the bronchioalveolar junction. After eight weeks, extensive hyperplasia and metaplasia can be detected however the mice never develop tumors nor do the hyperplastic and metaplastic lesions demonstrate overt neuroendocrine features. SV40 large T antigen, known for its ability to sequester p53 and Rb, was utilized in order to amplify the hyperplastic effect seen with ASCL1 overexpression alone. It is important to note that p53 and RB1 mutations are seen in nearly all cases of SCLC. The combination of ASCL1 overexpression with SV40 induced the formation of fast-growing adenocarcinomas, which upon further inspection were shown to express neuroendocrine markers (Linnoila, Zhao et al. 2000). This research demonstrates that inhibition of key pathways that are frequently mutated in pulmonary neuroendocrine tumors are required for ASCL1 to exert its tumorigenic effects, likely functioning in a lineage-specific manner to promote cancer growth.

Upstream regulation of ASCL1 expression is an evolving field, however several key experiments point to the MEK/ERK pathway playing an essential role. In a cell line model of MTC, estradiol-inducible RAF1 was sufficient to reduce transcript expression of ASCL1, along with a reduction in neuroendocrine markers such as calcitonin, and displayed marked morphologic changes including cell rounding and cessation of cell growth (Chen, Carson-Walter et al. 1996). Other work demonstrated that induction of RAf1 *in vivo* was sufficient to inhibit

growth of MTC tumor xenografts (Vaccaro, Chen et al. 2006). Pharmacological efforts to reduce ASCL1 expression similarly rely on activating the RAS/RAF/MEK/ERK cascade. Phorbol esters such as phorbol 12-myristate 12-acetate (PMA) are analogous of diacylglycerol and mediate their function in the cell by activating protein kinase C, and proliferating the signal through RAS/RAF/MEK/ERK (Tahara, Kadara et al. 2009). PMA is frequently used to probe the RAS/RAF/MEK/ERK cascade in cell culture experiments. Treatment of ASCL1+ neuroblastoma cells with PMA resulted in the rapid decrease of ASCL1 mRNA expression that is sustained over the course of several days (Benko, Winkelmann et al. 2011). A separate natural compound isolated from the hop plant, xanthohumol (XN), is also a potent activator of the RAS/RAF/MEK/ERK cascade. Treatment of MTC cells with XN reduces ASCL1 expression and inhibits growth by inducing apoptosis (Cook, Luo et al. 2010). Interestingly, a mouse model utilizing inducible H-RAS under the pulmonary neuroendocrine cell-specific cGRP promoter showed only the formation of bronchial adenocarcinomas with a loss of neuroendocrine features in the induced cells (Sunday, Haley et al. 1999). Taken together this research suggests that activation of the RAS/RAF/MEK/ERK cascade inhibits expression of ASCL1, leading to a loss of neuroendocrine properties, and that pharmacological intervention for ASCL1+ pulmonary tumors including SCLC and NE-NSCLC may be possible by targeting upstream regulators of ASCL1 expression.

Another regulator of ASCL1 expression is the Notch pathway. Notch receptors on the cell surface bind ligands such as delta and jagged, and transmit the signal through the nucleus via cleavage event that releases the Notch-intracellular domain (ICD). The ICD activates expression

of HES1, which directly represses expression of ASCL1 by binding to a proximal repressor element (Sriuranpong, Borges et al. 2002). In pulmonary neuroendocrine cells, as well as in most neuroendocrine cancers, the Notch pathway is inhibited. Overexpression of Notch ICD is sufficient to induce apoptosis in MTC cells, corresponding with a loss of ASCL1 expression (Kunnimalaiyaan, Vaccaro et al. 2006; Jaskula-Sztul, Pisarnturakit et al. 2011). In SCLC, overexpression of active Notch receptors correlated with profound cell cycle arrest and growth inhibition, leading to a similar ASCL1 reduction as seen in the MTC model (Sriuranpong, Borges et al. 2001). The identification of small molecules that can activate the Notch pathway may have therapeutic potential in ASCL1+ cancers, including SCLC (Pinchot, Jaskula-Sztul et al. 2011; Truong, Cook et al. 2011).

Of key importance for the study of lineage-dependence in human cancer is the discovery of the tumor cell of origin. SCLC likely develops from aberrant genetic signaling courtesy of the pulmonary neuroendocrine cell; however the discovery of NSCLC with neuroendocrine features suggests that neuroendocrine tumors may have a variety of cells of origin. To answer this critical question, Sutherland and colleagues inactivated p53 and RB1 in a variety of specialized lung cells and assayed for tumor formation *in vivo* (Sutherland, Proost et al. 2011). p53 and RB1 inactivated under the CMV promoter induced NE tumors in 40/47 mice tested, while 25/30 mice formed tumors under the cGRP PNEC-specific promoter. Surprisingly, 15/33 mice formed NE tumors from the SPC alveolar type 2 cell-specific promoter. Prior research demonstrates that a small percentage of type 2 cells express ASCL1 suggesting that these cells, while classically associated with the formation of NSCLC, also have the ability to transform into tumors with

neuroendocrine features (Li and Linnoila 2012). The formation of NE tumors from cGRP-driven p53/RB1 inactivation is in contrast to the cGRP-driven inducible H-Ras mouse model that develops bronchial adenocarcinomas (Sunday, Haley et al. 1999). The two different tumors arising from the same cell of origin demonstrates that different genetic lesions can drive divergent differentiation paths. Similarly, expressing constitutively active mutant KRAS in SCLC completely changes the phenotype of those cells, turning the SCLC into a mesenchymal NSCLC tumor (Falco, Baylin et al. 1990; Calbo, van Montfort et al. 2011). Such changes between SCLC and NSCLC have been previously noted in the clinic (Brereton, Mathews et al. 1978; Abeloff, Eggleston et al. 1979), while differentiation in the opposite direction, from NSCLC to SCLC, has been noted in patients treated with EGFR inhibitors (Sequist, Waltman et al. 2011). Whether NE-NSCLC is a subtype of lung cancer that exists along a continuum of differentiation between SCLC and NSCLC remains to be proven. The discovery of NE-NSCLC tumors in the clinic and the lack of specific treatment options for those patients necessitates the establishment of pre-clinical models that will encompass this important subtype.

1.3 Hypothesis and Specific Aims

The importance of ASCL1 in development and neuroendocrine tumors, including SCLC, has been demonstrated in several seminal reports. However, the discovery of prominent ASCL1 expression in NSCLC, a classic non-NE tumor, is surprising and merits further study. The hypothesis for this work is that ASCL1 acts a lineage-dependent oncogene in NSCLC with neuroendocrine features. Besides expression of ASCL1 itself, the downstream targets of ASCL1

will provide a molecular signature that will provide prognostic and diagnostic information. Finally, therapy targeted at ASCL1-dependent tumors can be achieved by attacking either upstream regulators of ASCL1 expression and/or the downstream genes ASCL1 regulates. To explore this hypothesis, three specific aims were developed:

1.3.1 Specific Aim One

To determine ASCL1 dependency in NE-NSCLC cell lines using si/shRNA knockdown approaches.

1.3.2 Specific Aim Two

To discover ASCL1 downstream targets and their functional and clinical relevance, including prognostic and diagnostic significance.

- **A.** Utilize chromatin immunoprecipitation followed by massively parallel sequencing (ChIP-Seq) performed on ASCL1-positive cell lines to determine the ASCL1 transcriptome.
- **B.** Determine if the ASCL1 transcriptome provides prognostic and/or diagnostic information in databases of resected lung cancer patient samples.
- **C.** Evaluate druggable targets downstream targets of ASCL1 for therapeutic potential in NE-NSCLC cell lines.

1.3.3 Specific Aim Three

To develop therapeutic targeting of the ASCL1 pathway in ASCL1-dependent lung cancers.

A. Show that upstream inhibition of ASCL1 regulators can induce potent cell death in ASCL1-dependent lung cancer cell lines.

B. Demonstrate that combining inhibition of upstream ASCL1 regulators with downstream ASCL1 targets is a viable route to therapy for ASCL1-driven lung cancers

CHAPTER TWO

MATERIALS AND METHODS

2.1 Materials

2.1.1 Lung Cell Lines

All human lung cancer cell lines used in this study were established by the John D. Minna and Adi F. Gazdar laboratories, and maintained in RPMI-1640 (Life Technologies, Inc.) supplemented with 5% or 10% fetal bovine serum, empirically determined per cell line, and grown in a humidified atmosphere with 5% CO_2 at 37°C (Phelps, Johnson et al. 1996). Lung cancer cell lines established at the National Cancer Institute (NCI) are denoted with the prefix H and lung cancer cell lines established at the University Of Texas Southwestern Medical Center Hamon Center for Therapeutic Oncology Research are annotated as HCC (Gazdar, Girard et al. 2010). Human bronchial epithelial cells (HBECs) immortalized with ectopic overexpression of CDK4 and hTERT were previously established in the Minna lab and cultured in KSFM (Gibco) supplemented with bovine pituitary extract and recombinant human epithelial growth factor (Ramirez, Sheridan et al. 2004). All cell lines have been DNA fingerprinted for provenance using the PowerPlex 1.2 kit (Promega) and confirmed to be the same as the DNA fingerprint

maintained either by the American Type Culture Collection (ATCC) or the Minna and Gazdar labs. The lines were also tested to be free of mycoplasma by e-Myco kit (Boca Scientific).

2.1.2 NSCLC Tissue Micro Array

Archived, formalin-fixed, paraffin-embedded tissues from surgically resected lung cancer specimens (lobectomies and pneumonectomies) containing tumor and adjacent normal epithelium tissues were obtained from the Lung Cancer Specialized Program of Research Excellence (SPORE) Tissue Bank at The University of Texas M. D. Anderson Cancer Center (Houston, TX), which has been approved by an institutional review board. The tissue specimens were histologically examined and classified using the 2004 World Health Organization classification system and 282 NSCLC samples (177 adenocarcinomas and 105 squamous cell carcinomas) were selected for our tissue microarray (TMA). TMAs were constructed using triplicate 1-mm diameter cores per tumor; each core included central, intermediate, and peripheral tumor tissue. Detailed clinical and pathologic information, including patient demographics, smoking history, smoking status, clinical and pathologic TNM stage, overall survival duration, and mutation status of KRAS and EGFR, was available for most cases.

2.2 Methods

2.2.1 Molecular Expression Analysis

Microarray Expression Analysis

Transcript data for the 207 lung cell lines, including SCLC, NSCLC, and HBEC/HSAEC lines, were profiled for genome wide mRNA expression using the Illumina WCG-V3 BeadChips array platform. Tumor cell RNA was isolated using the Qiagen RNeasy kit and total RNA quality was confirmed by formaldehyde gel and/or capillary electrophoresis on the Experion System (Bio-Rad). Total RNA was labeled, amplified, and re-analyzed for quality prior to hybridization by the UTSW Simmons Comprehensive Cancer Center Genomics Core.

MATRIX (MicroArray Transformation in Microsoft Excel) software 1.503 is a Microsoft Visual Basic program created by Dr. Luc Girard in the Minna Lab used to import and analyze microarray expression data. Using MATRIX, mRNA transcript expression was normalized across samples by the median value, then normalized expression signals were $\log_2$ transformed and color coded. For comparison between sample classes (such as NE-NSCLC vs. NSCLC cell lines), the ratio of $\log_2$-transformed signals from sample classes were generated and two-sample t-tests were performed using MATRIX to filter out non-significant differences in expression ($p < 0.01$).

Quantitative Real-Time PCR Analysis

Expression of ASCL1 and associated mRNA transcripts by quantitative real-time PCR (qPCR) was performed using TaqMan Assay probes (Applied Biosystems). The reverse transcriptase reaction was performed using the iScript cDNA synthesis kit (Bio-Rad) on RNA isolated using the miRNeasy kit (Qiagen). iTaq Supermix with Rox (Bio-Rad), a premade formula containing iTaq DNA polymerase, optimized buffers, nucleotides and Rox passive

detection dye, was used to perform the qPCR reaction. Reactions were run in triplicate wells on a 96-well plate in a 7300 Real Time PCR System (Applied Biosystems). 7300 System Software (Applied Biosystems) was used to derive Ct values and ΔCt values were calculated using GAPDH or 18s amplification as a control. TaqMan probes utilized in this study are listed in Table 2.1.

Protein Expression Analysis

Protein expression analysis was performed using standard Western blot (immunoblot) techniques. Cells in culture were washed twice in cold PBS, trypsinized, and snap frozen. Protein lysates were prepared using M-PER Mammalian Protein Extraction Reagent (Thermo Scientific) and boiled in protein dye containing B-mercaptoethanol. Cellular proteins were separated using 10% SDS/Polyacrylamide gel electrophoresis and electrotransferred to nitrocellulose membranes (Millipore) for two hours at 285mA. The membrane was blocked using 5% milk for one hour at room temperature, and then incubated overnight with primary antibody at 4°C with gentle shaking. Horseradish peroxidase-conjugated secondary antibody was applied for two hours at room temperature the following day. Protein expression was detected by enhanced chemiluminescence (Thermo Scientific). Primary antibodies are listed in Table 2.2.

Gene	RefSeq Number	TaqMan Assay
ALDH1A1	NM_000689.4	Hs00946916_m1
ASCL1	NM_004316.3	Hs04187546_g1
BCL2	NM_000633.2	Hs00608023_m1
CAV1	NM_001753.4	Hs00971716_m1
DLL1	NM_005618.3	Hs00194509_m1
DLL3	NM_016941.3	Hs01085096_m1
DUSP4	NM_001394.6	Hs01027785_m1
DUSP6	NM_001946.2	Hs04329643_s1
DUSP10	NM_007207.4	Hs00200527_m1
GAPDH	NM_002046.4	Hs02758991_g1
HES1	NM_005524.3	Hs00172878_m1
KIT	NM_000222.2	Hs00174029_m1
NEUROD1	NM_002500.4	Hs01922995_s1
NOTCH1	NM_017617.3	Hs01062014_m1
NR0B2	NM_021969.2	Hs00222677_m1
NRTN	NM_004558.3	Hs00177922_m1
PROM1	NM_006017.2	Hs01009250_m1
RET	NM_020630.4	Hs01120030_m1
TITF1	NM_003317.2	Hs00968940_m1
miR-153		000476
miR-375		000564

Table 2.1: TaqMan probes for qRT-PCR analysis.

Antibody	Company	Product Number
ALDH1A1	ABcam	Ab23375
ASCL1	BD Biosciences	556604
BCL2	Cell Signaling	2872
Cleaved Caspase3	Cell Signaling	9661
Cleaved PARP	Cell Signaling	9541
GAPDH	Imgenex	IMG-5019A-1
HSP-90	Santa Cruz Biotechnology	sc-13119
PARP	Cell Signaling	9542
Phospho ERK	Cell Signaling	9101
RET	Cell Signaling	3223
Total ERK	Cell Signaling	9102

Table 2.2: Primary antibodies used for immunoblot analysis.

2.2.2 Gene Silencing

siRNA-based Short Term Genetic Knockdown

Lung cancer cell lines were optimized for transfection conditions in 6-well and 96-well plates by monitoring lipid content and cell number, and measuring the proliferative differences between scramble oligo control (Qiagen) and toxic control (Qiagen). For 6-well experiments, 3-5 uL RNAiMAX (Invitrogen) was added to 500 uL serum-free RPMI-1640 and incubated at room temperature for 5 minutes. 20 nM siRNA was mixed, plated dropwise in 6-well plates, and complexed for 20 minutes. $200x10^5$ cells were added on top of the mixture, and incubated at 37°C for 72 hours prior to analysis. For 96-well experiments, 0.2-0.4 uL RNAiMAX was added to 10 uL RNAiMAX and incubated for 5 minutes at RT. 20 nM siRNA was added to the lipid mixture and then added to each well. $2x10^3$ cells were added in 90 uL RPMI supplemented with 5% or 10% FBS and incubated at 37°C for 5 days prior to proliferation analysis by MTS. siRNAs utilized in this study were purchased from Qiagen and are indicated in Table 2.3.

shRNA-based Long Term Genetic Knockdown

To silence expression of ASCL1 in lung cancer cells, a pGIPZ lentiviral vector targeted against ASCL1 was purchased from Open Biosystems (Clone ID: V2LHS_15337). Non-targeting shRNA was utilized as control. shASCL1 or shNTC was transformed into competent DH5α *E. coli.* Competent cells were thawed on ice, then incubated with 10 ng of shRNA vector DNA for 30 minutes. After incubation, cells were heat shocked at 42°C for 45 seconds, chilled on ice for 2 minutes, then incubated in 800 uL SOC media at 37°C for one hour with gentle

shaking prior to being streaked on LB agar containing 100 ug/mL ampicillin. Ampicillin-resistant colonies were selected and expanded in culture and plasmid DNA was isolated using a Qiagen HiSpeed Plasmid Midi kit. Restriction enzyme digests of plasmid DNA was performed and resolved by gel electrophoresis to confirm vector fidelity.

Lentivirus was created by transfection of 293T packaging cells with a three-plasmid system. 293T cells grown in RPMI-1640 supplemented with 5% FBS were transiently transfected with shRNA vector, pMD.G-VSVG, and pCMV-ΔR8.91 viral packaging plasmids using Fugene6 (Roche). Viral supernatant was harvested once per day for up to three days, passed through a 0.45 μm filter and stored as 1 mL aliquots at -80°C. The viral supernatant was used for transduction of lung cancer cells with 8 μg/mL polybrene (Sigma-Aldrich). Stable shRNA expressing lung cancer cells were generated after one week in culture with 4 ug/mL puromycin.

RNAi	Company	Product Number
shASCL1-pGIPZ	Thermo Scientific	V2LHS_15337
siASCL1-1	Qiagen	SI00062573
siASCL1-2	Qiagen	SI00062580
siASCL1-3	Qiagen	SI00062587
siBCL2	Qiagen	SI00299397
siCERK	Qiagen	SI00288029
siDUSP6	Qiagen	SI00030324
siERK1	Qiagen	SI00605997
siERK2	Qiagen	SI00300748
siKIT	Qiagen	SI02659531
siMEK1	Qiagen	SI00300699
siMEK2	Qiagen	SI02225090
siNR0B2	Qiagen	SI02757678
siRET	Qiagen	SI02224985

Table 2.3: RNAi-mediated knockdown constructs.

2.2.3 Fluorescence Activated Cell Sorting and Flow Cytometric-Based Assays

Cell Cycle Analysis

DNA content was measured from lung cancer cells following short-term genetic knockdown or treatment with small molecules to determine the cell cycle profile and measure apoptosis. Cells were fixed in 70% EtOH, added slowly during fixation to prevent clumping, for 15 minutes on ice or overnight at -20°C. Cells were incubated in buffered staining solution containing 0.05% Triton X-100, 0.1 mg/mL RNase A, and 50 μg/mL propidium iodide (PI) in PBS for 40 minutes at 37°C. Following incubation, 3 mL fresh PBS was added to quench the reaction, cells were spun at 1000 RPM for 5 minutes at room temperature, and then resuspendend in 0.5 mL PBS and analyzed using a FACScan or FACSCalibur flow cytometer. The Watson algorithm was performed in FlowJo software (Treestar) to determine the distribution and gating of cells in different states of DNA replication.

Annexin V Apoptosis Assay

Lung cancer cell lines transfected with siRNA targeting ASCL1 or control siRNA were profiled for annexin expression as a surrogate marker for apoptosis using the Annexin V kit (BD Biosciences). Following 48 hours transfection, cells were washed twice with PBS and disaggregated with 0.5% Trypsin-EDTA (Gibco). $1x10^6$ cells were resuspended in 1 mL of 1x binding buffer (BD Biosciences). 100 μL of cells were mixed with 5 μL Annexin V-FITC antibody and 2 μL 50 μg/mL PI. Cells were incubated for 15 minutes at room temperature in the

dark prior to adding 400 µL 1x binding buffer. Cells were profiled for Annexin V and PI expression using the FACSCalibur flow cytometer, and data analyzed using FlowJo software.

Expression Analysis

Lung cancer cell lines were analyzed for their expression of putative ASCL1 target genes CD117 and CD133 using flow cytometry. Briefly, cells were detached and disaggregated using 0.5% Trypsin-EDTA (Gibco) and resuspended in HBSS+ (HBSS containing 2% FBS and 10 µM HEPES) at a concentration of $1x10^6$ cells/mL. Cells were stained with fluorescently-conjugated antibodies against CD117 (BD Biosciences) and CD133 (Miltenyi Biotec) and incubated for 30 minutes at 4°C. Cells were then washed and resuspended in fresh HBSS+ and stained with PI to account for non-viable cells. Flow cytometric profiling was performed using a FACSCalibur flow cytometer and analyzed using FlowJo software (Treestar).

Aldefluor Assay

The Aldefluor kit (Stem Cell Technologies) was used to profile cells for aldehyde dehydrogenase activity (ALDH) as previously described (Ginestier, Hur et al. 2007). Cells were incubated with Aldefluor assay buffer containing the ALDH protein substrate BODIPY-aminoacetaldehyde (BAAA) for 45 minutes at 37°C. Cells that catalyze BAAA to its fluorescent product BODIPY-aminoacetate (BAA) were considered $ALDH^+$. Profiling gates for FACS were drawn relative to cell baseline fluorescence, which was determined by the addition of the ALDH-specific inhibitor diethylaminobenzaldehyde (DEAB) during the incubation and DEAB-treated

samples served as negative controls. After incubation, samples were resuspended in fresh assay buffer containing 1 μg/mL PI to mark non-viable cells. ALDH activity was profiled using the FACSCalibur flow cytometer and analyzed with FlowJo software.

2.2.4 Tumor Cell Growth Assays

Liquid Colony Formation Assay

Anchorage-dependent colony formation was performed by plating 500-2000 cells per well in a 6-well plate (9.5 cm^2 well area) in RPMI-1640 supplemented with either 5% or 10% FBS depending on the cell line utilized. Following a two-week incubation, colonies were stained with 0.5% methylene blue and counted using ImageJ software (NIH).

MTS Proliferation Assay

Relative cell growth was analyzed by MTS assay. Briefly, 100 uL of cells grown in 96-well plates were mixed with 20 uL MTS assay reagent consisting of tetrazolium compound and phenazine ethosulfate, an electron coupling reagent (Promega). Cells were incubated with MTS mixture until formation of soluble formazan product was observed, providing a relative readout of metabolically active cells. Relative absorbance of formazan was analyzed by plate reader at 490 nm and is directly proportional to the number of living cells in culture.

2.2.5 Drug Treatment Assays

Phorbol 12-myristate 13-acetate* in vitro *Treatments

Phorbol 12-myristate 13-acetate (PMA) was purchased from Sigma-Aldrich. HBEC-3KT and HCC1833 cells were plated in 6-well plates at a density of $2x10^5$ cells per well and allowed to adhere for 24 hours prior to treatment. PMA was added at a concentration of 1, 10, and 100 nM for 24 hours after which cells were harvested for cell cycle analysis, qRT-PCR, and immunoblot. Short-term treatments were performed in 6-well plates on $4x10^5$ HCC1833 cells treated for 30, 60, 90, 120, 150, and 180 minutes with 100 nM PMA. Each time point was harvested for qRT-PCR and immunoblot analysis.

Xanthohumol* in vitro *Treatments

Xanthohumol (XN) was purchased from Tocris Bioscience. HCC1833 cells were plated in 6-well plates at a density of $2x10^5$ cells per well and allowed to adhere for 24 hours. Cells were then treated for 24 hours with 10, 20, or 30 uM xanthohumol prior to harvesting for cell cycle analysis, qRT-PCR, and immunoblot. NCI-H1993 cells were treated for 24, 48, and 72 hours with 10, 20, or 30 uM XN and analyzed for apoptosis after each time point.

Sorafenib* in vitro *Treatments

Sorafenib (Nexavar) was purchased from Selleck Chemicals. NCI-H1755, HCC1833, and HBEC-3KT cells were plated at a density of $2x10^5$ cells per well in 6-well plates and allowed to adhere for 24 hours. Cells were treated for 24 hours with 10 nM, 100 nM, or 1 uM sorafenib prior to analyzing for protein expression and apoptosis.

AZD-6244* in vitro *Treatments

AZD-6244 (Selumetinib) was purchased from Selleck Chemicals. HCC1833 cells were plated at a density of $2x10^5$ cells per well in 6-well plates and allowed to adhere for 24 hours. Cells were treated for 24 hours with 100 nM, 500 nM, or 1 uM AZD-6244 prior to analyzing for protein expression and apoptosis.

ABT-263* in vitro *Treatments

ABT-263 (Navitoclax) was purchased from Selleck Chemicals. Lung cell lines including NCI-H1755, NCI-H1993, HCC1833, and HBEC-3KT were treated for 12-24 hours with 50 nM, 100 nM, and 500 nM ABT-263 in 6 well plates prior to assaying for apoptosis. For MTS growth proliferation experiments, cells were plated in 96-well plates at a density of $2x10^3$ to $4x10^3$ cells per well. Cells were allowed to adhere for 24 hours prior to 48-hour treatment with ABT-263 concentrations ranging from 1 nM to 100 uM. Drug combination treatments with PMA were performed in NCI-H1755, NCI-H1993, and HBEC-3KT cells. Briefly, $2x10^5$ to $3x10^5$ cells were plated in 6-welll plates and allowed to adhere for 24 hours. Cells were then treated with 50, 100, or 500 nM ABT-263, 1, 10, or 100 nM PMA, and 1 nM PMA together with 50, 100, or 500 nM ABT-263. Following treatment, cells were profiled for apoptosis by cell cycle analysis as described above.

ABT-263* in vivo *Xenograft Treatments

Non-obese diabetic/severe combined immunodeficiency (NOD/SCID) mice were utilized to characterize the response of subcutaneous tumors to treatment with ABT-263. All *in vivo* experiments were performed in female NOD/SCID mice bred by the UT Southwestern Mouse Breeding Core. The care and treatment of experimental animals were in accordance with institutional guidelines.

H1755 and H1993 cells were utilized for xenograft experiments. Paratopic implantations of lung cancer cells were carried out by injecting $1x10^6$ cells suspended in 100 uL PBS subcutaneously into the right flank. To minimize leakage at the injection site, 27½ gauge needles were used and the subcutaneous region was made accessible for injection by lifting the skin at the site of injection to alleviate pressure on the injected volume. Prior to subcutaneous injection, fur on the right flanks of mice was shaved off using electric clippers to improve detection of xenograft formation. Mice were monitored twice weekly and tumors, once formed, were measured by digital caliper. Tumor volumes were calculated as follows: $V_{tumor} = (\pi/6)(d_{large})(d_{small})^2$.

Tumors were allowed to grow to between 200 and 300 mm^3 prior to initiating treatment. Mice were grouped into vehicle-treated or ABT-263-treated cohorts in order to minimize standard deviation. Treatments were carried out by intraperitoneal injection of 50 uL DMSO or 50 uL 100mg/kg ABT-263 dissolved in DMSO daily for 14 days. 27½ gauge needles were used to minimize wounding at the point-of-entry and injection side was alternated each day. Tumor size was measured daily prior to injection. Mice were sacrificed 24 hours following the 14^{th}

treatment in the case of H1755 tumor xenografts, or following two weeks of observation for H1993 tumor xenografts.

2.2.6 Immunohistochemistry

Immunohistochemical (IHC) staining for ASCL1, BCL2, cGRP, and GRP was performed on TMA samples as follows: 5 μm-thick formalin-fixed, paraffin-embedded tissue sections were deparaffined, hydrated, heated in a Biocare decloaker for 30 minutes pretreated with Target Retreval Solution (Dako), and washed in Tris buffer. Peroxide blocking was performed with 3% H_2O_2 in methanol at room temperature for 15 minutes, followed by 35 minute incubations in Tris-buffered saline containing 15% FBS. Slides were incubated with the primary antibody (ASCL1 1:100) at room temperature for 65 minutes, washed with Tris-buffered saline, followed by incubation with Envision Dual Link+ Polymer-Labeled System (Dako) for 30 minutes. Staining was developed with chromogen substrate (Dako) for 5 minutes and then counterstained with hematoxylin, dehydrated, and mounted.

Expression was quantified using light microscopy (total magnification, 200x) and expression was quantified using a four-value intensity score (0, 1, 2, and 3) and the percent of IHC^+ tumor cells (0-100%). Intensity scores were defined as follows: 0 = no appreciable staining; 1 = barely detectable staining; 2 = readily appreciable staining; and 3 = dark brown epithelial cell staining. An expression score was obtained by multiplying the intensity and reactivity extension values (range 0 – 300). Expression scores from samples stained with the

ASCL1, BCL2, and GRP antibodies were dichotomized by their mean values into high or low staining categories.

2.2.7 ChIP-Seq Methods

Chromatin Immunoprecipitation, Sequence Library Preparation, and Alignment

10 million lung cancer cells were prepared for chromatin immunoprecipitation (ChIP) by washing twice with cold PBS followed by trypsinization. The cell lines utilized for ChIP were the following: H1755, HCC4018 (NE-NSCLC), H128, H1184, H2107 (SCLC), and control cell lines H524 and H526 (ASCL1-negative SCLC). Nuclei were liberated from cells by dounce homogenization and then fixed in 1% formaldehyde for 10 minutes at room temperature. Fixation was terminated by adding glycine to a final concentration of 0.125M. Chromatin was sheared by using a Diagenode Bioruptor for 30 minutes on high power with 30s:30s on:off cycles. 100 μg chromatin was immunoprecipitated with 5 μg affinity-purified mouse anti-ASCL1 antibody (BD Biosciences) followed by anti-mouse Dyna beads (Invitrogen). The immunoprecipitated chromatin was then purified with the Qiagen PCR Clean-up kit.

Prior to sequencing, ChIP quality was determined by qRT-PCR for known targets DLL1 and DLL3 as well as negative control regions. ChIP-Seq libraries were prepared using the NEBNext ChIP-Seq Library kit. Indexing primers and adapters were obtained from Illumina. Single-end sequencing of 50 bp was conducted for all samples on the Illumina High-Seq 2000 sequencer. The DNA sequencing data produced following ChIP and library preparation were aligned using Bowtie (Langmead, Trapnell et al. 2009). The parameters for running Bowtie are

"-S -n 2 -e 70 -l 20 -m 3 --time -p 12 --chunkmbs 512." The reference genome is HG19. Replicates were mapped individually and pooled together.

Peak Calling Using Model-Based Analysis for ChIP-Seq and DNA Motif Analysis

ChIP-Seq peaks were called using Model-Based Analysis for ChIP-Seq (MACS) software, version 1.4.0rc (Zhang, Liu et al. 2008). All reads that were mapped to more than one genomic region were removed in order to reduce ambiguity. Additionally, only one unique copy of each read was retained to prevent PCR bias. Reads from control ASCL1-negative cell lines H524 and H526 were pooled prior to comparison with ASCL1+ cell line reads. Peak calling was performed using default parameters in MACS. The cutoff for tag reads needed to retain a peak in each cell line varied from 11 to 19. Cutoff values were manually chosen based on visual inspection of ChIP-Seq peaks in the UCSC Genome Browser. Peaks appearing in ASCL1-negative control samples were subtracted from ASCL1+ samples.

After peak calling was performed in MACS on each cell line, a hierarchical clustering algorithm with complete linkage was used to identify consensus peaks in the ASCL1+ cell lines. A maximum distance of 300 bp between peak summits appearing in different samples was allowed for consideration of consensus peaks. For clusters of consensus peaks, a new summit was calculated from summits of member peaks weighted by fold change.

DNA motif analysis was performed using Heterogeometric Optimization of Motif EnRichment (HOMER) (Heinz, Benner et al. 2010). The parameters used for HOMER were "-S

15 -bits -size -50,50 -len 5,6,7,8,9,10 –keepFiles." The"-50,50" parameter informs HOMER to search for motifs within a 100 bp window centered around the summit of consensus peaks.

Gene Associations using Genomic Region Enrichment Annotation Tool

Consensus peaks identified using MACS were tabulated as 70 bp reads in a .BED file and uploaded to the Genomic Region Enrichment Annotation Tool (GREAT) server in order to correlate genomic peak location with genes (McLean, Bristor et al. 2010). Default parameters for gene association were used. GREAT defines a basal regulatory region for a gene within 5 kb upstream of the transcriptional start site (TSS) or 1 kb downstream and defines an extended regulatory region that exists within 1000 kb both up and downstream of the TSS. These rules were utilized to assign gene associations to the consensus peaks obtained from hierarchical clustering of peaks identified via MACS analysis.

Correlation of Associated Genes with Microarray Expression Data

Microarray expression data from the Minna lab in conjunction with ChIP-Seq gene-association data was utilized to find likely transcriptional targets of ASCL1. Only those cell lines utilized for ChIP-Seq (H1755, HCC4018, H128, H1184, and H2107) were used to compare gene expression of ASCL1 targets. A Pearson correlation was calculated for ASCL1 expression against every other gene in the genome. The genes with the highest positive correlation were chosen to compare against the ChIP-Seq associated gene list. The overlap of the ASCL1

microarray correlation analysis with the ChIP-Seq gene list resulted in a final list of targets whose overexpression is likely regulated by ASCL1.

Similarly, microarray expression analysis was used to determine $\log_2$ ratio differences in transcripts between ASCL1+ samples and the ASCL1-negative control lines. Comparison of gene expression differences of the ASCL1-associated genes between H1755, HCC4018, H128, H1184, H2107 versus H524 and H526 resulted in a list of ChIP-Seq target genes specifically upregulated in ASCL1+ samples.

2.2.8 Retrospective Survival Analysis

The prognostic performance of the gene lists associated with overexpression of putative ASCL1 target genes, either by correlation analysis or microarray $\log_2$ ratio analysis, was tested several patient data sets. These include the NCI Director's Challenge Consortium study, which contains genome-wide mRNA expression data and survival analysis on 442 resected lung adenocarcinomas; the Tomida Dataset of 117 resected lung adenocarcinomas; and the MD Anderson Cancer Center (MDACC) Spore Dataset containing 275 resected NSCLCs.

Overall survival time was defined as the time from the date of surgery (resection) until death or last follow-up contact. Some patients in the NCI Director's Challenge were followed for up to 17 years, so to avoid extrapolation of the prediction model, the comparison of survival times between predicted risk groups is truncated at five years.

The prediction model is built from a training set using Supervised Principal Component analysis and then validated in the testing set (Bair and Tibshirani 2004). Supervised Principal

Component analysis was implanted using the superPC R package using all default parameters. The testing set samples are divided into two equally sized risk groups by the median of the predicted risk scores. Survival curves are estimated by the Kaplan-Meier method and ranked according to the log-rank test. The hazard ratios were determined using Cox proportional-hazards model (Collet et al., 2003).

CHAPTER THREE

IDENTIFICATION OF A PRE-CLINCAL MODEL FOR NON-SMALL CELL LUNG CANCER WITH NEUROENDOCRINE FEATURES

3.1 Introduction

The mortality associated with lung cancer is due in part to the limitations of current therapies to effectively treat the pathologically and molecularly distinct subsets associated with the disease. In order to develop personalized, targeted medicine for the treatment of lung cancer we need to accurately classify tumors using a combination of features such as histologic and pathologic analysis, mRNA gene expression, response to therapy, and oncogene/tumor suppressor mutation status. Currently lung cancers are grouped into two main types, small cell lung cancer (SCLC) or non-small cell lung cancer (NSCLC). Patients presenting with NSCLC can be further subdivided into adenocarcinoma, squamous cell carcinoma, or large cell/neuroendocrine carcinoma (LCNEC) groups. Recent data suggests that the molecular heterogeneity of lung cancer is far greater than that which can be captured through histological analysis of tumor biopsies (West, Vidwans et al. 2012). Of particular interest are lung cancers with neuroendocrine features, such as SCLC and LCNEC, due to their significantly more aggressive nature compared to all other lung cancers (Garcia-Yuste, Matilla et al. 2008).

Non-small cell lung cancers with neuroendocrine (NE-NSCLC) features are difficult to diagnose and treat. Additionally, neuroendocrine differentiation and gene expression in NSCLC

is associated with significantly reduced survival in several studies (Schleusener, Tazelaar et al. 1996; Bhattacharjee, Richards et al. 2001). The established neuroendocrine subtype of NSCLC officially recognized by current staging methods is termed large cell neuroendocrine carcinoma (LCNEC), which represents approximately 2-3% of NSCLC cases (Skuladottir, Hirsch et al. 2002). Besides LCNEC, neuroendocrine features can appear in up to 10 to 20% of otherwise typical NSCLCs (Rekhtman 2010). In these tumors, neuroendocrine features such as positive staining for neuroendocrine markers by immunohistochemistry (IHC) may be present even if distinct neuroendocrine morphology is not. Confounding the study of neuroendocrine tumors in NSCLC is the discovery that certain typical NSCLCs, usually adenocarcinomas, have no overt neuroendocrine morphology or neuroendocrine marker IHC positivity yet express a wide range of neuroendocrine genes as measured by genome-wide mRNA expression array (Bhattacharjee, Richards et al. 2001). Although several large IHC studies performed on resected adenocarcinomas demonstrate neuroendocrine differentiation to be of no clinical utility (Ionescu, Treaba et al. 2007; Segawa, Takata et al. 2009; Sterlacci, Fiegl et al. 2009), other studies demonstrate that neuroendocrine gene expression in NSCLC can predict for poor prognosis (Schleusener, Tazelaar et al. 1996; Bhattacharjee, Richards et al. 2001; Pelosi, Pasini et al. 2003; Jones, Virtanen et al. 2004; Howe, Chapman et al. 2005). Regardless of the clinical activity of these tumors relative to other lung cancers, the fact remains that neuroendocrine differentiation in NSCLC is significant, representing up to 25% of all NSCLCs, and merits serious further study.

Perhaps most importantly, a pre-clinical model including cell lines and xenografts for NE-NSCLC has yet to be established. Pre-clinical models in lung cancer have been critical toward the study of and clinical implementation of targeted therapies in such subsets as EGFR mutant NSCLCs and EML4-ALK fusion NSCLCs (Pao, Miller et al. 2004; Choi, Soda et al. 2010). Studies of cell lines *in vitro* and *in vivo* via mouse xenografts are crucial to discover essential cellular dependencies that can be exploited therapeutically.

The goal of this study is to identify a pre-clinical model for non-small cell lung cancer with neuroendocrine features using cell lines previously established by the Minna and Gazdar labs. These cell lines will then serve as the backbone for molecular experiments in order to uncover clinical biomarkers to identify NE-NSCLC tumors and new therapies to treat them. If effective, this study will set the stage for advancing a biomarker and potential targeted therapy into clinical trials for patients with NE-NSCLC.

3.2 Results

3.2.1 Genome-Wide mRNA Expression Analysis of Lung Cell Lines

The establishment of lung cancer cell lines has been instrumental in bringing targeted therapies into the clinic, particularly for patients carrying activating mutations in the EGFR gene or patients with a fusion of the EML4 and ALK genes. Drs. John Minna and Adi Gazdar established the majority of lung cancer cell lines utilized in the world (Phelps, Johnson et al. 1996; Gazdar, Girard et al. 2010). As part of their work, extensive legacy data has been collected

for each cell line including tumor suppressor/oncogene mutation status, response to standard and experimental therapies, and most recently, genome-wide mRNA expression analysis.

207 lung cell lines including NSCLCs, SCLCs, and normal immortalized human bronchial or small airway epithelial cells (HBECs/HSAECs) were profiled for genome-wide mRNA expression using the Illumina V3 platform. Normalization across all samples was performed using MicroArray Transformation in Microsoft Excel (MATRIX) software 1.503 and $\log_2$-transformed. An unsupervised average-linkage clustering analysis using the Pearson Method resulted in a grouping of cell lines by histology (Figure 3.1A**)**, with NSCLC, HBEC/HSAEC, and SCLC clustering together. Interestingly, within the SCLC cluster are 11 NSCLC cell lines. This result is surprising due to the dramatic gene expression differences between typical SCLCs and typical NSCLCs. By grouping with SCLC, the assumption can be that the 11 NSCLC cell lines have a similar gene expression profile. Since SCLCs are an overt neuroendocrine tumor, highly expressing neuroendocrine genes, we can assume that the 11 potential NE-NSCLC cell lines also express neuroendocrine genes.

3.2.2 NE-NSCLC Cell Line Oncogenotype and Response to Chemotherapy

The putative NE-NSCLC cell lines are not categorized by any single histological subtype and include carcinoids (H720 and H727), adenocarcinomas (H969, H1385, H1755, HCC1833, HCC2374, and HCC4018), and large cell/neuroendocrine carcinomas (H1155, H1570, and H2106) (Figure 3.1B). The oncogenotype of NE-NSCLC includes 8 TP53 mutant cell lines, 5 KRAS mutant lines, and 1 BRAF mutant. None of the NE-NSCLC cell lines carry EGFR

mutations. Despite the gene expression similarities to SCLC, the NE-NSCLCs are distinct because of the presence of KRAS and BRAF mutations, which are never seen in SCLC. RB1 mutations, seen at a frequency of 75% to 90% in SCLC, appear in three out of the 11 NE-NSCLC cell lines**.** NE-NSCLC cell lines are not biased in terms of gender (5 male, 6 female) and have no significant correlation with response to chemotherapy (Table 3.1).

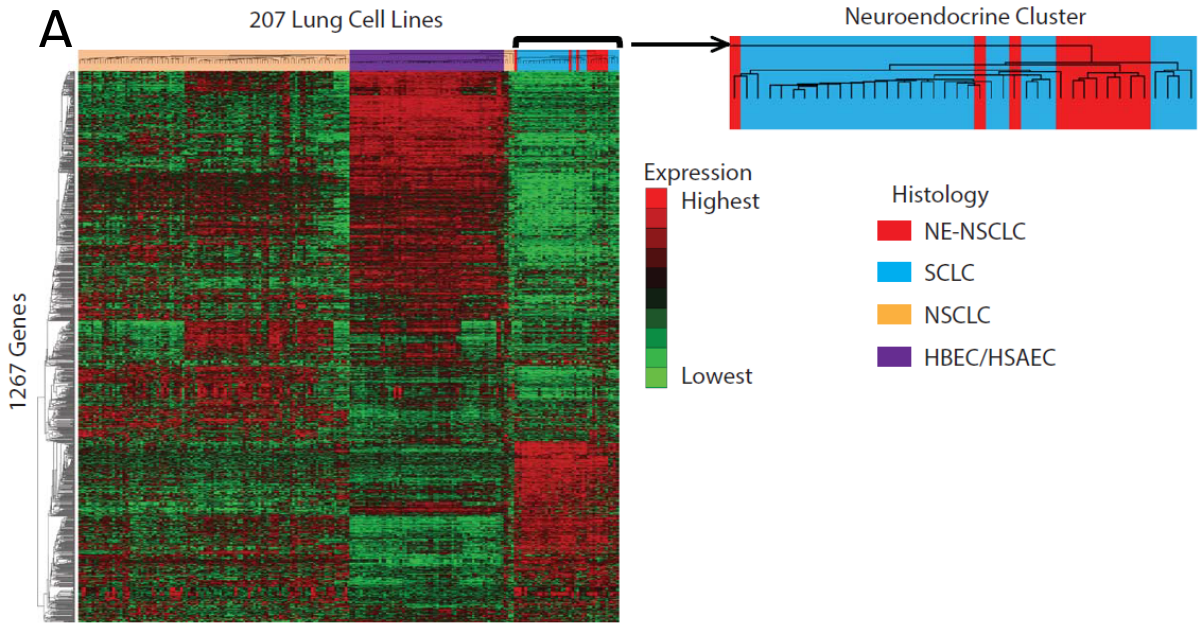

B

Cell Line	H720	H727	H969	H1155F	H1385	H1570	H1755	H2106	HCC1833	HCC2374	HCC4018
Type	CAR	CAR	AC	LCNE	AC	LC	AC	LCNE	AC	AC	AC
TP53	mt	mt	WT	mt	WT	WT	mt	mt	mt	mt	mt
KRAS	WT	mt	WT	mt	mt	mt	WT	WT	WT	mt	WT
RB1	mt	WT		mt	WT	WT	WT	mt			WT
EGFR	WT	WT	WT	WT	WT	WT	WT		WT	WT	WT
PIK3CA	WT	WT	WT	WT	WT	WT	WT	WT	WT	WT	WT
BRAF	WT	WT	WT	WT	WT	WT	mt	WT	WT	WT	WT
p16	WT	WT	WT	WT	mt	WT	mt			WT	WT
PTEN	WT	WT	WT	mt	WT	WT	WT			WT	WT
NRAS	WT	WT		WT	WT	WT	WT			WT	WT

Figure 3.1: Identification of a subset of non-small cell lung cancer cell lines with neuroendocrine features. Genome-wide mRNA expression data was used to cluster lung cell lines. (A) Clustering results demonstrate grouping of cell lines by histology. 11 NSCLC lines group together with SCLC, suggesting a common neuroendocrine gene expression signature. (B) Oncogenotype for the 11 putative NE-NSCLC cell lines showing mutation profile for common oncogenes and tumor suppressors.

Therapy	Log Ratio	T-test	Significance
Carboplatin	-0.37	0.1183	N.S.
Docetaxel	-0.44	0.2603	N.S.
Doxorubicin	-0.16	0.7485	N.S.
Etoposide	-0.49	0.4129	N.S.
Gemcitabine	-0.19	0.6823	N.S.
Gemcitabine/Cisplatin	0.49	0.3908	N.S.
Paclitaxel	-0.10	0.7352	N.S.
Paclitaxel/Carboplatin	-0.18	0.4968	N.S.
Pemetrexed	-1.10	0.1420	N.S.
Pemetrexed/Cisplatin	-0.42	0.4621	N.S.
Vinorelbine	-1.38	0.4037	N.S.

Table 3.1: Response of NE-NSCLC cell lines to chemotherapy. NE-NSCLC cell lines were profiled for their response to chemotherapy compared to typical NSCLC lines. Log ratio analysis was performed comparing log10(IC50) values of standard chemotherapy between NE-NSCLC and NSCLC cell lines. A higher log ratio indicates that NE-NSCLC lines are more resistant to a particular therapy. No chemotherapies showed a significant sensitization or resistance to NE-NSCLC cell lines.

3.2.3 Validation of Neuroendocrine Gene Expression in NE-NSCLC Cell Lines

To understand the gene expression differences between the putative NE-NSCLC lines and "typical" NSCLC lines, a $\log_2$ ratio analysis was performed to assay the differences between the two groups (Figure 3.2). Unsurprisingly, the 15 highest expressed genes in NE-NSCLC demonstrate an overrepresentation of neuroendocrine markers, including chromogranin A/B, synaptotagmin 4, secretogranin 2/3, and dopa decarboxylase, among others. The most differentially expressed gene between NE-NSCLC and NSCLC cell lines is ASCL1 (achaete-scute homolog 1, mASH1/hASH1), a transcription factor required for the development of several neural and endocrine cell types including pulmonary neuroendocrine cells.

A second gene expression analysis consisted of combining log ratio analysis with the significance of those ratios as measured by t-test. The resulting plot, termed volcano plot, is useful to display genes that are both highly expressed and highly significant between two separate populations. NE-NSCLC and NSCLC expression differences plotted as shown in Figure 3.3A reveals 69 genes that are expressed at a $\log_2$ ratio greater than 5.0 and a p-value lower than 0.001 ($-\log_{10}$ (t-test) as plotted). A clustering analysis on the 119 NSCLC cell lines using the 69 markers results in an exceptionally clean separation of NE-NSCLC from NSCLC cell lines (Figure 3.3B). ASCL1 is a member of this 69-gene signature and its location on the volcano plot is indicated.

High expression of ASCL1 in neuroendocrine tumors, particularly SCLC, has been noted for some time (Ball, Azzoli et al. 1993). The importance of ASCL1 in SCLC has also been studied via genetic knockdown studies. Those experiments showed that ASCL1 is required for

the survival of SCLC, however the discovery of high levels of ASCL1 expression in NSCLC is surprising and merits further study within this subset of cancers.

ASCL1 expression in a panel of 32 lung cancer cell lines was verified by TaqMan-based qRT-PCR analysis relative to expression of endogenous GAPDH. Expression of the ASCL1 gene is present only in neuroendocrine lung cancer lines, including SCLC and NE-NSCLC (Figure 3.4A). ASCL1 transcript is not detected in any typical NSCLC cell line suggesting its importance in neuroendocrine lung cancers. Several transcriptional targets of ASCL1 have been determined and include the Notch ligands Delta-like 1 and Delta-like 3 (DLL1, DLL3) (Castro, Skowronska-Krawczyk et al. 2006; Henke, Meredith et al. 2009; Castro, Martynoga et al. 2011). Expression of DLL1 measured by qRT-PCR shows a similar pattern of expression as ASCL1, with high transcript levels detected in SCLC and NE-NSCLC cell lines and minimal or no transcript detected in typical NSCLCs.

Western blot analysis of ASCL1 protein expression shows that ASCL1 protein is present in NE-NSCLC cell lines, but not typical NSCLC, mirroring the results demonstrated via microarray and qRT-PCR analysis (Figure 3.4B). Despite the high expression of ASCL1 in both NE-NSCLC and SCLC cell lines, it does not lie in a region of known amplification. Also, ASCL1 is never mutated in SCLC patient samples or cell lines. Due to the significant growth retardation and apoptotic effect seen in SCLC upon knockdown of ASCL1, the characterization of ASCL1 knockdown in NE-NSCLC also needs to be understood.

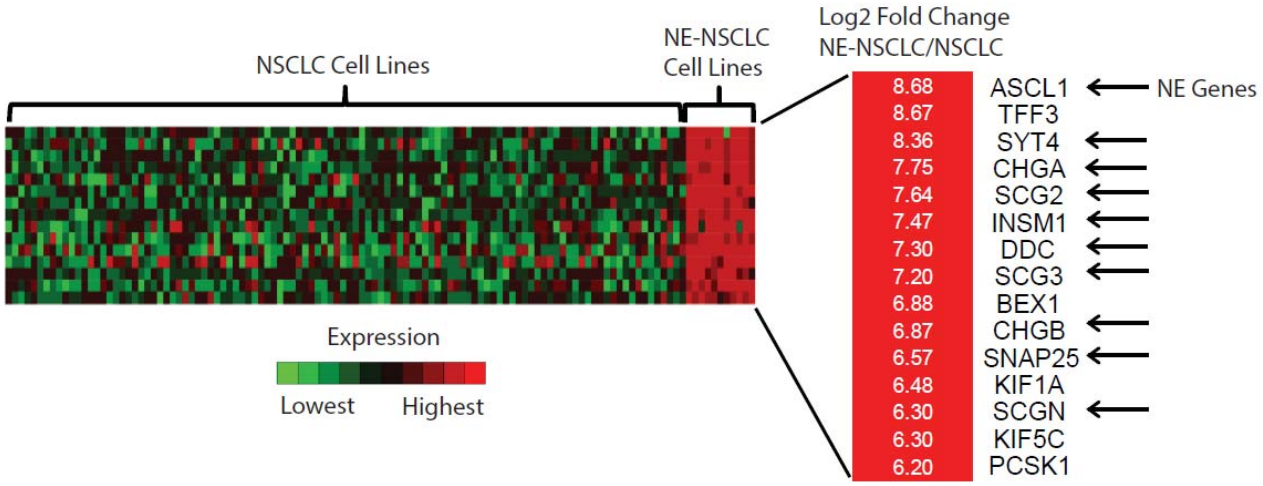

Figure 3.2: Log ratio analysis comparing NE-NSCLC and NSCLC cell lines gene expression. Log ratio analysis was used to identify the highest expressed genes in the NE-NSCLC subset compare to typical NSCLC lines. ASCL1 is the most abundant transcript. Neuroendocrine genes are highlighted and represent the majority of the highly expressed genes.

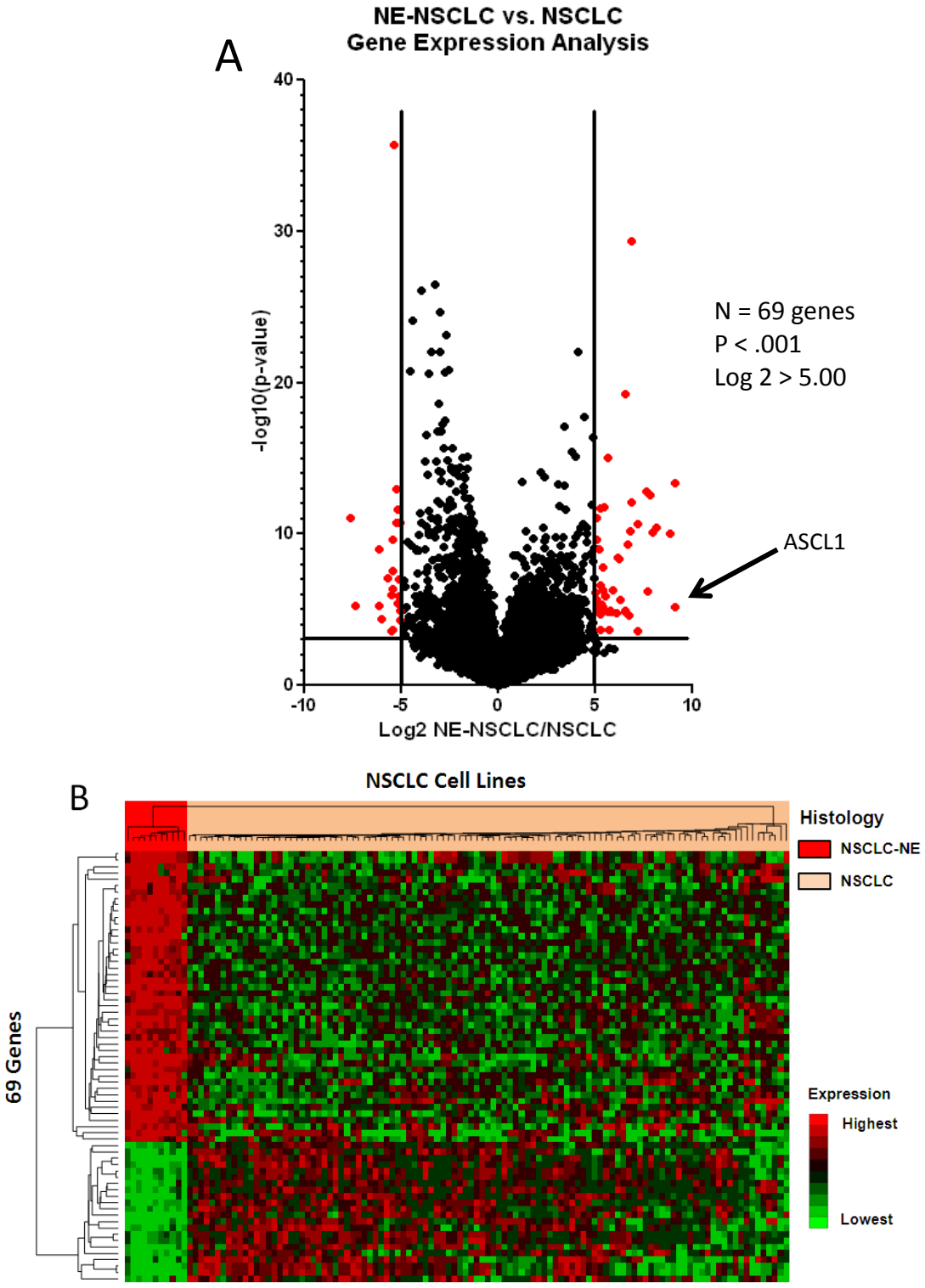
A
NE-NSCLC vs. NSCLC
Gene Expression Analysis
-log10(p-value)
Log2 NE-NSCLC/NSCLC
N = 69 genes
P < .001
Log 2 > 5.00
ASCL1
B
NSCLC Cell Lines
69 Genes
Histology
NSCLC-NE
NSCLC
Expression
Highest
Lowest

Figure 3.3: Detecting highly expressed and highly significant genes in NE-NSCLC. Log2 gene expression differences between NE-NSCLC and typical NSCLC cell lines were plotted along with the p-value (-log10(p-value)). Significant genes were chosen based on |log2 > 5.00| and p-value < 0.001. (A) The resulting volcano plot with the 69 most significant genes indicated in red. ASCL1 is highlighted. (B) The 69 genes were used to cluster the NSCLC cell lines and resulted in a clean separation of the NE-NSCLC and typical NSCLC lines.

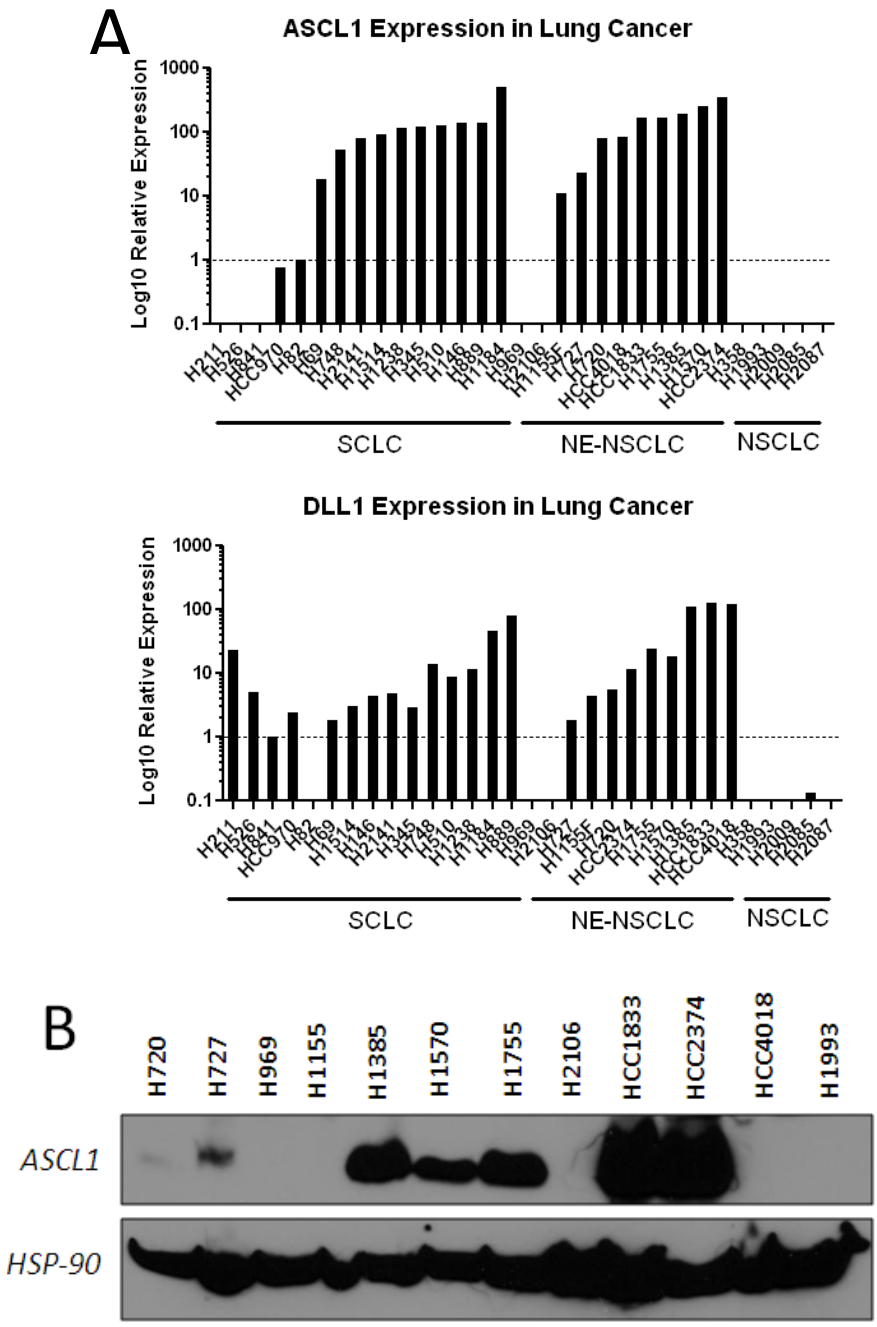

Figure 3.4: ASCL1 expression in lung cancer cell lines. (A) ASCL1 and DLL1 mRNA expression measured by qRT-PCR demonstrates high levels of transcript in neuroendocrine lung cancer lines compared to NSCLC. The expression pattern of DLL1 is very similar to that of ASCL1. (B) ASCL1 protein levels in NE-NSCLC cell lines.

3.2.4 Analysis of ASCL1 Knockdown in NE-NSCLC Cell Lines

ASCL1 has been implicated as an oncogene in SCLC, but its expression in a subset of NSCLC is surprising. Prior research utilizing short-hairpin RNAi methods showed that knockdown of ASCL1 in SCLC cell lines ACC-LC-172 (Osada, Tatematsu et al. 2005), DMS-53 (Osada , Tomida et al. 2008), and H1618 (Jiang, Collins et al. 2009) dramatically reduced cell viability, growth, proliferation, and survival. Similarly, knockdown of ASCL1 in a NSCLC line positive for ASCL1 expression, ACC-LC-91, demonstrated similar growth inhibitory effects. To test the panel of NE-NSCLC cell lines, ASCL1 expression was knocked down via transient siRNA and stable shRNA methods.

Knockdown of ASCL1 in NE-NSCLC cell lines H1755 and HCC1833 was performed with three different siRNAs targeting ASCL1. Reduced expression of ASCL1 transcript was detected in siASCL1-transfected cells. mRNA was decreased by 80% and 64% in H1755 and HCC1833, respectively, compared to control-transfected cells (Figure 3.5A**)**. DLL1, a transcriptional target gene of ASCL1, also shows decreased expression following ASCL1 knockdown, demonstrating the functional effect of the siRNAs.

ASCL1 protein levels were measured in H1755 and HCC1833 cells transfected with three different ASCL1-targeting siRNAs. In both cell lines, siASCL1-1, siASCL1-2, and siASCL1-3 significantly reduced ASCL1 protein levels compared to controls, which included an untransfected sample, lipid-only, siSCR-transfected, and siLUC-transfected (Figure 3.5B). siASCL1-3 consistently demonstrated the largest degree knockdown of ASCL1 protein levels and was utilized throughout the duration of these studies.

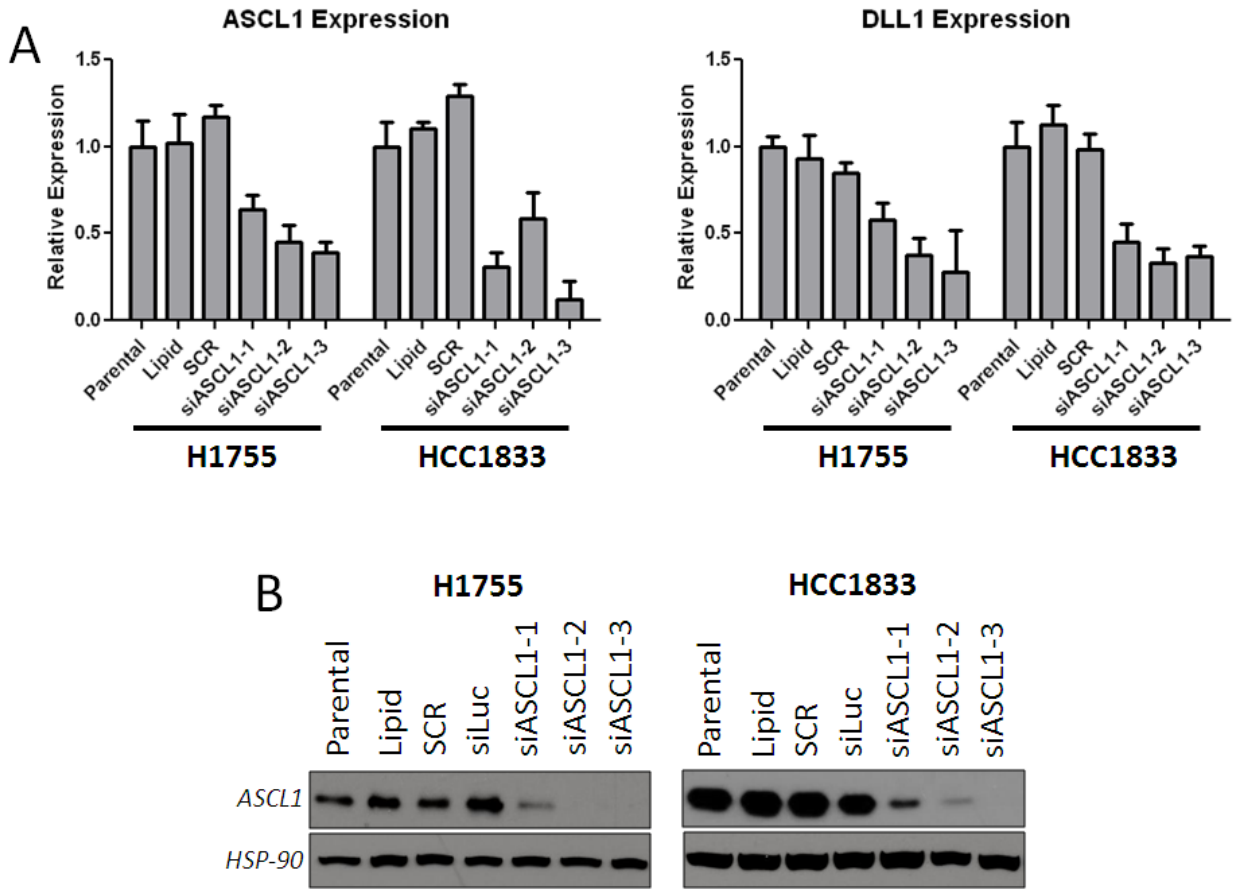

Figure 3.5: Validating ASCL1 knockdown in NE-NSCLC cell lines. siRNA-mediated knockdown was performed with 20 nM siRNA and profiled following 72 hours. (A) ASCL1 was knocked down using siRNA-mediated technology. ASCL1 expression was reduced compared to controls in both H1755 and HCC1833. The mRNA of the direct transcriptional target DLL1 was also reduced in all siASCL1-transfected cells. (B) ASCL1 protein is reduced in siASCL1-transfected H1755 and HCC1833 cells. This blot was stripped and reprobed with primary antibodies in subsequent experiments.

3.2.5 Proliferative and Apoptotic Effects in NE-NSCLC Cells Following ASCL1 Knockdown

Cell growth and proliferative effects were studied on H1755 and HCC1833 cells following ASCL1 knockdown using the MTS assay. The MTS assay uses cellular reductase enzyme activity as a surrogate marker for metabolic health, which is proportional to the number of healthy, viable cells. Reduction of ASCL1 by siASCL1-3 reduces proliferation in H1755 and HCC1833 by 60 to 70%. In both cells lines, siASCL1-3 inhibited growth to the same degree as the toxic oligo (siPLK) control-transfected cells. H1993, an ASCL1-negative NSCLC cell line, was unaffected by siASCL1-3 (Figure 3.6). Control-transfected cells, including cells-only, lipid-only, and siSCR had no statistical effect on cell growth as measured by MTS.

Next, colony forming ability following stable ASCL1 knockdown was measured. In this set of experiments, H1755 and HCC1833 ASCL1+ NE-NSCLC cell lines along with an ASCL1-negative cell line, H1993, were infected with lentivirus carrying an shRNA designed to inhibit expression of ASCL1. After infection, cells carrying the shASCL1 or shNTC control construct were selected for by puromycin antibiotic treatment. Following one week of selection, cells were imaged under fluorescent microscope for GFP expression in order to validate construct expression (Figure 3.7A) and the liquid colony formation assay was performed. 500-2000 cells were plated in 6-well plates and allowed to develop into colonies for 2 weeks. H1755 and HCC1833 shASCL1 cells demonstrated dramatically reduced colony forming ability compared to shNTC cells (Figure 3.7B). Colony formation in the stable knockdown cells was nearly completely eliminated. H1993 ASCL1-negative control cells infected with either shASCL1 or

shNTC showed no statistical difference in their ability to form colonies in liquid culture. Quantification of the number of colonies was performed by manual counting (Figure 3.7C).

The growth inhibitory effects seen with knockdown of ASCL1 may be the result of cytostatic or cytotoxic mechanisms. Cancer cells treated with cytostatic compounds prevent or slow tumor growth, however those treatments are often ineffective as the tumor cells remain and have the potential to quickly become resistant to treatment. Cytotoxic treatments, on the other hand, induce apoptosis or necrosis and have the potential to reduce tumor burden. If knockdown of ASCL1 induces apoptosis in NE-NSCLC, then it can serve as a potential starting point for finding therapies targeting this subset of lung cancer.

Cell cycle analysis can be utilized as a surrogate marker for apoptosis. Cells are stained with propidum iodide (PI), which is a dye that binds DNA by intercalating between the bases, and analyzed by flow cytometry. The amount of DNA is then quantified and related to the stages of the cell cycle using standard algorithms. Cellular apoptosis is analogous to the number of cells appearing in the sub-G1 phase of the cell cycle. The sub-G1 phase signifies a reduction of DNA content relative to the amount seen in the G0-1 phase. A reduction of DNA content in an intact cell signifies that apoptosis has begun and DNA is being degraded through the function of DNA nucleases, which are released only after the apoptotic cascade has initiated.

H1755 and HCC1833 cells were transfected with siASCL1-1, siASCL1-2, and siASCL1-3 along with control siRNAs siSCR and siLUC. Parental untransfected control and lipid-only control were also utilized, with the parental untransfected control serving as the baseline for cell cycle analysis. Following 72 hours of knockdown with siRNA in 6-well plates, one well was

isolated and prepared for cell cycle analysis. Cells were fixed, stained with PI, and analyzed for DNA content by flow cytometry. Cell cycle analysis on siASCL1-treated cells demonstrates a significant increase in the number of cells in the sub-G1 phase of the cell cycle, suggesting that knockdown of ASCL1 induces apoptosis. Apoptosis is quantifiably increased with all three ASCL1-targeting siRNAs, while the control siRNAs have little effect (Figure 3.8A). H1993 cells transfected with the same siRNAs show no significant difference in the amount of cells seen in the sub-G1 phase of the cell cycle indicating that ASCL1 knockdown induces apoptosis specifically in ASCL1-positive cell lines.

A separate marker for cellular apoptosis is the exposure of phosphatidylserine (PS) on the outer membrane of the cell. PS is generally flipped from the inner to the outer membrane during the early stages of apoptosis and can be used as a marker by utilizing an antibody that recognizes PS and is conjugated with a fluorescent label suitable for flow cytometric analysis.

H1755 cells were treated for 48 hours with 20 nM siSCR or siASCL1-3 and then prepared for flow cytometric analysis of outer-membrane PS. Compared to the siSCR control, siASCL1-3 treated cells had a significant shift in the number of PS-positive cells indicating a higher number of apoptotic cells (Figure 3.8B). This result mirrors what is seen by cell cycle analysis in H1755.

Cleavage of poly ADP ribose polymerase (PARP) is an apoptosis signal. PARP's main role in the cell is to detect and signal single-stranded DNA breaks to the single-strand repair machinery. PARP binds a broken DNA strand, undergoes a conformational change, and initiates its enzymatic ability to synthesize a poly-ADP ribose chain as a signal for other DNA-repairing

enzymes. During apoptosis PARP is cleaved by Caspase3 and Caspase7 resulting in 24 kDA and 89 kDA fragments. These fragments are biologically inactive and detection of the cleaved PARP fragments is a marker for cellular apoptosis.

H1755 and HCC1833 cells transfected with siASCL1-1, siASCL1-3, siASCL1-3 as well as parental, lipid-only, siSCR, and siLUC controls were harvested for western blot analysis. After 72 hours transfection with 20 nM siRNA, full-length and cleaved PARP (89 kDa) protein levels were measured. siASCL1-transfected cells in both H1755 and HCC1833 lines demonstrated an induction of PARP cleavage compared to control cells (Figure 3.8C). PARP cleavage was shown to act coincidentally with loss of ASCL1 protein expression, while control cells showed little or no induction of PARP cleavage, suggesting that loss of ASCL1 leads to apoptosis. These data suggest that ASCL1 is responsible for maintaining growth, proliferation, and survival of NE-NSCLC cell lines and that therapy targeting the ASCL1 pathway may be a viable route to therapy for this subset of lung cancers.

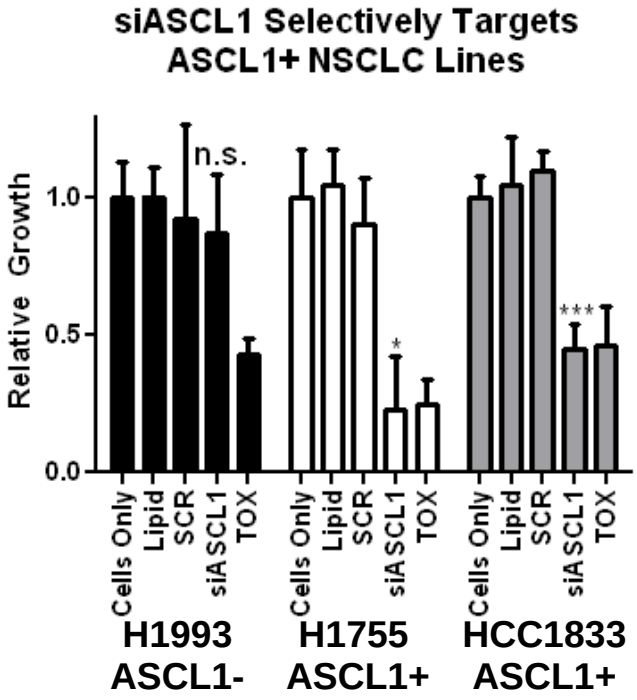

Figure 3.6: ASCL1 knockdown inhibits growth and proliferation. Knockdown of ASCL1 leads to growth reduction that is specific to NE-NSCLC cell lines. H1755 and HCC1833, following transfection, demonstrated loss of proliferation similar to toxic oligo while H1993 was unaffected by siASCL1. Viability was measured by MTS assay and calculated relative to untransfected control (* $p < 0.05$, *** $p < 0.005$).

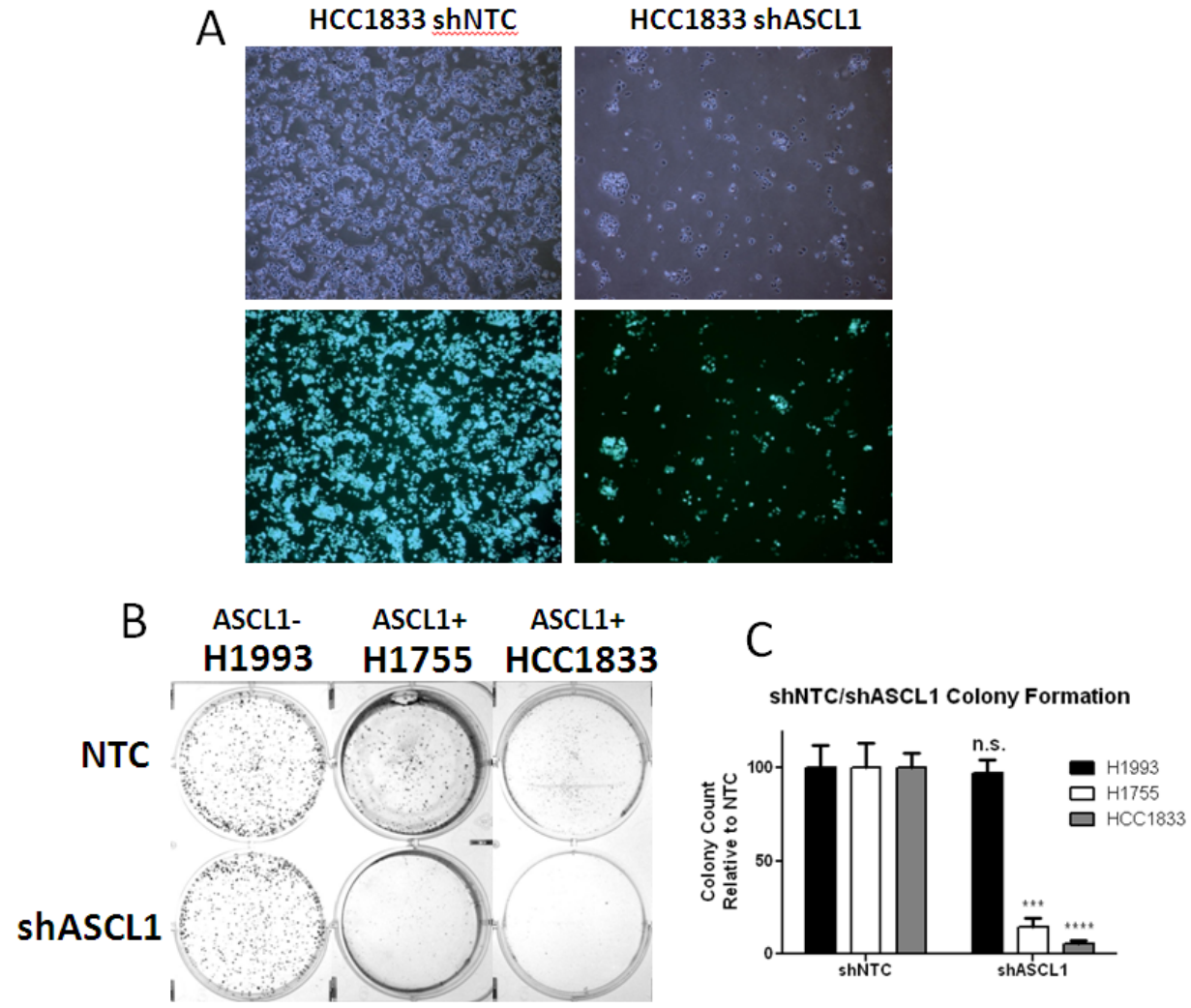

Figure 3.7: Stable knockdown of ASCL1 inhibits colony forming ability. ASCL1 stable knockdown was performed by infecting cells with shRNA targeting ASCL1 and subsequent antibiotic selection for 7 days. (A) Microscopy demonstrating integration of GFP-positive shNTC and shASCL1 constructs into HCC1833. The decrease in cell growth in shASCL1-infected HCC1833 is apparent. (B) Liquid colony formation assay demonstrated that NE-NSCLC cell lines H1755 and HCC1833 with stable knockdown of ASCL1 lose their ability to form anchorage-dependent colonies compared to shNTC-infected cells. H1993 is unaffected by shASCL1. (C) Quantification of colony forming ability (*** $p < 0.005$, **** $p < 0.001$).

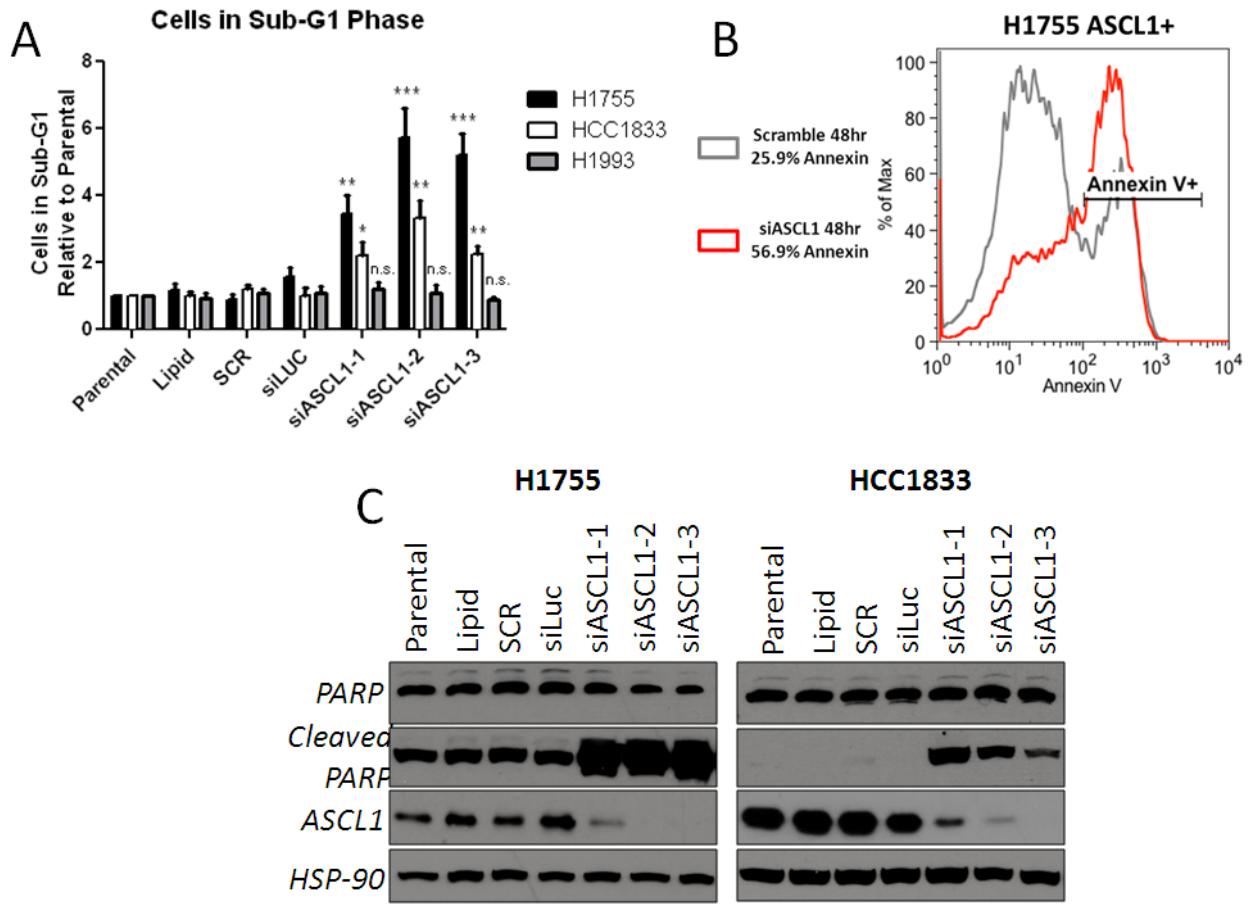

Figure 3.8: ASCL1 knockdown leads to apoptotic cell death. Inhibition of ASCL1 by siRNA results in apoptotic cell death that is detected by three methods. (A) Cell cycle analysis demonstrates siASCL1-transfected lines show a significant increase in the number of cells in the sub-G1 phase, which is analogous to apoptotic cells, compared to controls. The effect is specific to NE-NSCLC cell lines (* $p < 0.05$, ** $p < 0.01$, *** $p < 0.005$). (B) H1755 transfected with siASCL1 are more annexin positive compared to scrambled oligo control-transfected cells. (C) H1755 and HCC1833 transfected with siASCL1 demonstrate cleavage of PARP following knockdown. This blot was stripped and reprobed with primary antibodies in subsequent experiments.

3.3 Discussion

The future of cancer therapy relies on identifying certain patient populations that will respond to one treatment but not another based on the properties of the tumor and additionally creating specific drugs that target genetic pathways required for a particular tumor's formation, growth, and maintenance. An excellent example of this type of "targeted therapy" is the treatment of EGFR-mutant tumors in non-small cell lung cancer (NSCLC) with anti-EGFR agents such as erlotinib and cetuximab (Pao, Miller et al. 2004). In the case of EGFR-mutant tumors, a patient population is readily identifiable using a clinical test and a drug is available that targets the tumor-driving gene. While targeted therapies are being developed for lung cancers with similar genetic lesions, many aggressive subsets of lung cancer such as the group of neuroendocrine tumors remain without any available targeted drugs. The purpose of this study is to direct a similar approach towards developing therapies specific for pulmonary neuroendocrine tumors.

Aggressive neuroendocrine tumors of the lung account for approximately 25% of all lung cancer diagnoses and include small cell lung cancer (SCLC) and a subset of non-small cell lung cancer (NSCLC) known as large cell neuroendocrine carcinoma (Rekhtman 2010). Additionally, using genome-wide mRNA expression analyses, several groups have identified neuroendocrine differentiation in NSCLCs originally scored as adenocarcinomas (neuroendocrine-NSCLC or NE-NSCLC) (Bhattacharjee, Richards et al. 2001). Neuroendocrine tumors occur at a rate of 10-15% in NSCLC and have a much poorer prognosis than classic NSCLC. In fact, this subtype has a clinical outcome approaching that of small cell lung cancer, a disease with a five-year survival

rate of about 5% (Pelosi, Pasini et al. 2003; Howe, Chapman et al. 2005; Garcia-Yuste, Matilla et al. 2008; Gollard, Jhatakia et al. 2010). Neuroendocrine tumors represent a large portion of new lung cancer diagnoses each year in the United States (about 40,000 cases/year), yet relatively few advances have been made in terms of therapeutic management of this disease group (Rodriguez and Lilenbaum 2010). Patients with SCLC are treated with a regimen that has changed little in three decades. Patients with NE-NSCLC are treated no differently than other NSCLCs.

To address the lack of effective treatments for neuroendocrine lung cancers there has been a major push to develop representative pre-clinical models of the disease *in vitro* using cultured tumor lines and *in vivo* using mouse models. These tools have been instrumental in the discovery and implementation of targeted therapy for NSCLC with EGFR mutations and EML4-ALK fusions, which was greatly augmented by the availability of lung cancer cell lines. A pre-clinical model for NE-NSCLC would significantly increase our understanding of disease biology and positively impact the development of targeted therapies for up to 40,000 lung cancer patients per year.

In this study, using the large legacy datasets on lung cell lines from the Minna and Gazdar laboratories, including genome-wide mRNA expression microarrays and oncogene/tumor suppressor mutation data, a class of neuroendocrine non-small cell lung cancer cell lines was identified. These NE-NSCLC cell lines were derived from patients demonstrating a wide range of NSCLC histology, including adenocarcinomas, large cell/neuroendocrine carcinomas, and carcinoids. Despite their dramatic histological/pathological differences, the cell lines established

from these patients' tumors demonstrate very similar gene expression profiles, indicated by the high expression of neuroendocrine markers.

The first approach to identify NE-NSCLC cell lines involved an unsupervised, unbiased clustering analysis of the genome-wide mRNA expression data available on 207 lung cell lines. The cell lines utilized included 119 NSCLCs, 29 SCLCs, and 59 HBEC/HSAECs. Clustering was performed using the Pearson method with average linkage and resulted in a separation of cell lines by histological type, grouping together NSCLCs, HBEC/HSAECs, and SCLCs. However, with the SCLC cluster were 11 NSCLC cell lines. Due to their close association with SCLCs, which are known to be neuroendocrine cell lines, the assumption was made that the 11 NSCLCs employed a similar neuroendocrine gene expression profile and were termed NE-NSCLC cell lines.

No previous attempt has been made in the literature to develop a valid pre-clinical model for NE-NSCLC despite the knowledge that neuroendocrine gene expression occurs in NSCLC has existed for some time (Berendsen, de Leij et al. 1989). This is the first description of such a pre-clinical model. Interestingly, the lack of association of neuroendocrine gene expression with histological subtype in NSCLC suggests that neuroendocrine genes can be expressed in tumors of any origin. A diagnosis of neuroendocrine features should not be ruled out solely based on pathological analysis.

Expression of neuroendocrine genes in NE-NSCLC is similar to that of SCLC, and includes overexpression of known NE markers such as CHGA, CHGB, DDC, and SCG3. In addition, the lineage-specific transcription factor ASCL1 is widely expressed in NE-NSCLC and

SCLC cell lines. ASCL1 is required for the formation of pulmonary NE cells (PNECs) and is therefore known as a lineage transcription factor. Prior research has demonstrated the importance of ASCL1 in regulating the survival of SCLC. One of the first knockdown studies of ASCL1 in SCLC was performed in ACC-LC-91 cells (Osada, Tatematsu et al. 2005). Loss of ASCL1 in those cells led to cell cycle arrest, inhibition of proliferation, apoptosis, and decreased tumor growth *in vivo*. Similarly, transient knockdown of ASCL1 in H1618 resulted in inhibition of anchorage-independent colony forming ability, induction of apoptosis, and decreased proliferation (Jiang, Collins et al. 2009). In the SCLC cell line H1618, it was postulated that ASCL1 directly regulates the transcription of the cancer stem cell associated factors ALDH1A1 and CD133/PROM1 and the conclusion was made that ASCL1 regulates tumorigenicity in SCLC by controlling cancer stem cell populations. The goal of this study is to perform similar knockdown studies in NE-NSCLC cell lines to determine if ASCL1 is required for the growth of these tumors and subsequently if targeting the ASCL1 pathway can serve as a viable therapeutic option.

ASCL1 mRNA and protein expression was validated by qRT-PCR and western blot analysis, respectively. Transient knockdown studies were performed via transfection of short interfering RNA (siRNA) molecules targeting the ASCL1 gene. A benefit of discovering high ASCL1 expression in NSCLC is the propensity of NSCLCs to grow as single-layer, attached epithelial cells, making these cell lines amenable for transfection. This is in stark contrast to the *in vitro* behavior of SCLCs, which tend to grow as spheroids in suspension and are difficult if not impossible to transfect. Transfection conditions were determined for H1755 and HCC1833 NE-

NSCLC cell lines. Knockdown of ASCL1 in those cell lines resulted in decreased proliferation as measured by MTS assay and induction of apoptosis. Apoptosis was detected by positive annexin staining, accumulation of cells within the sub-G1 phase of the cell cycle, and cleavage of PARP. Similarly, long-term knockdown of ASCL1 through the use of stably introduced short-hairpin RNAs (shRNA) resulted in decreased anchorage-dependent colony forming ability. In both the transient and long-term knockdowns, loss of ASCL1 resulted in growth defects and cell death only in ASCL1+ cell lines. A control NSCLC cell line without ASCL1 expression was insensitive to siASCL1 and shASCL1 treatment demonstrating that only ASCL1+ NE-NSCLCs are vulnerable to knockdown.

The inhibition of growth and induction of cell death following knockdown of ASCL1 presents a therapeutic opportunity for ASCL1-dependent NE-NSCLCs. This effect is similar to that previously reported for SCLC by several groups indicating that lung cancers expressing ASCL1, irrespective of histology, are sensitive to knockdown of the gene (Osada, Tatematsu et al. 2005; Osada, Tomida et al. 2008; Jiang, Collins et al. 2009). Since ASCL1 is a known lineage transcription factor, required for the establishment of several specific neural and neuroendocrine cell types during development, including PNECs, the assumption can be made that ASCL1 functions as a lineage-dependent oncogene in lung cancer. Prior studies of lineage-dependent oncogenes including TTF1 in lung adenocarcinoma and SOX2 in lung squamous cell carcinoma revealed that TTF1 and SOX2 are highly amplified in a select group of those respective tumors (Kwei, Kim et al. 2008; Bass, Watanabe et al. 2009). However, SNP analysis demonstrates that despite the high expression of ASCL1, it is not amplified. Genome-wide DNA sequencing on

SCLC patient samples and SCLC cell line reveals that ASCL1 is also not mutated. The latter result is not surprising as ASCL1 is a short protein and there is likely selective pressure to maintain the wild-type conformation in order to maintain proper transcriptional fidelity.

ASCL1, as a basic helix-loop-helix (bHLH) transcription factor, is not likely to be involved in any processes besides dimerization and DNA binding to promote or inhibit DNA transcription. Therefore, the cell death phenotype associated with loss of ASCL1 expression is likely due to the loss of transcriptional activity of a downstream target or targets required for cancer cell survival. If decreased expression of a required downstream target results in cell death and that target is "druggable" or targetable with small molecule inhibitors, it can then become a viable therapeutic option for ASCL1-dependent lung cancers.

CHAPTER FOUR

PROGNOSTIC AND THERAPEUTIC IMPLICATIONS OF ASCL1 TRANSCRIPTIONAL TARGETS

4.1 Introduction

Transcription factors exert their biological function by binding to DNA and either promoting or inhibiting transcription of genes. Understanding the genetic targets of transcription factors has been instrumental in increasing our knowledge of developmental pathways activated during cell lineage establishment (McGill, Horstmann et al. 2002). During development, transcription factors act in a coordinated manner to ensure proper growth and differentiation of tissues, and often control or are controlled by pro-growth pathways. It is therefore unsurprising that cancers have learned to hijack transcription factor biology for their pro-tumorigenic potential. In the case of melanoma, a certain subset of those tumors amplifies the MITF transcription factor (Garraway, Widlund et al. 2005), which during development is required for the establishment of melanocytes (Goding 2000; Widlund and Fisher 2003). Subsequent analysis resulted in the identification of the RAS/RAF/MEK/ERK pathway as a modulator of MITF activity and led directly to the development of vemurafenib, a BRAF inhibitor, as an FDA-approved therapy for late-stage melanoma patients (Wellbrock, Rana et al. 2008; Chapman, Hauschild et al. 2011). This suggests that research focused on lineage-dependent transcription

factor oncogenes can result in the identification of actionable therapeutic targets with clinical applications.

ASCL1 is a potential lineage oncogene transcription factor in neuroendocrine lung cancers, including SCLC and NE-NSCLC. To date, few transcriptional targets of ASCL1 are known and the upstream signaling regulating ASCL1 is controversial at best. Validated downstream targets of ASCL1 include DLL1 and DLL3, members of the NOTCH pathway (Henke, Meredith et al. 2009; Castro, Martynoga et al. 2011; Kim, Ables et al. 2011). Recent publications suggest that ASCL1 regulates matrix metalloproteases (MMPs), drug-resistance genes (MGMT), and cyclin-dependent kinases (CDK5) (Demelash, Rudrabhatla et al. 2012; Wang, Jensen-Taubman et al. 2012). While each of these targets is important in their own context, it is unlikely that a single-target approach will provide enough resolution toward the identification of actionable therapeutic targets.

The past decade of research has brought to the forefront high-throughput technologies capable of genome-wide resolution. This technology has accelerated biological discovery and exponentially increased the ability to perform top-down research, particularly in the area of oncology. In this way, unbiased approaches can be utilized to discover genetic changes in cancer cells that have the potential to be exploited therapeutically. Comparisons to normal, non-tumorigenic cells will rule out broadly cytotoxic approaches and narrow efforts towards discovery of cancer-specific acquired vulnerabilities. Chromatin immunoprecipitation is an accepted method of understanding protein-DNA interactions and determining direct transcriptional control of a gene by a transcription factor or transcription factor complex. High-

throughput sequencing has developed that technology one step further by allowing for the identification of transcription factor binding sites on a genome-wide level. That is, chromatin immunoprecipitation followed by massively parallel DNA sequencing (ChIP-Seq) can provide a genome-wide transcriptome understanding of a single transcription factor. A transcriptome understanding of ASCL1 would provide a list of genes potentially regulated by ASCL1. This would serve as a starting point for discovering downstream targets of ASCL1 required for survival.

ASCL1 is primarily studied in mammalian cells within the context of neuronal differentiation. Neurogenesis during embryonic development is regulated in part by ASCL1, which promotes cell cycle exit in neuronal progenitors and allows for the differentiation of those stem cells into functional neurons (Bertrand, Castro et al. 2002; Ross, Greenberg et al. 2003). Overexpression of ASCL1 in neuronal stem cell cultures rapidly induces differentiation into functional neurons (Casarosa, Fode et al. 1999; Berninger, Guillemot et al. 2007; Geoffroy, Critchley et al. 2009), while loss of ASCL1 coincides with dramatic decrease of basal ganglia neurons (Casarosa, Fode et al. 1999; Horton, Meredith et al. 1999; Marin, Anderson et al. 2000; Yun, Fischman et al. 2002). In order to study the transcriptional network controlled by ASCL1 in neuronal cell populations, Castro and colleagues performed ChIP-Chip analysis on embryonic telencephalon and cultured neuronal stem cells (Castro, Martynoga et al. 2011). This study was able to utilize a genome-wide approach to study the full range of ASCL1 transcriptional targets in mouse brain and use that data to postulate how ASCL1 regulates neurogenesis during embryonic development. The authors discovered, through the combination of transcriptome and

expression analyses, that ASCL1 regulates a diverse network of genes with broad applications to many cellular processes. Common and known targets such as regulators of the Notch pathway were well represented along with regulation of genes that promote cell cycle exit. Prominently, ASCL1 was found to play a role in both early and late neurogenesis, however an unexpected finding was that ASCL1 positively regulates the expression of positive cell cycle regulators. The ChIP-Chip study therefore demonstrates that ASCL1, during embryonic neurogenesis, controls the development of neurons through the successive phases of proliferation, cell cycle exit, and differentiation. This research demonstrates how ASCL1 can act as a master regulator of cell lineage establishment by expertly coordinating the transcription of a large number of genes. Besides the effect on development, through the regulation of pro-tumorigenic positive cell cycle regulators, ASCL1 may also function as an oncogene in pre-neoplastic cells. Cancer cells may utilize and, indeed, learn to depend on, ASCL1 for these pro-growth effects. Despite the commonality of Notch signaling members discovered from the Castro study, the biological function of a transcription factor depends on many elements, including progenitor lineage, chromatin structure, and other context-dependent effects. Additionally, the context-dependent expression of transcriptional coregulators modulates DNA binding and can affect mRNA splicing. *Cis*-enhancer regions are also important in determining transcriptional regulation that is cell-type dependent. For these reasons, it is critical to determine the ASCL1 transcriptional profile in lung cancer, as the genes ASCL1 regulates in the lung may be quite different than those ASCL1 regulates during neurogenic differentiation.

The identification of ASCL1 dependence in a novel class of NE-NSCLC cell lines, as explained in the previous chapter, suggests that downstream targets of ASCL1 are required for cancer cell survival. In the following studies, ChIP-Seq analysis was performed on ASCL1+ SCLC and NE-NSCLC cell lines in an attempt to describe the transcriptional profile regulated by ASCL1. Multiple cell lines were chosen in order to gain a consensus understanding of ASCL1 target genes, as there may exist cell line context-dependent singular targets. Additionally, both SCLC and NE-NSCLC cell lines were utilized in the ChIP-Seq analysis due to the very similar gene expression profiles of the cell lines. Though the histological typing of the original patient tumors was dramatically different, the mRNA expression profiles of the resulting cell lines are similar, including high expression of ASCL1.

To date, ChIP-Seq analysis on lineage-dependent transcription factors in the lung has been limited to TTF1 amplified cell lines (Watanabe, Francis et al. 2013), which resulted in the identification of downstream targets with therapeutic potential for TTF1-dependent lung adenocarcinoma. The studies described in the following chapter represent the first cancer-specific transcriptome analysis of the ASCL1 transcription factor. The aim of this work is to identify a consensus ASCL1-specific gene regulatory network with the goal of extending this work towards finding actionable, survival-associated downstream targets that can serve as potential therapeutic interventions in the clinic for ASCL1-dependent lung cancers.

4.2 Results

4.2.1 Chromatin Immunoprecipitation of ASCL1-Positive Lung Cancer Cell Lines

DNA-protein interactions can be studied through chromatin immunoprecipitation (ChIP). ChIP was performed on five ASCL1+ cell lines, including SCLCs H128, H1184, H207 and NE-NSCLCs H1755 and HCC4018. 10 million cells were grown in mass culture prior to being fixed in formaldehyde and ASCL1 bound to DNA precipitated. The DNA prepared from the cells was then amplified and verified for biological fidelity. Known ASCL1 target genes include the Notch receptor ligands DLL1 and DLL3. qRT-PCR performed on those genes from the ASCL1-bound DNA demonstrates an enrichment of the known target sites (Figure 4.1) A negative control region with which ASCL1 is known not to bind does not demonstrate enrichment in ASCL1+ samples. For each ASCL1+ cell line, there exists enrichment in DLL1 and DLL3 DNA compared to the control regions. This demonstrates that the data obtained from ChIP is biologically accurate and amenable for massively parallel DNA sequencing.

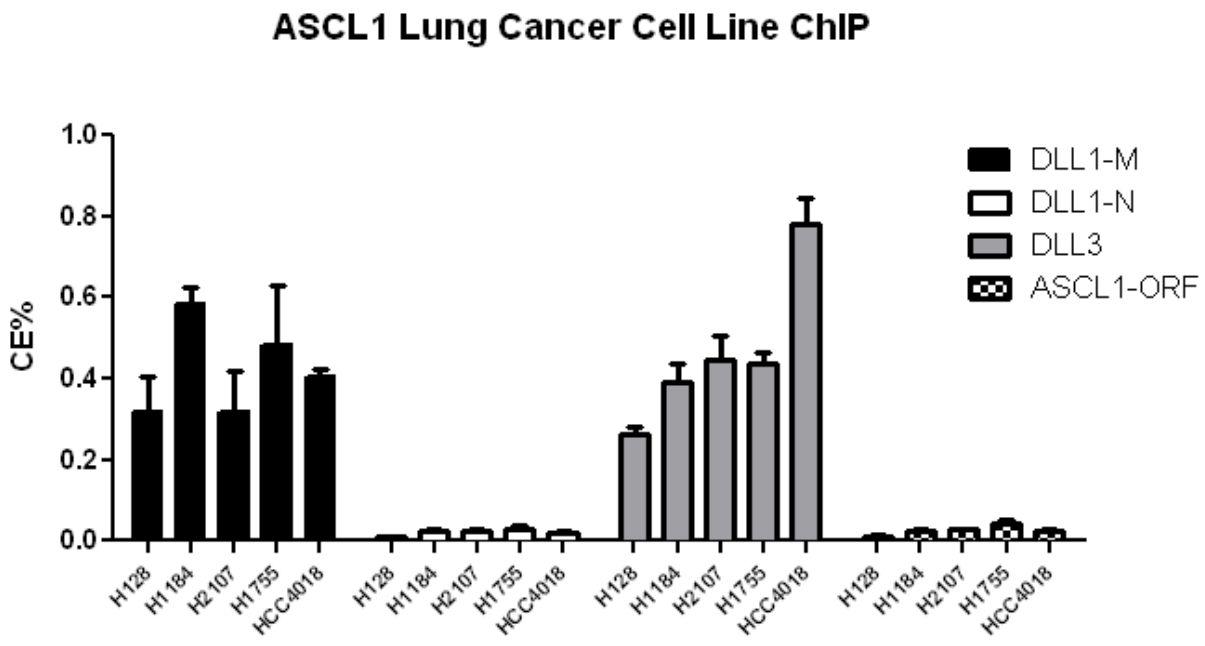

Figure 4.1: ASCL1 ChIP qRT-PCR of known target regions. ASCL1 ChIP performed on five ASCL1+ cell lines was tested for biological fidelity by qRT-PCR analysis of known target sites. ChIP efficiency is plotted. Each ASCL1+ DNA sample amplified known target regions in DLL1 and DLL3, while sites where ASCL1 is known not to bind (DLL1-N and ASCL1-ORF) are unamplified. This experiment performed by Mark Borromeo of the Jane Johnson lab, UTSW.

4.2.2 Massively Parallel DNA Sequencing of Cell Line ChIP Samples

The ability to perform genome-wide DNA sequencing of ChIP samples allows for obtaining a genome scale understanding of transcription factor binding. This data can be used to infer transcriptional targets. For the purposes of this study, ChIP-Seq on ASCL1 will be useful in identifying downstream targets of ASCL1 required for survival. Those deemed to be druggable, either with small molecules presently designed to hit those targets, or novel targets with therapeutically actionable domains can be used as potential treatments.

ChIP-Seq libraries on five ASCL1+ cell lines and two ASCL1-negative control SCLC lines (H524 and H526) were prepared using the NEBNext ChIP-Seq Library kit. Following the addition of indexing primers and adapters from Illumina, DNA samples were sequenced on the Illumina High-Seq 2000 sequencer. The number of mapped reads following alignment to the human reference genome (HG19) with Bowtie (Langmead, Trapnell et al. 2009) varied from 19 million to 73 million (Table 4.1).

Aligned reads were then processed for peak calling using Model-Based Analysis for ChIP-Seq (MACS) (Zhang, Liu et al. 2008). The number of ASCL1-bound peaks found by MACS for each sample is also available in Table 4.1. These peaks are visual representations of the number of sequence tags at a given genomic location and presumably correspond to ASCL1-bound sites. The peaks can then be analyzed based on their genomic location and used to infer peak-gene interactions. Relative peak heights normalized to the control samples are shown in Figure 4.2A and demonstrate significant signal enrichment compared to non-ASCL1 expressing control cell lines.

Transcription factors bind canonical DNA sequences within the promoter or regulatory regions of a given target gene. ASCL1 is a basic helix-loop-helix transcription factor and is known to bind E-box motifs (CANNTG). Using sequencing data it is possible to infer a common DNA binding motif for ASCL1 based on peak analysis. Heterogeometric Optimization of Motif EnRichment (HOMER) is a publically available program that searches the DNA within peak regions to find frequently recurring sequences that may correspond to common binding motifs (Heinz, Benner et al. 2010). Based on the analysis of peak-level sequencing data, HOMER discovered a canonical E-box binding site, CAGNTG, present in the majority of ASCL1 peaks in all five ASCL1+ cell lines (Figure 4.2B). The motif was present in 77% to 95% of all peaks indicating a strict degree of specificity for this canonical binding sequence (Table 4.1).

The ChIP-Seq analysis performed indicates a dramatic heterogeneity in the number and location of peaks in each of the ASCL1+ cell lines. Clustering analysis was therefore necessary to determine the location of shared peaks amongst all five ASCL1+ cell lines compared to controls. Hierarchical clustering was used to identify consensus peaks, with a maximum distance of 300 bp between peak summits allowed for consideration of consensus peaks. A new peak summit was then calculated from the summits of member peaks and weighted by fold change. This method resulted in the identification of 912 consensus peaks (Figure 4.2B) with a shared canonical CASSTG E-box site that appears in nearly 88% of those peaks. A BED file was then populated with the genomic locations of the 912 consensus peaks and prepared for peak-gene interaction analysis, which provides an estimate of genes transcriptionally regulated by ASCL1 due to their proximity to the consensus binding peaks of ASCL1 throughout the genome.

Sample	Reads	Peaks	% of Peaks with Primary Motif	P-Value for Motif
Shared	--	912	87.70%	1e-509
H128	19×10^6	8,363	70.43%	1e-3768
H1184	30×10^6	10,269	81.09%	1e-4825
H2107	67×10^6	8,914	94.94%	1e-4461
H1755	34×10^6	8,395	77.08%	1e-12512
HCC4018	73×10^6	4,329	84.71%	1e-2072

Table 4.1: ASCL1 ChIP-Seq data overview. Data gathered during ChIP-Seq analysis. Samples are labeled. "Shared" corresponds to common peaks among all five samples. The number of 50 bp reads was determined by Bowtie. Peaks were identified using MACS. Motif analysis was performed with HOMER. Computational analysis of ChIP-Seq data was performed by Tao Wang of the Yang Xie lab, UTSW.

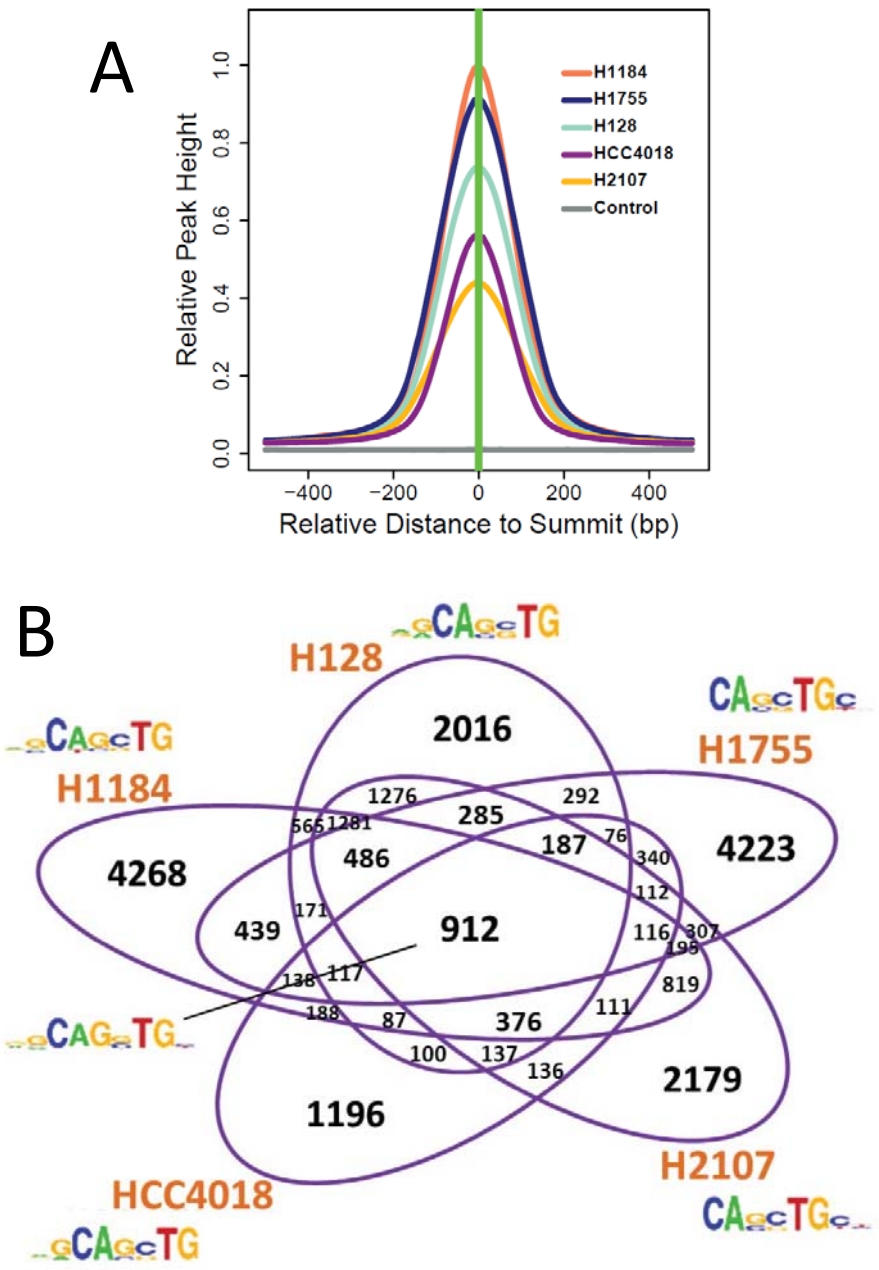

Figure 4.2: ASCL1 ChIP-Seq peak analysis. ASCL1-bound peaks were uncovered using MACS. (A) Relative peak height for the five ASCL1+ samples is displayed relative to the control samples. (B) Venn diagram demonstrating the number of peaks across the samples and the shared peaks between each sample. The most significant DNA binding motif present in each sample is displayed along with the consensus E-box motif across all samples.

4.2.3 Identifying ASCL1 Target Genes through Peak-Gene Interactions

Target genes of ASCL1 hold immense value as potential therapeutic targets due to the lethality seen in NE-NSCLC cell lines following ASCL1 knockdown. Identification of consensus ASCL1-bound peaks across a range of ASCL1+ cell lines presents the opportunity to gain a genome-wide transcriptome understanding of ASCL1. However, relating peaks to genes and inferring binding site-gene interactions is non-trivial due to the unequal spacing of genetic information throughout the human genome. For example, there exist many gene rich regions and many gene-poor regions. These gene poor regions – gene deserts – often contain an incredible amount of regulatory information. Transcription factor binding sites that occur in gene deserts are difficult to associate with the genes that a given particular transcription factor may regulate. Depending on sequence and context-specific clues, a transcription factor may regulate Gene A in one cell type and Gene B in another even if Gene A and Gene B are on the same chromosome and near a transcription factor binding site. These combinatorial regulatory codes are complex and prevent from simply assigning binding peaks to the nearest available gene. To process ChIP-Seq data and arrive at a list of genes that may correspond to transcription factor regulatory genes, the Bejerano lab developed a modeling algorithm that utilizes several rules in order to parse out peak-gene interactions that are most likely to be biologically active (McLean, Bristor et al. 2010).

Genomic Regions Enrichment of Annotations Tool (GREAT) is a program that integrates ChIP-Seq peak data with known genetic regulatory regions to develop a list of potentially regulated genes. The rules for flexible peak assignment are as follows: if a peak is within 5 kb

upstream or 1 kb downstream of the transcriptional start site (TSS) of a particular gene, then assign that peak only to those genes that fall within the range. This corresponds to a gene's basal regulatory region. If a peak falls within 1 Mb upstream of downstream of a gene, then assign that peak to all genes within the range. This corresponds to a gene's extended regulatory region. Using these rules, the 912 consensus ASCL1-bound peaks correspond to 1330 genes. The analysis performed by GREAT results in only 6 peaks that were unassigned and were not associated with any genes. 193 peaks were assigned one gene, 712 peaks were assigned two genes, and 1 peak was assigned three genes (Figure 4.3A). The 1330 genes resulting from GREAT analysis were mostly the result of long-range peak-gene interactions. 224 genes were determined to lie within 0-5 kb of the TSS, while the remaining genes interact with peaks at distances between 5 kb and 1 Mb (Figure 4.3B).

Besides providing a list of genes, GREAT also performs gene ontology analysis in order to discover commonly targeted pathways. Gene ontology (GO) analysis is useful for identifying biological themes from a large list of genes and may point to enrichment of various pathways. GO analysis performed on the 1330 genes potentially regulated by ASCL1 resulted in an enrichment of terms within the Notch pathway (Table 4.2) including the appearance of known ASCL1 targets DLL1 and DLL3 (Figure 4.4). The GO analysis, by demonstrating enrichment of Notch terms, suggests that the ChIP-Seq data are valid and biologically accurate.

ASCL1 expression is frequently associated with neuroendocrine gene expression. Loss of ASCL1 expression in several models is associated with inhibition of neuroendocrine features, such as loss of CHGA/CHGB, NCAM, and DDC expression. Prior work showed that

overexpression of ASCL1 is sufficient to induce expression of certain neuroendocrine markers (Osada, Tatematsu et al. 2005; Osada , Tomida et al. 2008) suggesting that ASCL1 is a lineage gene that also supports the neuroendocrine phenotype. GO analysis demonstrated that ASCL1 contains binding sites with the promoter regions of several neuroendocrine genes, including CDH2 (NCAM), GRP, INSM1, and SYT1 (Figure 4.5). It is likely, therefore, that ASCL1 promotes and supports the neuroendocrine phenotype in ASCL1+ lung cancer cell lines.

In the previous chapter, an unsupervised clustering analysis of genome-wide mRNA expression data revealed a cluster of neuroendocrine cell lines that contained all SCLC lines and the 11 NE-NSCLC lines. Following the development of the 1330 ASCL1-associated ChIP-Seq signature, a supervised clustering analysis was performed on the 207 lung cell lines to determine if putative ASCL1 targets were sufficient in grouping together the neuroendocrine cell lines. Using the Pearson method and average linkage clustering, 1006 gene targets remained following filtering, and those genes were sufficient to cluster the SCLC and NE-NSCLC separately from NSCLCs and HBECs/HSAECs suggesting that ASCL1 target genes may provide a biomarker to differentiate neuroendocrine lung tumors from non-neuroendocrine lung tumors, and also differentiate between NE cancers and normal cells (Figure 4.6).

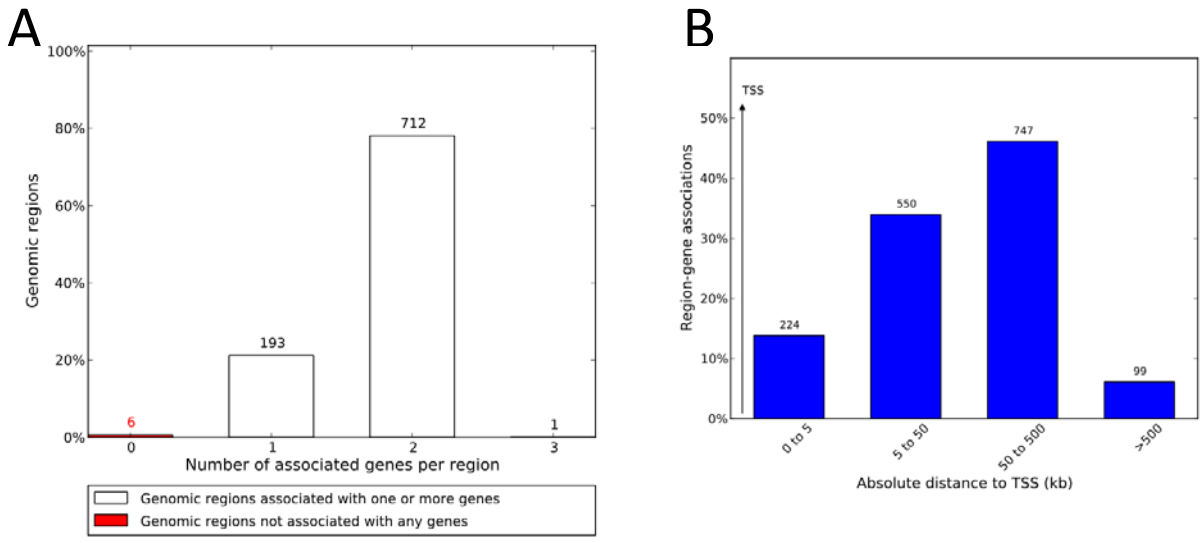

Figure 4.3: GREAT analysis of ASCL1 consensus peaks. ASCL1-bound peaks discovered from ChIP-Seq analysis were profiled for peak-gene interactions using the GREAT software package. (A) The majority of consensus peaks (712 of 912) were correlated with two genes. Only one peak was associated with three genes. Six peaks were not assigned to any genes. (B) The majority of peak-gene interactions are long range. Only 224 genes were within 0 to 5 kb of the transcriptional start site. 846 genes interacted with peaks at a distance of 50 to 1000 kb.

Gene	Peak Region (distance to TSS)
DLL1	Peak 703 (-1,435)
DLL3	Peak 300 (-880)
DLL4	Peak 152 (-790)
DTX1	Peak 93 (+58,658)
DTX2	Peak 770 (-87)
HES1	Peak 623 (+196,535)
HES5	Peak 412 (-4,668)
LFNG	Peak 755 (+4,542)
NCOR2	Peak 82 (-152,878), Peak 74 (-19,415)
NOTCH1	Peak 859 (+18,932), Peak 874 (+56,923)
PSENEN	Peak 333 (-4,550)
RBPJ	Peak 658 (+131,938)

Table 4.2: Notch pathway representation in ASCL1 ChIP-Seq analysis. The Notch pathway is a major regulator of ASCL1 expression. Validated ASCL1 targets include DLL1 and DLL3, which are used to signal to adjacent cells via Notch receptors to inhibit ASCL1 expression. The Notch pathway is strongly represented in the ASCL1 ChIP-Seq data, including DLL1 and DLL3, suggesting that the ASCL1 ChIP-Seq experiment maintains biological fidelity. Notch pathway genes were determined by gene ontology analysis. The peak region and the distance of that peak to the transcriptional start site of the gene are indicated.

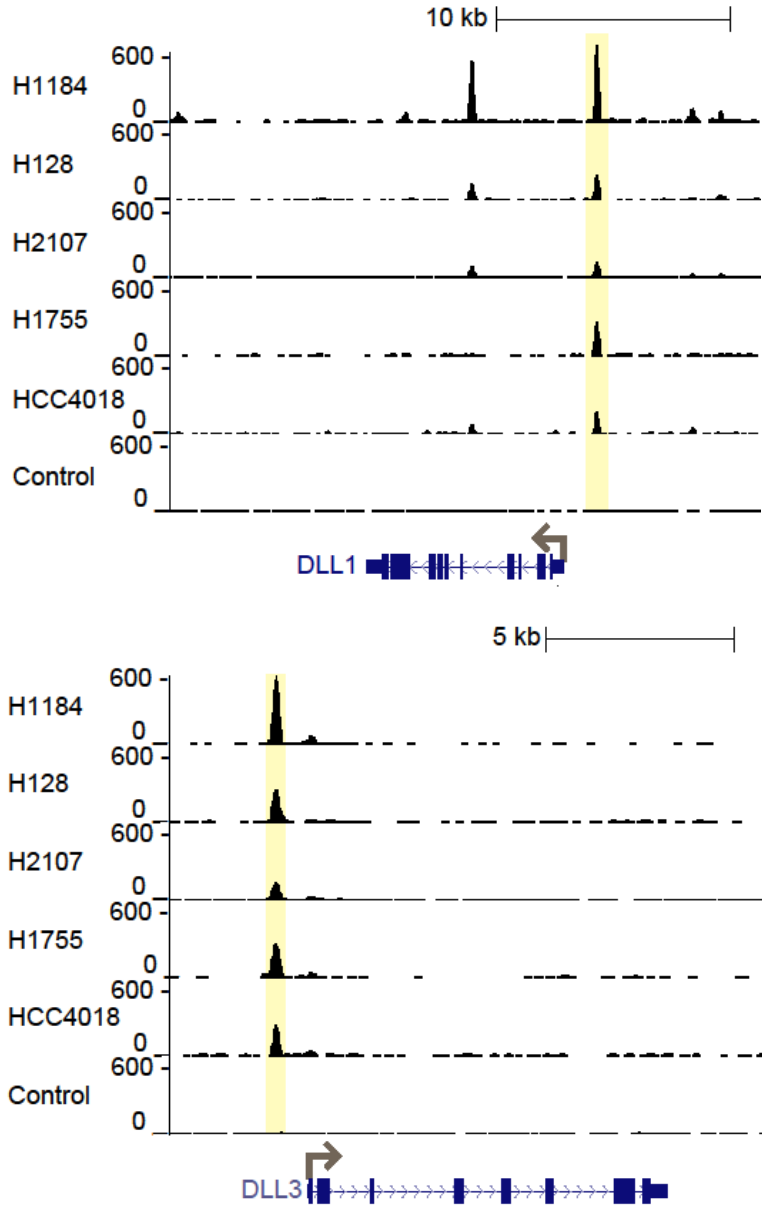

Figure 4.4: DLL1 and DLL3 contain ASCL1 binding peaks. DLL1 and DLL3 were verified ASCL1 transcriptional targets. ChIP-Seq data gathered on five ASCL1+ cells demonstrate consensus binding sites in each cell line compared to control. ASCL1-bound peaks are evident in the basal regulatory region (0 to 5 kb to TSS) of both genes. ChIP-Seq plots created by Tao Wang of the Yang Xie lab, UTSW.

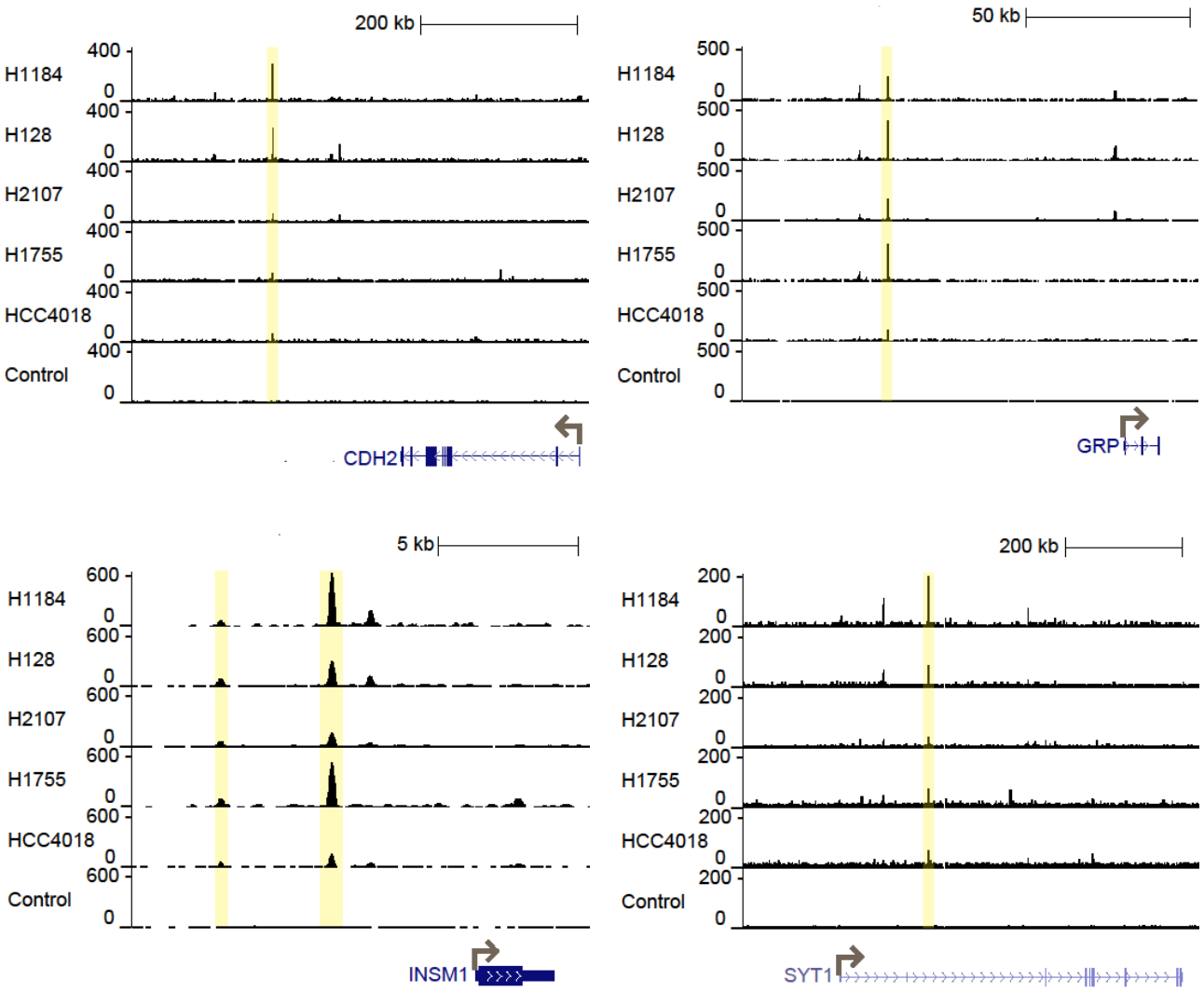

Figure 4.5: ASCL1 binding peaks are associated with common neuroendocrine genes. ChIP-Seq data suggest that ASCL1 regulates the expression of common neuroendocrine genes. CDH2 (NCAM), GRP (Bombesin), INSM1, and SYT1 are all significantly overexpressed in NE-NSCLC cell lines and each gene contains conserved ASCL1 E-box binding sites. These data suggest that ASCL1 regulates the neuroendocrine phenotype in ASCL1+ lung cancers including SCLC and NE-NSCLC

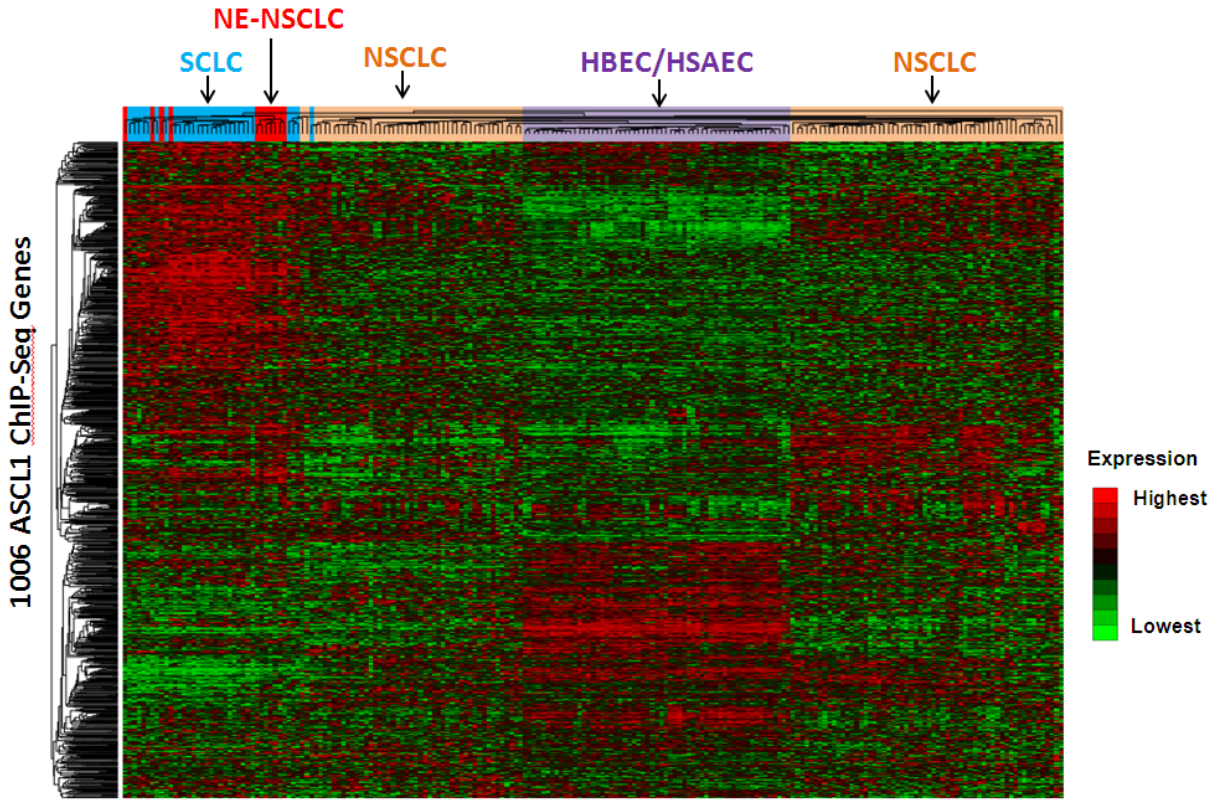

Figure 4.6: Clustering lung cell lines using genes identified from ASCL1 ChIP-Seq analysis. Supervised clustering using the Pearson Method (average linkage) was used to group 207 lung cell lines according to their expression of 1330 genes identified as putative ASCL1 targets from the ChIP-Seq analysis. Following filtering, 1006 genes remained. The clustering analysis was able to group together SCLC and NE-NSCLC cell lines separately from NSCLC and HBEC/HSAECs. Genes that are overexpressed in neuroendocrine cancers compared to NSCLC and HBEC/HSAECs are readily apparent.

4.2.4 Determining Prognostic Potential of ASCL1 Target Genes in NSCLC

Two separate methods were then used to determine overexpression of ASCL1 ChIP-Seq targets in ASCL1+ cell lines. First, the cohort of 11 NE-NSCLC and 29 SCLC cell lines profiled for genome-wide mRNA expression was used to find genes significantly positively correlated with ASCL1 expression. A significant positive correlation ($R > 0.70$ and $p < 0.01$) was found for 492 genes, of which 125 appeared in the ChIP-Seq GREAT analysis (125 of 1330). The 125 genes were then used to cluster all 119 NSCLC cell lines. 9 of 11 NE-NSCLC clustered together (Figure 4.7) with H1155 and H2106 dropping out. H1155 was previously shown to depend on a separate neurogenic transcription factor, NeuroD1, for survival (Osborne et al., 2013) while H2106 does not express ASCL1 transcript. This suggests that the 125-gene ASCL1 target overexpression signature is sufficient to group together NE-NSCLC cell lines that both express and depend on ASCL1 for survival.

The 125-gene signature was then tested for prognostic information by identifying patients at high risk for expressing the signature and then querying available survival data. The gene signature was tested on several patient data sets, including the MDACC SPORE database, the NCI Director's Challenge, and the Tomida dataset. For the purposes of this study, all tumors studied were lung adenocarcinomas. Initially the gene signature was trained on one dataset (ex. NCI Director's Challenge) using supervised principal component analysis (Bair and Tibshirani 2004) and the resulting continuous variable was then validated using a testing set (ex. Tomida dataset). The testing set was divided into two-equal sized risk groups using the median of the predicted risk scores. Survival data demonstrates that patients at high-risk for expressing the 125-

gene ASCL1 signature have poorer overall survival (Figure 4.8A-C) and this result is consistent in each dataset. Training on the NCI Director's Challenge and then using either the Tomida or MDACC SPORE datasets, significantly poorer survival is seen in patients with higher risk scores (more likely to express the gene signature) compared to those patients with lower risk scores. Similarly, training on the Tomida dataset and applying to MDACC SPORE or NCI and training on MDACC SPORE and applying to Tomida or NCI shows poorer survival for those patients at higher risk for expressing the gene signature. The survival data demonstrates that ASCL1 target gene expression is a poor prognostic indicator for lung adenocarcinoma. Prior studies indicated that neuroendocrine gene expression is a poor prognostic indicator in NSCLC and these results narrow the poor prognosis to just ASCL1 target genes.

The second method to identify overexpressed ASCL1 target genes utilized log ratio gene expression analysis between the cell lines used for ChIP-Seq. NE-NSCLCs H1755 and HCC4018 along with SCLCs H128, H1184, and H2107 were grouped together and compared to ASCL1-negative SCLCs H524 and H526. Log ratio analysis to discover significantly upregulated genes from the list of 1330 ASCL1 targets was performed using the MATRIX software developed by Girard et al (publication pending). 72 genes were found to be significantly upregulated and those genes were used to cluster the NSCLC cell lines (Figure 4.9). Similar to the previous analysis, the majority of the NE-NSCLC grouped together with the lone drop out being H2106, which does not express any ASCL1 transcript. Both the 125-gene and the 72-gene signatures are able to categorize the NE-NSCLC cell lines.

Similar to the prognostic abilities of the 125-gene signature, the 72-gene signature also predicts for poor survival in lung adenocarcinoma patients with higher risk of expressing the ASCL1 signature. In each case, the data demonstrate a significant separation of low risk and high risk patients (Figure 4.10A-C). Due to the long-term follow up of the data sets, it is more accurate to view prognosis out to the five-year mark, as beyond five years it is more likely that patients succumb to comorbidities rather than tumor burden. The five-year prognostic ability of the 125-gene and 72-gene signatures is generally more accurate than the overall prognosis. Despite the ability of the ASCL1 target gene signatures to predict for poor survival in retrospective analyses of patient datasets, the risk scores calculated via principal component analysis only provide prognosis and are not amendable for use as a diagnostic biomarker.

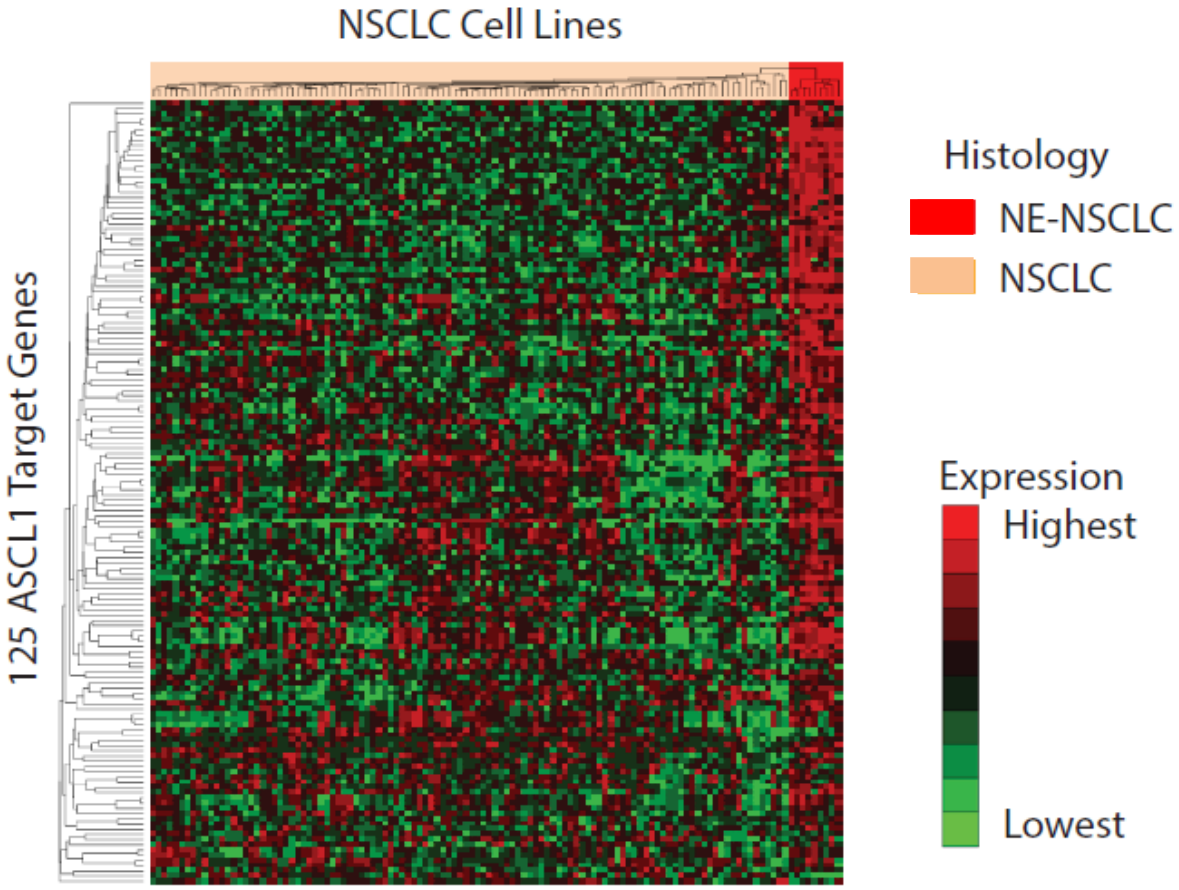

Figure 4.7: Clustering of NSCLC lines using 125-gene ASCL1 target gene signature. The 125-gene signature, identified by comparing genes highly correlated with ASCL1 expression and genes uncovered following ChIP-Seq analysis, was sufficient to group together the NE-NSCLC lines separately from typical NSCLC lines. H1155 and H2106 do not group with the remaining NE-NSCLC cell lines. H1155 is regulated by NeuroD1 while H2106 does not express ASCL1.

A

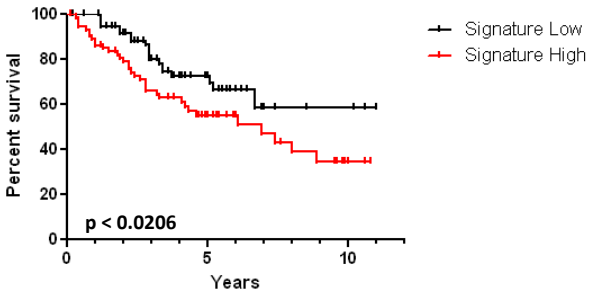
125 Gene NCI to MDACC SPORE
Overall Survival
Percent survival
Years
p < 0.0206
Signature Low
Signature High

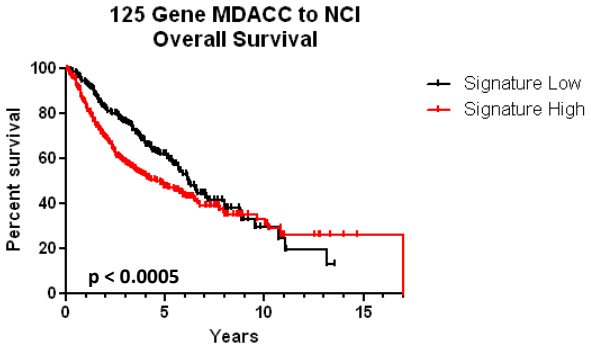
125 Gene MDACC to NCI
Overall Survival
Percent survival
Years
p < 0.0005
Signature Low
Signature High

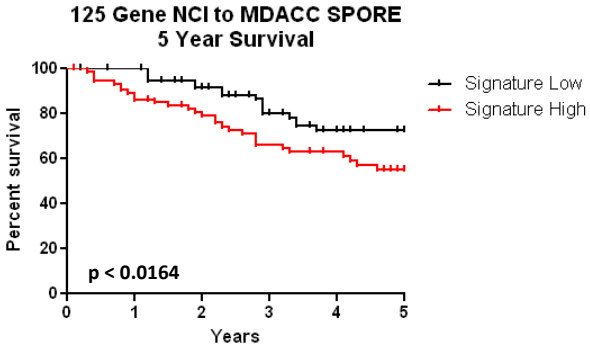
125 Gene NCI to MDACC SPORE
5 Year Survival
Percent survival
Years
p < 0.0164
Signature Low
Signature High

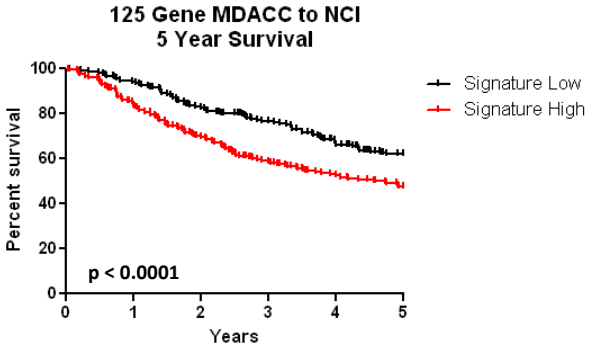
125 Gene MDACC to NCI
5 Year Survival
Percent survival
Years
p < 0.0001
Signature Low
Signature High

B

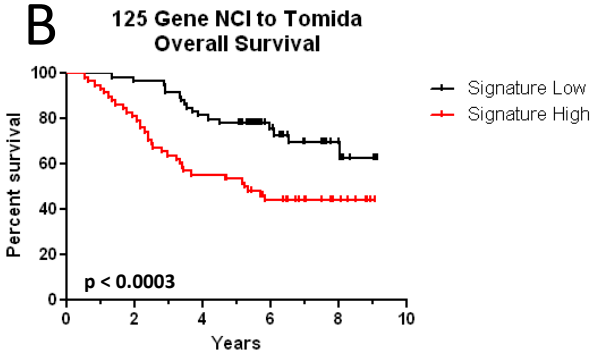
125 Gene NCI to Tomida
Overall Survival
Percent survival
Years
p < 0.0003
Signature Low
Signature High

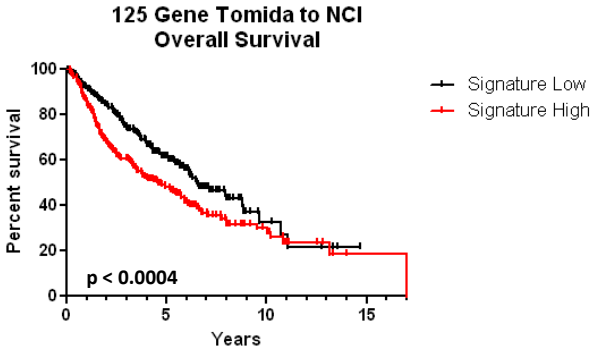
125 Gene Tomida to NCI
Overall Survival
Percent survival
Years
p < 0.0004
Signature Low
Signature High

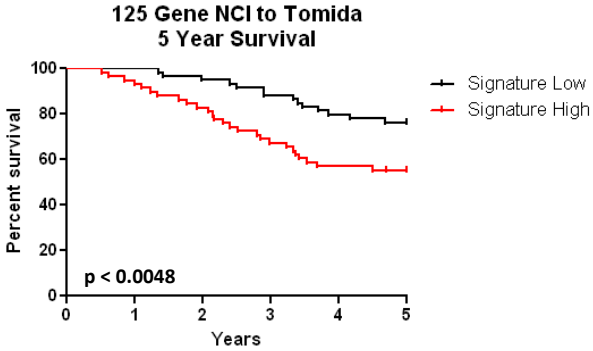
125 Gene NCI to Tomida
5 Year Survival
Percent survival
Years
p < 0.0048
Signature Low
Signature High

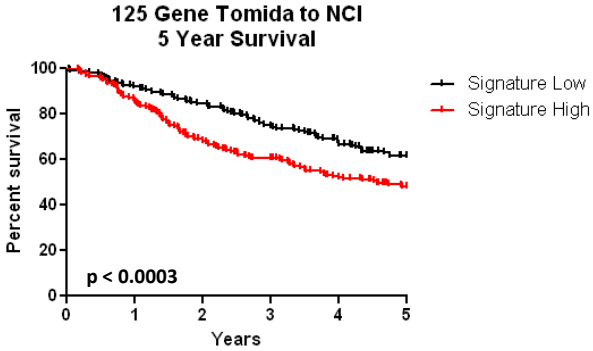
125 Gene Tomida to NCI
5 Year Survival
Percent survival
Years
p < 0.0003
Signature Low
Signature High

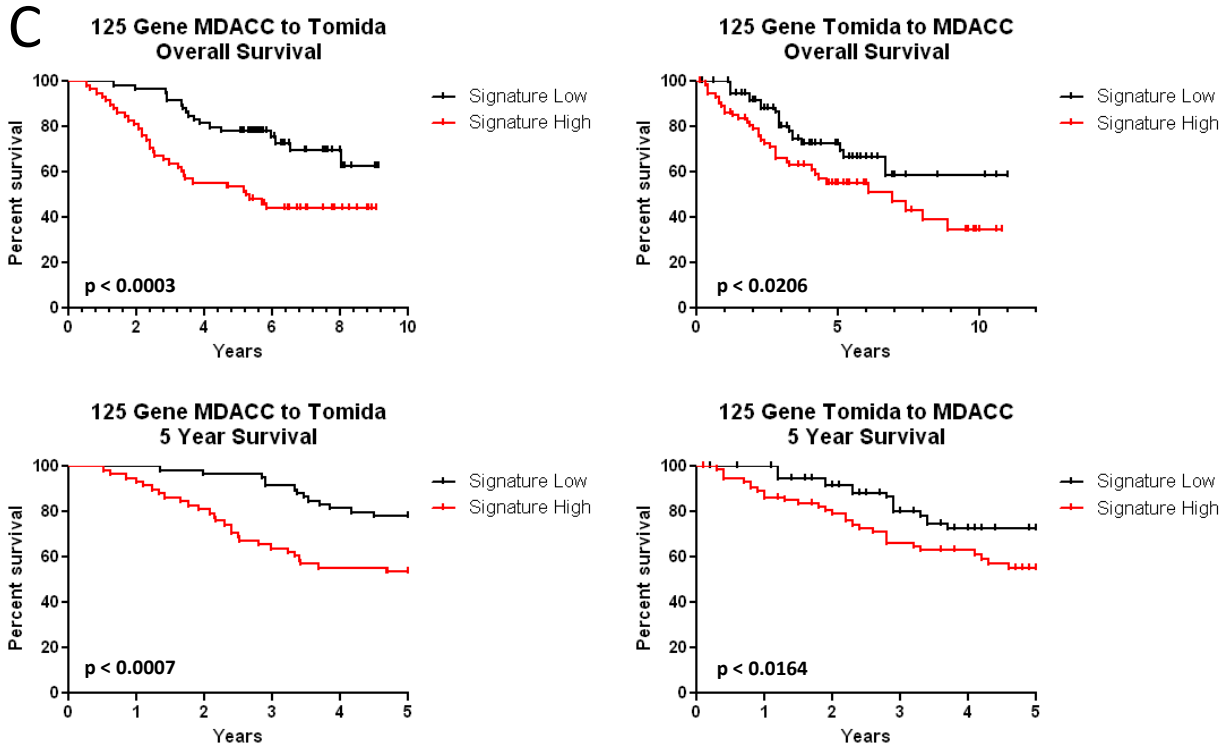

Figure 4.8: Prognostic potential of 125-gene ASCL1 target gene signature. Supervised principle component analysis was used on three different NSCLC patient datasets to determine prognostic potential of ASCL1 target genes. In each case, patients with a higher probability of expressing the gene signature demonstrated poorer survival. Overall and five-year survival rates are shown. (A) Left: Training set – NCI Director's Consortium, Testing set – MDACC SPORE. Right: Testing set – MDACC SPORE, Training set – NCI Director's Consortium. (B) Left: Training set – NCI Director's Consortium, Testing set – Tomida Adenocarcinoma. Right: Testing set – Tomida Adenocarcinoma, Training set – NCI Director's Consortium. (C) Left: Training set – MDACC SPORE, Testing set – Tomida Adenocarcinoma. Right: Testing set – MDACC SPORE, Training set – Tomida Adenocarcinoma. Significance between curves calculated using the Gehan-Breslow-Wilcoxon Test. Survival analysis performed by Tao Wang of the Yang Xie lab, UTSW.

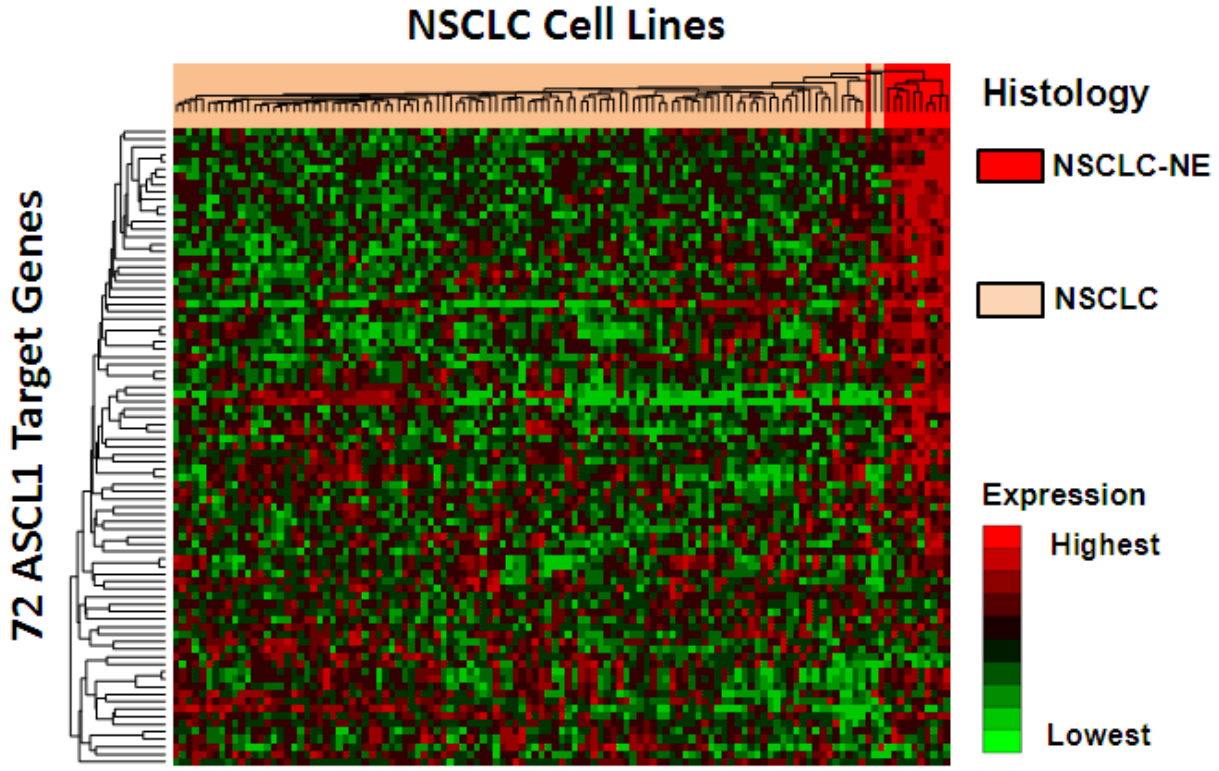

Figure 4.9: Clustering of NSCLC lines using 72-gene ASCL1 target gene signature. The 72-gene signature, identified by comparing log ratio differences between cell lines used for ASCL1 ChIP-Seq analysis (H128, H1184, H2107, H1755, and HCC4018 vs. H524 and H526) was correlated with genes uncovered following ChIP-Seq analysis. The 72-gene signature was used to cluster the NSCLC cell lines. 10 of 11 NE-NSCLC grouped separately from the remaining NSCLC lines. H2106 was the lone drop out, which is a cell line that does not express ASCL1.

A

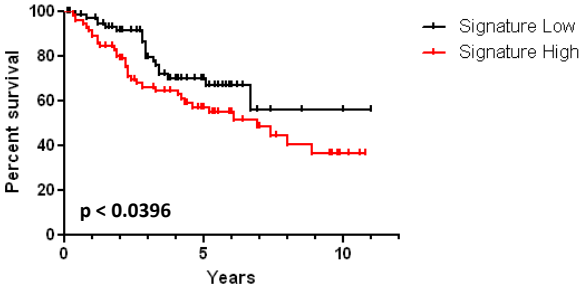
72 Gene NCI to MDACC SPORE
Overall Survival
Percent survival
Years
p < 0.0396
Signature Low
Signature High

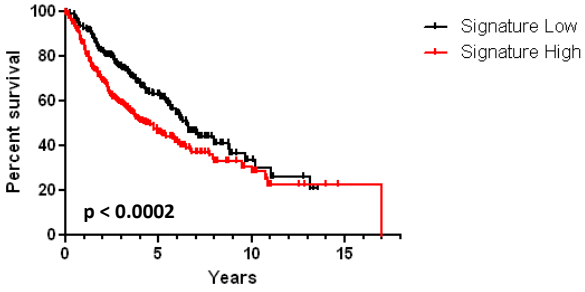
72 Gene MDACC SPORE to NCI
Overall Survival
Percent survival
Years
p < 0.0002
Signature Low
Signature High

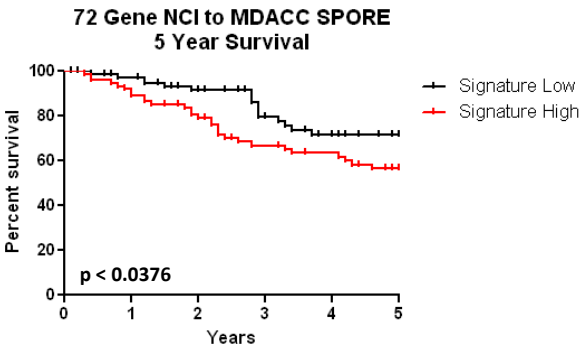
72 Gene NCI to MDACC SPORE
5 Year Survival
Percent survival
Years
p < 0.0376
Signature Low
Signature High

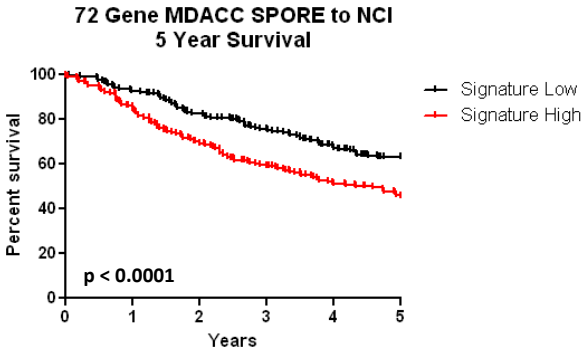
72 Gene MDACC SPORE to NCI
5 Year Survival
Percent survival
Years
p < 0.0001
Signature Low
Signature High

B

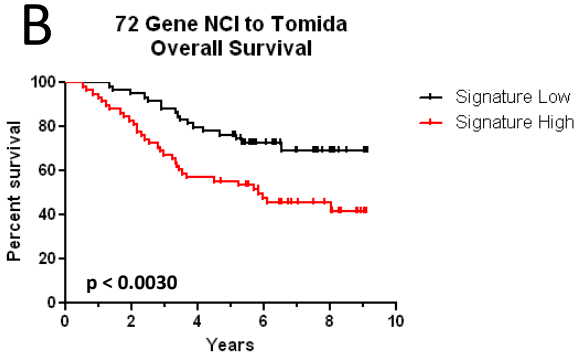
72 Gene NCI to Tomida
Overall Survival
Percent survival
Years
p < 0.0030
Signature Low
Signature High

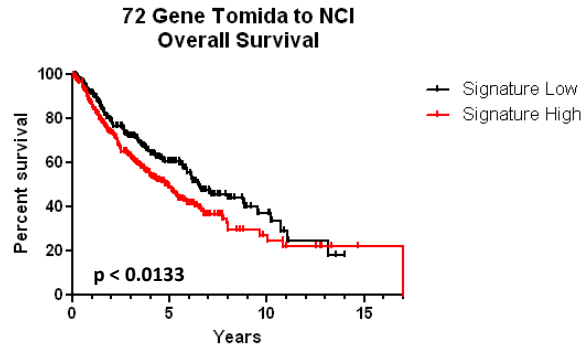
72 Gene Tomida to NCI
Overall Survival
Percent survival
Years
p < 0.0133
Signature Low
Signature High

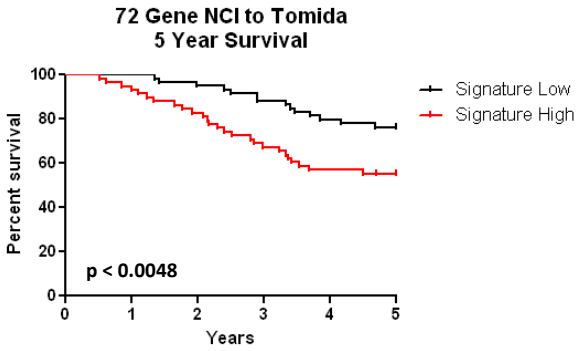
72 Gene NCI to Tomida
5 Year Survival
Percent survival
Years
p < 0.0048
Signature Low
Signature High

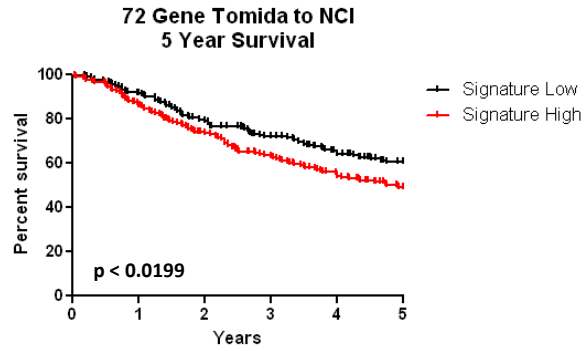
72 Gene Tomida to NCI
5 Year Survival
Percent survival
Years
p < 0.0199
Signature Low
Signature High

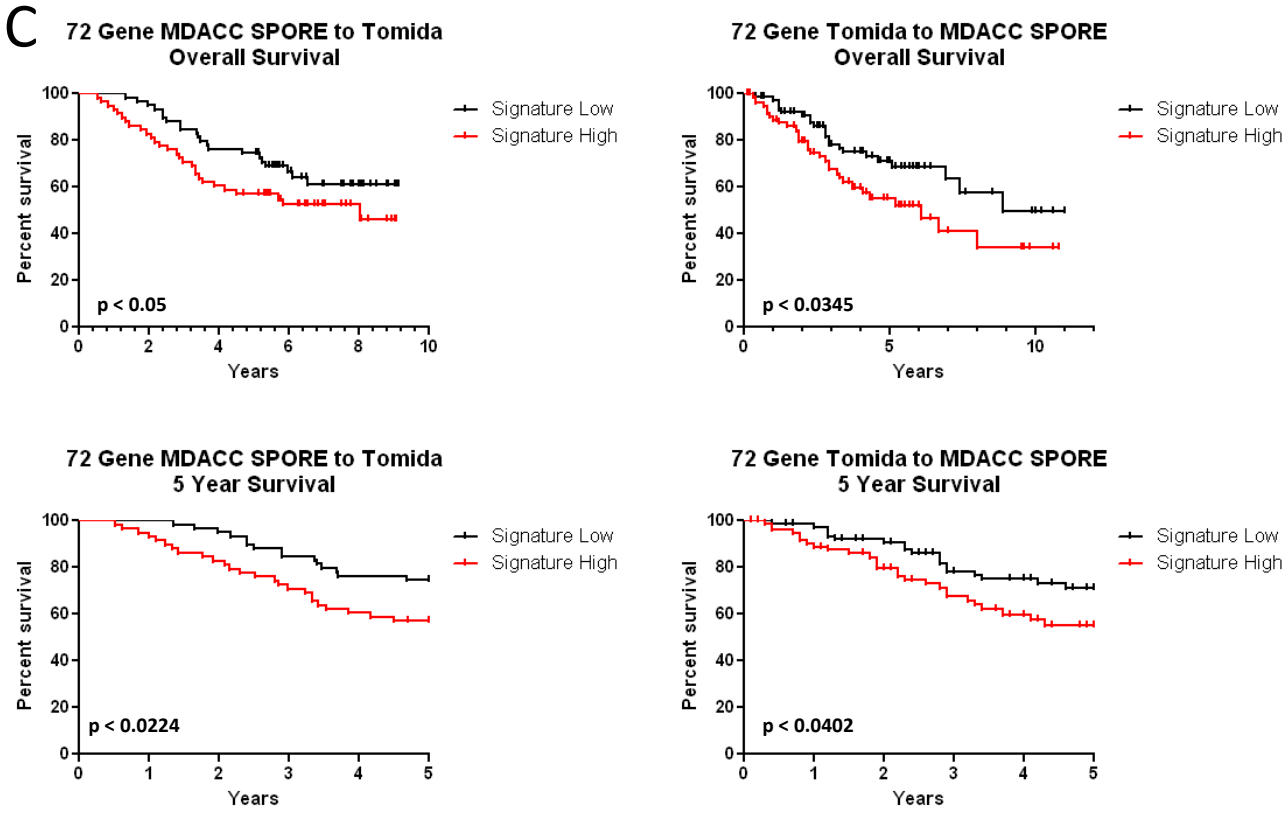

Figure 4.10: Prognostic potential of 72-gene ASCL1 target gene signature. Supervised principle component analysis was used on three different NSCLC patient datasets to determine prognostic potential of ASCL1 target genes. In each case, patients with a higher probability of expressing the gene signature demonstrated poorer survival. Overall and five-year survival rates are shown. (A) Left: Training set – NCI Director's Consortium, Testing set – MDACC SPORE. Right: Testing set – MDACC SPORE, Training set – NCI Director's Consortium. (B) Left: Training set – NCI Director's Consortium, Testing set – Tomida Adenocarcinoma. Right: Testing set – Tomida Adenocarcinoma, Training set – NCI Director's Consortium. (C) Left: Training set – MDACC SPORE, Testing set – Tomida Adenocarcinoma. Right: Testing set – MDACC SPORE, Training set – Tomida Adenocarcinoma. Significance between curves calculated using the Gehan-Breslow-Wilcoxon Test. Survival analysis performed by Tao Wang of the Yang Xie lab, UTSW.

4.2.5 Diagnostic Ability of ASCL1 Target Genes in Lung Adenocarcinoma

In 2001, the Meyerson group profiled 139 pathologically unremarkable lung adenocarcinomas for genome-wide mRNA expression using an early Affymetrix platform (Bhattacharjee, Richards et al. 2001). The group discovered that despite any overt histological differences the tumors could be subdivided into five subgroups based on their gene expression, with one of these subgroups demonstrating neuroendocrine gene expression. The neuroendocrine adenocarcinoma patients (~9% of the cohort) were found to have significantly reduced survival compared to the remaining non-neuroendocrine adenocarcinomas. Since ASCL1 expression in NSCLC cell lines is limited to approximately 10% of the population, and that ASCL1 expression along with other neuroendocrine markers defined the neuroendocrine/adenocarcinoma patients, there is considerable reason to expect that ASCL1 target genes may be able to categorize these patients as well.

The 125-gene ASCL1 target gene signature was used to cluster the lung adenocarcinoma patients from the Bhattacharjee study. Following filtering between platforms, 69 genes remained for the analysis. Using average linkage clustering via the Pearson method, the 69 genes were able to group together the neuroendocrine adenocarcinoma patients with a high degree of significance (Figure 4.11A). One patient previously identified to be a part of the neuroendocrine subgroup clustered outside of the ASCL1- target gene group and was replaced by another patient. Whether the reasoning behind this switch is significant or not remains to be seen. However, survival analysis on the patients grouped by the ASCL1 target gene signature demonstrates a nearly identical survival curve as found by the Meyerson group (Figure 4.11B). It is possible, therefore,

that since the ASCL1 target gene signature identified patients previously discovered to have a neuroendocrine phenotype, that it can be used as a diagnostic biomarker to select for such patients.

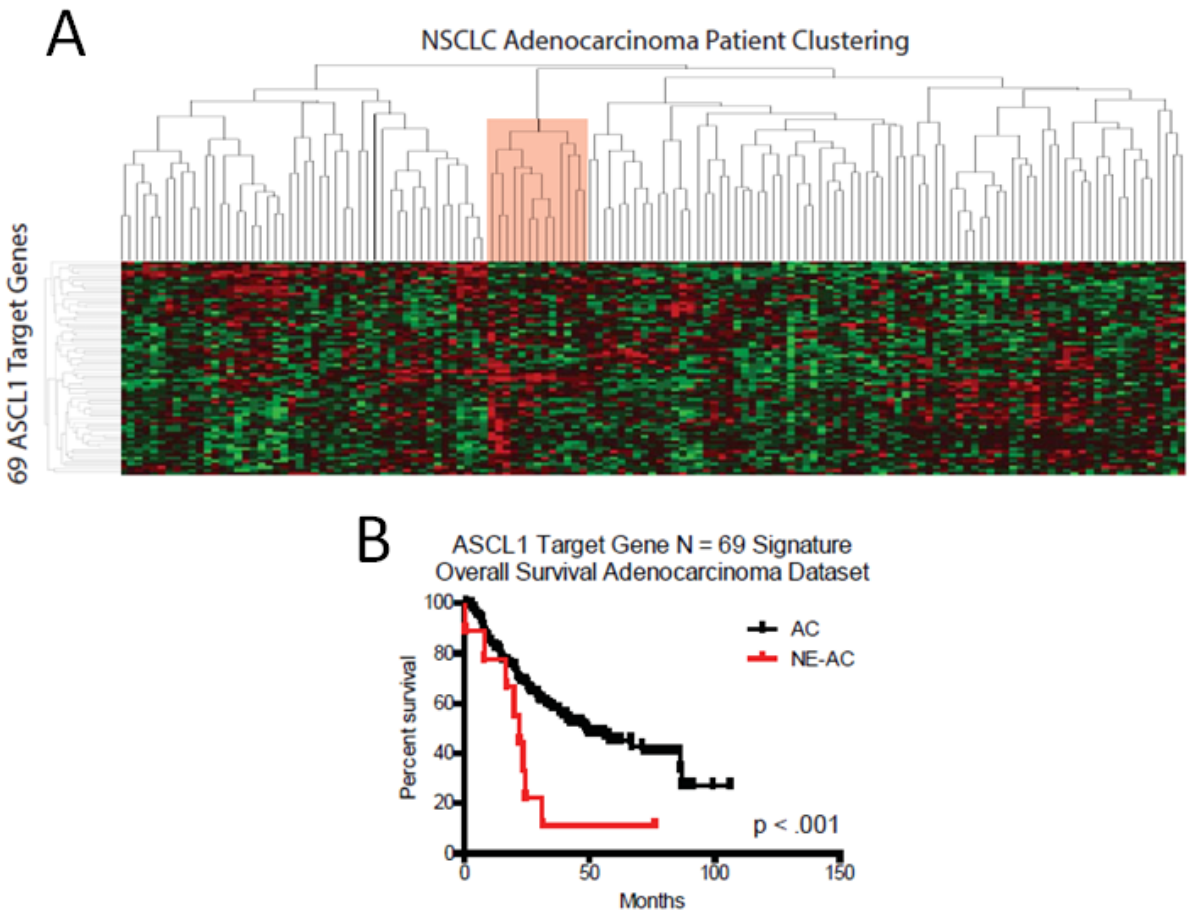

Figure 4.11: Diagnostic potential of ASCL1 target genes. Using an adenocarcinoma patient dataset previously shown to contain patients with a neuroendocrine gene signature, ASCL1 target genes were profiled for their ability to accurately identify those patients. (A) 69 genes from the 125-gene ASCL1 target gene signature remained for clustering analysis following filtering between Illumina V3 and Affymetrix platforms. Clustering was performed using the Pearson Method (average linkage analysis). Patients determined by the Meyerson group to be neuroendocrine are highlighted. (B) Survival analysis comparing the highlighted patients versus the remaining patients. Significance calculated using the Gehan-Breslow-Wilcoxon Test.

4.2.6 Uncovering Druggable Downstream Targets of ASCL1

The ultimate goal for targeted therapy in cancer is to uncover a clinically relevant subset of human cancer readily identifiable with a biomarker and to develop a treatment that is effective in those patients. In lung cancer, targeted therapy is available for patients that present with lung adenocarcinoma driven by the fusion of EML4-ALK genes (Soda, Choi et al. 2007). Such patients show dramatic response to Crizotinib compared to standard chemotherapy (Choi, Soda et al. 2010). NE-NSCLC cell lines are exquisitely sensitive to knockdown of ASCL1, however ASCL1 and other basic helix-loop-helix transcription factors are historically difficult to inhibit with small molecules. Due to the biological function of transcription factors, it is likely that a target or targets of ASCL1 mediate survival within the NE-NSCLC subset of cell lines. If such a target is druggable with a small molecule it immediately becomes of clinical utility as a treatment for ASCL1-driven lung cancers. To discover druggable ASCL1 targets, the list of 1330 ChIP-Seq genes was threaded through a database of the "druggable genome" published by Washington University St. Louis and accessible at dgidb.wustl.edu (manuscript in preparation).

Of the 1330 genes imported into the druggable genome database, 275 were deemed as potential drug targets (Table 4.3) and alone these genes are able to cluster SCLC and NE-NSCLC lines separately from NSCLC and HBEC/HSAECs (Figure 4.12). The genes can be grouped into multiple categories, including transporters, drug resistance genes, kinases, proteases, growth factors, and phosphatases, among others. The most populated categories include transporters (95 genes), kinases (69 genes), and tumor suppressors (56 genes). This list provides an intriguing categorization of hits to test against the NE-NSCLC cell lines. It is likely

that FDA approved drugs or drugs currently in clinical trials target these genes and may prove to be therapeutically active in the NE-NSCLC subset.

The most attractive therapeutic targets are those that are more likely to be overexpressed in ASCL1^{+} lung cancers compared to typical NSCLCs and normal lung cells. A log ratio analysis comparing the expression of the 275 druggable target genes between neuroendocrine lung cancer cell lines and non-neuroendocrine cell lines revealed 77 genes that were specifically overexpressed in neuroendocrine lung cancer lines (Figure 4.13). Significance was determined by t-test comparing the two groups. Each gene demonstrated a log 2 ratio greater than 1.00 between the neuroendocrine and non-neuroendocrine cell lines. Based on the expression analysis performed, these 77 genes represent a list of primary hits to screen in ASCL1-dependent lung cancer cell lines as potential therapeutic targets (Table 4.4).

Druggable ASCL1 Target Genes					
AACS	DGKB	HES6	NOMO3	S1PR1	TNS3
ABCA1	DIP2C	HNRNPU	NR0B2	SATB2	TP63
ABCB9	DMBX1	HSD17B14	NRCAM	SCN2A	TPCN1
ABP1	DMPK	HSPB1	NRTN	SEC11C	TRIB1
ADCK3	DPP9	ID2	NTHL1	SERPINH1	TRIB2
ADCY1	DTL	ID3	NUAK1	SERPINI1	TRIM9
ADK	DUSP10	IL10	NUAK2	SIK1	TRIO
ADRA2A	DUSP4	IL1B	OCA2	SLC12A4	TUBB
ALDH7A1	DUSP6	INHBB	ODC1	SLC22A23	TUBB2B
ANAPC2	E2F7	INPP5A	OXT	SLC24A6	TXNRD2
ARRB1	ECE1	IP6K3	P2RX2	SLC25A34	UBE2I
ASCL1	EP400	ITGA4	PANK1	SLC26A11	UBE2L3
ATF4	EPHB2	ITPKB	PARP12	SLC29A3	USP13
ATG4D	ERCC1	ITPR3	PBX3	SLC36A4	USP41
ATP5G2	ETNK2	JDP2	PDE4C	SLC44A1	USP48
ATP5G3	FABP6	JPH3	PDGFB	SLC4A8	USP54
BCL10	FAF1	KCNB2	PDZK1	SLC6A17	VGF
BCL2	FANCA	KCNC1	PEX5L	SLC6A3	VLDLR
BCL2L11	FBP1	KCNF1	PFKFB2	SLC7A11	WNK2
BCL6	FBXW7	KCNH2	PFKP	SLC7A4	WNT4
BCR	FGF21	KCNH3	PHF2	SLC7A5	WWOX
BIRC7	FGFRL1	KCNMA1	PHLPP1	SLC7A5P2	XPOT
BMP8B	FGGY	KCNT1	PHLPP2	SLCO2B1	YWHAZ
BTG2	FKBP9	KIF20B	PI4KAP2	SLCO3A1	ZADH2
C9orf3	FKBP9L	KITLG	PIK3C3	SMAD2	ZFHX3
CABLES2	FLNA	KLF4	PIM1	SMAD7	
CACHD1	FOXA2	KSR2	PITPNC1	SOCS1	
CACNA1A	FOXC1	LCAT	PKMYT1	SOX4	
CACNA1H	FUT1	LHX3	PLA2G10	SPHK1	
CAMK1D	FUT2	LPIN1	PLCG2	SPPL2B	
CAMK2B	FZD3	LRRC26	PNPLA8	SPTB	
CCRN4L	FZD5	LYPLAL1	POLD3	STAT5A	
CD34	GABRG3	MACF1	POLR2J	STAT5B	
CD9	GADD45G	MAD1L1	PPAP2C	STK32C	
CDC25B	GAS6	MAD2L1	PPIF	STK39	
CDK18	GCK	MALT1	PPM1F	SYT1	
CDK5RAP3	GGT2	MAN2A1	PPP2CB	SYT17	
CEBPB	GJA3	MAPK1	PROX1	SYT7	
CERK	GNAO1	MAPK9	PRSS8	TBXAS1	
CHKA	GPC3	MBOAT2	PTP4A3	TCF12	
CHORDC1	GPC4	MCRS1	PTPRN2	TCIRG1	
CLIC4	GPR114	MDC1	PTPRU	TERF1	
CLK1	GPR12	MELK	PYGB	TFDP1	
CNTNAP3	GPR6	MFSD2A	QSOX2	TGFB2	
COL22A1	GPR68	MFSD9	RAB4A	TGIF1	
CSNK2A1	GPR89B	MLXIPL	RBPJ	TLE1	
CYP11A1	GPRC5C	MPP3	RNF19A	TMX3	
CYP26B1	GRP	MTMR1	RPA3	TNFRSF18	
CYP51A1	HES1	NEK2	RPH3AL	TNK2	
DACT1	HES5	NFIA	RPS6KA3	TNS1	

Table 4.3: Druggable genes uncovered from ChIP-Seq analysis. From the list of 1330 genes identified from ASCL1 ChIP-Seq analysis, 275 were deemed as druggable. The genes were curated by the Drug Gene Interaction Database (dgidb.genome.wustl.edu).

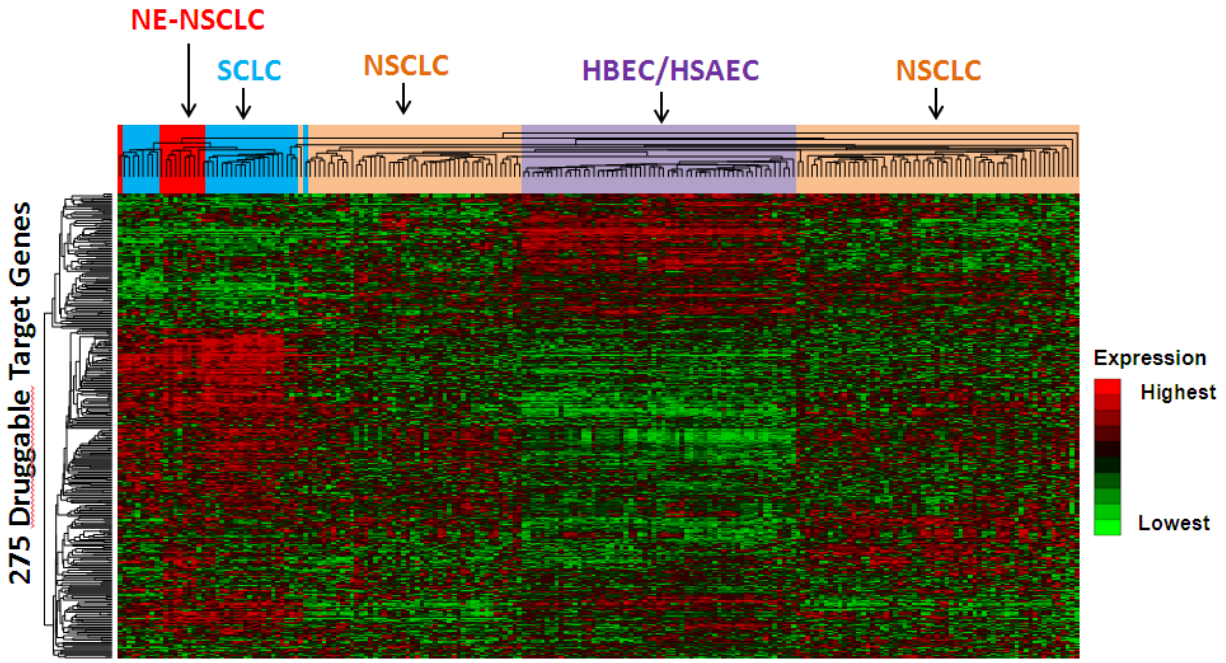

Figure 4.12: Clustering of lung cell lines using druggable ASCL1 target genes. The 275 druggable genes were used to cluster lung cell lines. Similar to the full 1330 target gene list, the druggable genes were sufficient to group together neuroendocrine lung cancer cell lines separately from NSCLC and HBEC/HSAEC lines. Average linkage clustering using the Pearson Method was applied to the gene signature. 10 of 11 NE-NSCLC cell lines grouped together within the SCLC lines suggesting a common gene signature within the global scope of the neuroendocrine lung cancers.

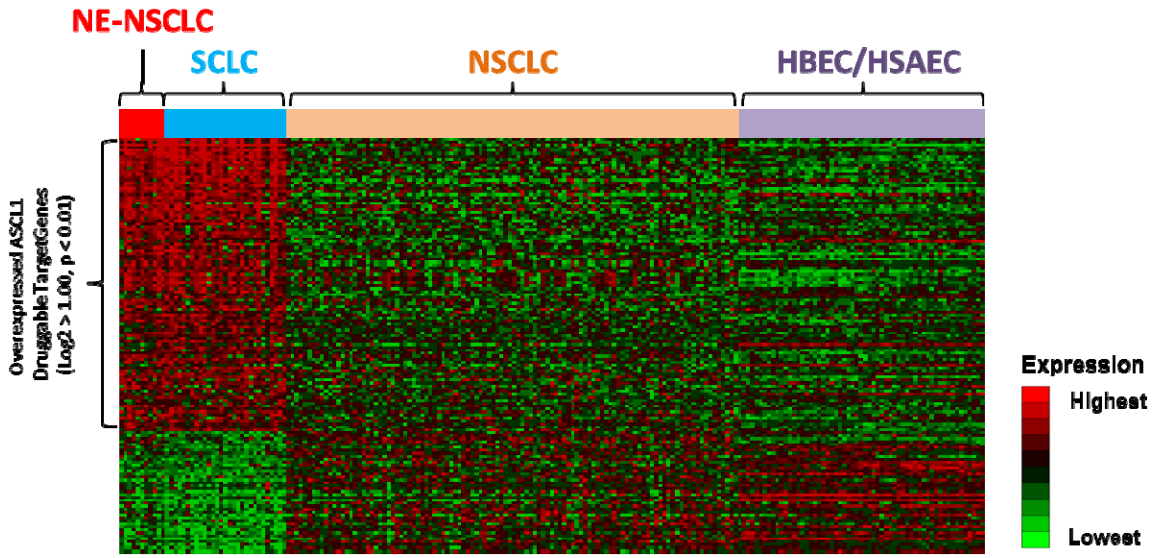

Figure 4.13: Identifying druggable ASCL1 target genes specifically overexpressed in neuroendocrine lung cancer cell lines. Log ratio analysis was performed to determine which druggable ASCL1 target genes were specifically overexpressed in neuroendocrine lung cancer cell lines compared to typical NSCLC lines and normal HBEC/HSAEC lines. 77 genes met the significance cutoff with a $p < 0.01$ and $\log 2 > 1.00$. These genes represent the most attractive therapeutic targets for ASCL1-dependent lung cancers.

Overexpressed ASCL1 Druggable Target Genes			
ADCK3	GAS6	LRRC26	SLC6A17
ADCY1	GCK	MFSD2A	SLC6A3
ASCL1	GNAO1	NR0B2	SLC7A4
ATG4D	GPC3	NRCAM	SLCO3A1
BCL2	GPR12	NRTN	SOX4
BMP8B	GPR6	NTHL1	SYT1
BTG2	GRP	ODC1	SYT7
CACNA1A	HES5	PBX3	TCF12
CACNA1H	HES6	PEX5L	TRIB2
CAMK1D	ID2	PHF2	TRIM9
CAMK2B	JPH3	PHLPP1	TUBB2B
CERK	KCNB2	PROX1	USP48
COL22A1	KCNC1	PTP4A3	VGF
DACT1	KCNF1	PTPRN2	WNK2
DGKB	KCNH2	SCN2A	WNT4
FABP6	KCNH3	SCN3A	WWOX
FOXA2	KCNJ11	SEC11C	ZADH2
FUT1	KCNT1	SLC22A23	
FZD3	KSR2	SLC36A4	
GADD45G	LHX3	SLC4A8	

Table 4.4: Druggable ASCL1 target genes overexpressed in neuroendocrine lung cancer cell lines. 77 druggable ASCL1 target genes were determined to be overexpressed in neuroendocrine lung cancer cell lines.

4.3 Discussion

Analysis of transcription factors deemed to be essential survival proteins in cancer can lead to novel therapeutic interventions. One way to study the function of transcription factors is to determine which downstream targets they regulate and how the downstream targets maintain cancer cell survival. Such a transcriptome analysis may provide a biological understanding of the pathways involved in regulating tumorigenesis while a detailed investigation of these pathways may provide druggable targets that demonstrate therapeutic potential in pre-clinical models.

In this study, the transcriptional targets of ASCL1 are determined by ChIP-Seq analysis, where protein-bound DNA is fixed, immunoprecipitated with the appropriate primary antibody, and DNA sequenced using massively parallel technologies able to cover the entire genome. In this way, DNA-protein interactions between ASCL1 and regulatory sequences can be determined and transcriptional regulation of genes inferred.

ChIP-Seq was performed on five ASCL1+ lung cancer cell lines, which included SCLCs H128, H1184, and H207 and NE-NSCLCs H1755 and HCC4018. Control samples included SCLC cell lines H524 and H526 that do not express ASCL1. Sequencing reads were first aligned to the human reference genome HG19 using Bowtie (Langmead, Trapnell et al. 2009). Stacks of 50 bp DNA reads, known as peaks, corresponding to ASCL1 binding sites were mapped using MACS (Zhang, Liu et al. 2008). Consensus peaks among all five ASCL1+ cell lines were profiled for peak-gene interactions using GREAT (McLean, Bristor et al. 2010), which resulted in a list of 1330 putative ASCL1 transcriptional targets.

Gene ontology analysis performed on the 1330 target genes revealed an overrepresentation of members of the Notch pathway, which included the validated ASCL1 target genes DLL1 and DLL3. The Notch pathway is central in regulating ASCL1 and neuroendocrine differentiation (Ball, Azzoli et al. 1993; Sriuranpong, Borges et al. 2002). When ASCL1 is expressed in primitive pulmonary neuroendocrine cells, it directs the expression of Notch ligands DLL1 and DLL3, which signal through the Notch pathway by binding to the extracellular domain of Notch receptors in adjacent cells. This signals the adjacent cell to repress ASCL1 expression and inhibit neuroendocrine differentiation. Recapitulation of this essential ASCL1 signaling pathway within the ChIP-Seq data in lung cancer cell lines demonstrates the fidelity of the experiment and suggests that novel transcriptional targets can be inferred from the list of 1330 putative ASCL1 genes. Additionally, ASCL1 is known to promote neuroendocrine differentiation, and several neuroendocrine genes are putative ASCL1 targets, including SYT1, CDH2, GRP, and INSM1.

ChIP-Seq analysis to discover downstream targets of transcription factors essential for survival is a novel approach towards discovering therapeutic options for cancer. Prior ChIP-Seq experiments performed on cancer cell lines were broad-spectrum analyses to discover binding motifs and co-occupancy transcription factors (Yu, Mani et al. 2010; Chng, Chang et al. 2012). Similarly, ChIP-Seq analysis of estrogen receptor (ER) in primary breast cancer was used to find global differences between tumors of varying clinical outcome (Ross-Innes, Stark et al. 2012). What has yet to be shown is that downstream targets of essential transcription factors discovered through ChIP-Seq analysis can be utilized as direct therapeutic interventions. ASCL1 ChIP-Seq

analysis performed in this study demonstrated a common E-box (CAGNTG) binding sequence present in all ASCL1+ samples, while also providing a gene list of 275 druggable targets.

Overall, the putative transcriptional targets of ASCL1 discovered via ChIP-Seq analysis have several uses. First, the initial list of 1330 genes relating to the 912 common peaks are sufficient to cluster together neuroendocrine lung cancer cell lines. Gene correlation analysis was then used to narrow the list of 1330 genes to 125. The 125 genes clustered together 9 of the 11 NE-NSCLC separately from the remaining typical NSCLCs, with the dropped out cell lines either depending on a different neurogenic transcription factor (H1155 and NeuroD1) or not expressing any ASCL1 (H2106). A separate filtering of the 1330 genes involved performing log ratio analysis between the five ASCL1+ cell lines (H128, H1184, H2107, H1755, and HCC4018) and the two ASCL1-negative cell lines (H524 and H526) utilized in the ChIP-Seq screen. This resulted in 72 putative ASCL1 target genes being significantly overexpressed in the ASCL1+ cell lines compared to the ASCL1-negative lines. The 72-gene signature was sufficient to group together 10 of the 11 NE-NSCLC cell lines, with H2106 constituting the lone drop out. In addition to clustering the cell lines, both the 125-gene and the 72-gene signatures were tested for prognostic utility. Previous reports demonstrated that expression of neuroendocrine genes in NSCLC is a poor prognostic indicator (Berendsen, de Leij et al. 1989; Schleusener, Tazelaar et al. 1996; Garcia-Yuste, Matilla et al. 2000; Bhattacharjee, Richards et al. 2001; Pelosi, Pasini et al. 2003; Howe, Chapman et al. 2005). In this study, transcriptional targets of ASCL1, a master neuroendocrine regulator, were predictors of poor prognosis in lung adenocarcinoma patients. The 125-gene and the 72-gene signatures were able to stratify patients into those at high and low-

risk for expressing ASCL1 targets. The patients with higher risk scores for expressing ASCL1 target genes demonstrated poorer survival, consistent with previous reports indicating unfavorable performance for NSCLCs with neuroendocrine features. In addition to poor prognosis, ASCL1 target genes also demonstrated the capacity to pick out patients previously determined to have neuroendocrine features, suggesting biomarker potential.

The initial list of 1330 putative ASCL1 targets was analyzed for druggable genes as described earlier. 275 targets were identified and categorized into a variety of groups, including kinases, transporters, and enzymes, among others. 77 of these were found to be specifically overexpressed in neuroendocrine lung cancer cell lines. Determination of which downstream druggable downstream targets of ASCL1 are essential for survival will require a significant effort. One way to study the necessity of the druggable genes is to create a mini-library siRNA screen that can measure viability post-knockdown. This method is attractive and can be performed in semi-high-throughput however concerns about off-target effects limit the effectiveness of this approach. Similarly, a small-molecule screen can be designed where drugs known to inhibit any of the 77 overexpressed target genes can be titrated against ASCL1-dependent cell lines and measured for inhibition of growth. This approach is the most likely to lead to a potential therapeutic option for ASCL1-dependent lung cancers, however it is prohibitively expensive. A proof-of-concept shotgun approach is first necessary to demonstrate that downstream targets of ASCL1 can be useful therapeutic options prior to proceeding with a larger unbiased method such as an siRNA mini-library or small molecule drug screen. The

following chapter will explain how two ASCL1 target genes with currently available therapies establish heterogeneous responses in ASCL1-dependent cell lines.

CHAPTER FIVE

THERAPEUTIC INDICATIONS OF ASCL1 TRANSCRIPTIONAL TARGETS IN NE-NSCLC CELL LINES

5.1 Introduction

Developing targeted therapy for a readily identifiable subclass of cancer is the ultimate goal of cancer research. Lung cancer research has produced several such targeted therapies in the last 15 years. First, patients with mutations in the EGFR gene demonstrate marked response to anti-EGFR therapies such as erlotinib and cetuximab (Pao, Miller et al. 2004). These patients can be detected with a simple immunohistochemistry test of a tumor biopsy specimen (Ulivi, Puccetti et al. 2013). A second targeted therapy exists for lung cancer patients presenting with a fusion of the EML4-ALK genes. These patients can also be detected with a simple IHC test and exhibit dramatic sensitivity to the MET inhibitor crizotinib (Kwak, Bang et al. 2010). Discovering a similar "Achilles heel" in ASCL1-dependent cancers would bring a therapeutic option to a large number of patients, as both SCLCs and NE-NSCLCs depend on ASCL1 for survival.

The ChIP-Seq studies described in the previous chapter suggests that 77 potential ASCL1 transcriptional targets are druggable, overexpressed, and present attractive therapeutic options. Despite recent advances in siRNA and small-molecule screening technologies, the associated

expenses are prohibitive and in the case of siRNA screens, off-target effects are difficult to isolate from on-target effects. A shotgun approach to find the most attractive therapeutic options was taken in this study to demonstrate that ASCL1 transcriptional targets can indeed indicate therapeutic effects in pre-clinical models. This can be used as evidence to undertake a more unbiased approach targeting all druggable ASCL1 genes in an siRNA or small molecule screen.

Two putative ASCL1 target genes were chosen for further analysis in NE-NSCLC cell lines. RET, a receptor tyrosine kinase, and BCL2, an anti-apoptotic regulator, are attractive therapeutic targets due to the availability of current small molecule inhibitors that target each respective protein and the wealth of available literature on both genes.

The RET proto-oncogene was first discovered to be rearranged in NIH-3T3 cells following transfection of DNA from human lymphoma cells (Takahashi, Ritz et al. 1985). As a canonical receptor tyrosine kinase, RET binds a ligand (GDNF) and initiates a downstream signaling cascade (Knowles, Murray-Rust et al. 2006). RET is involved in the development of several organs and systems during development (Arighi, Borrello et al. 2005) and is found to be mutated in a number of cancers. Mutations of RET are found in a subset of colorectal cancer as well as hereditary and sporadic thyroid cancer (Qi, Ma et al. 2011). Activating point mutations in the kinase domain of RET cause multiple endocrine neoplasia type 2 (MEN2), which is a disease that constitutes several familial cancers including medullary thyroid carcinoma (MTC), pheochromocytoma, parathyroid neoplasia, and ganglioneuromatosis of the gastroenteric mucosa (Moline and Eng 2011). Interestingly, all of the prior tissues contain ASCL1 in their developmental history. MEN2 underscores RET's involvement in neuroendocrine cancers and

suggests it may be involved in other NE tumors such as NE-NSCLC. Recently, two RET inhibitors were approved by the FDA for treatment of late-stage (metastatic) MTC in patients who are ineligible for surgery. Vandetinib and cabozantinib are multi-kinase inhibitors that have increased specificity for RET (Nagilla, Brown et al. 2012; Wells, Robinson et al. 2012). Though NE-NSCLC does not appear to be associated with mutations in RET, it is possible that pro-survival signaling through RET may mediate tumorigenic effects in pulmonary neuroendocrine tumors, especially if RET is determined to be a transcriptional target of ASCL1.

BCL2 is also an attractive therapeutic target. BCL2 exerts its pro-tumorigenic effects by inhibiting the polymerization of BAX and BAK along the mitochondrial membrane thereby preventing the release of cytochrome C into the cytoplasm (Chipuk, Moldoveanu et al. 2010). Once cytochrome C diffuses from the mitochondria into the cytoplasm, it constitutes a critical apoptotic stimulus and activates caspase 9, which in turn initiates the signaling cascade responsible for destroying the cell from within (Jiang and Wang 2000). BCL2 is also involved in development of tissues. Its transcriptional regulation by the melanocyte master regulator MITF is necessary for the survival of the melanocyte lineage during early development (McGill, Horstmann et al. 2002). Based on its anti-apoptotic function, BCL2 is a prime suspect for a pre-neoplastic cell to take advantage of and co-opt for further pro-tumorigenic development. Small molecule inhibitors of BCL2 are available. Abbott Laboratories has developed a trio of molecules, ABT-737, ABT-263, and ABT-199, as BCL2 inhibitors (Chauhan, Velankar et al. 2007; Hann, Daniel et al. 2008; Shoemaker, Mitten et al. 2008; Tse, Shoemaker et al. 2008; Souers, Leverson et al. 2013). ABT-199 is the third generation inhibitor and exhibits excellent

specificity for BCL2. ABT-737 and its oral analog ABT-263 demonstrate nanomolar specificity for BCL2 but also inhibit the related family members BCL-w and BCL-XL, the latter of which is responsible for the most prevalent side effect observed during clinical trials. Since BCL-XL mediates platelet survival, patients treated with ABT-263 were prone to developing thrombocytopenia (Rudin, Hann et al. 2012). This observation, in turn, led to the development of ABT-199, which is likely to ameliorate unwanted side effects through improved specificity for BCL2. Clinical trials for ABT-199 are currently ongoing.

SCLC cell lines highly express BCL2 and treatment of SCLC xenografts with ABT-737 and ABT-263 showed dramatic results in several models (Hann, Daniel et al. 2008; Shoemaker, Mitten et al. 2008). H146 cells injected subcutaneously into the mouse flank were allowed to grow until reaching approximately 250 mm^3 and subsequently treated for 21 consecutive days with 100 mg/kg ABT-263. This treatment modality resulted in tumor regression compared to vehicle control demonstrating the effectiveness of BCL2 inhibition in SCLC.

Due to the effective tumor suppressive effect of BCL2 inhibition, it is possible that ASCL1 mediates its pro-survival effect in pulmonary neuroendocrine tumors including SCLC and NE-NSCLC via transcriptional regulation of BCL2. In this model, ASCL1 would bind the regulatory region of BCL2, activate its transcription and use BCL2 as an anti-apoptotic regulator to maintain cancer cell survival. In turn, knockdown of ASCL1 and/or inhibition of BCL2 would relieve this anti-apoptotic block and induce cancer cell death. Demonstrating direct transcriptional regulation of BCL2 by ASCL1 would have significant impact in both the cancer setting as well as the developmental setting, as ASCL1 may regulate survival of early pulmonary

neuroendocrine progenitor cells by initiating BCL2 transcription and maintaining the lineage during development.

5.2 Results

5.2.1 Analysis of RET as an ASCL1 Transcriptional Target

ChIP-Seq performed on ASCL1+ cell lines as described in the previous chapter suggests that the RET receptor tyrosine kinase is a potential ASCL1 transcriptional target in NE-NSCLC cell lines. RET expression was verified using qRT-PCR and it was determined that RET mRNA transcript is abundant in NE-NSCLC cell lines (Figure 5.1A). SCLC cell lines also express RET but not in every case and typical NSCLC do not express RET. ASCL1 binding sites appear in the first intron of RET in H1755 and HCC4018 lines suggesting a potential regulatory interaction in NE-NSCLC (Figure 5.1B).

Knockdown of ASCL1 using siRNAs resulted in a decrease of RET mRNA in H1755 and HCC1833 NE-NSCLC cell lines (Figure 5.2A). All three siRNAs targeting ASCL1 demonstrated a reduction of RET mRNA. Protein expression was analyzed 72-hours post-transfection and it was found that RET protein is similarly decreased after ASCL1 knockdown (Figure 5.2B) suggesting a direct transcriptional activation of RET by ASCL1.

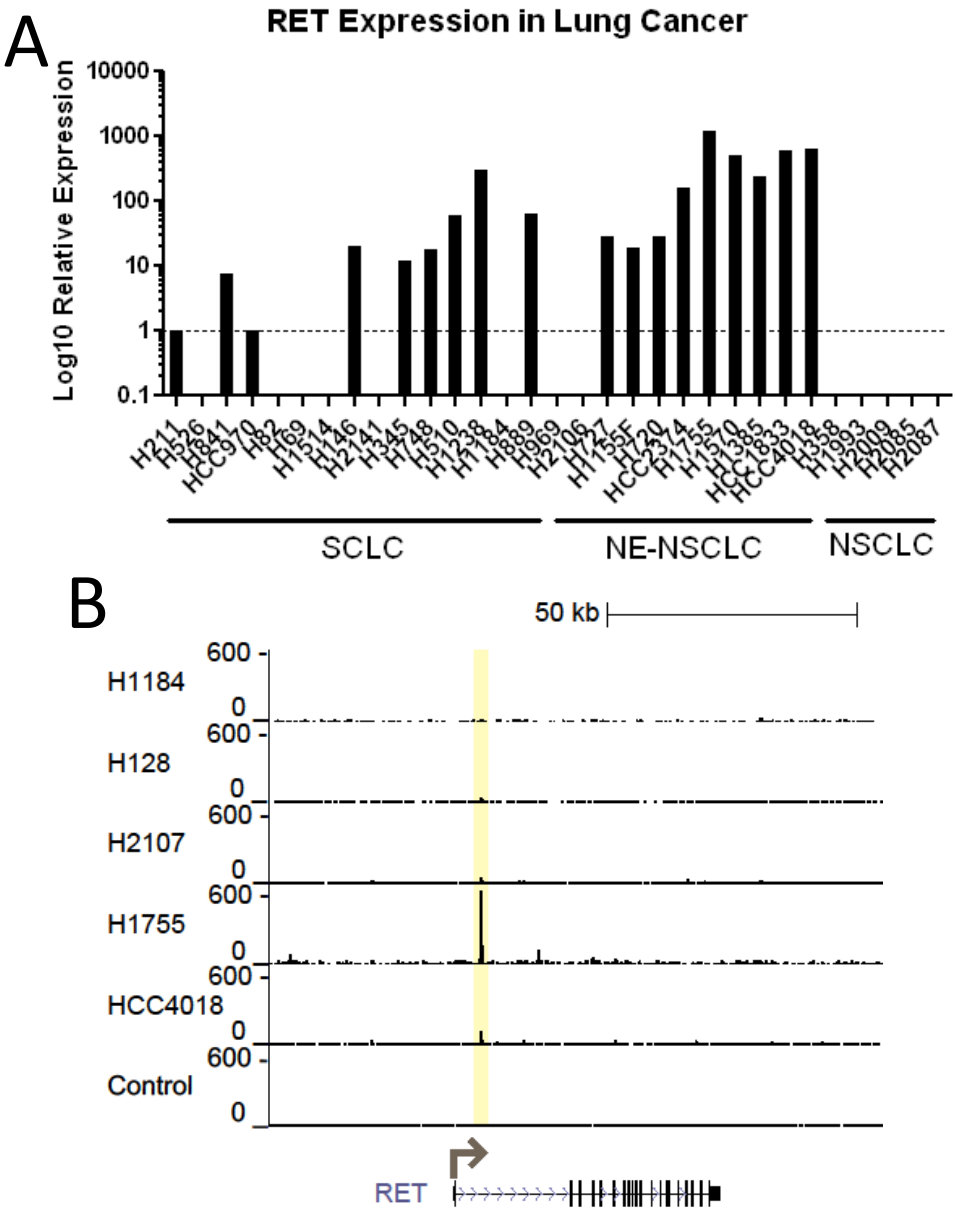

Figure 5.1: RET is highly expressed in NE-NSCLC and potentially regulated by ASCL1. (A) RET expression was determined in lung cancer cell lines using qRT-PCR analysis. RET is highly expressed in nearly every NE-NSCLC cell line. SCLC also express RET but not in every cell line. NSCLC lines do not express RET. (B) ASCL1-bound peaks are present in NE-NSCLC cell lines H1755 and HCC4018. RET may be preferentially regulated by ASCL1 in NE-NSCLC compared to SCLC cell lines.

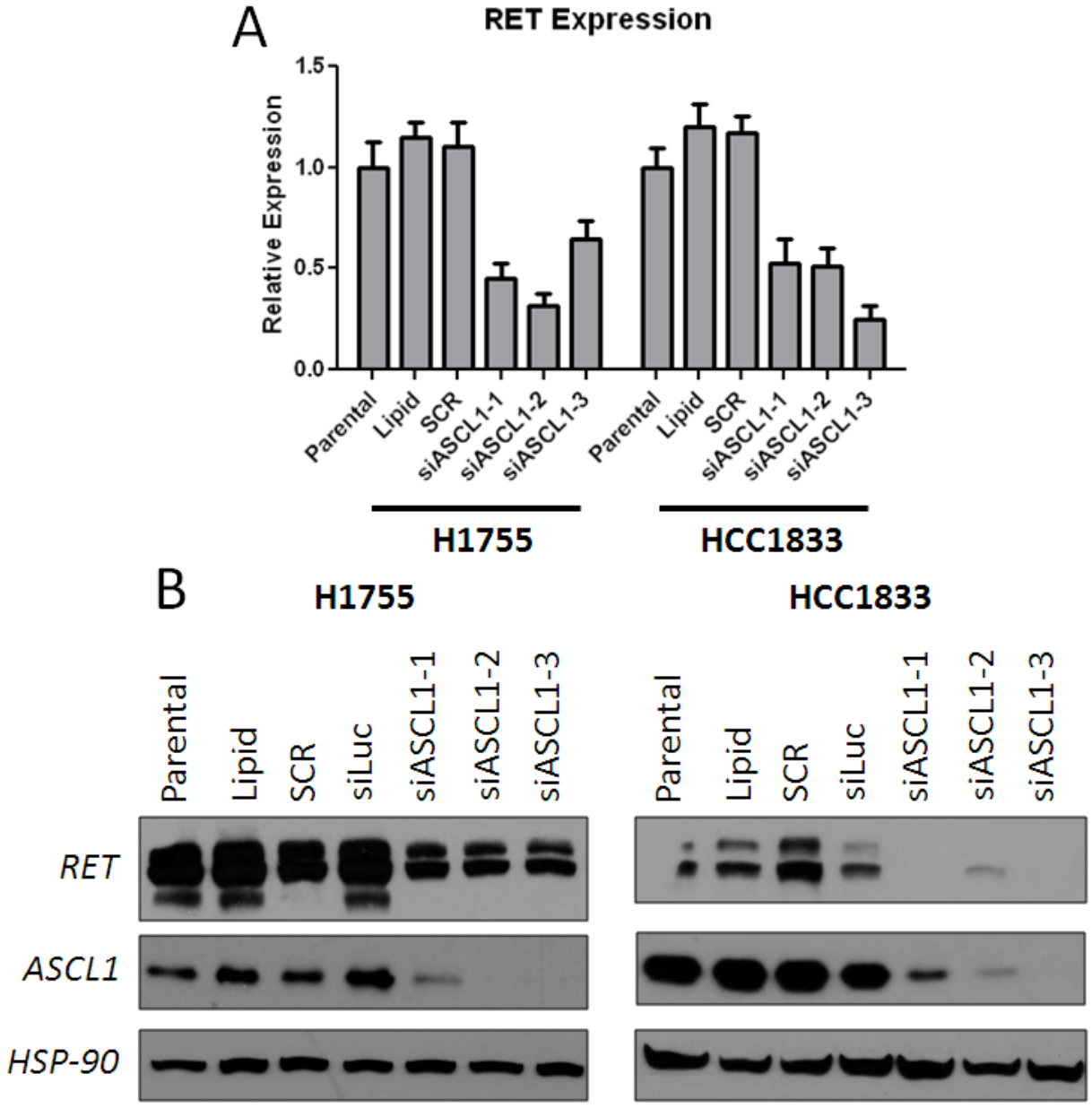

Figure 5.2: RET expression is regulated by ASCL1. ASCL1 was knocked down using siRNA-mediated methods. 20 nM siRNA was transfected into NE-NSCLC cell lines for 72 hours. (A) Knockdown of ASCL1 in H1755 and HCC1833 results in a significant decrease of RET mRNA as compared to controls. (B) Knockdown of ASCL1 results in an inhibition of RET protein expression in H1755 and HCC1833 demonstrating transcriptional regulation of RET by ASCL1. This blot was stripped and reprobed with primary antibodies in subsequent experiments.

5.2.2 Analysis of RET Inhibition on Cell Growth and Apoptosis in NE-NSCLC Cell Lines

Knockdown of ASCL1 results in a reduction of RET mRNA transcript and protein. In this series of experiments, knockdown and inhibition of RET was tested directly to determine if survival of ASCL1-dependent NE-NSCLC cell lines dependent on the expression and function of RET. Apoptosis was measured by analyzing the relative number of cells appearing in the sub-G1 phase of the cell cycle. Knockdown of RET was unable to completely phenocopy the apoptotic effect seen with knockdown of ASCL1, however a quantifiable amount of apoptosis was induced over scrambled control-transfected cells. The relative amount of apoptosis was approximately two-fold enriched over control in H1755 and about three-fold enriched in HCC1833 (Figure 5.3A). The induction of apoptosis with siRET suggests that inhibition of RET with one of the available small molecule inhibitors may prove to be a potential therapy for NE-NSCLCs.

Cabozantinib (CZ) is a small molecule inhibitor of MET, VEGFR2, and RET. The drug was recently granted FDA approval for the treatment of progressive, metastatic medullary thyroid cancer (Nagilla, Brown et al. 2012). CZ was studied for its effectiveness in inhibiting the growth of NE-NSCLC compared to typical NSCLC cell lines using the five-day MTS assay, where cells are plated for 24 hours and then treated with drug for the following four days. Dose-response curves were generated and IC50 values calculated using DIVISA (manuscript in preparation). The average IC50 for the NE-NSCLC cell lines H1155, H1755, and HCC1833 was 3.1, 2.35, and 2 μM, respectively (Figure 5.3B). For typical NSCLC cell lines the IC50 value was very similar to that observed in NE-NSCLC with the exception of H1703, which co-amplifies the PDGF receptor and PDGF ligand (McDermott, Ames et al. 2009). CZ, as a multi-

tyrosine kinase inhibitor, is effective in inhibiting PDGFR and as a consequence demonstrates specificity in H1703. Despite demonstrating induction of apoptosis following genetic RET knockdown, inhibition of RET with CZ does not lead to a dramatic reduction in growth nor demonstrate the required low-nanomolar IC50, which is preferred for a kinase inhibitor.

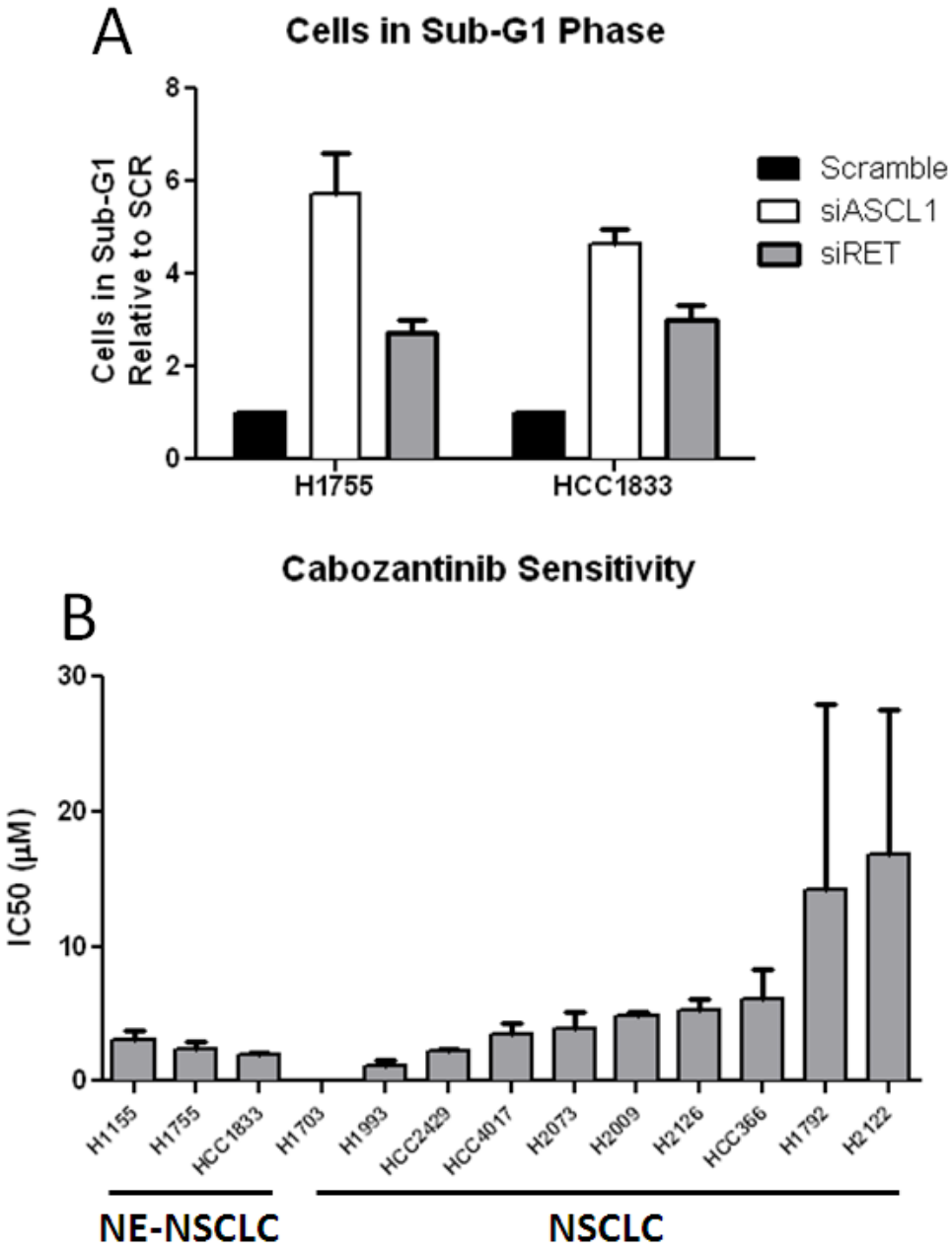

Figure 5.3: Effect of RET inhibition of growth and survival. (A) Knock down of RET induces apoptosis in H1755 and HCC1833 although the effect does not phenocopy knockdown of ASCL1. (B) Treatment of NE-NSCLC lines with a RET inhibitor does not appear to bes selective for ASCL1+ lines compared to typical NSCLC lines. H1703 (IC50 = 0.005 μM) is the only exquisitely sensitive line to cabozantinib on account of focal amplification of PDGF and PDGFR. Cabozantinib MTS assays performed by Mike Peyton of the John Minna lab, UTSW.

5.2.3 Testing BCL2 as a Direct Transcriptional Target of ASCL1

BCL2 is an anti-apoptotic regulator that inhibits cell death by antagonizing the oligomerization of BAX and BAK along the mitochondrial membrane and preventing the release of cytochrome C from the mitochondria into the cytoplasm (Chipuk, Moldoveanu et al. 2010). ChIP-Seq analysis performed on ASCL1+ cell lines shows that ASCL1 contains several conserved binding sites within the BCL2 second intronic region (Figure 5.4A) in each cell line tested, suggesting that ASCL1 has a role in regulating BCL2 expression. Additionally, BCL2 is highly expressed in most neuroendocrine lung cancer lines compared to typical NSCLC lines (Figure 5.4B).

To test BCL2 transcriptional regulation by ASCL1, siRNA-mediated knockdown of ASCL1 was performed in NE-NSCLC cell lines H1755 and HCC1833. After 72 hours, knockdown of ASCL1 resulted in a significant decrease of BCL2 mRNA in both H1755 and HCC1833 (Figure 5.5A). All three siRNAs targeting ASCL1 demonstrated a reduction of BCL2 transcript. Similarly, immunoblot analysis shows a reduction of BCL2 protein following ASCL1 knockdown (Figure 5.5B). These data indicate a direct transcriptional regulation of BCL2 by ASCL1.

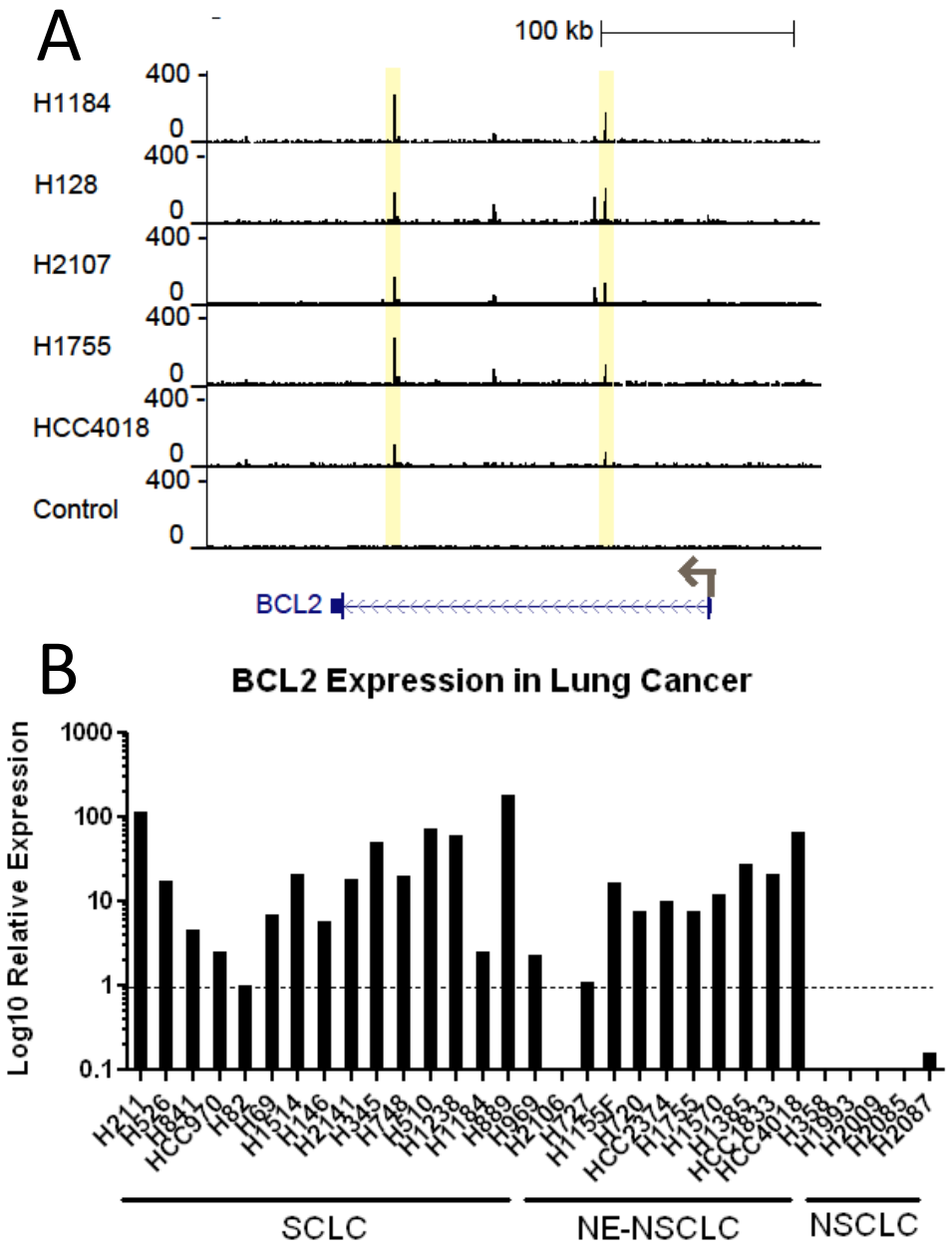

Figure 5.4: BCL2 is a potential target of ASCL1 and highly expressed in neuroendocrine lung cancers. (A) ChIP-Seq data showing binding of ASCL1 to two conserved regions with the BCL2 second intron. (B) BCL2 expression was measured in lung cancer cell lines using qRT-PCR analysis. BCL2 is highly expressed in nearly every neuroendocrine lung cancer line (SCLC and NE-NSCLC) and generally not expressed in typical NSCLC cell lines.

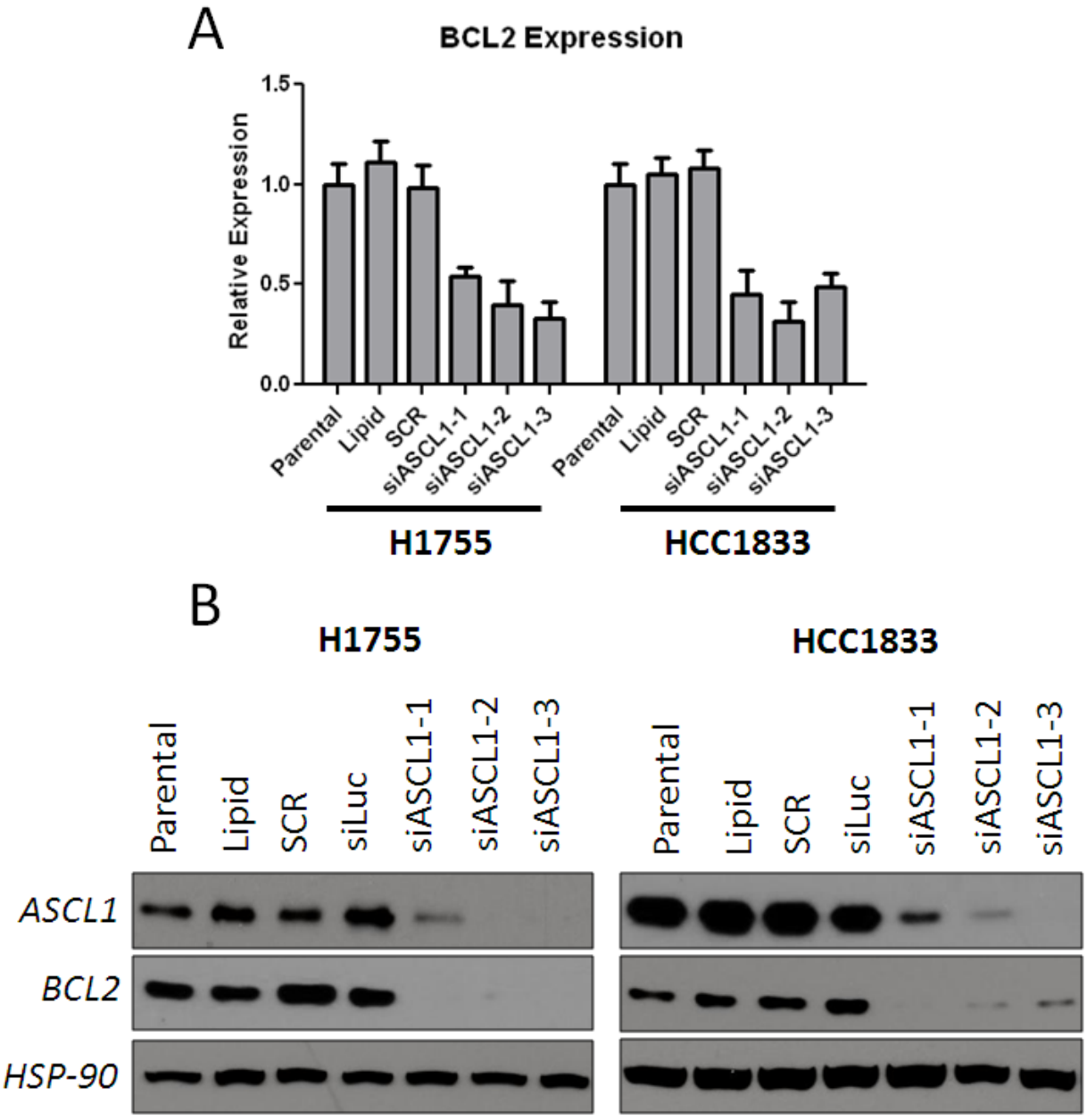

Figure 5.5: BCL2 is a transcriptional target of ASCL1 in NE-NSCLC lines. ASCL1 was knocked down using siRNA-mediated methods. 20 nM siRNA was transfected into NE-NSCLC cell lines for 72 hours. (A) Knockdown of ASCL1 in H1755 and HCC1833 results in a significant decrease of BCL2 mRNA as compared to controls. (B) Knockdown of ASCL1 results in an inhibition of BCL2 protein expression in H1755 and HCC1833 demonstrating transcriptional regulation of BCL2 by ASCL1.

5.2.4 Analysis of BCL2 Inhibition on the Growth and Survival of NE-NSCLC Cell Lines

BCL2 is an attractive therapeutic target because several specific small molecule inhibitors have been developed and have already completed or are currently undergoing clinical investigation in patients with different types of cancer (Kang and Reynolds 2009). As a transcriptional target of ASCL1, it is possible that BCL2 mediates survival of the ASCL1-dependent lung cancer cell lines. To test if BCL2 is directly required for survival, siRNA-mediated knockdown was performed and assayed for apoptotic cell death. After 72-hours knockdown with siBCL2, both H1755 and HCC1833 demonstrated an increased number or cells in the sub-G1 phase of the cell cycle compared to scrambled control-transfected cells (Figure 5.6A-B). H1993, a typical NSCLC cell line that does not express either ASCL1 or BCL2 was unaffected by BCL2 knockdown demonstrating that NE-NSCLC cell lines are uniquely sensitive to genetic inhibition of BCL2.

As a transcriptional target whose primary function is to prevent apoptosis, it is likely that BCL2 acts downstream of ASCL1 and does not feedback on the expression of ASCL1. To test if this is indeed the case, siRNA-mediated knockdown of BCL2 and ASCL1 was performed in HCC1833 cells. An immunoblot was utilized to show that knockdown of BCL2 has no effect on ASCL1 expression, while ASCL1 knockdown reduces both BCL2 and ASCL1 protein (Figure 5.6C). This evidence enhances the fact that BCL2 is a transcriptional target of ASCL1 that acts downstream to mediate survival of NE-NSCLC cells.

ABT-263 is an orally available, potent inhibitor of BCL2. Prior reports show that it has dramatic efficacy in reducing tumor in SCLC tumor xenograft models (Shoemaker, Mitten et al.

2008). The effectiveness of ATB-263 to induce apoptosis was tested in HBEC-3KT cells, H1993 typical NSCLC cells, and in H1755 and HCC1833. Following 24 hours of treatment, ABT-263 was found to induce striking levels of apoptosis only in the NE-NSCLC cell lines (Figure 5.7A). Both HBEC-3KT cells and H1993 did not reach significance in terms of apoptosis induction as measured by the relative number of cells in the sub-G1 phase of the cell cycle. Compared to DMSO control-treated cells, HBEC-3KT and H1993 cells could tolerate up to 500 nM ABT-263 for 24 hours without any apoptotic effects. H1755 and HCC1833, however, began showing significant apoptosis at 50 nM ABT-263 for H1755 and 100 nM ABT-263 for HCC1833. Qualitatively, H1755 cells began displaying evidence of apoptosis in cell culture including cell rounding and detachment following four hours of treatment with ABT-263, underscoring the ability of this drug to induce cell death in NE-NSCLC. To show that H1755 enters apoptosis rapidly following treatment with ABT-263, cells were harvested following 12 hours of treatment with 50, 100, or 500 nM ABT-263 and prepared for immunoblot. Western blot analysis showed a dose-dependent induction of cleaved PARP and cleaved Caspase3 following 12 hours of treatment with ABT-263 indicating a rapid entry of H1755 cells into apoptosis (Figure 5.7B).

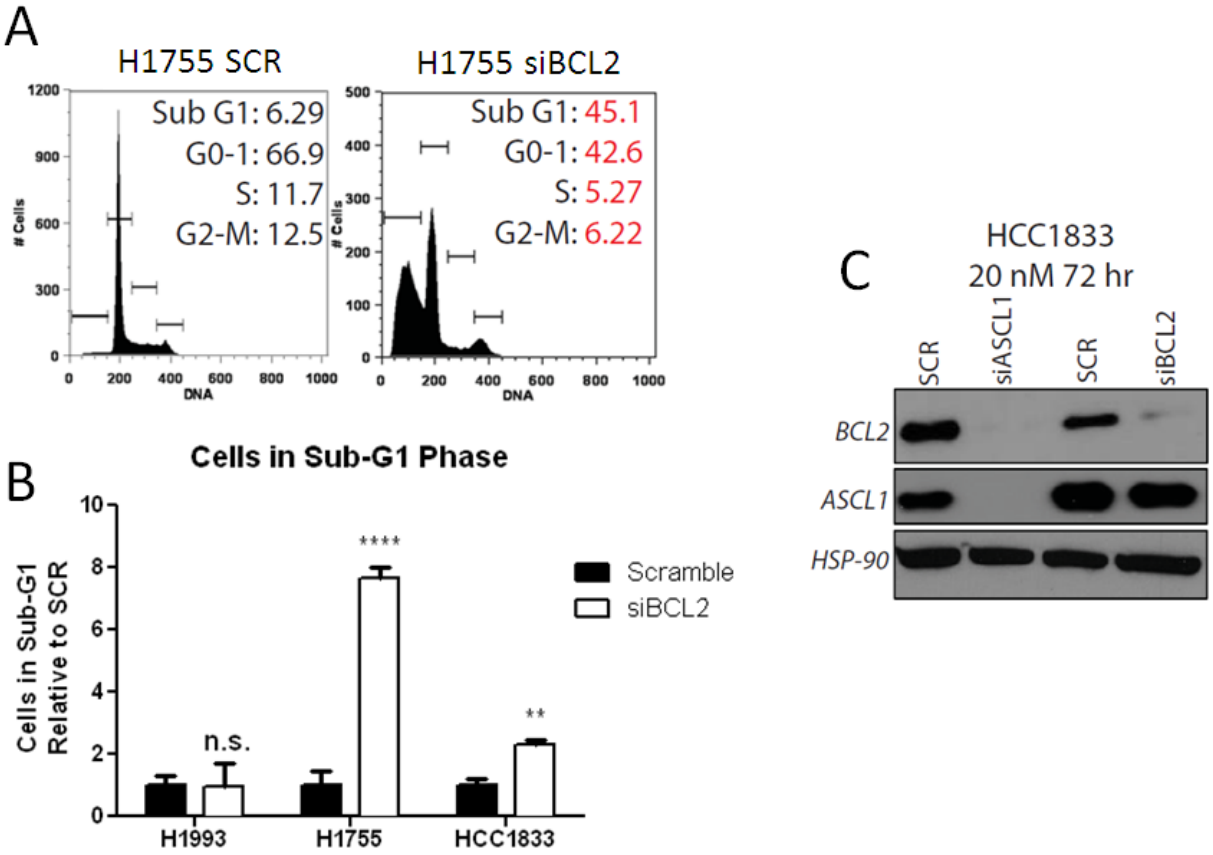

Figure 5.6: Analysis of BCL2 knockdown in NE-NSCLC cell lines. (A) Knockdown of BCL2 in H1755 leads to significant cell cycle abnormalities. An increase in the number of cells in the sub-G1 (apoptotic) phase is indicated following siRNA-mediated knockdown of BCL2. (B) Quantification of cells in the sub-G1 phase relative to scramble oligo-control. H1993 cells are unaffected by knockdown of BCL2 while NE-NSCLC cell lines H1755 and HCC1833 show a significant induction of apoptosis (** $p < 0.01$, **** $p < 0.001$). (C) Knockdown of BCL2 in HCC1833 does not reduce ASCL1 protein levels demonstrating that BCL2 acts downstream of ASCL1.

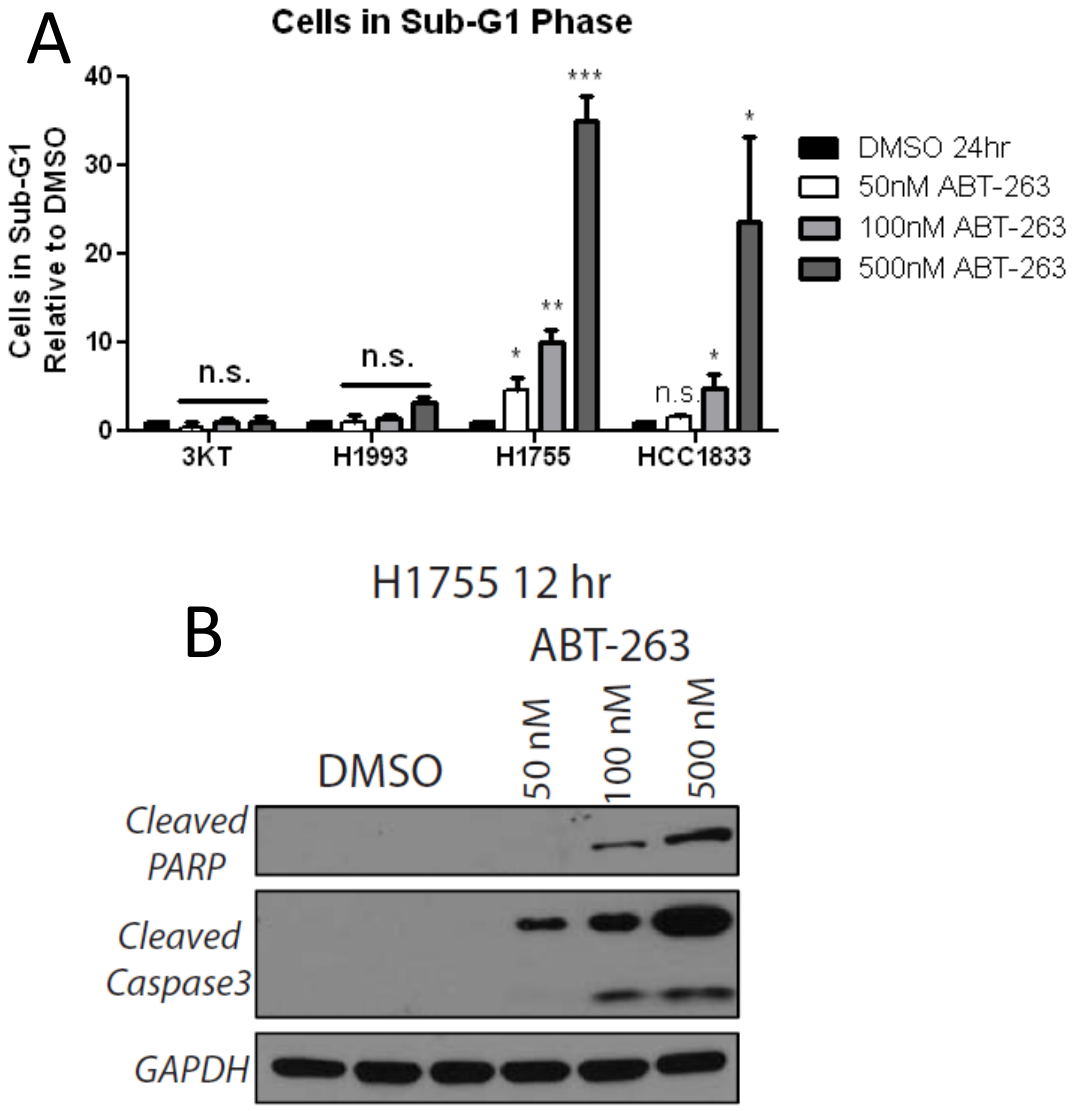

Figure 5.7: Inhibition of BCL2 with the small molecule ABT-263. (A) Treatment of cells with ABT-263 demonstrates a heterogeneous response in lung cell lines. Normal immortalized HBEC-3KT cells and typical NSCLC H1993 cells show no induction of apoptosis following treatment with ABT-263. H1755 and HCC1833 are uniquely sensitive, demonstrating cell death after treatment. Cells were allowed to adhere for 24 hours prior to treatment with ABT-263 for a subsequent 24 hours (* $p < 0.05$, ** $p < 0.01$, *** $p < 0.005$). (B) H1755 cells were profiled for apoptotic markers following 12 hour treatment with ABT-263. Following treatment, H1755 demonstrated induction of cleaved PARP and cleaved Caspase 3.

5.2.5 Efficacy of BCL2 Inhibition in vivo *Demonstrates Therapeutic Potential*

ABT-263 was tested in mouse xenografts to determine if BCL2 inhibition is specifically effective in NE-NSCLC H1755 tumors compared to typical NSCLC H1993 tumors. One million cells suspended in PBS were injected into the right subcutaneous flank region of female NOD/SCID mice and tumors grown until reaching an average volume of approximately 250 mm^3. Tumors were size-matched and split into two groups – those receiving vehicle control and those receiving ABT-263. ABT-263 or vehicle control was delivered by intraperitoneal injection at a daily dose of 100 mg/kg for 14 consecutive days. Tumors were measured daily by caliper measurement.

H1993, following 14 days treatment, showed no difference in tumor growth rate or tumor volume (Figure 5.8A). Tumors were allowed to grow another 14 days without treatment with volume measurements taken every three days, and no differences between control and ABT-263-treated mice could be detected. H1755, on the other hand, demonstrated dramatic tumor regression following treatment with ABT-263. After 14 days, ABT-263 treated xenografts averaged 68.7 mm^3 post-treatment after starting at an average of 290 mm^3 (Figure 5.8B). One day after the last injection, H1755 mice were sacrificed and tumors dissected. Compared to vehicle control-treated mice, ABT-263-treated mice presented with much smaller tumors (Figure 5.8C). The average weight of a vehicle-treated tumor was 1.46 grams while ABT-263 treated tumors averaged 0.06 grams, constituting a highly significant reduction of tumor burden (Figure 5.8D). These data provide a valuable proof-of-concept for the indication of BCL2 targeting in ASCL1-dependent NE-NSCLCs.

Tissue sections taken from xenograft tumors shows that vehicle-treated H1755 exhibits marked neuroendocrine features, including a high mitotic index and cellular fasciculations (Figure 5.9). The mitotic index is apparent in higher magnification images, and is indicated by the red arrows in Figure 5.9. H1755 xenografts treated with ABT-263 show absolutely no necrotic tissue, which is surprising given the apoptotic nature of the BCL2 inhibitor. Additionally, ABT-263-treated xenografts show a differentiated phenotype, including features commonly seen in pulmonary carcinoids such as the organization of cells into primitive ductal structures. This data suggests that BCL2-treated tumors undergo apoptotic cell death quickly following initial treatment and that outgrowth of a tumor with carcinoid-like morphology may constitute a mechanism of resistance.

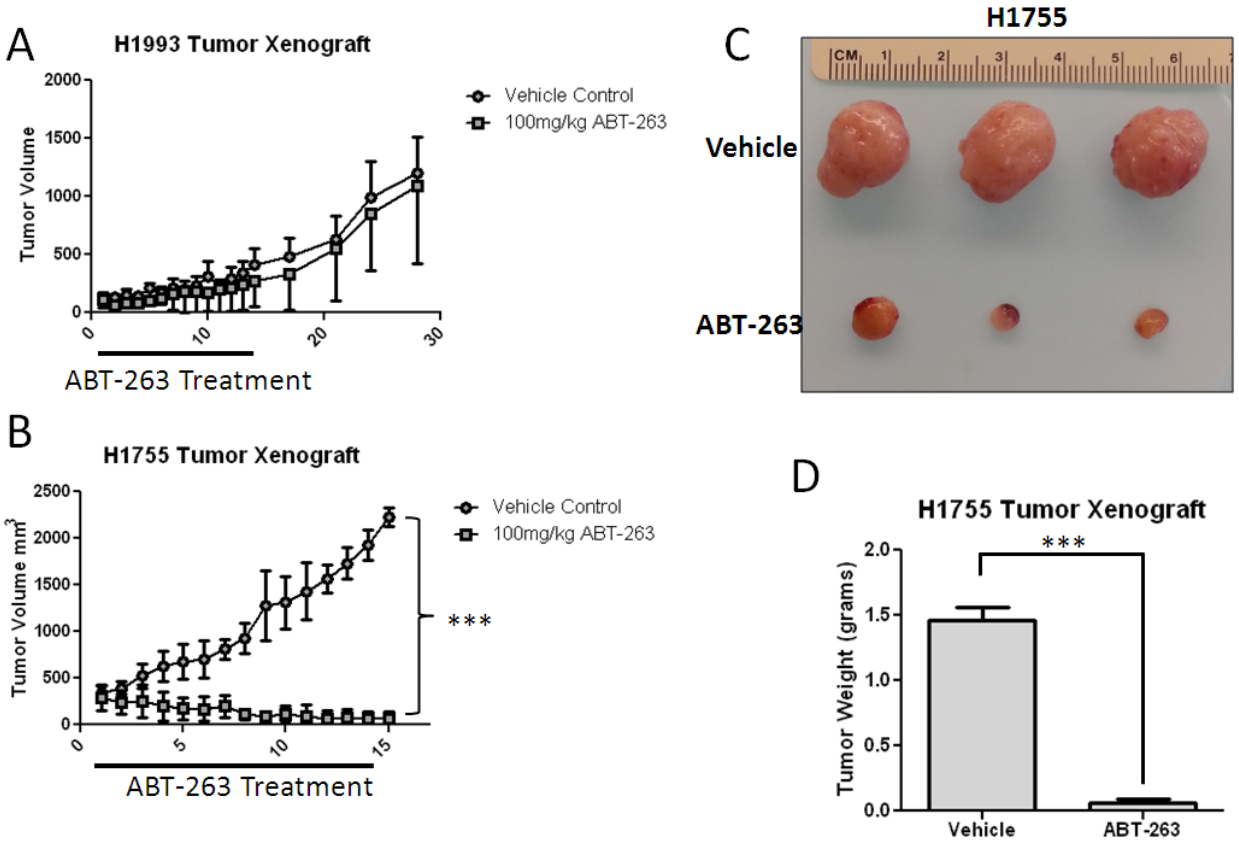

Figure 5.8: BCL2 inhibition demonstrates efficacy in vivo. (A) H1993 tumor xenografts treated with 100 mg/kg ABT-263 for 14 consecutive days did not demonstrate significant growth difference from vehicle-treated control. (B) H1755 treated with 100 mg/kg ABT-263 for 14 consecutive days showed a reduction of tumor volume compared to vehicle control (*** $p < 0.001$). (C) H1755 tumors treated with ABT-263 are dramatically reduced in size compared to vehicle-treated controls. (D) ABT-263-treated tumors are significantly smaller than tumors from vehicle-treated mice (*** $p < 0.001$).

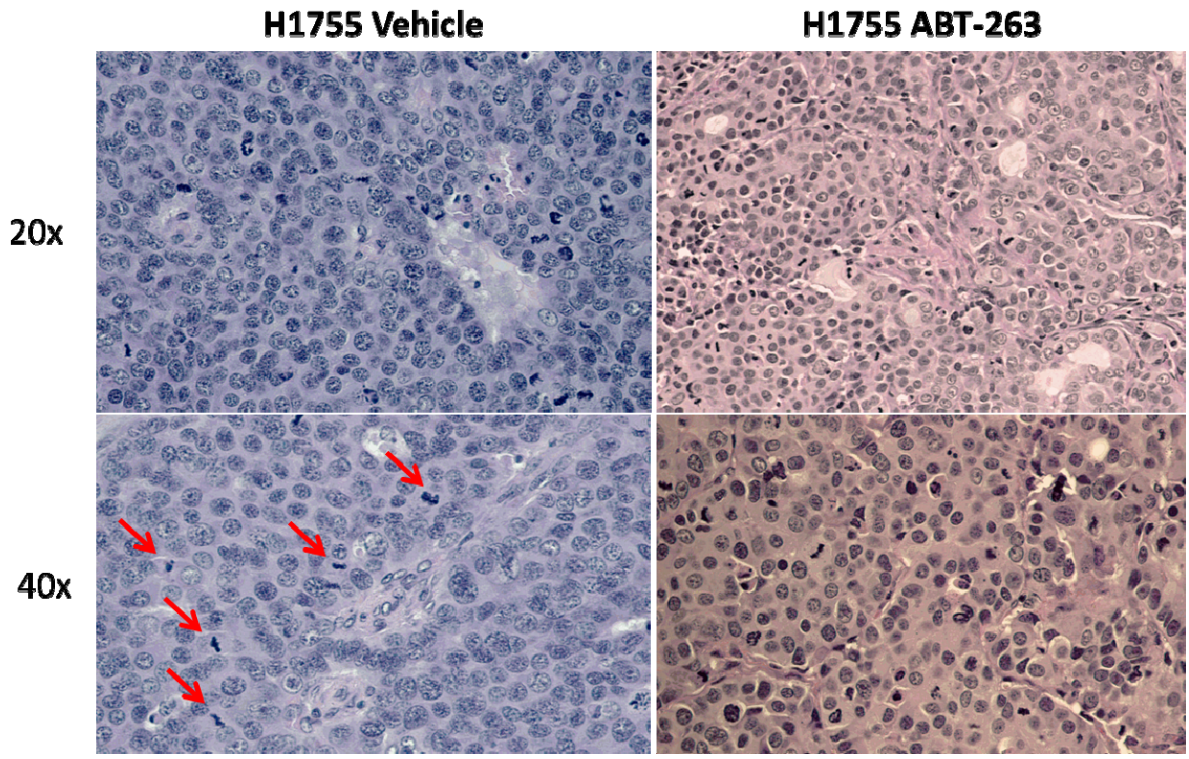

Figure 5.9: H1755 xenografts treated with ABT-263 exhibit differentiated phenotype. Hemotoxylin and eosin staining of tissue samples harvested from H1755 xenografts treated with vehicle control or ABT-263. Vehicle-treated tumors demonstrate neuroendocrine properties, including a high mitotic index (indicated by red arrows). ABT-263-treated tumors show differentiated phenotype including the apparent organization of cells into ductal structures, mimicking features seen in pulmonary carcinoids.

5.2.6 ALDH1A1 is not a Conserved ASCL1 Transcriptional Target

A prior article suggested that ASCL1 mediates its oncogenic effect by regulating the tumor initiating or cancer stem cell component of SCLCs (Jiang, Collins et al. 2009). ALDH activity has been previously shown to be a marker for cancer stem cells in the lung (Sullivan, Spinola et al. 2010). By showing that ASCL1 binds to the proximal promoter of the cancer stem cell marker ALDH1A1, the group made the assumption that ASCL1 participates in regulating tumor initiating cells in SCLC.

The striking tumorigenicity and rate of relapse of SCLC compared to NSCLC may be explained by the cancer stem cell model. If a large percentage of the tumor is composed of cells with stem-like activity, then the assumption can be made that relapse can occur far easier compared to a tumor with a small percentage of stem-like cells. The Aldefluor assay performed on neuroendocrine lung cancer lines showed that ALDH activity is dramatically elevated compared to typical NSCLC lines (Figure 5.10A) suggesting that neuroendocrine tumors have a greater stem-like phenotype. If ASCL1 regulation of the ALDH population is validated, it would suggest that ASCL1 is indeed a regulator of stemness in these tumors.

ChIP-Seq data gathered from five ASCL1+ cell lines, including SCLC, do not show any binding peaks for ASCL1 within the promoter or extended regulatory regions of ALDH1A1 (Figure 5.10B). Next, knockdown of ASCL1 using siRNAs in H1755 did not result in a reduction of ALDH1A1 mRNA suggesting that ASCL1 does not transcriptionally regulate this cancer stem cell marker (Figure 5.10C). Finally, siRNA-mediated knockdown of ASCL1 does not result in a reduction of ALDH1A1 protein (Figure 5.10D). These data do not validate

ALDH1A1 as a conserved transcriptional target of ASCL1. It is possible that ASCL1 regulates ALDH1A1 in a context-dependent manner.

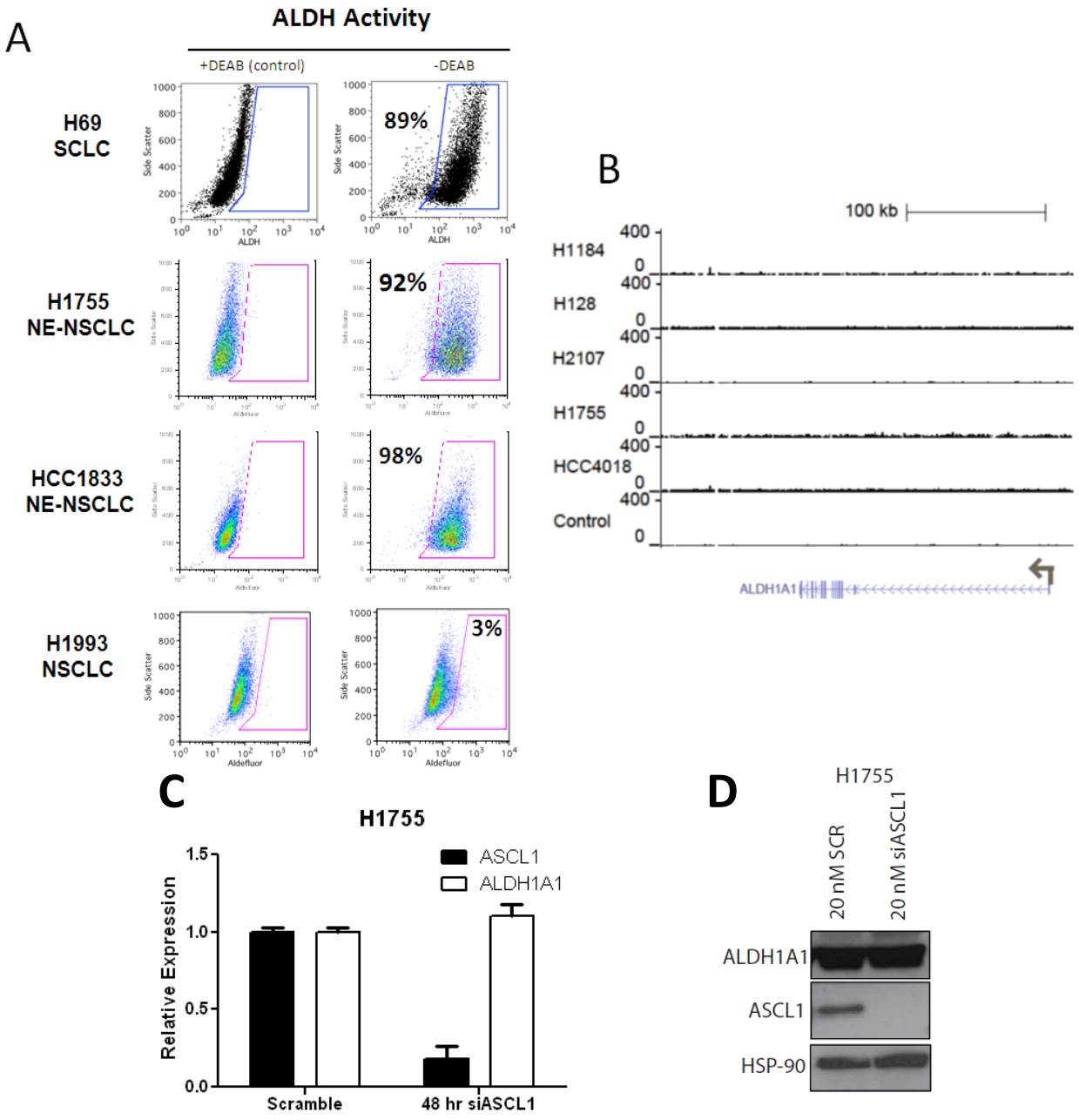

Figure 5.10: ALDH1A1 is not a conserved transcriptional target of ASCL1. (A) ALDH activity is significantly elevated in neuroendocrine lung cancer cell lines compared to typical NSCLCs. (B) ASCL1 ChIP-Seq analysis suggests that ASCL1 does not bind near the ALDH1A1 locus. (C) Knockdown of ASCL1 does not result in inhibition of ALDH1A1 mRNA transcript. (D) Knockdown of ASCL1 does not inhibit ALDH1A1 protein expression.

5.3 Discussion

In this chapter, two potential downstream targets of ASCL1 discovered via ChIP-Seq analysis were tested for their ability to induce a therapeutic response in ASCL1-dependent NE-NSCLC cell lines. RET, a receptor tyrosine kinase, binds the glial-derived neurotrophic factor (GDNF) family of ligands and activates signaling through the MEK/ERK, PI3K/AKT, and RHO/FAK pathways (Knowles, Murray-Rust et al. 2006). RET is critical player in the development of different cell types, playing major roles in the proper differentiation of the kidney and enteric nervous system (Arighi, Borrello et al. 2005). Recently RET has gained interest as a druggable target in cancer due to the appearance of activating mutations in MTC (Figlioli, Landi et al. 2013). Although RET is not mutated in the majority of lung cancer, including the subset of neuroendocrine lung cancers, the possibility existed that RET played a major role in the survival of ASCL1-dependent cancers.

RET was validated as a transcriptional target of ASCL1 following ASCL1 knockdown. RET mRNA transcript and protein loss were discovered coincident with inhibition of ASCL1 expression demonstrating transcriptional regulation of RET by ASCL1. Next, genetic inhibition of RET expression via siRNA-mediated knockdown resulted in an induction of apoptosis in the NE-NSCLC cell lines H1755 and HCC1833, suggesting that inhibition of RET may be a potential therapeutic avenue in ASCL1-dependent tumors. However, treatment of NE-NSCLC cell lines with a RET inhibitor did not demonstrate specificity for the NE-NSCLC subset compared to typical NSCLC cells. The IC50 for cabozantinib (CZ) in NE-NSCLC was approximately 2 μM, which is not low enough to merit clinical consideration. Effective

inhibition, for example in K562 BCR-ABL mutant lines treated with imatinib, would occur in the low nanomolar range (O'Hare, Pollock et al. 2004). Interestingly, H1703, a typical NSCLC cell line, was exquisitely sensitive to CZ treatment demonstrating an IC50 of 5 nM. H1703 contains a focal amplification of PDGF and PDGFR, the latter of which is potently inhibited by CZ (McDermott, Ames et al. 2009). Despite the attractiveness of discovering that the RET tyrosine kinase is a transcriptional target of ASCL1, it can be concluded from this study that RET is not specifically required for ASCL1-dependent cancers for survival, and that RET-targeted therapy in this cohort of tumors is not clinically useful.

The second ASCL1 transcriptional target studied in this chapter was BCL2. As an anti-apoptotic factor, BCL2 is an attractive gene for cancer to subvert in order to maintain survival and promote the tumorigenic phenotype. Anti-BCL2 therapy is therefore an attractive clinical intervention in cancers that rely on BCL2. SCLC highly expresses BCL2 and treatment of a number of SCLC xenografts with ABT-263, a BCL2 inhibitor, demonstrated tumor reduction following daily oral administration of the drug (Shoemaker, Mitten et al. 2008). Due to the effectiveness of ABT-263 *in vivo*, a clinical trial was undertaken to study the effect of BCL2 inhibition in patients with relapsed SCLC (Rudin, Hann et al. 2012). In spite of the effectiveness in pre-clinical models, ABT-263 showed partial response in one patient and stable disease in nine others out of a total of 39 patients suggesting that alone, ABT-263 is not sufficient to induce response in SCLC. However, all patients were treated previously with at least one therapy so the possibility remains that ABT-263 may be effective in treatment-naïve SCLC and ineffective in drug-resistant SCLCs. Another complication with ABT-263 was the prevalence of grade III-IV

thrombocytopenia (41% of patients) secondary to inhibition of BCL-xL, the BCL2 family member isoform responsible for maintaining survival of platelets (Debrincat, Josefsson et al. 2012). To address this problem, Abbott has created a third generation BCL2 inhibitor that eliminates the inhibition of BCL-xL and likely ameliorates the associated thrombocytopenia (Souers, Leverson et al. 2013). ABT-199 is currently undergoing clinical trial enrollment. Due to the high expression level of BCL2 in NE-NSCLC cell lines and the potential regulation of the gene by ASCL1, it is possible that BCL2 inhibition is a promising route to therapy in these tumors.

Following ASCL1 knockdown in H1755 and HCC1833, it was discovered that BCL2 mRNA transcript and protein are also significantly reduced demonstrating transcriptional control of BCL2 by ASCL1. To determine if ASCL1-mediated survival is controlled directly by BCL2, direct genetic inhibition of BCL2 was performed via siRNA knockdown. Reduction of BCL2 led to apoptosis following 72 hours of siRNA transfection in both H1755 and HCC1833 while H1993 control cells were unaffected by BCL2 knockdown relative to scrambled control-treated cells. To test the effectiveness of BCL2 small molecule therapy, ABT-263 was added to normal immortalized bronchial epithelial cells (HBEC-3KT), a typical NSCLC line (H1993), and NE-NSCLC lines (H1755 and HCC1833). ABT-263 was able to dramatically induce apoptosis in the ASCL1+/BCL2+ NE-NSCLC lines while sparing HBEC-3KT and H1993. Similarly, treatment of mouse xenograft tumors with ABT-263 showed remarkable effectiveness in H1755 tumors and no effect in H1993 tumors, suggesting that BCL2-targeted therapy may be an excellent treatment modality for ASCL1-dependent NE-NSCLC tumors.

Analysis of tissues from vehicle-treated and ABT-263-treated tumors provides a wealth of information supporting the use of BCL2 inhibitors for ASCL1-dependent cancers. First, H1755, developed from a patient with lung adenocarcinoma, demonstrates marked neuroendocrine features such as a high mitotic index. Next, ABT-263-treated tumors show no necrosis following two weeks of treatment, indicating that tumor regression occurs quickly following administration of drug, and that the resulting carcinoid-like tumor may constitute a mechanism of resistance for BCL2-sensitive tumors. Interestingly, the failure of BCL2 targeted therapy in SCLC clinical trials may be attributed to a drug-resistant feature of advanced SCLCs. Perhaps BCL2 targeted therapy will be more effective as frontline therapy for patients with SCLC prior to the outgrowth of a resistant subpopulation such as the one seen in the H1755 ABT-263-treated xenograft.

The effectiveness of BCL2 inhibition in H1755 xenograft tumors may be promoted by using ABT-199 rather than ABT-263. At the maximum dose of 100 mg/kg of ABT-263, toxicities were beginning to become apparent, including evidence of thrombocytopenia highlighted by the appearance of black, tarry stools. A higher dose may be achievable with the use of ABT-199 that may not only induce tumor regression but perhaps demonstrate complete remission in H1755. In addition to relieving the inhibition of BCL-xL and sparing platelets, ABT-199 also lowers its IC50 against BCL2 making it the most potent inhibitor of BCL2 ever developed (Souers, Leverson et al. 2013). These combinations make it an attractive drug for use in SCLC or NE-NSCLC and should make ABT-199 an intriguing drug to follow through clinical trials for these tumors.

Lineage transcription factors have previously been implicated in regulating genes such as BCL2 in order to mediate survival. It appears likely that ASCL1 follows a similar pattern during tumorigenesis and likely during development. The ability of ASCL1 to positively regulate BCL2 expression indicates that ASCL1 controls lineage survival and that neuroendocrine lung cancers take advantage of this mechanism in order to maintain the tumorigenic phenotype. Attacking lineage-related genes that mediate survival is therefore an attractive therapeutic possibility.

Interestingly, ASCL1 does not appear to regulate ALDH1A1, which was identified previously as a transcriptional target (Jiang, Collins et al. 2009). This suggests the likely scenario that ASCL1 regulates a different set of targets depending on the cellular context. Cancer genomes have incredible variation even within the subset of neuroendocrine lung cancers. Though the association of ASCL1 with the cancer stem cell niche is exceptionally interesting and potentially groundbreaking, to develop therapeutic indications for all ASCL1-dependent pulmonary tumors it is critical to study conserved transcriptional targets such as BCL2.

CHAPTER SIX

UPSTREAM REGULATION OF ASCL1

6.1 Introduction

ASCL1, as a neurogenic transcription factor, has gained much interest lately for its ability to reprogram cells into neurons. Using different types of starting cells, including fibroblasts, induced pluripotent stem cells, glial cells, and pericytes, ASCL1 along with other transcription factors can be used to differentiate those cells into diverse neural cells such as retinal progenitors, dopaminergic neurons, and neural stem cells (Adler, Grigsby et al. 2012; Karow, Sanchez et al. 2012; Zhao, He et al. 2012; Pollak, Wilken et al. 2013; Theka, Caiazzo et al. 2013). Along with ASCL1's ability to regulate development of neuroendocrine tissues such as pulmonary neuroendocrine cells, there exists a wealth of data about the function of ASCL1. However, besides the Notch pathway-mediated regulation of its expression little is known about the upstream regulation of ASCL1. Understanding the pathway(s) that maintain ASCL1 expression in cells may promote the development of novel cancer therapeutics that focus on inhibiting those pathways in order to reduce ASCL1 expression and thereby inhibit the survival of ASCL1-dependent cancers, including SCLC and NE-NSCLC.

The Notch pathway is part of a conserved developmental pathway, active in *Drosophila* and mammals, which inhibits neural/neuroendocrine differentiation in cells adjacent to those expressing ASCL1 (Sriuranpong, Borges et al. 2002). Briefly, ASCL1 regulates the transcription

of Notch ligands DLL1 and DLL3, which are then expressed on the cell surface and interact with Notch receptors of adjacent cells (Ball 2004). The resulting Notch pathway activation in adjacent cells turns on transcription of HES1, which binds to a common repressor motif in the ASCL1 promoter region and inhibits ASCL1 expression in the adjacent cell. Knowledge of this pathway has been utilized to show that activating the Notch pathway inhibits neuroendocrine cancer cell growth. Overexpression of the Notch intracellular domain (ICD) was sufficient to inhibit cell proliferation and reduce the neuroendocrine phenotype of MTC cells *in vitro* and *in vivo* (Kunnimalaiyaan, Vaccaro et al. 2006; Jaskula-Sztul, Pisarnturakit et al. 2011). Similarly, overexpression of Notch1 in human pancreatic carcinoid BON cells resulted in an upregulation of HES1, reduction in neuroendocrine markers including ASCL1, and inhibition of growth (Nakakura, Sriuranpong et al. 2005). This effect is also evident in lung cancer. Recombinant adenoviruses were used to deliver Notch1, Notch2, and HES1 in human SCLC cell lines H209 and DMS-53. Induction of the Notch proteins caused profound growth arrest, which was associated with G1 block secondary to upregulation of p21 and p27kip1 (Sriuranpong, Borges et al. 2001). Notch activation also led to a reduction of ASCL1 mRNA. Interestingly, in the SCLC model, induction of HES1 alone did not reduce growth or inhibit ASCL1 expression suggesting that other members of the Notch pathway may be required to regulate its expression. The Notch pathway is classically known as oncogenic, or tumor promoting, but it displays paradoxical tumor suppressive effects in neuroendocrine tumors expressing ASCL1. Current efforts are underway to develop small molecule Notch pathway activators and evaluate them for therapeutic

efficacy in pre-clinical models including SCLC and MTC, among others (Pinchot, Jaskula-Sztul et al. 2011; Truong, Cook et al. 2011).

Using a cell line model of MTC, a group of researchers from Johns Hopkins discovered that induction of Raf1 signaling could reduce expression of ASCL1 mRNA transcript (Chen, Carson-Walter et al. 1996; Vaccaro, Chen et al. 2006). Silencing of ASCL1 was discovered in parallel with reduction of RET expression, which was described in the previous chapter as a transcriptional target of ASCL1. In addition to loss of ASCL1 expression, the authors noted profound morphological changes, including cell rounding and cessation of growth. This important experiment introduced activation of the MEK/ERK pathway as a way to reduce levels of ASCL1 and inhibit neuroendocrine differentiation. Two small molecules have been used in cancer pre-clinical models to activate the MEK/ERK pathway: xanthohumol (XN) and phorbol 12-myristate 13-acetate (PMA). PMA is a diacylglycerol mimic and activates the MEK/ERK pathway by acting as a PKC agonist (Tahara, Kadara et al. 2009). The cellular targets of XN are yet to be determined. XN-treated MTC cells demonstrated activated ERK1/2 signaling, reduction of ASCL1 expression, inhibition of growth, and repression of neuroendocrine markers (Cook, Luo et al. 2010). In a neuroblastoma-derived cell line, PMA-treated Kelly cells showed a rapid reduction of ASCL1 mRNA and protein that was sustained for several days (Benko, Winkelmann et al. 2011). This research suggests that activation of the MEK/ERK pathway with small molecules may be a potential therapeutic option in neuroendocrine tumors that depend on ASCL1.

SCLC cell lines were also studied for their ability to reduce ASCL1 expression following upregulation of the MEK/ERK pathway. H249 cells infected with virus carrying the Ras gene completely inhibited the expression of ASCL1 and lost their neuroendocrine properties (Borges, Linnoila et al. 1997). Literature exists supporting activation of the MEK/ERK pathway is also important in inhibiting the formation of neuroendocrine tumors. A mouse model of human cancer where Raf-1 is expressed in an inducible manner only from pulmonary neuroendocrine cells (PNEC) via the cGRP promoter results in tumors appearing as bronchial adenocarcinomas with no overt neuroendocrine features (Sunday, Haley et al. 1999). This is in stark contrast to other mouse models utilizing PNECs as the cell-of-origin, which result in tumors that closely resemble human SCLC (Sutherland, Proost et al. 2011). Additionally, there is clinical evidence that SCLC has the ability to differentiate into a NSCLC phenotype (Falco, Baylin et al. 1990). Whether this is a true differentiation event or an outgrowth of a combined SCLC/NSCLC tumor remains to be determined. Interestingly, a clinical case where NSCLC differentiated into SCLC has also been reported. Patients with an EGFR-mutant NSCLC treated with anti-EGFR therapy became resistant to either erlotinib or gefitinib and developed SCLC that was sensitive to standard SCLC therapy, even though the original EGFR mutation was retained (Sequist, Waltman et al. 2011). While the authors did not speculate on a biological reason behind the transition from NSCLC to SCLC, it is possible that inhibition of the MEK/ERK pathway following EGFR inhibition with gefitinib or erlotinib allowed for a de-repression of the neuroendocrine phenotype and development of SCLC.

In this study, HCC1833 NE-NSCLC cells were studied for their reliance on inhibiting the MEK/ERK pathway to maintain survival and ASCL1 expression. Additionally, a combination therapy utilizing upstream inhibition of ASCL1 and downstream inhibition of the ASCL1 target gene BCL2 was studied as a therapeutic option for NE-NSCLC.

6.2 Results

6.2.1 Analysis of MEK/ERK Activation on ASCL1 Expression and Cell Survival

Activation of the MEK/ERK pathway was tested in HCC1833, an ASCL1+ NE-NSCLC cell line, using two small molecule compounds: PMA and XN. HCC1833 cells and HBEC-3KT were plated in six well plates overnight prior to treatment with DMSO control or 1, 10, or 100 nM PMA for 24 hours. RNA was extracted after treatment and analyzed for ASCL1 expression differences between the treatment groups. ASCL1 mRNA transcript levels in HCC1833 were significantly decreased in the PMA-treated cells compared to DMSO control-treated cells (Figure 6.1A). HBEC-3KT control cells showed no ASCL1 expression before or after treatment. Additionally, ASCL1 protein levels were measured by immunoblot and PMA-treated HCC1833 cells exhibited loss of ASCL1 protein (Figure 6.1B). This data demonstrates that the MEK/ERK pathway activator PMA is sufficient to reduce levels of ASCL1 protein, and that this loss of expression is likely transcriptional in nature.

The ability of PMA to modulate survival in ASCL1+ HCC1833 cells was measured by cell cycle analysis and calculating the relative number of cells in the sub-G1 (apoptotic) phase.

HCC1833 and HBEC-3KT cells treated for 24 hours with 1 nM PMA were analyzed for their cell cycle status. HBEC-3KT cells were totally unaffected by PMA while HCC1833 cells indicated both a G2-M block and a dramatic increase in apoptotic cells (Figure 6.2A). The relative percentage of cells in the sub-G1 phase was calculated for HBEC-3KT and HCC1833 cells treated with 1, 10, or 100 nM PMA compared to DMSO control (Figure 6.2B). HBEC-3KT cells were insensitive to PMA up to 100 nM, while HCC1833 cells showed significant induction of apoptosis at all three concentrations of PMA tested. An immunoblot for the apoptotic marker cleaved PARP was performed on HCC1833 cells treated with DMSO, 1, 10, or 100 nM PMA. PARP cleavage was readily detected after 24 hours treatment with PMA (Figure 6.2C). PMA is therefore able to reduce the expression of ASCL1 and also induce apoptotic cell death, analogous to the effect seen when ASCL1 is knocked down by siRNA methods.

Previous research performed on a neuroblastoma-derived cell line showed that PMA rapidly reduced ASCL1 mRNA transcript (Benko, Winkelmann et al. 2011). The ability of PMA to rapidly reduce ASCL1 mRNA expression in HCC1833 NE-NSCLC cells was measured in a short-term time-course assay where HCC1833 cells were treated with 100 nM PMA for up to three hours. Cells were harvested every 30 minutes and analyzed by qRT-PCR for ASCL1 mRNA expression. Protein lysates were prepared to study ERK activation and ASCL1 protein levels. PMA treatment for 30 minutes did not result in a significant decrease of ASCL1 mRNA, although phospho-ERK levels were dramatically elevated at this time point indicating an activation of the MEK/ERK pathway. After one hour of treatment, ASCL1 transcript was significantly reduced compared to DMSO control and this was followed by time-dependent

reduction up to 150 minutes of treatment. ASCL1 protein reduction was detected after three hours of PMA treatment (Figure 6.3A-B). Interestingly, phospho-ERK levels do not remain elevated after 24 hours, suggesting that perhaps ERK inhibition may also be involved in regulating ASCL1 expression (Figure 6.3C).

XN is a different compound that is reported to activate ERK signaling in the literature (Cook, Luo et al. 2010). HCC1833 cells were treated with XN and analyzed for ASCL1 expression and survival differences. Following 24 hours of treatment with 10, 20, and 30 uM XN, HCC1833 cells exhibited loss of ASCL1 mRNA expression (Figure 6.4A). The magnitude of loss of transcript is much greater in cells treated with 30 uM XN compared to 10 uM. ASCL1 protein is also lost in XN-treated cells in a dose-dependent manner (Figure 6.4B). Similar to the effects seen in PMA-treated cells, XN is also able to reduce ASCL1 mRNA and protein levels.

HCC1833 cells treated with 10, 20, and 30 uM XN demonstrate a dose-dependent cleavage of PARP compared to DMSO control-treated cells, indicating apoptotic cell death is occurring in concert with the reduction of ASCL1 transcript and protein (Figure 6.4B). H1993 NSCLC cells lacking ASCL1 expression and HCC1833 cells were treated with 10, 20, or 30 uM XN and analyzed for apoptotic cell death using the cell cycle assay. H1993 cells treated for up to 72 hours were insensitive to XN and showed no significant induction of apoptosis over DMSO control-treated cells. On the contrary, HCC1833 cells showed an increase in apoptotic cells at the 20 and 30 uM levels that were significantly increased over DMSO control-treated cells (Figure 6.4C). Taken together these results demonstrate that activation of the MEK/ERK pathway using small molecule pathway agonists is sufficient to reduce ASCL1 mRNA and protein expression

while inducing apoptotic cell death that is specific to NE-NSCLC cells. Additionally, these treatments spare normal HBEC-3KT cells and typical non-NE NSCLC H1993 cells suggesting that activation of MEK/ERK is a potential therapeutic option for ASCL1-dependent lung cancers.

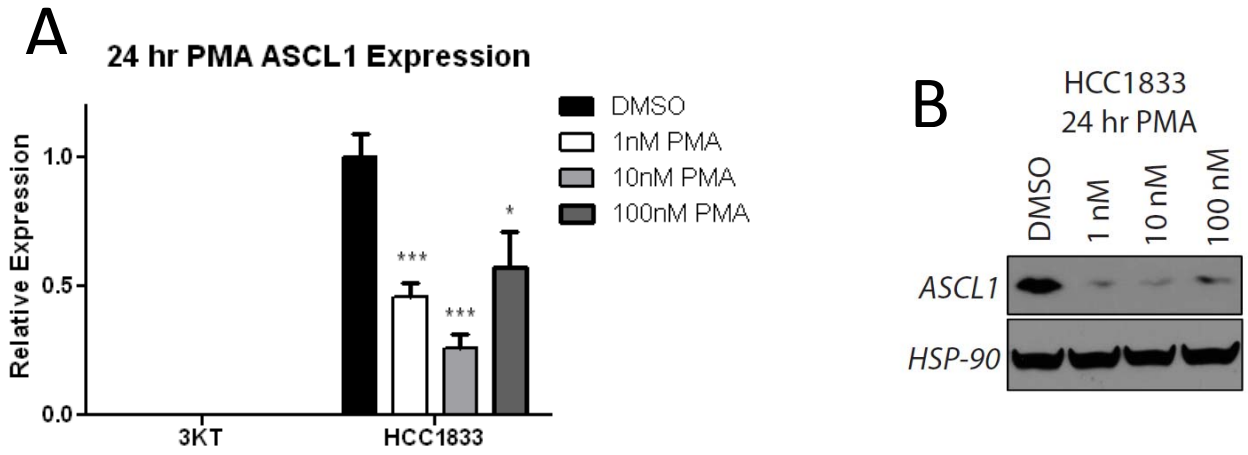

Figure 6.1: PMA inhibits ASCL1 expression in NE-NSCLC. (A) Treatment of HCC1833 with nanomolar concentrations of PMA for 24 hours rapidly inhibits ASCL1 mRNA expression. (B) ASCL1 protein levels are inhibited following 24 hours treatment with PMA.

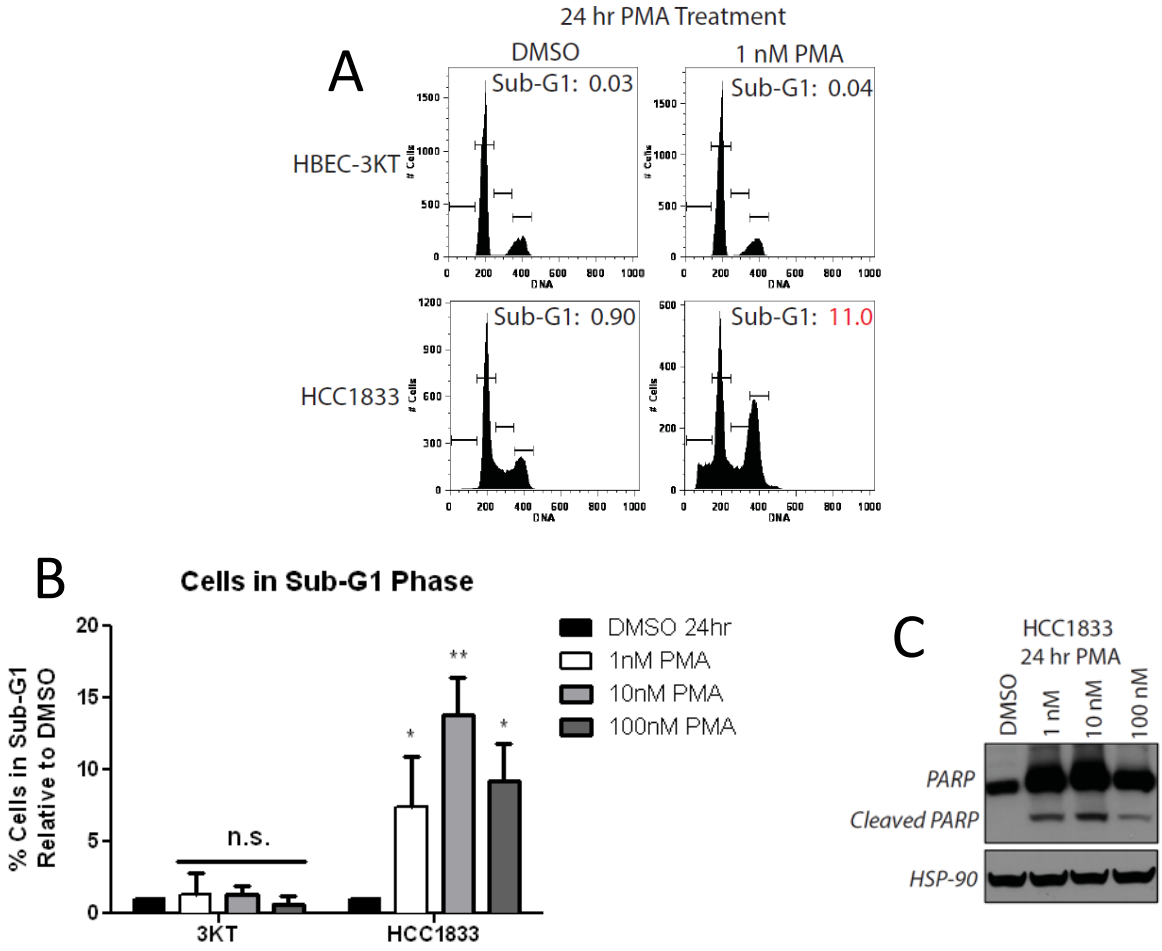

Figure 6.2: PMA treatment induces apoptosis in HCC1833. (A) Cell cycle analysis following 24 hours treatment of HCC1833 with either DMSO or 1 nM PMA demonstrates an induction of apoptosis as measured by the relative number of cells in the sub-G1 phase. A block in the G2-M phase of the cell cycle is also observed. (B) Quantification of apoptotic cells following treatment with PMA. HBEC-3KT cells are unaffected by PMA while HCC1833 cells show induction of apoptosis that is ~10 fold increased over DMSO control-treated cells (* $p < 0.05$, ** $p < 0.01$). (C) Treatment with PMA results in PARP cleavage, indicating apoptosis in HCC1833.

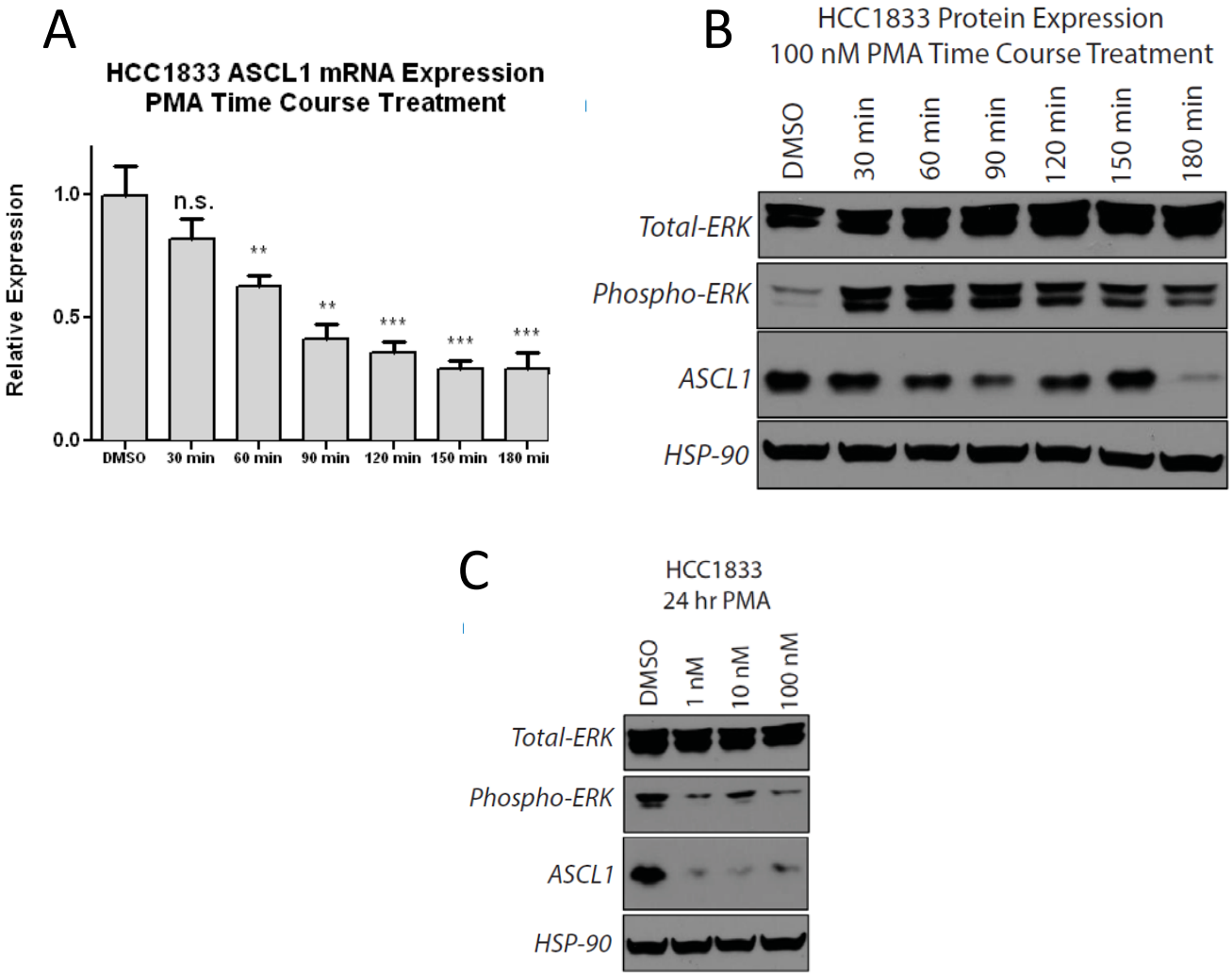

Figure 6.3: PMA induces rapid degradation of ASCL1 while elevating ERK activity. (A) A short time course treatment of HCC1833 cells with 100 nM PMA induces a rapid loss of ASCL1 mRNA expression. ASCL1 mRNA is significantly reduced following 1 hour of treatment (** $p < 0.01$, *** $p < 0.005$). (B) Western blot analysis shows that ASCL1 protein expression is lost following 3 hours treatment with 100 nM PMA. Phospho-ERK activity is induced immediately following treatment and is sustained. (C) Following 24 hours of treatment, loss of ASCL1 expression is retained. Phospho-ERK activity is reduced to below baseline after 24 hours.

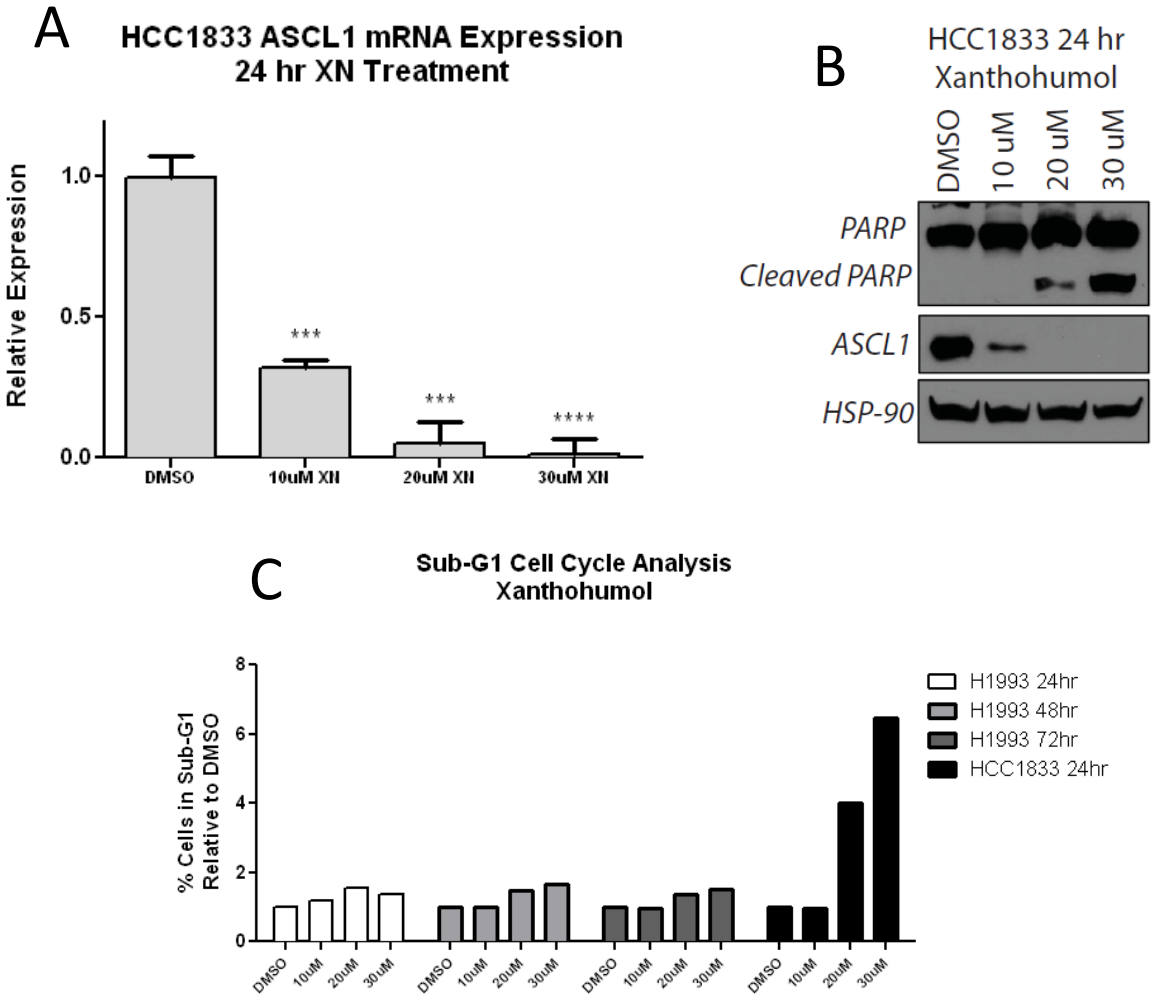

Figure 6.4: Xanthohumol reduces ASCL1 expression and induces apoptosis. (A) Treatment of HCC1833 cells with XN for 24 hours dramatically reduces ASCL1 mRNA expression (*** $p < 0.005$, **** $p < 0.001$). (B) XN induces loss of ASCL1 protein and induction of cleaved PARP that is dose-dependent. (C) XN treatment induces apoptosis in HCC1833 after 24 hours as measured by cell cycle analysis. H1993 was tested for sensitivity to XN for up to 72 hours. No induction of apoptosis was measured at any concentration of XN.

6.2.2 Combining Upstream and Downstream Therapeutic Targeting of the ASCL1 Pathway

Knockdown of ASCL1 is an effective method of reducing the viability of NE-NSCLC cell lines, which implicates the ASCL1 pathway as a therapeutic target for such tumors in the clinic. ChIP-Seq analysis and subsequent experiments showed that the critical anti-apoptotic factor BCL2 is a transcriptional target of ASCL1. Next, inhibition of BCL2 by siRNA or small molecule induced cell death specifically in ASCL1-dependent lung cancer cell lines. This effect was recapitulated *in vivo* when the BCL2 inhibitor ABT-263 was effective in reducing tumor burden in an ASCL+ cell line but not an ASCL-negative line. Finally, it was determined that ASCL1 expression is regulated by the MEK/ERK pathway in NE-NSCLC cells. Activation of the pathway by small molecule agonists resulted in decreased ASCL1 expression and induction of apoptosis. In this study, BCL2 inhibition was combined with MEK/ERK activation via PMA in order to understand if targeting the ASCL1 pathway by inhibiting its expression upstream while simultaneously repressing a downstream transcriptional target is an effective way to induce dramatic cell death.

Three cell lines were utilized for the combination therapy study – normal HBEC-3KTs, a non-NE NSCLC line H1993, and the NE-NSCLC line HCC1833. All three cell lines were treated with DMSO or 1, 10, or 100 nM PMA as well as DMSO or 50, 100, or 500 nM ABT-263. The combination therapy consisted of cells being treated with DMSO control or 1 nM PMA in addition to 50, 100, and 500 nM ABT-263. Cells were treated for 24 hours and then assayed for apoptosis using cell cycle analysis. As reported earlier, treatment of HBEC-3KT and H1993 cells with PMA results in no quantifiable difference in apoptotic levels compared to DMSO-treated

cells. HCC1833, however, retains the cell death phenotype and shows an induction of apoptosis that is increased approximately 10-fold over baseline DMSO compared to PMA-treated cells (Figure 6.5). HBEC-3KT and H1993 cells treated with the BCL2 inhibitor ABT-263 show no significant induction of apoptosis compared to cells treated with DMSO. HCC1833 cells, as described in the previous chapter, are exquisitely sensitive to 500 nM ABT-263, demonstrating a 25-fold induction of apoptosis over baseline. Cells treated with the combination of 1 nM PMA and varying concentrations of ABT-263 showed a heterogeneous response. HBEC-3KT cells showed a modest dose-dependent induction of apoptosis compared to baseline DMSO-treated cells suggesting that the combination of PMA and ABT-263 may be somewhat toxic to normal cells. H1993 cells treated with the combination of PMA and ABT-263 did not show a dramatic additional induction of apoptosis compared to cells treated with either single agent alone. HCC1833 cells, however, were incredibly sensitive to the combination of PMA and ABT-263, particularly when 500 nM of ABT-263 was used. At that concentration, a 50-fold induction of apoptosis over baseline was detected signifying dramatic sensitivity of NE-NSCLC cells to reduction of ASCL1 expression with concurrent inhibition of a downstream ASCL1 target. This is a proof-of-principle result that indicates targeting the ASCL1 pathway upstream and downstream has therapeutic implications in ASCL1-dependent lung cancers.

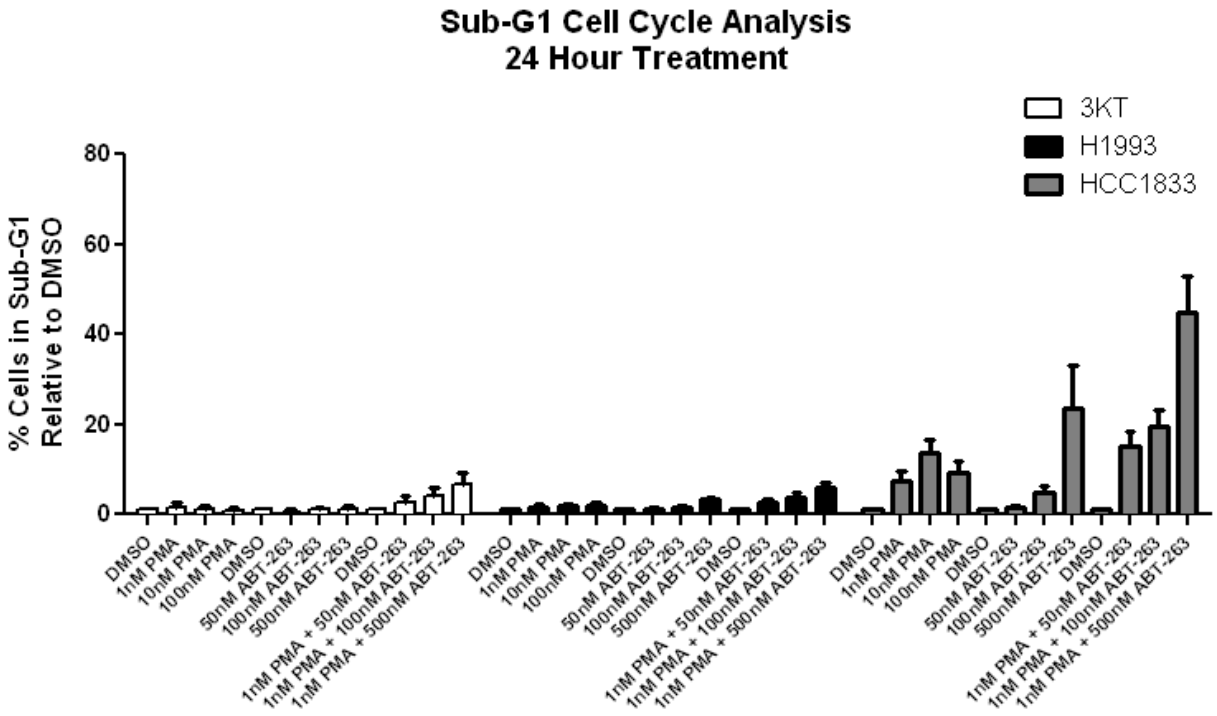

Figure 6.5: Combination therapy with PMA and ABT-263 induces massive cell death in NE-NSCLC cells. Inhibition of BCL2 with ABT-263 was combined with PMA to measure the effect of targeting the ASCL1 pathway upstream and downstream in lung cell lines. HBEC-3KT, H1993, and HCC1833 cells were treated with PMA alone, ABT-263 alone, or the combination of 1 nM PMA and 50, 100, or 500 nM ABT-263. 3KT cells remained resistant to PMA, ABT-263, and only began showing slight induction of apoptosis when the combination therapy was applied. H1993 cells were resistant to all treatments. HCC1833 cells showed a 50-fold increase in the number of apoptotic cells in response to the combination therapy compared to DMSO control-treated cells.

6.2.3 Analysis of MEK/ERK Inhibition on ASCL1 Expression and NE-NSCLC Survival

Previously, it was shown that inhibition of ASCL1 with PMA, a MEK/ERK pathway activator, eventually resulted in reduced ERK phosphorylation after 24 hours of treatment. To determine if MEK/ERK pathway inhibition played a role in the regulation of ASCL1 expression, siRNA-mediated knockdown experiments were performed. In this study, HCC1833 cells were transfected with siRNAs targeting ASCL1, MEK1, MEK2, ERK1, ERK2, and a simultaneous knockdown targeting ASCL1 and MEK1. ASCL1 protein expression as well as phospho-ERK expression was analyzed 72 hours post-transfection. This study demonstrated that knockdown of ASCL1 cleanly reduces ASCL1 protein expression while MEK1, MEK2, ERK1, or ERK2 inhibition had no effect on ASCL1 levels (Figure 6.6). Each siRNA targeting the MEK/ERK pathway showed significant reduction in phospho-ERK levels indicating that the primary target of the siRNA was inhibited. A surprising result is that knockdown of ASCL1 actually activated ERK phosphorylation to a significant degree suggesting that ASCL1, when expressed in HCC1833, actively represses the ERK pathway. Even in the presence of siMEK1, which completely inhibited ERK phosphorylation on its own, siASCL1-3 still showed a rescue of phospho-ERK. This indicates that the MEK/ERK pathway not only regulates ASCL1 expression, but that ASCL1 is also involved in regulating its repression establishing a probable double-negative feedback loop.

Additionally, repression of the MEK/ERK pathway using currently available small molecule inhibitors was also tested. Sorafenib is a multi-kinase inhibitor that potently targets VEGFR, PDGFR, and RAF (Wilhelm, Adnane et al. 2008). It is currently approved for the

treatment of advanced clear cell carcinoma and primary hepatocellular carcinoma (Escudier, Eisen et al. 2007; Llovet, Ricci et al. 2008). Sorafenib was used to treat HCC1833 cells, which were subsequently assayed for survival and ASCL1 protein expression. Despite using concentrations as high as 1 uM, sorafenib was ineffective in reducing ASCL1 protein expression in either H1755 or HCC1833 following 24 hours of treatment (Figure 6.7A). Additionally, treatment for up to 72 hours resulted in no induction of apoptosis over baseline DMSO control-treated cells (Figure 6.7B). A second MEK/ERK pathway inhibitor is AZD-6244, also known as selumetinib (Yeh, Marsh et al. 2007). It inhibits MEK1 and MEK2 with potent efficiency and is currently being tested in clinical trials for a variety of tumor types, including NSCLC, as well as tumors with BRAF mutations such as melanoma (Catalanotti, Solit et al. 2013). AZD-6244 was used to treat HCC1833 cells for up to 72 hours with concentrations of 100 nM, 500 nM, and 1 uM. This drug was unable to inhibit ASCL1 protein expression in HCC1833 and treatment for up to 72 hours resulted in no induction of apoptosis, mirroring the results seen with (Figure 6.7C-D). These results, together with data gathered from the genetic siRNA-mediated inhibition of MEK1/2 and ERK1/2, indicate that inhibition of the MEK/ERK pathway is not able to reduce ASCL1 expression or induce apoptosis and is unlikely to yield therapeutically useful results if used in the clinic against ASCL1-dependent lung cancers.

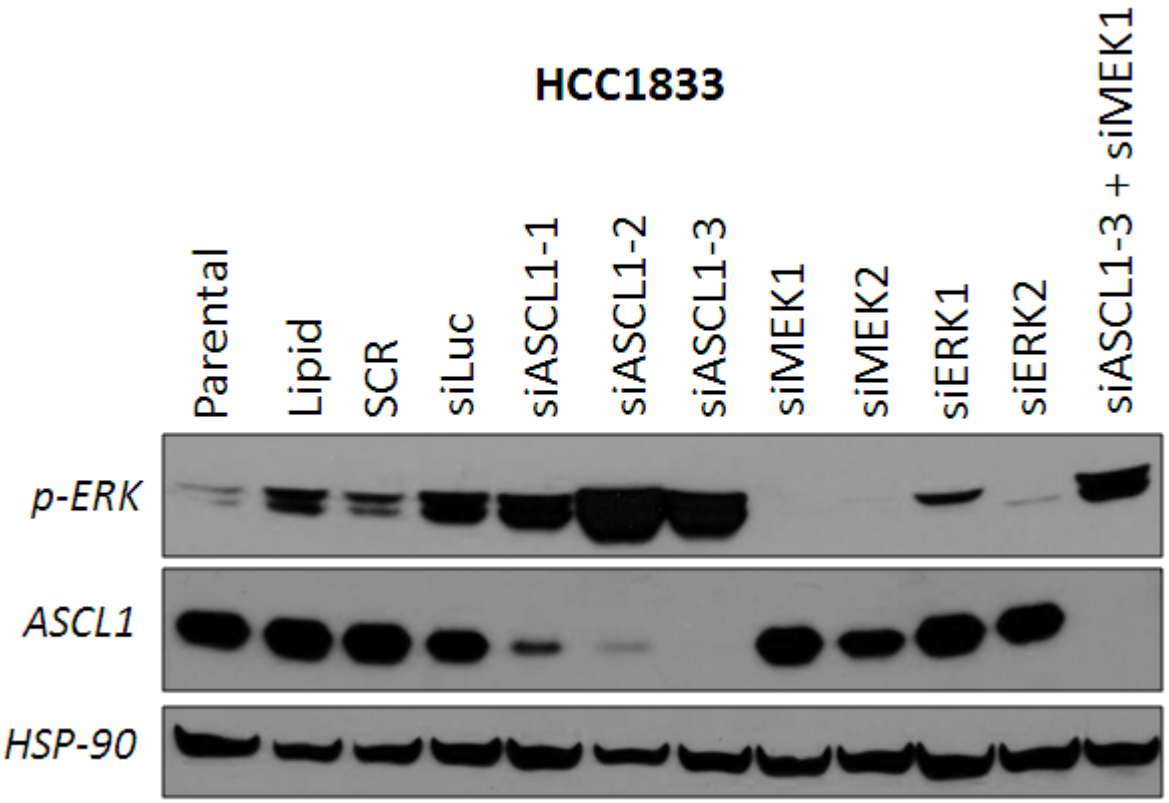

Figure 6.6: ASCL1 represses ERK activity. Knockdown of ASCL1 in HCC1833 using siRNAs induced an induction of ERK activity as measured by phospho-ERK. Inhibition of the MEK/ERK pathway resulted in no reduction of ASCL1 protein. Co-knockdown of ASCL1 and MEK1 was still able to rescue ERK activity, demonstrating that ASCL1 actively repressed the ERK pathway.

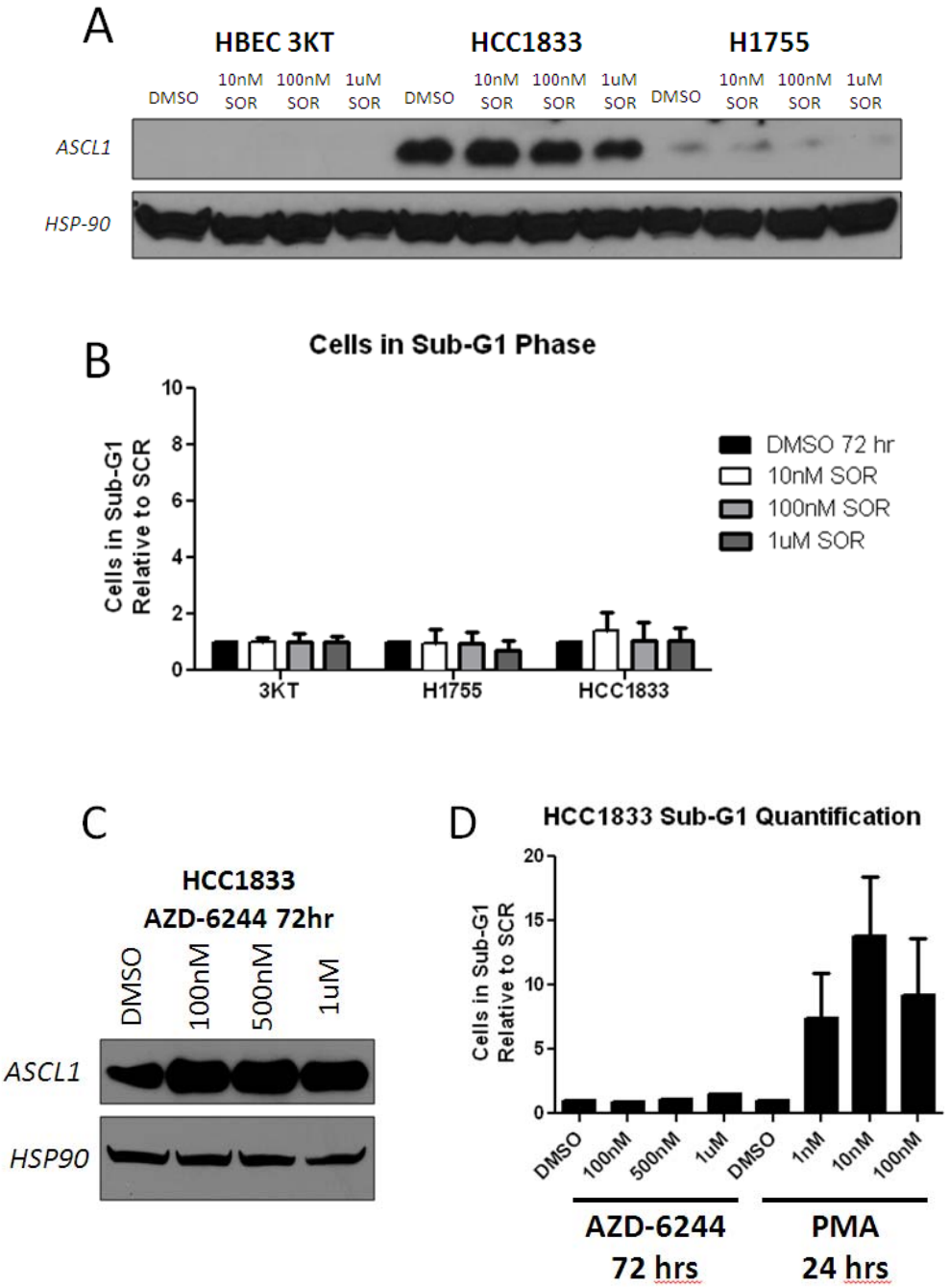

Figure 6.7: Inhibition of the MEK/ERK pathway with small molecules does not reduce ASCL1 expression or induce cell death in NE-NSCLC. (A) Treatment with Sorafenib does not reduce ASCL1 protein in H1755 or HCC1833. (B) Sorafenib does not induce cell death in NE-NSCLC cells following 72 hours of treatment. (C) AZD-6244 does not reduce ASCL1 protein expression following 72 hours of treatment in HCC1833. (D) AZD-6244 treatment in HCC1833 for 72 hours does not lead to cell death. PMA induction of apoptosis is shown as a reference.

6.3 Discussion

Little is known about the upstream regulation of ASCL1 despite a wealth of knowledge available about the downstream function of the gene. In the previous chapter it was shown that inhibition of a critical downstream transcriptional target of ASCL1, BCL2, was sufficient to induce tumor regression in mouse models of NE-NSCLC. This chapter focused on studying the upstream regulation of ASCL1 to determine if inhibition of ASCL1 expression was possible using small molecules and whether that inhibition resulted in cell death. A well-known regulator of ASCL1 is the Notch pathway, where activation of Notch receptors via ligand binding activates HES1, which directly inhibits the expression of ASCL1 (Sriuranpong, Borges et al. 2002). Activation of the Notch pathway either by overexpression of the full Notch receptors or the intracellular binding domain was sufficient to reduce ASCL1 expression and induce cell death in SCLC and MTC pre-clinical models (Sriuranpong, Borges et al. 2001; Jaskula-Sztul, Pisarnturakit et al. 2011). This is an example of how paradoxical activation of a common oncogenic pathway can be tumor suppressive based on the context. It remains to be determined whether Notch pathway activation with small molecules is a suitable route to therapy for neuroendocrine cancers such as SCLC or NE-NSCLC. The pitfalls associated with treating patients with a drug that activates an oncogenic pathway may be too much to overcome, although this must be proven first in pre-clinical studies as well as clinical trials in patients. Efforts are currently underway to discover novel small molecules that activate the Notch pathway with high specificity (Pinchot, Jaskula-Sztul et al. 2011). Resveratrol was identified from a screen of over 7,000 compounds as a Notch activator, and subsequent experiments showed it was able to induce

a dose-dependent growth inhibition in pancreatic and lung carcinoid cells, as well as a reduction in the expression of ASCL1 (Truong, Cook et al. 2011). Xenograft studies were performed with resveratrol injected daily, which resulted in a slowing of carcinoid tumor growth without grossly affecting morbidity or mortality. More work involving resveratrol is needed, particularly for other tumors that may be sensitive to Notch activation like SCLC or NE-NSCLC. It will be interesting to determine if the pairing of resveratrol and ABT-263 will be sufficient to inhibit tumor growth in ASCL1-dependent lung cancers.

Prior research showed that activating MEK/ERK signaling could inhibit neuroendocrine differentiation in various cancers, particularly in medullary thyroid carcinoma and SCLC. Induction of Raf-1 in MTC cells was sufficient to reduce ASCL1 and neuroendocrine gene expression, while simultaneously inhibiting growth (Chen, Carson-Walter et al. 1996; Vaccaro, Chen et al. 2006). Similarly, a mouse model of inducible Raf-1 under the control of the cGRP promoter resulted in tumors that displayed bronchial adenocarcinoma morphology with no neuroendocrine features (Sunday, Haley et al. 1999). Small molecule activators of the MEK/ERK pathway include xanthohumol (XN) and phorbol 12-myristate 13-acetate (PMA). XN-treated MTC cells showed an activation of the MEK/ERK pathway, reduction of ASCL1 expression, and inhibition of growth (Cook, Luo et al. 2010). PMA was able to rapidly reduce ASCL1 expression in a neuroblastoma-derived cell line (Benko, Winkelmann et al. 2011). Both compounds were used to treat HCC1833 NE-NSCLC cells and both displayed similar results. XN and PMA-treated cells showed a rapid reduction of ASCL1 mRNA and protein, which was associated with an induction of apoptosis. Analogous to the Notch pathway story, it was

discovered that activation of the classically pro-oncogenic MEK/ERK pathway was actually tumor suppressive in ASCL1-dependent HCC1833 cells.

The activation of two well-studied oncogenic pathways resulting in tumor suppressive effects in ASCL1-dependent cancers is a surprising result. The possibility exists that both the Notch pathway and the MEK/ERK pathway are required for the proper developmental regulation of pulmonary neuroendocrine cells and that the genetic information required by the cell to respond to cues from the Notch and MEK/ERK pathways is still encoded even after a cell becomes neoplastic. Further research is required to determine what cellular changes occur during the activation of the MEK/ERK pathway that result in a rapid decrease of ASCL1 mRNA transcript.

The study of PMA treatment in HCC1833 led to a surprising result, namely the inhibition of ERK phosphorylation following 24 hours of treatment suggesting that MEK/ERK inhibition may play a role in the regulation of ASCL1. siRNA-mediated knockdown experiments demonstrated that MEK1, MEK2, ERK1, and ERK2 inhibition was not sufficient to reduce ASCL1 expression. This result was validated by using small molecule inhibitors of MEK1/2 and RAF that included sorafenib and AZD-6244. A novel outcome was that knockdown of ASCL1 resulted in a significant increase in ERK phosphorylation, demonstrating that ASCL1 actively represses the MEK/ERK pathway. Even when ASCL1 is knocked down in the presence of siMEK1, which completely represses ERK phosphorylation on its own, there was still a full rescue of phospho-ERK demonstrating that this repression is potentially ERK-specific. The pathway involved in the regulation of ERK by ASCL1 has yet to be determined. It is likely that

ASCL1 directs the transcription of genes that repress ERK phosphorylation. ChIP-Seq data from the five ASCL1+ cell lines suggests that ASCL1 regulates several dual specificity phosphatases (DUSPs), which act on various stages of the mitogen-activated protein kinase (MAPK) pathway, including MEK/ERK, to remove activating phosphates (Caunt and Keyse 2013). Once ASCL1 is repressed, DUSPs are no longer expressed in the cell and are unable to inhibit the activation of MAPK and more specifically ERK1/2, which would result in an increased phosphorylated state of the protein as seen here. If proven to be true, then DUSPs regulated by ASCL1 would become a prime therapeutic target. Inhibition of DUSPs would activate MEK/ERK, rapidly reduce ASCL1 expression, and induce cell death. Taking advantage of the double-negative feedback loop involving ASCL1 may produce dramatically increased cell death compared to targeting downstream effectors.

A proof-of-principle experiment was performed to show that combination therapy involving inhibition of ASCL1 by modulating upstream regulatory pathways along with inhibition of BCL2, a downstream target, would lead to extensive cell death in NE-NSCLC cells. HCC1833 treated with the combination of PMA and ABT-263 resulted in a 50-fold increase of cell death over DMSO-treated baseline. This effect suggests that the ASCL1 pathway is absolutely required for cell survival in NE-NSCLC and that attacking it using a combination of rationally-devised drugs results in a therapeutically viable option. The next step is to determine whether this effect translate to an *in vivo* setting by treating mice with PMA and ABT-263 in combination. Preliminary studies showed that PMA is dangerously toxic when dissolved in

DMSO and injected I.P. into female NOD/SCID mice even though PMA has been used in human clinical trials and passed phase one dose-escalation studies.

Despite the toxicity of PMA *in vivo*, the fact that the MEK/ERK pathway regulates ASCL1 is important in determining novel therapies aimed at improving clinical outcome for lung cancers dependent on ASCL1. Pulmonary neuroendocrine tumors, including SCLC and NE-NSCLC, appear at a rate of approximately 40,000 per year so a highly specific upstream inhibitor of ASCL1 expression may be an incredibly lucrative treatment option if proven effective in pre-clinical models.

CHAPTER SEVEN

CONCLUSION AND ONGOING STUDIES

7.1 Conclusion

Non-small cell lung cancers with neuroendocrine features are difficult to diagnose and treat, and no consensus has been reached as to how they should be managed clinically. This confounding subtype of lung cancer is made even more difficult to study because of the lack of an established pre-clinical model. The meteoric rise of high-throughput technologies in biological research has expanded the ability to study cancers on a genome-wide level. It is now possible to ascertain the expression of every single mRNA in a tumor and determine each DNA mutation using next generation sequencing technologies. This advancement is making it possible to utilize massive amounts of data in order to reclassify tumors. Early returns of data from the "genome-wide era" suggest that lung cancer is an incredibly heterogeneous disease with pathological typing unlikely to capture the diverse nature of these tumors. Accurate diagnosis is paramount to providing the best treatment options for lung cancer patients. In this study, genome-wide approaches were taken to discover a pre-clinical model for NSCLC with neuroendocrine features, with subsequent studies indicating ways to therapeutically target this subset of cancer.

The objective of this dissertation was to identify NSCLC cell lines with neuroendocrine features and to rationally determine actionable therapeutic targets specific for these tumors. To this end, the most salient findings include (Figure 7.1):

1. Genome-wide mRNA expression profiling identified a cluster of NSCLC cell lines with neuroendocrine gene expression similar to SCLC. ASCL1 is the highest expressed gene in NE-NSCLC cell lines and is essential for their survival (Chapter Three).

2. ChIP-Seq analysis performed on ASCL1+ cell lines determined a gene signature predicting for poor prognosis in lung adenocarcinoma patients as well as serving as a diagnostic biomarker (Chapter Four).

3. BCL2 and RET are direct downstream targets of ASCL1. Inhibition of BCL2 using ABT-263, a drug currently in clinical trials, led to dramatic cell death *in vitro* and tumor regression *in vivo* in NE-NSCLC (Chapter Five).

4. A double negative feedback loop exists between ASCL1 and the MEK/ERK pathway. Activation of MEK/ERK using small molecule pathway agonists inhibited the expression of ASCL1 and induced cell death. Inhibition of ASCL1 activated ERK activity (Chapter Six).

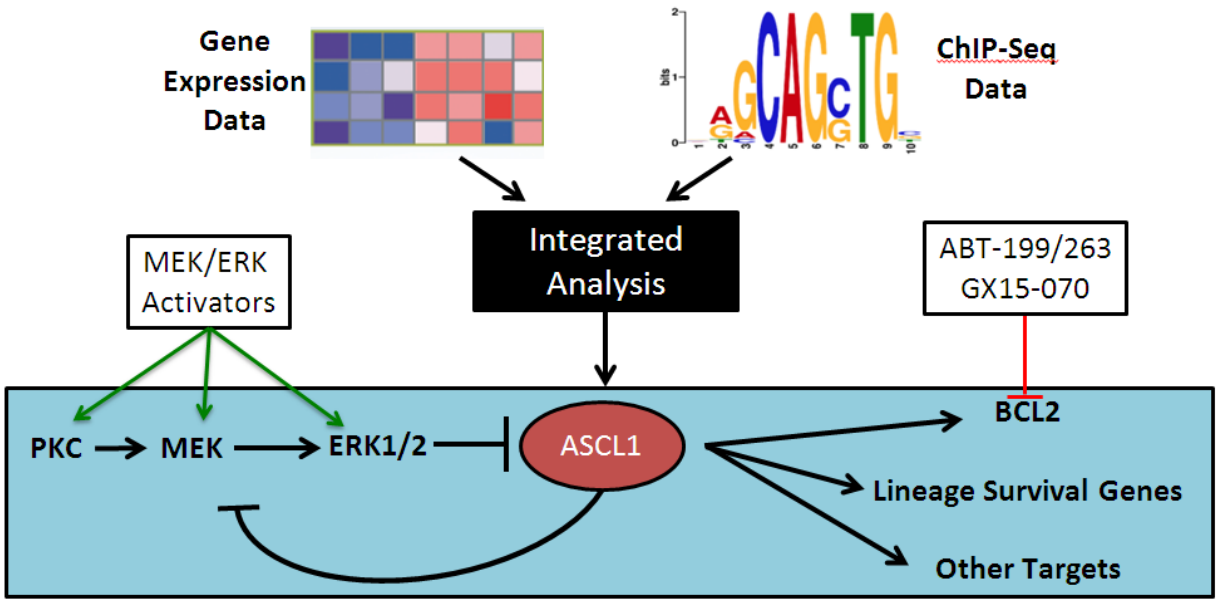

Figure 7.1: ASCL1 lineage dependence model. The combination of gene expression and ChIP-Seq analysis was used to discover ASCL1 is a lineage oncogene in a novel subset of NSCLC with neuroendocrine features. Subsequent experiments detailed that ASCL1 expression is regulated by activation of the MEK/ERK pathway and that ASCL1 actively represses ERK activation. BCL2 is a lineage survival factor that is directly regulated by ASCL1. Inhibition of BCL2 with small molecules and/or activation of the MEK/ERK pathway are potential routes to therapy for NE-NSCLC.

7.2 Ongoing and Unpublished Studies

In the previous chapters, ASCL1 was established as a lineage oncogene in a new class of NSCLC with neuroendocrine features. Downstream targets of ASCL1 were used to predict for poor prognosis in retrospective analyses of lung cancer patient datasets. Target genes of ASCL1 were also used to demonstrate biomarker ability in a dataset previously used to determine patients with neuroendocrine features. Druggable downstream targets include RET and BCL2, with BCL2 inhibition proving to be a major therapeutic intervention in ASCL1-dependent NE-NSCLC cells. The proof-of-concept of BCL2 is attractive, however it is unlikely that BCL2 is the only gene the mediate survival in NE-NSCLC. A complete analysis of ASCL1 downstream targets needs to be performed. To this end, microarray analysis performed before and after knockdown of ASCL1 was recently undertaken. This experiment was conducted in H1755 and HCC1833 cell lines and, combined with the ChIP-Seq target list, should provide for an accurate understanding of "true" ASCL1 transcriptional targets.

Mini-library siRNA screens are useful to study the effect of knocking down groups of related genes and assaying their importance to cell growth. Mini libraries have been created to study nuclear hormone receptors and coregulators (120 genes), chromatin remodelers (102 genes), and cancer stem cell-related genes (40 genes). Many NSCLC cell lines as well as normal HBEC lines have been profiled against these libraries. It will be important to determine the effect of knocking down these genes in NE-NSCLC ASCL1-dependent lines. Presently, the cancer stem cell mini library has been screened against H1755 and HCC1833 because of the fact that it contains a pooled siRNA targeting ASCL1. This screen was an independent validation of the

growth inhibition caused by knock down of ASCL1 using completely different siRNA sequences (Figure 7.2). Knockdown of ASCL1 was only effective in reducing proliferation in H1755 and HCC1833 while producing no significant phenotype in the remaining NSCLC lines and HBECs. The effect of knocking down various genes involved in stem cell pathways will need to be studied in NE-NSCLC lines for potential exploitation for therapy. Additionally, profiling ASCL1-dependent lines against the other siRNA libraries will provide a wealth of information on how these cell lines function compared to typical NSCLC and HBECs. Any pertinent data gained can then be utilized to postulate rational drug interventions for the therapeutic targeting of this subset of lung cancers.

Micro-RNAs (microRNAs, miRs) are short interfering RNA molecules that modulate gene expression by binding to the 3' UTR region of mRNA transcripts (He and Hannon 2004). Previous research indicated that ASCL1 directs the transcription of miR-375 (validated by ASCL1 ChIP-Seq data), which is involved in regulating levels of the YAP1 transcription factor (Nishikawa, Osada et al. 2011). miRs are an attractive therapeutic target and "miR replacement therapy" is currently being pursued by several pharmaceutical groups. To study the differential expression of miRs in ASCL1+ cell lines compared to ASCL1-negative lines, a miR microarray was performed. H2171, H889, HCC1833, and H1755 served as ASCL1+ lines while H1993 and H2087 served as ASCL1-negative lines. The highest expressed microRNA was miR-153, which is located in the intronic portion of the PTPRN and PTPRN2 genes (Figure 7.3A-B). PTPRN2 is a potential ASCL1 target gene as determined by ChIP-Seq analysis, meaning that miR-153 is likely transcribed in concert with PTPRN2 (Figure 7.3C). Whether miR-153 is important for the

survival of ASCL1-dependent cell lines remains to be determined. One of the top predicted target genes for miR-153 is the neurogenic transcription factor NeuroD1 (Figure 7.3D). If ASCL1 regulates miR-153, which in turn regulates NeuroD1, it will establish a novel regulatory circle tying together two critical developmental transcription factors.

One major difference between SCLC and NSCLC is that KRAS mutations never appear in SCLC, even though about 30% of NSCLC carry them (Sekido, Fong et al. 2003). Additionally, RAF mutations are also conspicuously absent from SCLC patient samples. This is an interesting observation given that MEK/ERK activation promotes inhibition of neuroendocrine differentiation both *in vitro* and *in vivo*. The possibility exists that SCLC patients gain KRAS mutations and then those tumors differentiate into NSCLCs. Insertion of the Ras gene into a SCLC line has long been known as a method for inducing differentiation into a NSCLC phenotype (Falco, Baylin et al. 1990). More recent work has involved inserting KRAS into the p53/RB1 knockout mouse that spontaneously produces human-like SCLC tumors (Calbo, van Montfort et al. 2011). The tumors containing KRAS developed a mesenchymal NSCLC phenotype suggesting that activation of the MAPK pathway is central in this differentiation cascade. Perhaps more importantly, it establishes an incredibly important biological link between SCLC and NSCLC that merits further study. Combined with the knowledge that MAPK activation reduces ASCL1 expression, it is likely that ASCL1 plays a central role in the switch between SCLC and NSCLC. A key observation is that five of the 11 NE-NSCLC contain KRAS mutations. It is possible that NE-NSCLC is simply a subtype that is uncovered as a result of SCLC tumors gaining MAPK pathway activating mutations and

differentiating into NSCLC. NE-NSCLC may lie along a continuum of differentiation between SCLC and NSCLC once the MAPK pathway is activated. Interestingly, the development of SCLC from a subset of patients with EGFR mutant NSCLC treated with erlotinib/gefitinib suggests that this differentiation pathway may work in reverse (Sequist, Waltman et al. 2011). EGFR inhibition would reduce MAPK pathway activation and allow for the increased expression of ASCL1 and development of a neuroendocrine tumor. Further study is needed to connect these links and establish a lineage of differentiation between SCLC and NSCLC. Presently, a SCLC cell line H889 was infected with oncogenic KRAS and following 10 days of selection in blasticidin media, those cells demonstrated an attached, mesenchymal NSCLC phenotype, which is in stark contrast to the floating, clustered SCLC phenotype of the vector-only infected cells (Figure 7.4). Xenograft studies will be performed to determine if the H889-KRASC12 cells result in tumors with a different histology compared to the parental H889-pL6 cells.

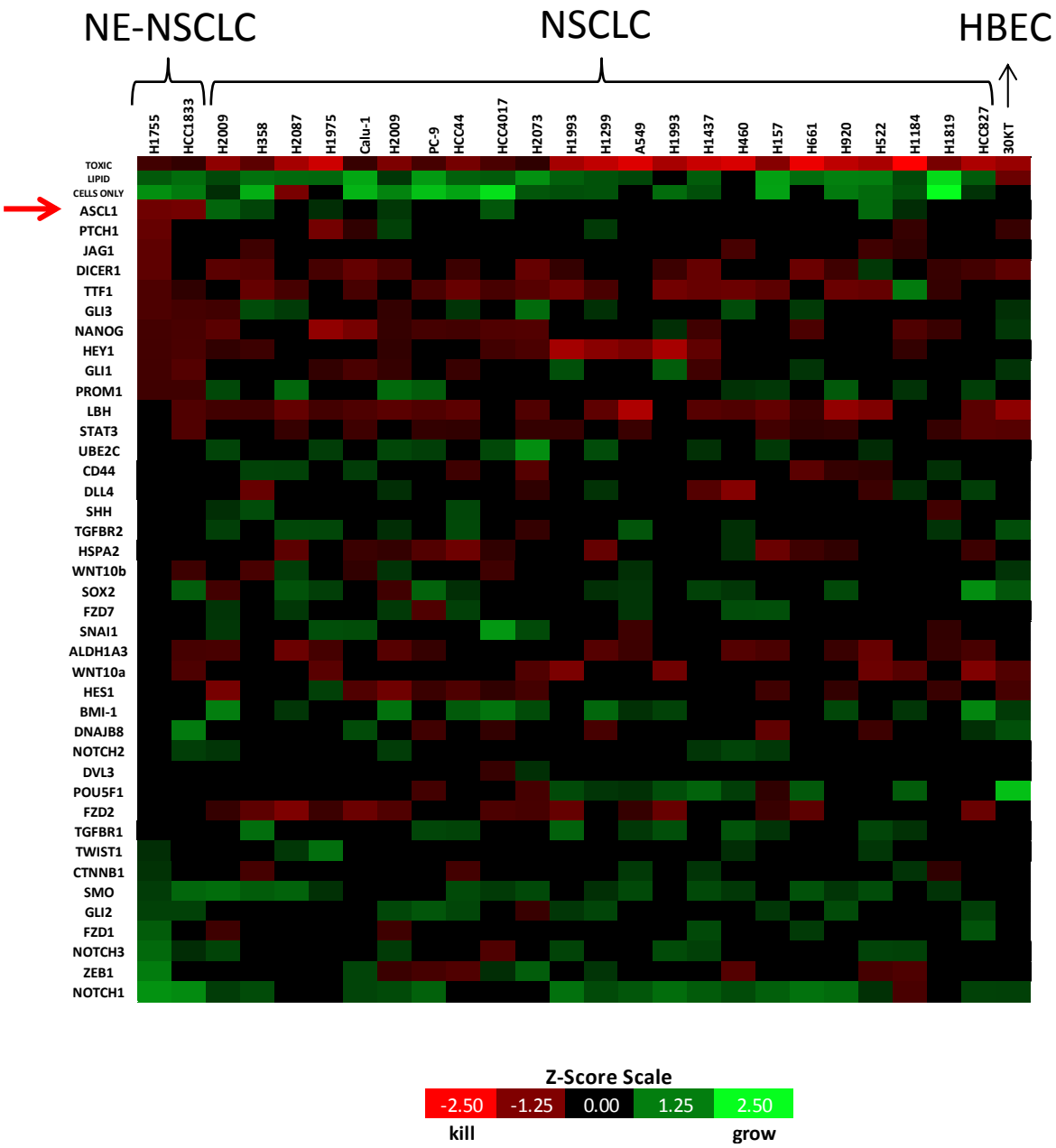

Figure 7.2: NSCLC cell line growth response to knockdown of stem cell-related genes. siRNA mini-library screen was developed to target cancer stem cell-related genes. H1755 and HCC1833 are the only cell lines demonstrating growth inhibition following knockdown of ASCL1. Mini libraries targeting other genes including nuclear receptor/coregulators and chromatin modifiers will be tested against NE-NSCLC cell lines to determine growth response.

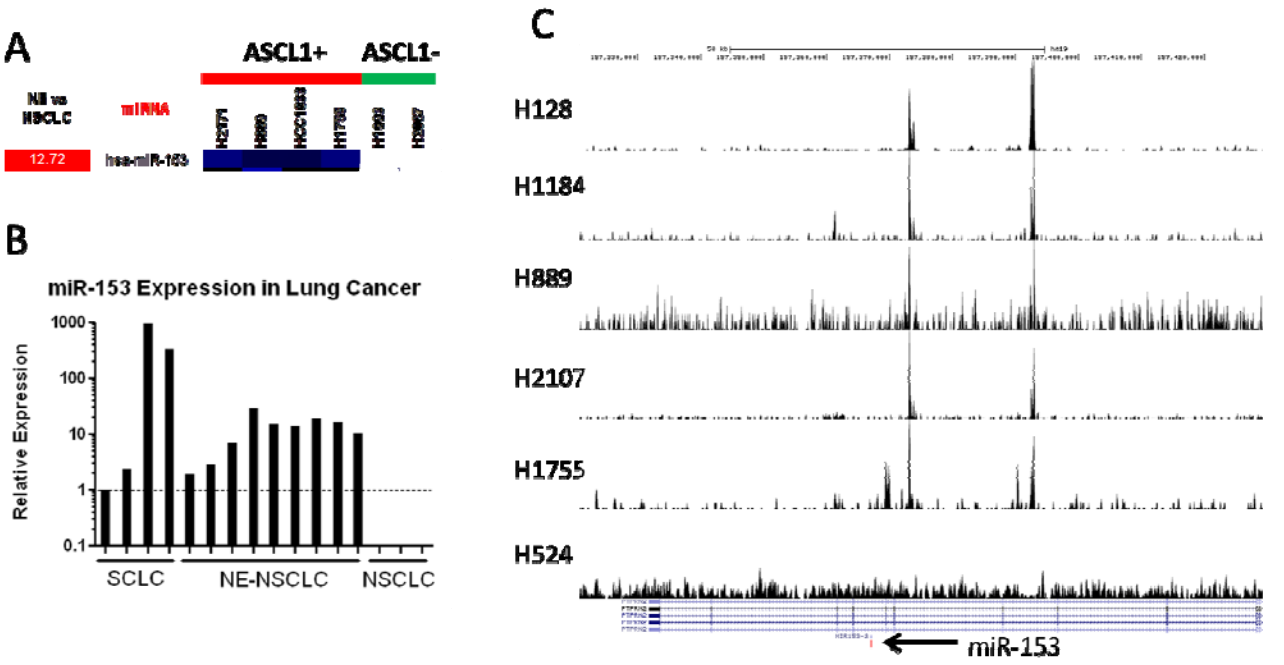
A
ASCL1+
ASCL1-
NE vs NSCLC
miRNA
12.72
hsa-miR-153
H2171
H889
HCC1833
H1703
H1299
H3667
B
miR-153 Expression in Lung Cancer
Relative Expression
1000
100
10
1
0.1
SCLC
NE-NSCLC
NSCLC
C
H128
H1184
H889
H2107
H1755
H524
miR-153

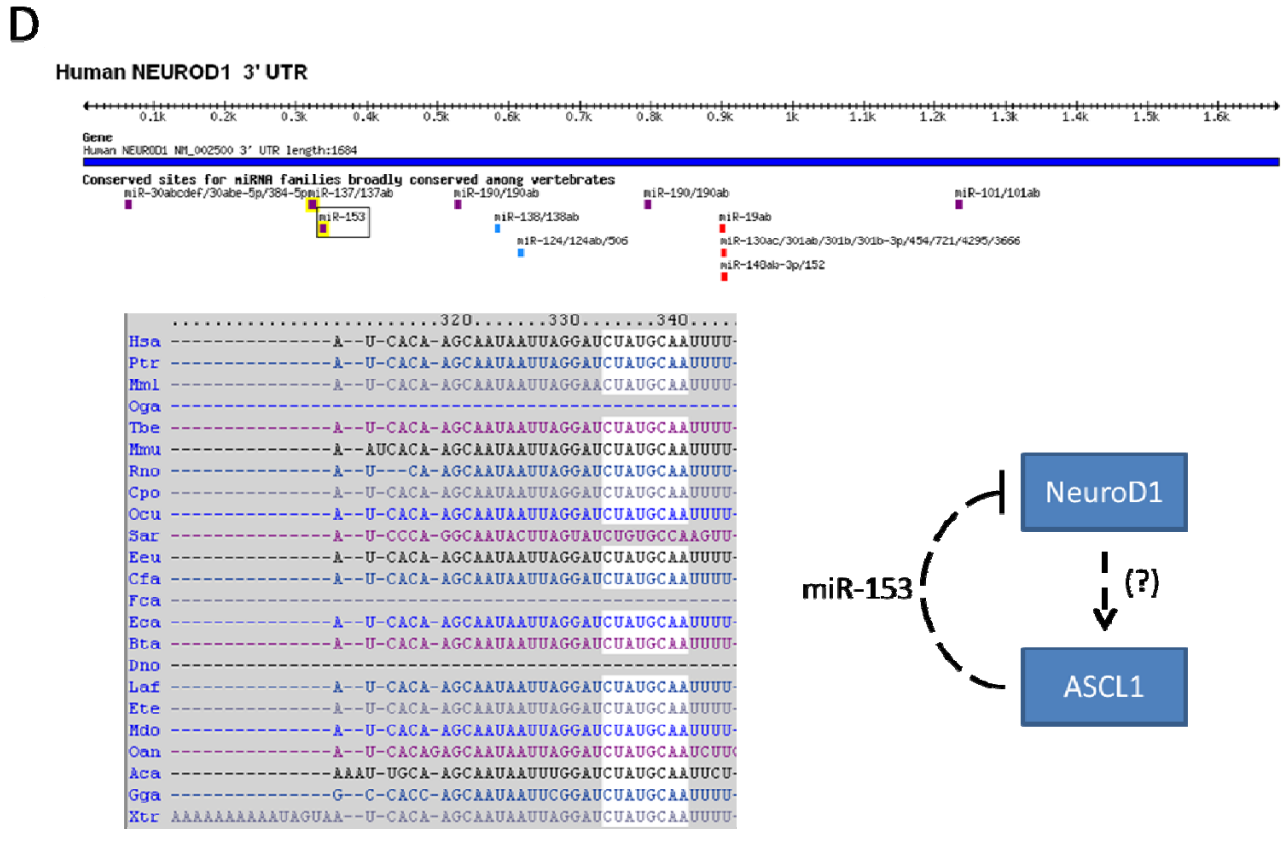
D
Human NEUROD1 3' UTR
Gene
Human NEUROD1 NM_002500 3' UTR length:1684
Conserved sites for miRNA families broadly conserved among vertebrates
miR-30abcdef/30abe-5p/384-5p
miR-137/137ab
miR-153
miR-190/190ab
miR-138/138ab
miR-124/124ab/506
miR-190/190ab
miR-19ab
miR-130ac/301ab/301b/301b-3p/454/721/4295/3666
miR-140ab-3p/152
miR-101/101ab
Hsa
Ptr
Mml
Oga
Tbe
Mmu
Rno
Cpo
Ocu
Sar
Eeu
Cfa
Fca
Eca
Bta
Dno
Laf
Ete
Mdo
Oan
Aca
Gga
Xtr
NeuroD1
miR-153
(?)
ASCL1

Figure 7.3: miR-153 is highly expressed in ASCL1+ cell lines. (A) Microarray expression shows that miR-153 is the highest expressed microRNA in a group of ASCL1+ cell lines compared to two ASCL1-negative NSCLC lines. (B) miR-153 expression was validated by qRT-PCR analysis. miR-153 is highly expressed in neuroendocrine lung cancer lines and not expressed in typical NSCLC lines, following the pattern set by ASCL1 expression. (C) miR-153 is located with the intron of the PTPRN2 gene, which contains several conserved ASCL1 binding sites as determined by ChIP-Seq analysis. (D) NeuroD1 is a predicted target gene for miR-153 as suggested by TargetScan analysis of the NeuroD1 3' UTR region. The possibility for a regulatory axis involving ASCL1, miR-153, and NeuroD1 exists.

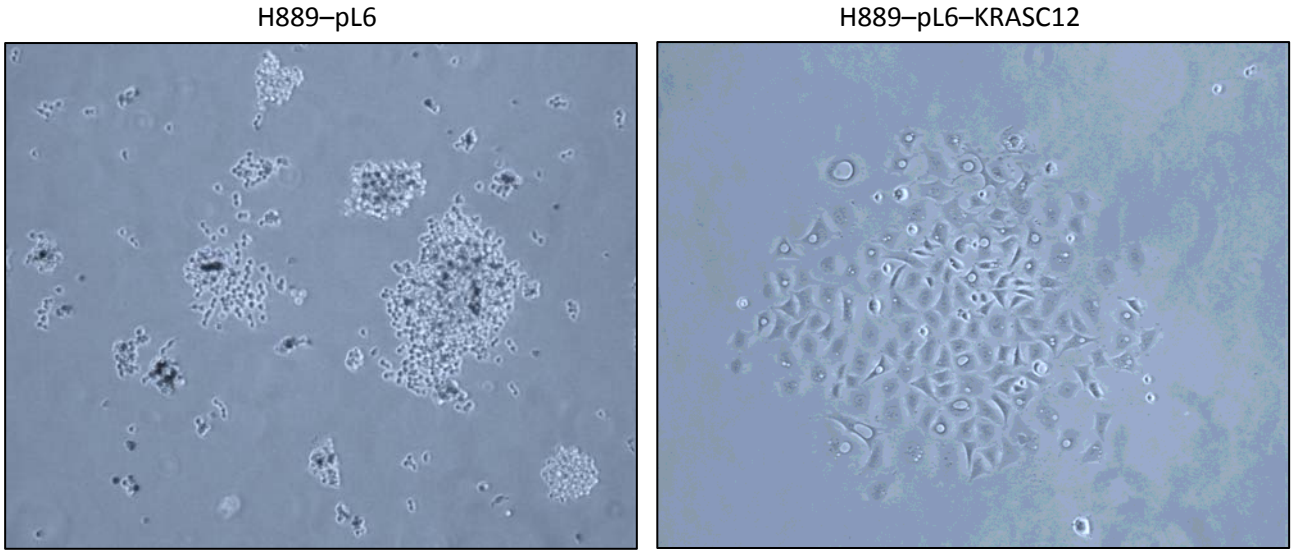

Figure 7.4: Mutant KRAS transforms SCLC cell lines. H889 cells infected with mutant KRAS (C12) showed a dramatic phenotypic change. H889-pL6 control vector cells grow identically to parental H889 cells. Following the addition of KRAS-C12, H889 cells grow attached and resemble epithelial NSCLC cells in culture.

7.3 Perspectives on Pulmonary Neuroendocrine Tumors

Neuroendocrine tumors of the lung are a complicated subset of cancer. As the cancer field turns to identifying acquired vulnerabilities, there is a marked lack of novel therapeutic targets for tumors like SCLC or NE-NSCLC. SCLC in particular is maddeningly difficult to handle in the clinic, as the therapeutic indication for its treatment has remained largely unchanged for the last three decades. The time to develop novel interventions for neuroendocrine lung cancers has arrived. With the advent of genome-wide technologies, it is possible to know more about cancers than ever before. This study takes advantage of genome-wide mRNA profiling and massively parallel sequencing in order to understand how a transcription factor essential for survival mediates its oncogenic effects within lung cancer cells. Previous research performed in SCLC has arrived at a similar conclusion – ASCL1 is a lineage oncogene in neuroendocrine lung cancers. The upstream regulation of the gene and the critical downstream targets it regulates are all potential therapeutic targets for both NE-NSCLC and SCLC and need to be studied further in pre-clinical models to evaluate their efficacy. The proof-of-concept experiments detailed in Chapter Five indicating BCL2 as a gene critical for survival suggests that this approach to studying cancer can ultimately result in therapeutic targets with clinical implications. Other druggable genes are likely involved in mediating survival of ASCL1-dependent tumors and those acquired vulnerabilities will become apparent with further research.

The exciting possibility of linking SCLC and NSCLC through a single genetic change is likely to bring forth many new potential therapeutic options. This effect, though first described nearly 25 years ago, is understudied and may result in a profound change in the treatment and

diagnosis of lung cancer. Experiments to discover the mechanism behind how the MAPK pathway regulates ASCL1 and differentiation between neuroendocrine and non-neuroendocrine lung tumors will reveal whether this pathway can be exploited for treatment purposes.

BIBLIOGRAPHY

Abate-Shen, C. (2002). "Deregulated homeobox gene expression in cancer: cause or consequence?" Nat Rev Cancer 2(10): 777-785.

Abbona, G., M. Papotti, L. Viberti, L. Macri, A. Stella and G. Bussolati (1998). "Chromogranin A gene expression in non-small cell lung carcinomas." J Pathol 186(2): 151-156.

Abeloff, M. D., J. C. Eggleston, G. Mendelsohn, D. S. Ettinger and S. B. Baylin (1979). "Changes in morphologic and biochemical characteristics of small cell carcinoma of the lung. A clinicopathologic study." Am J Med 66(5): 757-764.

Adler, A. F., C. L. Grigsby, K. Kulangara, H. Wang, R. Yasuda and K. W. Leong (2012). "Nonviral direct conversion of primary mouse embryonic fibroblasts to neuronal cells." Mol Ther Nucleic Acids 1: e32.

Arighi, E., M. G. Borrello and H. Sariola (2005). "RET tyrosine kinase signaling in development and cancer." Cytokine Growth Factor Rev 16(4-5): 441-467.

Asamura, H., T. Kameya, Y. Matsuno, M. Noguchi, H. Tada, Y. Ishikawa, T. Yokose, S. X. Jiang, T. Inoue, K. Nakagawa, K. Tajima and K. Nagai (2006). "Neuroendocrine neoplasms of the lung: a prognostic spectrum." J Clin Oncol 24(1): 70-76.

Bair, E. and R. Tibshirani (2004). "Semi-supervised methods to predict patient survival from gene expression data." PLoS Biol 2(4): E108.

Ball, D. W. (2004). "Achaete-scute homolog-1 and Notch in lung neuroendocrine development and cancer." Cancer Lett 204(2): 159-169.

Ball, D. W., C. G. Azzoli, S. B. Baylin, D. Chi, S. Dou, H. Donis-Keller, A. Cumaraswamy, M. Borges and B. D. Nelkin (1993). "Identification of a human achaete-scute homolog highly expressed in neuroendocrine tumors." Proc Natl Acad Sci U S A 90(12): 5648-5652.

Balsara, B. R. and J. R. Testa (2002). "Chromosomal imbalances in human lung cancer." Oncogene 21(45): 6877-6883.

Bass, A. J., H. Watanabe, C. H. Mermel, S. Yu, S. Perner, R. G. Verhaak, S. Y. Kim, L. Wardwell, P. Tamayo, I. Gat-Viks, A. H. Ramos, M. S. Woo, B. A. Weir, G. Getz, R. Beroukhim, M. O'Kelly, A. Dutt, O. Rozenblatt-Rosen, P. Dziunycz, J. Komisarof, L. R. Chirieac, C. J. Lafargue, V. Scheble, T. Wilbertz, C. Ma, S. Rao, H. Nakagawa, D. B. Stairs, L. Lin, T. J. Giordano, P. Wagner, J. D. Minna, A. F. Gazdar, C. Q. Zhu, M. S. Brose, I. Cecconello, U. R. Jr, S. K. Marie, O. Dahl, R. A. Shivdasani, M. S. Tsao, M. A. Rubin, K. K. Wong, A. Regev, W. C. Hahn, D. G. Beer, A. K. Rustgi and M. Meyerson (2009). "SOX2 is an

amplified lineage-survival oncogene in lung and esophageal squamous cell carcinomas." Nat Genet 41(11): 1238-1242.

Batra, S. K., S. Castelino-Prabhu, C. J. Wikstrand, X. Zhu, P. A. Humphrey, H. S. Friedman and D. D. Bigner (1995). "Epidermal growth factor ligand-independent, unregulated, cell-transforming potential of a naturally occurring human mutant EGFRvIII gene." Cell Growth Differ 6(10): 1251-1259.

Benko, E., A. Winkelmann, J. C. Meier, P. B. Persson, H. Scholz and M. Fahling (2011). "Phorbol-Ester Mediated Suppression of hASH1 Synthesis: Multiple Ways to Keep the Level Down." Front Mol Neurosci 4: 1.

Berendsen, H. H., L. de Leij, S. Poppema, P. E. Postmus, A. Boes, H. J. Sluiter and H. The (1989). "Clinical characterization of non-small-cell lung cancer tumors showing neuroendocrine differentiation features." J Clin Oncol 7(11): 1614-1620.

Berman, J. (2005). "Modern classification of neoplasms: reconciling differences between morphologic and molecular approaches." BMC Cancer 5: 100.

Berman, J. J. (2004). "Tumor taxonomy for the developmental lineage classification of neoplasms." BMC Cancer 4: 88.

Berninger, B., F. Guillemot and M. Gotz (2007). "Directing neurotransmitter identity of neurones derived from expanded adult neural stem cells." Eur J Neurosci 25(9): 2581-2590.

Bertrand, N., D. S. Castro and F. Guillemot (2002). "Proneural genes and the specification of neural cell types." Nat Rev Neurosci 3(7): 517-530.

Bhattacharjee, A., W. G. Richards, J. Staunton, C. Li, S. Monti, P. Vasa, C. Ladd, J. Beheshti, R. Bueno, M. Gillette, M. Loda, G. Weber, E. J. Mark, E. S. Lander, W. Wong, B. E. Johnson, T. R. Golub, D. J. Sugarbaker and M. Meyerson (2001). "Classification of human lung carcinomas by mRNA expression profiling reveals distinct adenocarcinoma subclasses." Proc Natl Acad Sci U S A 98(24): 13790-13795.

Bondy, P. K. (1981). "The pattern of ectopic hormone production in lung cancer." Yale J Biol Med 54(3): 181-185.

Borges, M., R. I. Linnoila, H. J. van de Velde, H. Chen, B. D. Nelkin, M. Mabry, S. B. Baylin and D. W. Ball (1997). "An achaete-scute homologue essential for neuroendocrine differentiation in the lung." Nature 386(6627): 852-855.

Bourke, L., P. Kirkbride, R. Hooper, A. J. Rosario, T. J. Chico and D. J. Rosario (2013). "Endocrine therapy in prostate cancer: time for reappraisal of risks, benefits and cost-effectiveness?" Br J Cancer 108(1): 9-13.

Brereton, H. D., M. M. Mathews, J. Costa, C. H. Kent and R. E. Johnson (1978). "Mixed anaplastic small-cell and squamous-cell carcinoma of the lung." Ann Intern Med 88(6): 805-806.

Brewster, R., J. Lee and A. Ruiz i Altaba (1998). "Gli/Zic factors pattern the neural plate by defining domains of cell differentiation." Nature 393(6685): 579-583.

Burbee, D. G., E. Forgacs, S. Zochbauer-Muller, L. Shivakumar, K. Fong, B. Gao, D. Randle, M. Kondo, A. Virmani, S. Bader, Y. Sekido, F. Latif, S. Milchgrub, S. Toyooka, A. F. Gazdar, M. I. Lerman, E. Zabarovsky, M. White and J. D. Minna (2001). "Epigenetic inactivation of RASSF1A in lung and breast cancers and malignant phenotype suppression." J Natl Cancer Inst 93(9): 691-699.

Burmer, G. C., P. S. Rabinovitch and L. A. Loeb (1991). "Frequency and spectrum of c-Ki-ras mutations in human sporadic colon carcinoma, carcinomas arising in ulcerative colitis, and pancreatic adenocarcinoma." Environ Health Perspect 93: 27-31.

Calbo, J., E. van Montfort, N. Proost, E. van Drunen, H. B. Beverloo, R. Meuwissen and A. Berns (2011). "A functional role for tumor cell heterogeneity in a mouse model of small cell lung cancer." Cancer Cell 19(2): 244-256.

Campos-Ortega, J. A. and E. Knust (1990). "Genetic and molecular mechanisms of neurogenesis in Drosophila melanogaster." J Physiol (Paris) 84(1): 1-10.

Campuzano, S., L. Carramolino, C. V. Cabrera, M. Ruiz-Gomez, R. Villares, A. Boronat and J. Modolell (1985). "Molecular genetics of the achaete-scute gene complex of D. melanogaster." Cell 40(2): 327-338.

Casarosa, S., C. Fode and F. Guillemot (1999). "Mash1 regulates neurogenesis in the ventral telencephalon." Development 126(3): 525-534.

Castro, D. S., B. Martynoga, C. Parras, V. Ramesh, E. Pacary, C. Johnston, D. Drechsel, M. Lebel-Potter, L. G. Garcia, C. Hunt, D. Dolle, A. Bithell, L. Ettwiller, N. Buckley and F. Guillemot (2011). "A novel function of the proneural factor Ascl1 in progenitor proliferation identified by genome-wide characterization of its targets." Genes Dev 25(9): 930-945.

Castro, D. S., D. Skowronska-Krawczyk, O. Armant, I. J. Donaldson, C. Parras, C. Hunt, J. A. Critchley, L. Nguyen, A. Gossler, B. Gottgens, J. M. Matter and F. Guillemot (2006). "Proneural bHLH and Brn proteins coregulate a neurogenic program through cooperative binding to a conserved DNA motif." Dev Cell 11(6): 831-844.

Catalanotti, F., D. B. Solit, M. P. Pulitzer, M. F. Berger, S. N. Scott, T. Iyriboz, M. E. Lacouture, K. S. Panageas, J. D. Wolchok, R. D. Carvajal, G. K. Schwartz, N. Rosen and P. B. Chapman (2013). "Phase II trial of MEK inhibitor selumetinib (AZD6244, ARRY-142886) in patients with BRAFV600E/K-mutated melanoma." Clin Cancer Res 19(8): 2257-2264.

Caunt, C. J. and S. M. Keyse (2013). "Dual-specificity MAP kinase phosphatases (MKPs): shaping the outcome of MAP kinase signalling." FEBS J 280(2): 489-504.

Chapman, P. B., A. Hauschild, C. Robert, J. B. Haanen, P. Ascierto, J. Larkin, R. Dummer, C. Garbe, A. Testori, M. Maio, D. Hogg, P. Lorigan, C. Lebbe, T. Jouary, D. Schadendorf, A. Ribas, S. J. O'Day, J. A. Sosman, J. M. Kirkwood, A. M. Eggermont, B. Dreno, K. Nolop, J. Li, B. Nelson, J. Hou, R. J. Lee, K. T. Flaherty and G. A. McArthur (2011). "Improved survival with vemurafenib in melanoma with BRAF V600E mutation." N Engl J Med 364(26): 2507-2516.

Chauhan, D., M. Velankar, M. Brahmandam, T. Hideshima, K. Podar, P. Richardson, R. Schlossman, I. Ghobrial, N. Raje, N. Munshi and K. C. Anderson (2007). "A novel Bcl-2/Bcl-X(L)/Bcl-w inhibitor ABT-737 as therapy in multiple myeloma." Oncogene 26(16): 2374-2380.

Chejfec, G., I. Cosnow, N. S. Gould, A. N. Husain and V. E. Gould (1990). "Pulmonary blastoma with neuroendocrine differentiation in cell morules resembling neuroepithelial bodies." Histopathology 17(4): 353-358.

Chen, H., E. B. Carson-Walter, S. B. Baylin, B. D. Nelkin and D. W. Ball (1996). "Differentiation of medullary thyroid cancer by C-Raf-1 silences expression of the neural transcription factor human achaete-scute homolog-1." Surgery 120(2): 168-172; discussion 173.

Chen, H., A. Thiagalingam, H. Chopra, M. W. Borges, J. N. Feder, B. D. Nelkin, S. B. Baylin and D. W. Ball (1997). "Conservation of the Drosophila lateral inhibition pathway in human lung cancer: a hairy-related protein (HES-1) directly represses achaete-scute homolog-1 expression." Proc Natl Acad Sci U S A 94(10): 5355-5360.

Chin, L. (2003). "The genetics of malignant melanoma: lessons from mouse and man." Nat Rev Cancer 3(8): 559-570.

Chipuk, J. E., T. Moldoveanu, F. Llambi, M. J. Parsons and D. R. Green (2010). "The BCL-2 family reunion." Mol Cell 37(3): 299-310.

Chng, K. R., C. W. Chang, S. K. Tan, C. Yang, S. Z. Hong, N. Y. Sng and E. Cheung (2012). "A transcriptional repressor co-regulatory network governing androgen response in prostate cancers." EMBO J 31(12): 2810-2823.

Choi, Y. L., M. Soda, Y. Yamashita, T. Ueno, J. Takashima, T. Nakajima, Y. Yatabe, K. Takeuchi, T. Hamada, H. Haruta, Y. Ishikawa, H. Kimura, T. Mitsudomi, Y. Tanio and H. Mano (2010). "EML4-ALK mutations in lung cancer that confer resistance to ALK inhibitors." N Engl J Med 363(18): 1734-1739.

Classon, M. and E. Harlow (2002). "The retinoblastoma tumour suppressor in development and cancer." Nat Rev Cancer 2(12): 910-917.

Cook, M. R., J. Luo, M. Ndiaye, H. Chen and M. Kunnimalaiyaan (2010). "Xanthohumol inhibits the neuroendocrine transcription factor achaete-scute complex-like 1, suppresses proliferation, and induces phosphorylated ERK1/2 in medullary thyroid cancer." Am J Surg 199(3): 315-318; discussion 318.

Cork, A. (1983). "Chromosomal abnormalities in leukemia." Am J Med Technol 49(10): 703-714.

D'Angelo, S. P. and M. C. Pietanza (2010). "The molecular pathogenesis of small cell lung cancer." Cancer Biol Ther 10(1): 1-10.

Dauger, S., F. Guimiot, S. Renolleau, B. Levacher, B. Boda, C. Mas, V. Nepote, M. Simonneau, C. Gaultier and J. Gallego (2001). "MASH-1/RET pathway involvement in development of brain stem control of respiratory frequency in newborn mice." Physiol Genomics 7(2): 149-157.

Davies, H., G. R. Bignell, C. Cox, P. Stephens, S. Edkins, S. Clegg, J. Teague, H. Woffendin, M. J. Garnett, W. Bottomley, N. Davis, E. Dicks, R. Ewing, Y. Floyd, K. Gray, S. Hall, R. Hawes, J. Hughes, V. Kosmidou, A. Menzies, C. Mould, A. Parker, C. Stevens, S. Watt, S. Hooper, R. Wilson, H. Jayatilake, B. A. Gusterson, C. Cooper, J. Shipley, D. Hargrave, K. Pritchard-Jones, N. Maitland, G. Chenevix-Trench, G. J. Riggins, D. D. Bigner, G. Palmieri, A. Cossu, A. Flanagan, A. Nicholson, J. W. Ho, S. Y. Leung, S. T. Yuen, B. L. Weber, H. F. Seigler, T. L. Darrow, H. Paterson, R. Marais, C. J. Marshall, R. Wooster, M. R. Stratton and P. A. Futreal (2002). "Mutations of the BRAF gene in human cancer." Nature 417(6892): 949-954.

Davis, P. K. and R. K. Brackmann (2003). "Chromatin remodeling and cancer." Cancer Biol Ther 2(1): 22-29.

de la Chapelle, A. (2004). "Genetic predisposition to colorectal cancer." Nat Rev Cancer 4(10): 769-780.

Debrincat, M. A., E. C. Josefsson, C. James, K. J. Henley, S. Ellis, M. Lebois, K. L. Betterman, R. M. Lane, K. L. Rogers, M. J. White, A. W. Roberts, N. L. Harvey, D. Metcalf and B. T. Kile (2012). "Mcl-1 and Bcl-x(L) coordinately regulate megakaryocyte survival." Blood 119(24): 5850-5858.

Demelash, A., P. Rudrabhatla, H. C. Pant, X. Wang, N. D. Amin, C. D. McWhite, X. Naizhen and R. I. Linnoila (2012). "Achaete-scute homologue-1 (ASH1) stimulates migration of lung cancer cells through Cdk5/p35 pathway." Mol Biol Cell 23(15): 2856-2866.

Dong, J., G. Jiang, Y. W. Asmann, S. Tomaszek, J. Jen, T. Kislinger and D. A. Wigle (2010). "MicroRNA networks in mouse lung organogenesis." PLoS One 5(5): e10854.

Du, J., H. R. Widlund, M. A. Horstmann, S. Ramaswamy, K. Ross, W. E. Huber, E. K. Nishimura, T. R. Golub and D. E. Fisher (2004). "Critical role of CDK2 for melanoma growth linked to its melanocyte-specific transcriptional regulation by MITF." Cancer Cell 6(6): 565-576.

Dukers, D. F., J. C. van Galen, C. Giroth, P. Jansen, R. G. Sewalt, A. P. Otte, H. C. Kluin-Nelemans, C. J. Meijer and F. M. Raaphorst (2004). "Unique polycomb gene expression pattern in Hodgkin's lymphoma and Hodgkin's lymphoma-derived cell lines." Am J Pathol 164(3): 873-881.

Dupin, E. and N. M. Le Douarin (2003). "Development of melanocyte precursors from the vertebrate neural crest." Oncogene 22(20): 3016-3023.

Escudier, B., T. Eisen, W. M. Stadler, C. Szczylik, S. Oudard, M. Siebels, S. Negrier, C. Chevreau, E. Solska, A. A. Desai, F. Rolland, T. Demkow, T. E. Hutson, M. Gore, S. Freeman, B. Schwartz, M. Shan, R. Simantov and R. M. Bukowski (2007). "Sorafenib in advanced clear-cell renal-cell carcinoma." N Engl J Med 356(2): 125-134.

Falco, J. P., S. B. Baylin, R. Lupu, M. Borges, B. D. Nelkin, R. K. Jasti, N. E. Davidson and M. Mabry (1990). "v-rasH induces non-small cell phenotype, with associated growth factors and receptors, in a small cell lung cancer cell line." J Clin Invest 85(6): 1740-1745.

Fantl, V., R. Smith, S. Brookes, C. Dickson and G. Peters (1993). "Chromosome 11q13 abnormalities in human breast cancer." Cancer Surv 18: 77-94.

Fenaux, P. and L. Degos (1997). "Differentiation therapy for acute promyelocytic leukemia." N Engl J Med 337(15): 1076-1077.

Figlioli, G., S. Landi, C. Romei, R. Elisei and F. Gemignani (2013). "Medullary thyroid carcinoma (MTC) and RET proto-oncogene: mutation spectrum in the familial cases and a meta-analysis of studies on the sporadic form." Mutat Res 752(1): 36-44.

Fraga, M. F., E. Ballestar, A. Villar-Garea, M. Boix-Chornet, J. Espada, G. Schotta, T. Bonaldi, C. Haydon, S. Ropero, K. Petrie, N. G. Iyer, A. Perez-Rosado, E. Calvo, J. A. Lopez, A. Cano, M. J. Calasanz, D. Colomer, M. A. Piris, N. Ahn, A. Imhof, C. Caldas, T. Jenuwein and M. Esteller (2005). "Loss of acetylation at Lys16 and trimethylation at Lys20 of histone H4 is a common hallmark of human cancer." Nat Genet 37(4): 391-400.

Garcia-Bellido, A. and J. F. de Celis (2009). "The complex tale of the achaete-scute complex: a paradigmatic case in the analysis of gene organization and function during development." Genetics 182(3): 631-639.

Garcia-Yuste, M., J. M. Matilla, T. Alvarez-Gago, J. L. Duque, F. Heras, L. J. Cerezal and G. Ramos (2000). "Prognostic factors in neuroendocrine lung tumors: a Spanish Multicenter Study.

Spanish Multicenter Study of Neuroendocrine Tumors of the Lung of the Spanish Society of Pneumonology and Thoracic Surgery (EMETNE-SEPAR)." Ann Thorac Surg 70(1): 258-263.

Garcia-Yuste, M., J. M. Matilla and F. Gonzalez-Aragoneses (2008). "Neuroendocrine tumors of the lung." Curr Opin Oncol 20(2): 148-154.

Garraway, L. A. and W. R. Sellers (2006). "From integrated genomics to tumor lineage dependency." Cancer Res 66(5): 2506-2508.

Garraway, L. A. and W. R. Sellers (2006). "Lineage dependency and lineage-survival oncogenes in human cancer." Nat Rev Cancer 6(8): 593-602.

Garraway, L. A., B. A. Weir, X. Zhao, H. Widlund, R. Beroukhim, A. Berger, D. Rimm, M. A. Rubin, D. E. Fisher, M. L. Meyerson and W. R. Sellers (2005). ""Lineage addiction" in human cancer: lessons from integrated genomics." Cold Spring Harb Symp Quant Biol 70: 25-34.

Garraway, L. A., H. R. Widlund, M. A. Rubin, G. Getz, A. J. Berger, S. Ramaswamy, R. Beroukhim, D. A. Milner, S. R. Granter, J. Du, C. Lee, S. N. Wagner, C. Li, T. R. Golub, D. L. Rimm, M. L. Meyerson, D. E. Fisher and W. R. Sellers (2005). "Integrative genomic analyses identify MITF as a lineage survival oncogene amplified in malignant melanoma." Nature 436(7047): 117-122.

Garst, J. (2007). "Topotecan: An evolving option in the treatment of relapsed small cell lung cancer." Ther Clin Risk Manag 3(6): 1087-1095.

Gazdar, A. F. (1992). "The molecular biology of lung cancer." Tohoku J Exp Med 168(2): 239-245.

Gazdar, A. F., L. Girard, W. W. Lockwood, W. L. Lam and J. D. Minna (2010). "Lung cancer cell lines as tools for biomedical discovery and research." J Natl Cancer Inst 102(17): 1310-1321.

Geoffroy, C. G., J. A. Critchley, D. S. Castro, S. Ramelli, C. Barraclough, P. Descombes, F. Guillemot and O. Raineteau (2009). "Engineering of dominant active basic helix-loop-helix proteins that are resistant to negative regulation by postnatal central nervous system antineurogenic cues." Stem Cells 27(4): 847-856.

Ginestier, C., M. H. Hur, E. Charafe-Jauffret, F. Monville, J. Dutcher, M. Brown, J. Jacquemier, P. Viens, C. G. Kleer, S. Liu, A. Schott, D. Hayes, D. Birnbaum, M. S. Wicha and G. Dontu (2007). "ALDH1 is a marker of normal and malignant human mammary stem cells and a predictor of poor clinical outcome." Cell Stem Cell 1(5): 555-567.

Goding, C. R. (2000). "Mitf from neural crest to melanoma: signal transduction and transcription in the melanocyte lineage." Genes Dev 14(14): 1712-1728.

Gollard, R., S. Jhatakia, M. Elliott and M. Kosty (2010). "Large cell/neuroendocrine carcinoma." Lung Cancer 69(1): 13-18.

Gontan, C., A. de Munck, M. Vermeij, F. Grosveld, D. Tibboel and R. Rottier (2008). "Sox2 is important for two crucial processes in lung development: branching morphogenesis and epithelial cell differentiation." Dev Biol 317(1): 296-309.

Grier, D. G., A. Thompson, A. Kwasniewska, G. J. McGonigle, H. L. Halliday and T. R. Lappin (2005). "The pathophysiology of HOX genes and their role in cancer." J Pathol 205(2): 154-171.

Guillemot, F., L. C. Lo, J. E. Johnson, A. Auerbach, D. J. Anderson and A. L. Joyner (1993). "Mammalian achaete-scute homolog 1 is required for the early development of olfactory and autonomic neurons." Cell 75(3): 463-476.

Gupta, P. B., C. Kuperwasser, J. P. Brunet, S. Ramaswamy, W. L. Kuo, J. W. Gray, S. P. Naber and R. A. Weinberg (2005). "The melanocyte differentiation program predisposes to metastasis after neoplastic transformation." Nat Genet 37(10): 1047-1054.

Hann, C. L., V. C. Daniel, E. A. Sugar, I. Dobromilskaya, S. C. Murphy, L. Cope, X. Lin, J. S. Hierman, D. L. Wilburn, D. N. Watkins and C. M. Rudin (2008). "Therapeutic efficacy of ABT-737, a selective inhibitor of BCL-2, in small cell lung cancer." Cancer Res 68(7): 2321-2328.

Harbour, J. W., S. L. Lai, J. Whang-Peng, A. F. Gazdar, J. D. Minna and F. J. Kaye (1988). "Abnormalities in structure and expression of the human retinoblastoma gene in SCLC." Science 241(4863): 353-357.

He, L. and G. J. Hannon (2004). "MicroRNAs: small RNAs with a big role in gene regulation." Nat Rev Genet 5(7): 522-531.

Heinlein, C. A. and C. Chang (2004). "Androgen receptor in prostate cancer." Endocr Rev 25(2): 276-308.

Heinz, S., C. Benner, N. Spann, E. Bertolino, Y. C. Lin, P. Laslo, J. X. Cheng, C. Murre, H. Singh and C. K. Glass (2010). "Simple combinations of lineage-determining transcription factors prime cis-regulatory elements required for macrophage and B cell identities." Mol Cell 38(4): 576-589.

Hemesath, T. J., E. Steingrimsson, G. McGill, M. J. Hansen, J. Vaught, C. A. Hodgkinson, H. Arnheiter, N. G. Copeland, N. A. Jenkins and D. E. Fisher (1994). "microphthalmia, a critical factor in melanocyte development, defines a discrete transcription factor family." Genes Dev 8(22): 2770-2780.

Henke, R. M., D. M. Meredith, M. D. Borromeo, T. K. Savage and J. E. Johnson (2009). "Ascl1 and Neurog2 form novel complexes and regulate Delta-like3 (Dll3) expression in the neural tube." Dev Biol 328(2): 529-540.

Hirota, S., K. Isozaki, Y. Moriyama, K. Hashimoto, T. Nishida, S. Ishiguro, K. Kawano, M. Hanada, A. Kurata, M. Takeda, G. Muhammad Tunio, Y. Matsuzawa, Y. Kanakura, Y. Shinomura and Y. Kitamura (1998). "Gain-of-function mutations of c-kit in human gastrointestinal stromal tumors." Science 279(5350): 577-580.

Hirsch, M. R., M. C. Tiveron, F. Guillemot, J. F. Brunet and C. Goridis (1998). "Control of noradrenergic differentiation and Phox2a expression by MASH1 in the central and peripheral nervous system." Development 125(4): 599-608.

Horton, S., A. Meredith, J. A. Richardson and J. E. Johnson (1999). "Correct coordination of neuronal differentiation events in ventral forebrain requires the bHLH factor MASH1." Mol Cell Neurosci 14(4-5): 355-369.

Howe, M. C., A. Chapman, K. Kerr, M. Dougal, H. Anderson and P. S. Hasleton (2005). "Neuroendocrine differentiation in non-small cell lung cancer and its relation to prognosis and therapy." Histopathology 46(2): 195-201.

Huber, K., B. Bruhl, F. Guillemot, E. N. Olson, U. Ernsberger and K. Unsicker (2002). "Development of chromaffin cells depends on MASH1 function." Development 129(20): 4729-4738.

Ionescu, D. N., D. Treaba, C. B. Gilks, S. Leung, D. Renouf, J. Laskin, R. Wood-Baker and A. M. Gown (2007). "Nonsmall cell lung carcinoma with neuroendocrine differentiation--an entity of no clinical or prognostic significance." Am J Surg Pathol 31(1): 26-32.

Iorio, M. V. and C. M. Croce (2012). "MicroRNA dysregulation in cancer: diagnostics, monitoring and therapeutics. A comprehensive review." EMBO Mol Med 4(3): 143-159.

Iso, T., V. Sartorelli, C. Poizat, S. Iezzi, H. Y. Wu, G. Chung, L. Kedes and Y. Hamamori (2001). "HERP, a novel heterodimer partner of HES/E(spl) in Notch signaling." Mol Cell Biol 21(17): 6080-6089.

Ito, T., N. Udaka, T. Yazawa, K. Okudela, H. Hayashi, T. Sudo, F. Guillemot, R. Kageyama and H. Kitamura (2000). "Basic helix-loop-helix transcription factors regulate the neuroendocrine differentiation of fetal mouse pulmonary epithelium." Development 127(18): 3913-3921.

Jacobsen, T. L., K. Brennan, A. M. Arias and M. A. Muskavitch (1998). "Cis-interactions between Delta and Notch modulate neurogenic signalling in Drosophila." Development 125(22): 4531-4540.

Jaskula-Sztul, R., P. Pisarnturakit, M. Landowski, H. Chen and M. Kunnimalaiyaan (2011). "Expression of the active Notch1 decreases MTC tumor growth in vivo." J Surg Res 171(1): 23-27.

Jemal, A., R. Siegel, E. Ward, T. Murray, J. Xu and M. J. Thun (2007). "Cancer statistics, 2007." CA Cancer J Clin 57(1): 43-66.

Jensen-Taubman, S., X. Y. Wang and R. I. Linnoila (2010). "Achaete-scute homologue-1 tapers neuroendocrine cell differentiation in lungs after exposure to naphthalene." Toxicol Sci 117(1): 238-248.

Jensen, S. M., A. F. Gazdar, F. Cuttitta, E. K. Russell and R. I. Linnoila (1990). "A comparison of synaptophysin, chromogranin, and L-dopa decarboxylase as markers for neuroendocrine differentiation in lung cancer cell lines." Cancer Res 50(18): 6068-6074.

Ji, L. and J. A. Roth (2008). "Tumor suppressor FUS1 signaling pathway." J Thorac Oncol 3(4): 327-330.

Jiang, T., B. J. Collins, N. Jin, D. N. Watkins, M. V. Brock, W. Matsui, B. D. Nelkin and D. W. Ball (2009). "Achaete-scute complex homologue 1 regulates tumor-initiating capacity in human small cell lung cancer." Cancer Res 69(3): 845-854.

Jiang, X. and X. Wang (2000). "Cytochrome c promotes caspase-9 activation by inducing nucleotide binding to Apaf-1." J Biol Chem 275(40): 31199-31203.

Jimenez, F. and J. A. Campos-Ortega (1979). "A region of the Drosophila genome necessary for CNS development." Nature 282(5736): 310-312.

Jogi, A., P. Persson, A. Grynfeld, S. Pahlman and H. Axelson (2002). "Modulation of basic helix-loop-helix transcription complex formation by Id proteins during neuronal differentiation." J Biol Chem 277(11): 9118-9126.

Johnson, J. E., S. J. Birren and D. J. Anderson (1990). "Two rat homologues of Drosophila achaete-scute specifically expressed in neuronal precursors." Nature 346(6287): 858-861.

Jones, M. H., C. Virtanen, D. Honjoh, T. Miyoshi, Y. Satoh, S. Okumura, K. Nakagawa, H. Nomura and Y. Ishikawa (2004). "Two prognostically significant subtypes of high-grade lung neuroendocrine tumours independent of small-cell and large-cell neuroendocrine carcinomas identified by gene expression profiles." Lancet 363(9411): 775-781.

Kameda, Y., T. Nishimaki, M. Miura, S. X. Jiang and F. Guillemot (2007). "Mash1 regulates the development of C cells in mouse thyroid glands." Dev Dyn 236(1): 262-270.

Kang, M. H. and C. P. Reynolds (2009). "Bcl-2 inhibitors: targeting mitochondrial apoptotic pathways in cancer therapy." Clin Cancer Res 15(4): 1126-1132.

Karow, M., R. Sanchez, C. Schichor, G. Masserdotti, F. Ortega, C. Heinrich, S. Gascon, M. A. Khan, D. C. Lie, A. Dellavalle, G. Cossu, R. Goldbrunner, M. Gotz and B. Berninger (2012). "Reprogramming of pericyte-derived cells of the adult human brain into induced neuronal cells." Cell Stem Cell 11(4): 471-476.

Kewley, R. J., M. L. Whitelaw and A. Chapman-Smith (2004). "The mammalian basic helix-loop-helix/PAS family of transcriptional regulators." Int J Biochem Cell Biol 36(2): 189-204.

Kho, A. T., Q. Zhao, Z. Cai, A. J. Butte, J. Y. Kim, S. L. Pomeroy, D. H. Rowitch and I. S. Kohane (2004). "Conserved mechanisms across development and tumorigenesis revealed by a mouse development perspective of human cancers." Genes Dev 18(6): 629-640.

Kim, E. J., J. L. Ables, L. K. Dickel, A. J. Eisch and J. E. Johnson (2011). "Ascl1 (Mash1) defines cells with long-term neurogenic potential in subgranular and subventricular zones in adult mouse brain." PLoS One 6(3): e18472.

Kluger, Y., Z. Lian, X. Zhang, P. E. Newburger and S. M. Weissman (2004). "A panorama of lineage-specific transcription in hematopoiesis." Bioessays 26(12): 1276-1287.

Knowles, P. P., J. Murray-Rust, S. Kjaer, R. P. Scott, S. Hanrahan, M. Santoro, C. F. Ibanez and N. Q. McDonald (2006). "Structure and chemical inhibition of the RET tyrosine kinase domain." J Biol Chem 281(44): 33577-33587.

Kunnimalaiyaan, M., A. M. Vaccaro, M. A. Ndiaye and H. Chen (2006). "Overexpression of the NOTCH1 intracellular domain inhibits cell proliferation and alters the neuroendocrine phenotype of medullary thyroid cancer cells." J Biol Chem 281(52): 39819-39830.

Kwak, E. L., Y. J. Bang, D. R. Camidge, A. T. Shaw, B. Solomon, R. G. Maki, S. H. Ou, B. J. Dezube, P. A. Janne, D. B. Costa, M. Varella-Garcia, W. H. Kim, T. J. Lynch, P. Fidias, H. Stubbs, J. A. Engelman, L. V. Sequist, W. Tan, L. Gandhi, M. Mino-Kenudson, G. C. Wei, S. M. Shreeve, M. J. Ratain, J. Settleman, J. G. Christensen, D. A. Haber, K. Wilner, R. Salgia, G. I. Shapiro, J. W. Clark and A. J. Iafrate (2010). "Anaplastic lymphoma kinase inhibition in non-small-cell lung cancer." N Engl J Med 363(18): 1693-1703.

Kwei, K. A., Y. H. Kim, L. Girard, J. Kao, M. Pacyna-Gengelbach, K. Salari, J. Lee, Y. L. Choi, M. Sato, P. Wang, T. Hernandez-Boussard, A. F. Gazdar, I. Petersen, J. D. Minna and J. R. Pollack (2008). "Genomic profiling identifies TITF1 as a lineage-specific oncogene amplified in lung cancer." Oncogene 27(25): 3635-3640.

Langmead, B., C. Trapnell, M. Pop and S. L. Salzberg (2009). "Ultrafast and memory-efficient alignment of short DNA sequences to the human genome." Genome Biol 10(3): R25.

Lasorella, A., M. Noseda, M. Beyna, Y. Yokota and A. Iavarone (2000). "Id2 is a retinoblastoma protein target and mediates signalling by Myc oncoproteins." Nature 407(6804): 592-598.

Li, Y. and R. I. Linnoila (2012). "Multidirectional differentiation of Achaete-Scute homologue-1-defined progenitors in lung development and injury repair." Am J Respir Cell Mol Biol 47(6): 768-775.

Linnoila, R. I. (2006). "Functional facets of the pulmonary neuroendocrine system." Lab Invest 86(5): 425-444.

Linnoila, R. I., A. Sahu, M. Miki, D. W. Ball and F. J. DeMayo (2000). "Morphometric analysis of CC10-hASH1 transgenic mouse lung: a model for bronchiolization of alveoli and neuroendocrine carcinoma." Exp Lung Res 26(8): 595-615.

Linnoila, R. I., B. Zhao, J. L. DeMayo, B. D. Nelkin, S. B. Baylin, F. J. DeMayo and D. W. Ball (2000). "Constitutive achaete-scute homologue-1 promotes airway dysplasia and lung neuroendocrine tumors in transgenic mice." Cancer Res 60(15): 4005-4009.

Llovet, J. M., S. Ricci, V. Mazzaferro, P. Hilgard, E. Gane, J. F. Blanc, A. C. de Oliveira, A. Santoro, J. L. Raoul, A. Forner, M. Schwartz, C. Porta, S. Zeuzem, L. Bolondi, T. F. Greten, P. R. Galle, J. F. Seitz, I. Borbath, D. Haussinger, T. Giannaris, M. Shan, M. Moscovici, D. Voliotis and J. Bruix (2008). "Sorafenib in advanced hepatocellular carcinoma." N Engl J Med 359(4): 378-390.

Lumachi, F., G. Luisetto, S. M. Basso, U. Basso, A. Brunello and V. Camozzi (2011). "Endocrine therapy of breast cancer." Curr Med Chem 18(4): 513-522.

Marin, O., S. A. Anderson and J. L. Rubenstein (2000). "Origin and molecular specification of striatal interneurons." J Neurosci 20(16): 6063-6076.

Marino, S., M. Vooijs, H. van Der Gulden, J. Jonkers and A. Berns (2000). "Induction of medulloblastomas in p53-null mutant mice by somatic inactivation of Rb in the external granular layer cells of the cerebellum." Genes Dev 14(8): 994-1004.

McDermott, U., R. Y. Ames, A. J. Iafrate, S. Maheswaran, H. Stubbs, P. Greninger, K. McCutcheon, R. Milano, A. Tam, D. Y. Lee, L. Lucien, B. W. Brannigan, L. E. Ulkus, X. J. Ma, M. G. Erlander, D. A. Haber, S. V. Sharma and J. Settleman (2009). "Ligand-dependent platelet-derived growth factor receptor (PDGFR)-alpha activation sensitizes rare lung cancer and sarcoma cells to PDGFR kinase inhibitors." Cancer Res 69(9): 3937-3946.

McGill, G. G., M. Horstmann, H. R. Widlund, J. Du, G. Motyckova, E. K. Nishimura, Y. L. Lin, S. Ramaswamy, W. Avery, H. F. Ding, S. A. Jordan, I. J. Jackson, S. J. Korsmeyer, T. R. Golub and D. E. Fisher (2002). "Bcl2 regulation by the melanocyte master regulator Mitf modulates lineage survival and melanoma cell viability." Cell 109(6): 707-718.

McLean, C. Y., D. Bristor, M. Hiller, S. L. Clarke, B. T. Schaar, C. B. Lowe, A. M. Wenger and G. Bejerano (2010). "GREAT improves functional interpretation of cis-regulatory regions." Nat Biotechnol 28(5): 495-501.

Meuwissen, R., S. C. Linn, R. I. Linnoila, J. Zevenhoven, W. J. Mooi and A. Berns (2003). "Induction of small cell lung cancer by somatic inactivation of both Trp53 and Rb1 in a conditional mouse model." Cancer Cell 4(3): 181-189.

Miki, M., D. W. Ball and R. I. Linnoila (2012). "Insights into the achaete-scute homolog-1 gene (hASH1) in normal and neoplastic human lung." Lung Cancer 75(1): 58-65.

Modi, S., A. Kubo, H. Oie, A. B. Coxon, A. Rehmatulla and F. J. Kaye (2000). "Protein expression of the RB-related gene family and SV40 large T antigen in mesothelioma and lung cancer." Oncogene 19(40): 4632-4639.

Moline, J. and C. Eng (2011). "Multiple endocrine neoplasia type 2: an overview." Genet Med 13(9): 755-764.

Muller, C. and A. Leutz (2001). "Chromatin remodeling in development and differentiation." Curr Opin Genet Dev 11(2): 167-174.

Nagamura-Inoue, T., T. Tamura and K. Ozato (2001). "Transcription factors that regulate growth and differentiation of myeloid cells." Int Rev Immunol 20(1): 83-105.

Nagilla, M., R. L. Brown and E. E. Cohen (2012). "Cabozantinib for the treatment of advanced medullary thyroid cancer." Adv Ther 29(11): 925-934.

Nakakura, E. K., V. R. Sriuranpong, M. Kunnimalaiyaan, E. C. Hsiao, K. E. Schuebel, M. W. Borges, N. Jin, B. J. Collins, B. D. Nelkin, H. Chen and D. W. Ball (2005). "Regulation of neuroendocrine differentiation in gastrointestinal carcinoid tumor cells by notch signaling." J Clin Endocrinol Metab 90(7): 4350-4356.

Nishi, T. and H. Saya (1991). "Neurofibromatosis type 1 (NF1) gene: implication in neuroectodermal differentiation and genesis of brain tumors." Cancer Metastasis Rev 10(4): 301-310.

Nishikawa, E., H. Osada, Y. Okazaki, C. Arima, S. Tomida, Y. Tatematsu, A. Taguchi, Y. Shimada, K. Yanagisawa, Y. Yatabe, S. Toyokuni, Y. Sekido and T. Takahashi (2011). "miR-375 is activated by ASH1 and inhibits YAP1 in a lineage-dependent manner in lung cancer." Cancer Res 71(19): 6165-6173.

O'Hare, T., R. Pollock, E. P. Stoffregen, J. A. Keats, O. M. Abdullah, E. M. Moseson, V. M. Rivera, H. Tang, C. A. Metcalf, 3rd, R. S. Bohacek, Y. Wang, R. Sundaramoorthi, W. C. Shakespeare, D. Dalgarno, T. Clackson, T. K. Sawyer, M. W. Deininger and B. J. Druker (2004).

"Inhibition of wild-type and mutant Bcr-Abl by AP23464, a potent ATP-based oncogenic protein kinase inhibitor: implications for CML." Blood 104(8): 2532-2539.

Omholt, K., A. Platz, L. Kanter, U. Ringborg and J. Hansson (2003). "NRAS and BRAF mutations arise early during melanoma pathogenesis and are preserved throughout tumor progression." Clin Cancer Res 9(17): 6483-6488.

Osada, H., Y. Tatematsu, Y. Yatabe, Y. Horio and T. Takahashi (2005). "ASH1 gene is a specific therapeutic target for lung cancers with neuroendocrine features." Cancer Res 65(23): 10680-10685.

Osada, H., S. Tomida, Y. Yatabe, Y. Tatematsu, T. Takeuchi, H. Murakami, Y. Kondo, Y. Sekido and T. Takahashi (2008). "Roles of achaete-scute homologue 1 in DKK1 and E-cadherin repression and neuroendocrine differentiation in lung cancer." Cancer Res 68(6): 1647-1655.

Pao, W., V. Miller, M. Zakowski, J. Doherty, K. Politi, I. Sarkaria, B. Singh, R. Heelan, V. Rusch, L. Fulton, E. Mardis, D. Kupfer, R. Wilson, M. Kris and H. Varmus (2004). "EGF receptor gene mutations are common in lung cancers from "never smokers" and are associated with sensitivity of tumors to gefitinib and erlotinib." Proc Natl Acad Sci U S A 101(36): 13306-13311.

Park, K. S., L. G. Martelotto, M. Peifer, M. L. Sos, A. N. Karnezis, M. R. Mahjoub, K. Bernard, J. F. Conklin, A. Szczepny, J. Yuan, R. Guo, B. Ospina, J. Falzon, S. Bennett, T. J. Brown, A. Markovic, W. L. Devereux, C. A. Ocasio, J. K. Chen, T. Stearns, R. K. Thomas, M. Dorsch, S. Buonamici, D. N. Watkins, C. D. Peacock and J. Sage (2011). "A crucial requirement for Hedgehog signaling in small cell lung cancer." Nat Med 17(11): 1504-1508.

Pelosi, G., F. Pasini, A. Sonzogni, F. Maffini, P. Maisonneuve, A. Iannucci, A. Terzi, G. De Manzoni, E. Bresaola and G. Viale (2003). "Prognostic implications of neuroendocrine differentiation and hormone production in patients with Stage I nonsmall cell lung carcinoma." Cancer 97(10): 2487-2497.

Perk, J., A. Iavarone and R. Benezra (2005). "Id family of helix-loop-helix proteins in cancer." Nat Rev Cancer 5(8): 603-614.

Perou, C. M., T. Sorlie, M. B. Eisen, M. van de Rijn, S. S. Jeffrey, C. A. Rees, J. R. Pollack, D. T. Ross, H. Johnsen, L. A. Akslen, O. Fluge, A. Pergamenschikov, C. Williams, S. X. Zhu, P. E. Lonning, A. L. Borresen-Dale, P. O. Brown and D. Botstein (2000). "Molecular portraits of human breast tumours." Nature 406(6797): 747-752.

Phelps, R. M., B. E. Johnson, D. C. Ihde, A. F. Gazdar, D. P. Carbone, P. R. McClintock, R. I. Linnoila, M. J. Matthews, P. A. Bunn, Jr., D. Carney, J. D. Minna and J. L. Mulshine (1996). "NCI-Navy Medical Oncology Branch cell line data base." J Cell Biochem Suppl 24: 32-91.

Pinchot, S. N., R. Jaskula-Sztul, L. Ning, N. R. Peters, M. R. Cook, M. Kunnimalaiyaan and H. Chen (2011). "Identification and validation of Notch pathway activating compounds through a novel high-throughput screening method." Cancer 117(7): 1386-1398.

Pollak, J., M. S. Wilken, Y. Ueki, K. E. Cox, J. M. Sullivan, R. J. Taylor, E. M. Levine and T. A. Reh (2013). "ASCL1 reprograms mouse Muller glia into neurogenic retinal progenitors." Development 140(12): 2619-2631.

Post, L. C., M. Ternet and B. L. Hogan (2000). "Notch/Delta expression in the developing mouse lung." Mech Dev 98(1-2): 95-98.

Puri, P. L., V. Sartorelli, X. J. Yang, Y. Hamamori, V. V. Ogryzko, B. H. Howard, L. Kedes, J. Y. Wang, A. Graessmann, Y. Nakatani and M. Levrero (1997). "Differential roles of p300 and PCAF acetyltransferases in muscle differentiation." Mol Cell 1(1): 35-45.

Qi, X. P., J. M. Ma, Z. F. Du, R. B. Ying, J. Fei, H. Y. Jin, J. S. Han, J. Q. Wang, X. L. Chen, C. Y. Chen, W. T. Liu, J. J. Lu, J. G. Zhang and X. N. Zhang (2011). "RET germline mutations identified by exome sequencing in a Chinese multiple endocrine neoplasia type 2A/familial medullary thyroid carcinoma family." PLoS One 6(5): e20353.

Ramirez, R. D., S. Sheridan, L. Girard, M. Sato, Y. Kim, J. Pollack, M. Peyton, Y. Zou, J. M. Kurie, J. M. Dimaio, S. Milchgrub, A. L. Smith, R. F. Souza, L. Gilbey, X. Zhang, K. Gandia, M. B. Vaughan, W. E. Wright, A. F. Gazdar, J. W. Shay and J. D. Minna (2004). "Immortalization of human bronchial epithelial cells in the absence of viral oncoproteins." Cancer Res 64(24): 9027-9034.

Reifenberger, J., C. B. Knobbe, A. A. Sterzinger, B. Blaschke, K. W. Schulte, T. Ruzicka and G. Reifenberger (2004). "Frequent alterations of Ras signaling pathway genes in sporadic malignant melanomas." Int J Cancer 109(3): 377-384.

Rekhtman, N. (2010). "Neuroendocrine tumors of the lung: an update." Arch Pathol Lab Med 134(11): 1628-1638.

Righi, L., M. Volante, I. Rapa, G. V. Scagliotti and M. Papotti (2007). "Neuro-endocrine tumours of the lung. A review of relevant pathological and molecular data." Virchows Arch 451 Suppl 1: S51-59.

Ringrose, L. and R. Paro (2004). "Epigenetic regulation of cellular memory by the Polycomb and Trithorax group proteins." Annu Rev Genet 38: 413-443.

Rodina, A., M. Vilenchik, K. Moulick, J. Aguirre, J. Kim, A. Chiang, J. Litz, C. C. Clement, Y. Kang, Y. She, N. Wu, S. Felts, P. Wipf, J. Massague, X. Jiang, J. L. Brodsky, G. W. Krystal and G. Chiosis (2007). "Selective compounds define Hsp90 as a major inhibitor of apoptosis in small-cell lung cancer." Nat Chem Biol 3(8): 498-507.

Rodriguez, E. and R. C. Lilenbaum (2010). "Small cell lung cancer: past, present, and future." Curr Oncol Rep 12(5): 327-334.

Ross-Innes, C. S., R. Stark, A. E. Teschendorff, K. A. Holmes, H. R. Ali, M. J. Dunning, G. D. Brown, O. Gojis, I. O. Ellis, A. R. Green, S. Ali, S. F. Chin, C. Palmieri, C. Caldas and J. S. Carroll (2012). "Differential oestrogen receptor binding is associated with clinical outcome in breast cancer." Nature 481(7381): 389-393.

Ross, S. E., M. E. Greenberg and C. D. Stiles (2003). "Basic helix-loop-helix factors in cortical development." Neuron 39(1): 13-25.

Rowley, J. D. (1973). "Letter: A new consistent chromosomal abnormality in chronic myelogenous leukaemia identified by quinacrine fluorescence and Giemsa staining." Nature 243(5405): 290-293.

Rudin, C. M., C. L. Hann, E. B. Garon, M. Ribeiro de Oliveira, P. D. Bonomi, D. R. Camidge, Q. Chu, G. Giaccone, D. Khaira, S. S. Ramalingam, M. R. Ranson, C. Dive, E. M. McKeegan, B. J. Chyla, B. L. Dowell, A. Chakravartty, C. E. Nolan, N. Rudersdorf, T. A. Busman, M. H. Mabry, A. P. Krivoshik, R. A. Humerickhouse, G. I. Shapiro and L. Gandhi (2012). "Phase II study of single-agent navitoclax (ABT-263) and biomarker correlates in patients with relapsed small cell lung cancer." Clin Cancer Res 18(11): 3163-3169.

Sakamoto, K., O. Ohara, M. Takagi, S. Takeda and K. Katsube (2002). "Intracellular cell-autonomous association of Notch and its ligands: a novel mechanism of Notch signal modification." Dev Biol 241(2): 313-326.

Sato, M., D. S. Shames, A. F. Gazdar and J. D. Minna (2007). "A translational view of the molecular pathogenesis of lung cancer." J Thorac Oncol 2(4): 327-343.

Sattler, M. and R. Salgia (2003). "Molecular and cellular biology of small cell lung cancer." Semin Oncol 30(1): 57-71.

Sawa, M., K. Yamamoto, T. Yokozawa, H. Kiyoi, A. Hishida, T. Kajiguchi, M. Seto, A. Kohno, K. Kitamura, Y. Itoh, N. Asou, N. Hamajima, N. Emi and T. Naoe (2005). "BMI-1 is highly expressed in M0-subtype acute myeloid leukemia." Int J Hematol 82(1): 42-47.

Schindler, T., W. Bornmann, P. Pellicena, W. T. Miller, B. Clarkson and J. Kuriyan (2000). "Structural mechanism for STI-571 inhibition of abelson tyrosine kinase." Science 289(5486): 1938-1942.

Schleusener, J. T., H. D. Tazelaar, S. H. Jung, S. S. Cha, P. J. Cera, J. L. Myers, E. T. Creagan, R. M. Goldberg and R. F. Marschke, Jr. (1996). "Neuroendocrine differentiation is an independent prognostic factor in chemotherapy-treated nonsmall cell lung carcinoma." Cancer 77(7): 1284-1291.

Segawa, Y., S. Takata, M. Fujii, I. Oze, Y. Fujiwara, Y. Kato, A. Ogino, E. Komori, S. Sawada, M. Yamashita, R. Nishimura, N. Teramoto and S. Takashima (2009). "Immunohistochemical detection of neuroendocrine differentiation in non-small-cell lung cancer and its clinical implications." J Cancer Res Clin Oncol 135(8): 1055-1059.

Sekido, Y., K. M. Fong and J. D. Minna (2003). "Molecular genetics of lung cancer." Annu Rev Med 54: 73-87.

Sequist, L. V., B. A. Waltman, D. Dias-Santagata, S. Digumarthy, A. B. Turke, P. Fidias, K. Bergethon, A. T. Shaw, S. Gettinger, A. K. Cosper, S. Akhavanfard, R. S. Heist, J. Temel, J. G. Christensen, J. C. Wain, T. J. Lynch, K. Vernovsky, E. J. Mark, M. Lanuti, A. J. Iafrate, M. Mino-Kenudson and J. A. Engelman (2011). "Genotypic and histological evolution of lung cancers acquiring resistance to EGFR inhibitors." Sci Transl Med 3(75): 75ra26.

Sharpless, E. and L. Chin (2003). "The INK4a/ARF locus and melanoma." Oncogene 22(20): 3092-3098.

Sherr, C. J. and F. McCormick (2002). "The RB and p53 pathways in cancer." Cancer Cell 2(2): 103-112.

Shimizu, E., A. Coxon, G. A. Otterson, S. M. Steinberg, R. A. Kratzke, Y. W. Kim, J. Fedorko, H. Oie, B. E. Johnson, J. L. Mulshine and et al. (1994). "RB protein status and clinical correlation from 171 cell lines representing lung cancer, extrapulmonary small cell carcinoma, and mesothelioma." Oncogene 9(9): 2441-2448.

Shoemaker, A. R., M. J. Mitten, J. Adickes, S. Ackler, M. Refici, D. Ferguson, A. Oleksijew, J. M. O'Connor, B. Wang, D. J. Frost, J. Bauch, K. Marsh, S. K. Tahir, X. Yang, C. Tse, S. W. Fesik, S. H. Rosenberg and S. W. Elmore (2008). "Activity of the Bcl-2 family inhibitor ABT-263 in a panel of small cell lung cancer xenograft models." Clin Cancer Res 14(11): 3268-3277.

Simpson, P. (1990). "Lateral inhibition and the development of the sensory bristles of the adult peripheral nervous system of Drosophila." Development 109(3): 509-519.

Skinner, M. K., A. Rawls, J. Wilson-Rawls and E. H. Roalson (2010). "Basic helix-loop-helix transcription factor gene family phylogenetics and nomenclature." Differentiation 80(1): 1-8.

Skov, B. G., M. Krasnik, S. Lantuejoul, T. Skov and E. Brambilla (2008). "Reclassification of neuroendocrine tumors improves the separation of carcinoids and the prediction of survival." J Thorac Oncol 3(12): 1410-1415.

Skuladottir, H., F. R. Hirsch, H. H. Hansen and J. H. Olsen (2002). "Pulmonary neuroendocrine tumors: incidence and prognosis of histological subtypes. A population-based study in Denmark." Lung Cancer 37(2): 127-135.

Smit, V. T., A. J. Boot, A. M. Smits, G. J. Fleuren, C. J. Cornelisse and J. L. Bos (1988). "KRAS codon 12 mutations occur very frequently in pancreatic adenocarcinomas." Nucleic Acids Res 16(16): 7773-7782.

Soda, M., Y. L. Choi, M. Enomoto, S. Takada, Y. Yamashita, S. Ishikawa, S. Fujiwara, H. Watanabe, K. Kurashina, H. Hatanaka, M. Bando, S. Ohno, Y. Ishikawa, H. Aburatani, T. Niki, Y. Sohara, Y. Sugiyama and H. Mano (2007). "Identification of the transforming EML4-ALK fusion gene in non-small-cell lung cancer." Nature 448(7153): 561-566.

Song, H., E. Yao, C. Lin, R. Gacayan, M. H. Chen and P. T. Chuang (2012). "Functional characterization of pulmonary neuroendocrine cells in lung development, injury, and tumorigenesis." Proc Natl Acad Sci U S A 109(43): 17531-17536.

Sorlie, T., C. M. Perou, R. Tibshirani, T. Aas, S. Geisler, H. Johnsen, T. Hastie, M. B. Eisen, M. van de Rijn, S. S. Jeffrey, T. Thorsen, H. Quist, J. C. Matese, P. O. Brown, D. Botstein, P. E. Lonning and A. L. Borresen-Dale (2001). "Gene expression patterns of breast carcinomas distinguish tumor subclasses with clinical implications." Proc Natl Acad Sci U S A 98(19): 10869-10874.

Souers, A. J., J. D. Leverson, E. R. Boghaert, S. L. Ackler, N. D. Catron, J. Chen, B. D. Dayton, H. Ding, S. H. Enschede, W. J. Fairbrother, D. C. Huang, S. G. Hymowitz, S. Jin, S. L. Khaw, P. J. Kovar, L. T. Lam, J. Lee, H. L. Maecker, K. C. Marsh, K. D. Mason, M. J. Mitten, P. M. Nimmer, A. Oleksijew, C. H. Park, C. M. Park, D. C. Phillips, A. W. Roberts, D. Sampath, J. F. Seymour, M. L. Smith, G. M. Sullivan, S. K. Tahir, C. Tse, M. D. Wendt, Y. Xiao, J. C. Xue, H. Zhang, R. A. Humerickhouse, S. H. Rosenberg and S. W. Elmore (2013). "ABT-199, a potent and selective BCL-2 inhibitor, achieves antitumor activity while sparing platelets." Nat Med 19(2): 202-208.

Sriuranpong, V., M. W. Borges, R. K. Ravi, D. R. Arnold, B. D. Nelkin, S. B. Baylin and D. W. Ball (2001). "Notch signaling induces cell cycle arrest in small cell lung cancer cells." Cancer Res 61(7): 3200-3205.

Sriuranpong, V., M. W. Borges, C. L. Strock, E. K. Nakakura, D. N. Watkins, C. M. Blaumueller, B. D. Nelkin and D. W. Ball (2002). "Notch signaling induces rapid degradation of achaete-scute homolog 1." Mol Cell Biol 22(9): 3129-3139.

Sterlacci, W., M. Fiegl, W. Hilbe, J. Auberger, G. Mikuz and A. Tzankov (2009). "Clinical relevance of neuroendocrine differentiation in non-small cell lung cancer assessed by immunohistochemistry: a retrospective study on 405 surgically resected cases." Virchows Arch 455(2): 125-132.

Sullivan, J. P. and J. D. Minna (2010). "Tumor oncogenotypes and lung cancer stem cell identity." Cell Stem Cell 7(1): 2-4.

Sullivan, J. P., M. Spinola, M. Dodge, M. G. Raso, C. Behrens, B. Gao, K. Schuster, C. Shao, J. E. Larsen, L. A. Sullivan, S. Honorio, Y. Xie, P. P. Scaglioni, J. M. DiMaio, A. F. Gazdar, J. W. Shay, Wistuba, II and J. D. Minna (2010). "Aldehyde dehydrogenase activity selects for lung adenocarcinoma stem cells dependent on notch signaling." Cancer Res 70(23): 9937-9948.

Sun, J. M., M. J. Ahn, J. S. Ahn, S. W. Um, H. Kim, H. K. Kim, Y. S. Choi, J. Han, J. Kim, O. J. Kwon, Y. M. Shim and K. Park (2012). "Chemotherapy for pulmonary large cell neuroendocrine carcinoma: similar to that for small cell lung cancer or non-small cell lung cancer?" Lung Cancer 77(2): 365-370.

Sunday, M. E., K. J. Haley, K. Sikorski, S. A. Graham, R. L. Emanuel, F. Zhang, Q. Mu, A. Shahsafaei and D. Hatzis (1999). "Calcitonin driven v-Ha-ras induces multilineage pulmonary epithelial hyperplasias and neoplasms." Oncogene 18(30): 4336-4347.

Sutherland, K. D., N. Proost, I. Brouns, D. Adriaensen, J. Y. Song and A. Berns (2011). "Cell of origin of small cell lung cancer: inactivation of Trp53 and Rb1 in distinct cell types of adult mouse lung." Cancer Cell 19(6): 754-764.

Tahara, E., H. Kadara, L. Lacroix, D. Lotan and R. Lotan (2009). "Activation of protein kinase C by phorbol 12-myristate 13-acetate suppresses the growth of lung cancer cells through KLF6 induction." Cancer Biol Ther 8(9): 801-807.

Takahashi, M., J. Ritz and G. M. Cooper (1985). "Activation of a novel human transforming gene, ret, by DNA rearrangement." Cell 42(2): 581-588.

Tal, M., M. Wetzler, Z. Josefberg, A. Deutch, M. Gutman, D. Assaf, R. Kris, Y. Shiloh, D. Givol and J. Schlessinger (1988). "Sporadic amplification of the HER2/neu protooncogene in adenocarcinomas of various tissues." Cancer Res 48(6): 1517-1520.

Tallman, M. S., J. W. Andersen, C. A. Schiffer, F. R. Appelbaum, J. H. Feusner, A. Ogden, L. Shepherd, C. Willman, C. D. Bloomfield, J. M. Rowe and P. H. Wiernik (1997). "All-trans-retinoic acid in acute promyelocytic leukemia." N Engl J Med 337(15): 1021-1028.

Theka, I., M. Caiazzo, E. Dvoretskova, D. Leo, F. Ungaro, S. Curreli, F. Manago, M. T. Dell'anno, G. Pezzoli, R. R. Gainetdinov, A. Dityatev and V. Broccoli (2013). "Rapid Generation of Functional Dopaminergic Neurons From Human Induced Pluripotent Stem Cells Through a Single-Step Procedure Using Cell Lineage Transcription Factors." Stem Cells Transl Med.

Toma, J. G., H. El-Bizri, F. Barnabe-Heider, R. Aloyz and F. D. Miller (2000). "Evidence that helix-loop-helix proteins collaborate with retinoblastoma tumor suppressor protein to regulate cortical neurogenesis." J Neurosci 20(20): 7648-7656.

Tomizawa, Y., Y. Sekido, M. Kondo, B. Gao, J. Yokota, J. Roche, H. Drabkin, M. I. Lerman, A. F. Gazdar and J. D. Minna (2001). "Inhibition of lung cancer cell growth and induction of

apoptosis after reexpression of 3p21.3 candidate tumor suppressor gene SEMA3B." Proc Natl Acad Sci U S A 98(24): 13954-13959.

Torii, M., F. Matsuzaki, N. Osumi, K. Kaibuchi, S. Nakamura, S. Casarosa, F. Guillemot and M. Nakafuku (1999). "Transcription factors Mash-1 and Prox-1 delineate early steps in differentiation of neural stem cells in the developing central nervous system." Development 126(3): 443-456.

Truong, M., M. R. Cook, S. N. Pinchot, M. Kunnimalaiyaan and H. Chen (2011). "Resveratrol induces Notch2-mediated apoptosis and suppression of neuroendocrine markers in medullary thyroid cancer." Ann Surg Oncol 18(5): 1506-1511.

Tse, C., A. R. Shoemaker, J. Adickes, M. G. Anderson, J. Chen, S. Jin, E. F. Johnson, K. C. Marsh, M. J. Mitten, P. Nimmer, L. Roberts, S. K. Tahir, Y. Xiao, X. Yang, H. Zhang, S. Fesik, S. H. Rosenberg and S. W. Elmore (2008). "ABT-263: a potent and orally bioavailable Bcl-2 family inhibitor." Cancer Res 68(9): 3421-3428.

Ucar, A., V. Vafaizadeh, H. Jarry, J. Fiedler, P. A. Klemmt, T. Thum, B. Groner and K. Chowdhury (2010). "miR-212 and miR-132 are required for epithelial stromal interactions necessary for mouse mammary gland development." Nat Genet 42(12): 1101-1108.

Ulivi, P., M. Puccetti, L. Capelli, E. Chiadini, S. Bravaccini, D. Calistri, W. Zoli, D. Amadori and P. Candoli (2013). "Molecular determinations of EGFR and EML4-ALK on a single slide of NSCLC tissue." J Clin Pathol.

Vaccaro, A., H. Chen and M. Kunnimalaiyaan (2006). "In-vivo activation of Raf-1 inhibits tumor growth and development in a xenograft model of human medullary thyroid cancer." Anticancer Drugs 17(7): 849-853.

Vachtenheim, J., I. Horakova, H. Novotna, P. Opaalka and H. Roubkova (1995). "Mutations of K-ras oncogene and absence of H-ras mutations in squamous cell carcinomas of the lung." Clin Cancer Res 1(3): 359-365.

Visvader, J. E. (2009). "Keeping abreast of the mammary epithelial hierarchy and breast tumorigenesis." Genes Dev 23(22): 2563-2577.

Voronova, A., A. Fischer, T. Ryan, A. Al Madhoun and I. S. Skerjanc (2011). "Ascl1/Mash1 is a novel target of Gli2 during Gli2-induced neurogenesis in P19 EC cells." PLoS One 6(4): e19174.

Wang, J. H. (2012). "Mechanisms and impacts of chromosomal translocations in cancers." Front Med 6(3): 263-274.

Wang, X. Y., S. M. Jensen-Taubman, K. M. Keefe, D. Yang and R. I. Linnoila (2012). "Achaete-scute complex homolog-1 promotes DNA repair in the lung carcinogenesis through matrix

metalloproteinase-7 and O(6)-methylguanine-DNA methyltransferase." PLoS One 7(12): e52832.

Warburton, D., M. Schwarz, D. Tefft, G. Flores-Delgado, K. D. Anderson and W. V. Cardoso (2000). "The molecular basis of lung morphogenesis." Mech Dev 92(1): 55-81.

Watanabe, H., J. M. Francis, M. S. Woo, B. Etemad, W. Lin, D. F. Fries, S. Peng, E. L. Snyder, P. R. Tata, F. Izzo, A. C. Schinzel, J. Cho, P. S. Hammerman, R. G. Verhaak, W. C. Hahn, J. Rajagopal, T. Jacks and M. Meyerson (2013). "Integrated cistromic and expression analysis of amplified NKX2-1 in lung adenocarcinoma identifies LMO3 as a functional transcriptional target." Genes Dev 27(2): 197-210.

Wechsler-Reya, R. and M. P. Scott (2001). "The developmental biology of brain tumors." Annu Rev Neurosci 24: 385-428.

Weinstein, I. B. (2002). "Cancer. Addiction to oncogenes--the Achilles heal of cancer." Science 297(5578): 63-64.

Wellbrock, C., S. Rana, H. Paterson, H. Pickersgill, T. Brummelkamp and R. Marais (2008). "Oncogenic BRAF regulates melanoma proliferation through the lineage specific factor MITF." PLoS One 3(7): e2734.

Wells, S. A., Jr., B. G. Robinson, R. F. Gagel, H. Dralle, J. A. Fagin, M. Santoro, E. Baudin, R. Elisei, B. Jarzab, J. R. Vasselli, J. Read, P. Langmuir, A. J. Ryan and M. J. Schlumberger (2012). "Vandetanib in patients with locally advanced or metastatic medullary thyroid cancer: a randomized, double-blind phase III trial." J Clin Oncol 30(2): 134-141.

West, L., S. J. Vidwans, N. P. Campbell, J. Shrager, G. R. Simon, R. Bueno, P. A. Dennis, G. A. Otterson and R. Salgia (2012). "A novel classification of lung cancer into molecular subtypes." PLoS One 7(2): e31906.

Widlund, H. R. and D. E. Fisher (2003). "Microphthalamia-associated transcription factor: a critical regulator of pigment cell development and survival." Oncogene 22(20): 3035-3041.

Wiggins, J. F., L. Ruffino, K. Kelnar, M. Omotola, L. Patrawala, D. Brown and A. G. Bader (2010). "Development of a lung cancer therapeutic based on the tumor suppressor microRNA-34." Cancer Res 70(14): 5923-5930.

Wilhelm, S. M., L. Adnane, P. Newell, A. Villanueva, J. M. Llovet and M. Lynch (2008). "Preclinical overview of sorafenib, a multikinase inhibitor that targets both Raf and VEGF and PDGF receptor tyrosine kinase signaling." Mol Cancer Ther 7(10): 3129-3140.

Winslow, M. M., T. L. Dayton, R. G. Verhaak, C. Kim-Kiselak, E. L. Snyder, D. M. Feldser, D. D. Hubbard, M. J. DuPage, C. A. Whittaker, S. Hoersch, S. Yoon, D. Crowley, R. T. Bronson,

D. Y. Chiang, M. Meyerson and T. Jacks (2011). "Suppression of lung adenocarcinoma progression by Nkx2-1." Nature 473(7345): 101-104.

Wistuba, II, A. F. Gazdar and J. D. Minna (2001). "Molecular genetics of small cell lung carcinoma." Semin Oncol 28(2 Suppl 4): 3-13.

Wong, A. J., S. H. Bigner, D. D. Bigner, K. W. Kinzler, S. R. Hamilton and B. Vogelstein (1987). "Increased expression of the epidermal growth factor receptor gene in malignant gliomas is invariably associated with gene amplification." Proc Natl Acad Sci U S A 84(19): 6899-6903.

Xiang, R., D. Liao, T. Cheng, H. Zhou, Q. Shi, T. S. Chuang, D. Markowitz, R. A. Reisfeld and Y. Luo (2011). "Downregulation of transcription factor SOX2 in cancer stem cells suppresses growth and metastasis of lung cancer." Br J Cancer 104(9): 1410-1417.

Yeh, T. C., V. Marsh, B. A. Bernat, J. Ballard, H. Colwell, R. J. Evans, J. Parry, D. Smith, B. J. Brandhuber, S. Gross, A. Marlow, B. Hurley, J. Lyssikatos, P. A. Lee, J. D. Winkler, K. Koch and E. Wallace (2007). "Biological characterization of ARRY-142886 (AZD6244), a potent, highly selective mitogen-activated protein kinase kinase 1/2 inhibitor." Clin Cancer Res 13(5): 1576-1583.

Yu, J., R. S. Mani, Q. Cao, C. J. Brenner, X. Cao, X. Wang, L. Wu, J. Li, M. Hu, Y. Gong, H. Cheng, B. Laxman, A. Vellaichamy, S. Shankar, Y. Li, S. M. Dhanasekaran, R. Morey, T. Barrette, R. J. Lonigro, S. A. Tomlins, S. Varambally, Z. S. Qin and A. M. Chinnaiyan (2010). "An integrated network of androgen receptor, polycomb, and TMPRSS2-ERG gene fusions in prostate cancer progression." Cancer Cell 17(5): 443-454.

Yun, K., S. Fischman, J. Johnson, M. Hrabe de Angelis, G. Weinmaster and J. L. Rubenstein (2002). "Modulation of the notch signaling by Mash1 and Dlx1/2 regulates sequential specification and differentiation of progenitor cell types in the subcortical telencephalon." Development 129(21): 5029-5040.

Zhang, Y., T. Liu, C. A. Meyer, J. Eeckhoute, D. S. Johnson, B. E. Bernstein, C. Nusbaum, R. M. Myers, M. Brown, W. Li and X. S. Liu (2008). "Model-based analysis of ChIP-Seq (MACS)." Genome Biol 9(9): R137.

Zhao, J., H. He, K. Zhou, Y. Ren, Z. Shi, Z. Wu, Y. Wang, Y. Lu and J. Jiao (2012). "Neuronal transcription factors induce conversion of human glioma cells to neurons and inhibit tumorigenesis." PLoS One 7(7): e41506.